



Copyright Undertaking

This thesis is protected by copyright, with all rights reserved.

By reading and using the thesis, the reader understands and agrees to the following terms:

1. The reader will abide by the rules and legal ordinances governing copyright regarding the use of the thesis.
2. The reader will use the thesis for the purpose of research or private study only and not for distribution or further reproduction or any other purpose.
3. The reader agrees to indemnify and hold the University harmless from and against any loss, damage, cost, liability or expenses arising from copyright infringement or unauthorized usage.

IMPORTANT

If you have reasons to believe that any materials in this thesis are deemed not suitable to be distributed in this form, or a copyright owner having difficulty with the material being included in our database, please contact lbsys@polyu.edu.hk providing details. The Library will look into your claim and consider taking remedial action upon receipt of the written requests.

**STUDY ON HYBRID RENEWABLE ENERGY
AND ELECTRICAL ENERGY STORAGE
SYSTEMS FOR POWER SUPPLY TO
BUILDINGS IN URBAN AREAS**

LIU JIA

PhD

The Hong Kong Polytechnic University

2021

The Hong Kong Polytechnic University
Department of Building Services Engineering

**Study on Hybrid Renewable Energy
and Electrical Energy Storage
Systems for Power Supply to
Buildings in Urban Areas**

Liu Jia

A thesis submitted in partial fulfillment of the requirements for the degree of

Doctor of Philosophy

April 2021

CERTIFICATE OF ORIGINALITY

I hereby declare that this thesis is my own work and that, to the best of my knowledge and belief, it reproduces no material previously published or written, nor material that has been accepted for the award of any other degree or diploma, except where due acknowledgement has been made in the text.

_____ (Signed)

Liu Jia (Name of student)

Department of Building Services Engineering

The Hong Kong Polytechnic University

Hong Kong SAR, China

April 2021

ABSTRACT

Abstract of thesis entitled: Study on hybrid renewable energy and electrical energy storage systems for power supply to buildings in urban areas

Submitted by : Liu Jia

For the degree of : Doctor of Philosophy

at The Hong Kong Polytechnic University in April 2021

The building sector accounts for 30% of the global final energy use and 28% of energy-related carbon emissions in 2019 as the largest contributor in the world, where reductions of 13% and 50% are expected to be achieved by 2040 from 2018 levels according to the International Energy Agency's sustainable development scenario. Renewable energy is projected to share up to 86% of total electricity generation and all buildings must adopt renewable energy strategies by 2050, to meet net-zero energy and net-zero carbon requirements at community scales. It is of great significance to develop renewable energy applications for power supply to buildings and communities in urban areas, as majority of carbon emissions in a country are mainly attributed to just several domestic cities. Especially for high-density cities like Hong Kong, the second largest carbon emitter in China, its building sector accounts for over 90% of total electricity consumption and 60% of carbon emissions. Renewable energy sources, such as solar photovoltaic power and wind power, are usually intermittent and unstable depending on weather conditions, and therefore not consistent with the fluctuating building energy demand. So electrical energy storage

technologies, such as battery and hydrogen storage, should be integrated with renewable energy systems to enhance the energy autonomy and flexibility.

This thesis presents a comprehensive and systematic study on the hybrid renewable energy and electrical energy storage systems for power supply to both a single building and building communities in urban regions, for achieving carbon neutrality in the near future. The novel energy management strategies, flexible grid integration models, robust system planning optimizations, and systematic peer-to-peer energy trading management and optimization platforms are proposed for the hybrid renewable energy and storage system developments. Applications of typical electrical energy storage technologies are investigated, including stationary battery storage, mobile battery vehicle storage, mobile hydrogen vehicle storage and their hybrids, by practical experiments, transient system simulations (TRNSYS), coupled multi-objective optimizations (jEplus+EA), techno-economic-environmental assessments and sensitivity analyses.

Firstly, novel energy management strategies, robust energy planning, improved technical and economic evaluation criteria, and integrated design optimization approaches of hybrid renewable energy and storage systems are developed in this thesis, for power supply **to a single building** in urban areas by establishing transient simulation models validated by practical experiments.

Specifically, an effective design optimization framework of a photovoltaic and battery storage system is developed for a real low-energy building in Shenzhen of China, proposing a novel energy management strategy considering the battery cycling aging, grid relief and local time-of-use pricing. Both single-criterion and multi-criterion optimizations are conducted by comprehensively considering technical, economic and environmental performances of the system.

Meanwhile, improved technical and economic optimization criteria of hybrid renewable energy and storage systems are proposed for typical system applications in a standard high-rise

residential building in Hong Kong, including photovoltaic systems, hybrid photovoltaic-wind systems and hybrid photovoltaic-wind-battery systems. A comprehensive technical optimization criterion is proposed integrating the energy supply, battery storage, building demand and grid relief indicators. And the improved levelized cost of energy considering detailed renewable energy benefits is formulated including the feed-in tariff, transmission loss saving, network expansion saving and carbon reduction benefits. The practical experiments on a photovoltaic and battery storage system, under the maximizing self-consumption and time-of-use strategies, are conducted to study the system performance and validate the energy balance based battery and energy management models.

Moreover, a robust energy planning and optimization approach for hybrid photovoltaic-wind systems integrated with stationary battery and mobile hydrogen vehicle storage is developed, for a typical high-rise residential building in Hong Kong, considering different vehicle-to-building schedules. Two energy management strategies with different priorities of battery and hydrogen storage operations are proposed to compare and optimize the impact of charging and discharging orders of the battery tank and hydrogen vehicle storage on the system technical and economic performances. Multiple design criteria including the supply performance, grid integration and lifetime net present value are formulated, to size the hybrid system and select the optimal energy management strategy. Four decision-making strategies based on the minimum distance to the utopia point and analytical hierarchy process methods are applied, to determine the final optimum solutions for major stakeholders with different preferences (i.e. the end-user, transmission system operator and investor) for high-rise residential building applications within urban contexts.

Secondly, novel time-of-use grid penalty cost business models, peer-to-peer energy trading price models, time-of-use peer-to-peer energy trading management and optimization platforms of

hybrid renewable energy and electrical energy storage systems are proposed, for power supply **to a large-scale net-zero energy building community** integrated with hydrogen vehicles and battery vehicles in urban areas with high power flexibility and grid economy.

In detail, novel time-of-use grid penalty cost business models for hybrid renewable energy and storage systems are developed to improve the power flexibility and economy between net-zero energy community systems and the utility grid. A net-zero energy building community is established with fundamental units of university campus, commercial office and high-rise residential building groups, based on actual energy use data and simulations as per surveys and codes in Hong Kong. Hybrid renewable energy systems integrated with stationary batteries and three hydrogen vehicle groups following different cruise schedules are firstly applied for power supply to the community microgrid as shared energy supply and storage. Four net-zero energy building and community scenarios are established with multi-objective optimizations to size the renewable energy and storage systems.

Additionally, a dynamic peer-to-peer energy trading management platform is developed for the diversified net-zero energy community powered by hybrid renewable energy and hydrogen vehicle storage systems, with innovative peer trading price model and time-of-use peer trading management approaches. An individual peer-to-peer energy trading price model is proposed to allocate individual peer selling/buying price to each building group according to its intrinsic supply demand feature and grid import price in the diversified community. The time-of-use peer energy trading management strategies for both uniform and individual energy trading price modes are further developed based on the time-of-use grid penalty cost model, to improve the power flexibility and economy of the utility grid. The techno-economic-environmental performances of peer-to-peer energy trading management cases are then clarified compared with the baseline case

with only peer-to-grid energy trading. The lifetime net present value of hybrid renewable energy and hydrogen vehicle storage systems in the current cost and future cost scenarios is discussed, to provide economic references for key stakeholders to develop net-zero energy communities.

Furthermore, the peer-to-peer energy trading management and optimization approaches are developed for hybrid renewable energy systems with energy storage of hydrogen and battery vehicles applied in the diversified net-zero energy community. Typical net-zero energy community models are developed and compared with different energy storage vehicle types (hydrogen vehicle/battery vehicle) and energy trading modes (peer-to-grid/peer-to-peer). Multi-objective peer-to-peer trading optimizations of the net-zero energy community integrated with both hydrogen vehicles and battery vehicles are conducted to find optimal configurations of vehicle numbers and time-of-use management operations. An improved peer-to-peer trading management strategy is further proposed considering the peer trading priority and complementary operations of hybrid vehicle storages, to enhance the grid integration, decarbonisation and economy. It provides significant references for stakeholders to apply renewable energy and green vehicle storage systems towards carbon neutrality in integrated building and transport sectors in urban areas.

The above study on hybrid renewable energy and electrical energy storage systems for power supply to both a single building and large-scale communities can help researchers and policy makers to evaluate the technical, economic and environmental feasibility, regarding the energy demand, energy supply, energy storage, energy management and grid integration aspects. The systematic research methodology and framework on the hybrid renewable energy and storage systems can provide significant guidance for relative stakeholders to develop renewable energy applications in the integrated building and transport sectors to accelerate the progress of carbon neutrality within urban contexts.

PUBLICATIONS DURING PHD STUDY

Journal papers:

- [1] **Liu J**, Chen X, Cao S, Yang H. Overview on hybrid solar photovoltaic-electrical energy storage technologies for power supply to buildings. *Energy Conversion and Management*. 2019; 187:103-21.
- [2] **Liu J**, Chen X, Yang H, Li Y. Energy storage and management system design optimization for a photovoltaic integrated low-energy building. *Energy*. 2020; 190:116424.
- [3] **Liu J**, Wang M, Peng J, Chen X, Cao S, Yang H. Techno-economic design optimization of hybrid renewable energy applications for high-rise residential buildings. *Energy Conversion and Management*. 2020; 213:112868.
- [4] **Liu J**, Cao S, Chen X, Yang H, Peng J. Energy planning of renewable applications in high-rise residential buildings integrating battery and hydrogen vehicle storage. *Applied Energy*. 2021; 281:116038.
- [5] **Liu J**, Chen X, Yang H, Shan K. Hybrid renewable energy applications in zero-energy buildings and communities integrating battery and hydrogen vehicle storage. *Applied Energy*. 2021; 290:116733.
- [6] **Liu J**, Yang H, Zhou Y. Peer-to-peer energy trading of net-zero energy communities with renewable energy systems integrating hydrogen vehicle storage. *Applied Energy*. 2021; 298:117206.
- [7] **Liu J**, Yang H, Zhou Y. Peer-to-peer trading optimizations on diversified net-zero energy community integrated with energy storage of hydrogen and battery vehicles. (*Under Review of Applied Energy*)

Conference papers:

- [1] **Liu J**, Chen X, Yang H. Energy management of solar photovoltaic-battery energy systems in buildings. *18th International Conference on Sustainable Energy Technologies*. 20-22 August 2019. Kuala Lumpur, Malaysia.
- [2] **Liu J**, Chen X, Yang H. Investigation of hybrid photovoltaic-wind system with battery storage for high-rise buildings in Hong Kong. *Applied Energy Symposium: MIT A+B*. 12-14 August, 2020. Cambridge / Virtual.
- [3] **Liu J**, Yang H, Chen X, Shan K. Study on hybrid renewable energy with battery and hydrogen vehicle storage applications in a zero-energy building community in Hong Kong. *Applied Energy Symposium 2020: Low carbon cities and urban energy systems*. 10-17 October 2020. Tokyo / Virtual.
- [4] **Liu J**, Yang H. Comparison of renewable energy systems with battery vehicles and hydrogen vehicles for application in a zero-energy community in Hong Kong. *International Conference on Applied Energy 2020*. 1-10 December 2020. Bangkok / Virtual.

ACKNOWLEDGEMENTS

This thesis summarizes three years of work with valuable help and support from many people.

First and foremost, I would like to express my deepest appreciation to my chief supervisor, Prof. Yang Hongxing, for his great support on accepting me to start the PhD career, for his professional guidance on my research and kind encouragement on my life. I feel extremely grateful as one of his students for his generous and significant support during this period.

My sincere gratitude is given to my co-supervisor Dr. Cao Sunliang, for his professional guidance on learning TRNSYS simulation and conducting research. Great appreciation is also offered to Dr. Chen Xi for his valuable help and important support on my research and life.

I am also grateful for helpful support and suggestions from Prof. Lu Lin. My sincere thanks are also given to Prof. Wang Shengwei for his valuable support on the software license and data sources. And many thanks to Prof. Peng Jinqing in Hunan University and Dr. Li Yutong in Shenzhen Institute of Building Research for offering the experimental platforms. Appreciation is also given to Dr. Ma Tao in Shanghai Jiao Tong University for his continuous suggestions and help on my research. I am also grateful to Dr. Shan Kui for his kind help on data sources.

I would also thank all members in the Renewable Energy Research Group for their valuable help and kind advices on both research and life during my PhD study. The teachers and staff in the Hong Kong Polytechnic University deserve my sincere appreciation as well for their services.

Last but not least, I would like to thank my dear family and friends for their selfless support and accompany in this three years. Special thanks are expressed to my dear sister, Ms. Liu Yuan, I would never finish my PhD study without her continuous encouragement and strong help.

TABLE OF CONTENTS

CERTIFICATE OF ORIGINALITY	I
ABSTRACT	II
PUBLICATIONS DURING PHD STUDY	VII
ACKNOWLEDGEMENTS	IX
TABLE OF CONTENTS.....	X
LIST OF FIGURES	XVIII
LIST OF TABLES	XXV
NOMENCLATURE	XXVII
CHAPTER 1 INTRODUCTION.....	1
1.1 Research background	1
1.2 Global development status and prospects of renewable energy and electrical energy storage systems	4
1.2.1 Global development status and prospects of solar photovoltaic and wind power	4
1.2.2 Global development status and prospects of electrical energy storage technologies	6
1.3 Research aims and objectives.....	12
1.4 Research framework and organization.....	15
CHAPTER 2 LITERATURE REVIEW	21

2.1 Feasibility analysis of hybrid renewable energy and storage systems for a single building and communities.....	21
2.2 Design optimization of hybrid renewable energy and storage systems for a single building and communities.....	25
2.3 Peer-to-peer energy trading in communities with hybrid renewable energy and storage systems	29
2.4 Research gaps on hybrid renewable energy and storage systems for a single building and communities	33
CHAPTER 3 SYSTEM MODELING AND EVALUATION METHODOLOGY OF HYBRID RENEWABLE ENERGY AND STORAGE SYSTEMS FOR BUILDINGS.....	36
3.1 System modelling of renewable energy and storage systems for a single building and communities	37
3.1.1 Solar photovoltaic modelling.....	37
3.1.2 Wind turbine modelling.....	37
3.1.3 Stationary battery storage and battery vehicle storage modelling.....	38
3.1.4 Hydrogen vehicle storage modelling.....	39
3.1.5 Grid integration with power interaction limits and time-of-use grid penalty cost business model	40
3.1.6 Uniform and individual peer energy trading price models of hybrid renewable energy and storage systems	43

3.2 System design optimization methods, decision-making strategies and evaluation indicators	47
3.2.1 Optimization methods and decision-making strategies	47
3.2.2 Techno-economic-environmental evaluation indicators of hybrid renewable energy and storage systems	50
CHAPTER 4 EXPERIMENTAL TEST AND MODEL VALIDATION OF SOLAR PHOTOVOLTAIC AND BATTERY STORAGE SYSTEMS IN BUILDINGS.	60
4.1 Experiment design of the solar photovoltaic and battery storage system	60
4.2 Experimental results and model validation	65
CHAPTER 5 DESIGN OPTIMIZATION OF A SOLAR PHOTOVOLTAIC AND BATTERY STORAGE SYSTEM FOR A SINGLE LOW-ENERGY BUILDING	68
5.1 Framework of design optimization of the solar photovoltaic and battery storage system for the single low-energy building	68
5.2 Low-energy building with the solar photovoltaic and battery storage system in Shenzhen	70
5.3 System modelling and management of the solar photovoltaic and battery storage system	73
5.4 System design optimization of the solar photovoltaic and battery storage system	76
5.5 Techno-economic-environmental performances of the solar photovoltaic and battery storage system	82
5.5.1 Energy supply performance analysis	82
5.5.2 Battery health performance analysis	84

5.5.3 Grid relief performance analysis	85
5.5.4 System economic and environmental performances analysis	87
5.6 Post-optimization sensitivity analysis of the solar photovoltaic and battery storage system	90
5.6.1 Local sensitivity analysis.....	91
5.6.2 Global sensitivity analysis	93
5.7 Summary of design optimization of solar photovoltaic and battery storage systems for the single low-energy building.....	96
CHAPTER 6 ENERGY PLANNING OF RENEWABLE ENERGY SYSTEMS WITH BATTERY AND HYDROGEN VEHICLE STORAGE FOR A SINGLE HIGH-RISE BUILDING.....	99
6.1 Load profile of a typical high-rise residential building in Hong Kong.....	100
6.2 Development of battery storage based renewable energy systems for the high-rise building	102
6.2.1 Framework of battery storage based renewable energy systems for the high-rise building	102
6.2.2 System modelling and multi-objective optimization of battery storage based renewable energy systems for the high-rise building.....	104
6.2.3 Techno-economic feasibility results of renewable energy applications for the high-rise building.....	109

6.2.4 Summary of battery storage based renewable energy systems for the high-rise building	119
6.3 Development of battery and hydrogen vehicle storage based renewable energy systems for the high-rise building	121
6.3.1 Framework of battery and hydrogen vehicle storage based renewable energy systems for the high-rise building	121
6.3.2 System modelling of battery and hydrogen vehicle storage based renewable energy systems for the high-rise building	123
6.3.3 Design optimization of battery and hydrogen vehicle storage based renewable energy systems for the high-rise building	129
6.3.4 Techno-economic-environmental analysis of battery and hydrogen vehicle storage based renewable energy systems for the high-rise building	135
6.3.5 Summary of battery and hydrogen vehicle storage based renewable energy systems for the high-rise building	143
CHAPTER 7 SYSTEM OPTIMIZATION OF RENEWABLE ENERGY SYSTEMS WITH BATTERY AND HYDROGEN VEHICLE STORAGE FOR A NET-ZERO ENERGY COMMUNITY	146
7.1 Framework of renewable energy systems with battery and hydrogen vehicle storage for the net-zero energy community	146
7.2 Load profile of a diversified building community with three building groups	148

7.3 System modelling of renewable energy systems with battery and hydrogen vehicle storage for the net-zero energy community	150
7.4 Design optimization of renewable energy systems with battery and hydrogen vehicle storage for the net-zero energy community	155
7.4.1 Design optimization variables and objectives of the hybrid system	155
7.4.2 Design optimization results of net-zero energy buildings and community	157
7.5 Techno-economic-environmental results of renewable energy systems with battery and hydrogen vehicle storage for the community	158
7.5.1 System supply performance of net-zero energy buildings and community	158
7.5.2 Economic performance and decarbonisation potential of net-zero energy buildings and community	161
7.6 Sensitivity analysis on time-of-use grid penalty cost model.....	170
7.7 Summary of renewable energy systems with battery and hydrogen vehicle storage for the net-zero energy community.....	172
 CHAPTER 8 PEER-TO-PEER ENERGY TRADING OPTIMIZATION OF A NET-ZERO ENERGY COMMUNITY WITH RENEWABLE ENERGY SYSTEMS INTEGRATING HYDROGEN VEHICLE AND BATTERY VEHICLE STORAGE	 175
8.1 Peer-to-peer energy trading of net-zero energy communities with renewable energy systems integrating hydrogen vehicle storage.....	175

8.1.1 Framework of peer energy trading of the net-zero energy community with renewable energy and hydrogen vehicle storage systems.....	175
8.1.2 System modelling of peer energy trading of the net-zero energy community with renewable energy and hydrogen vehicle storage systems	178
8.1.3 Energy management of five net-zero energy community cases with renewable energy and hydrogen vehicle storage systems.....	181
8.1.4 Peer energy trading results of the net-zero energy community with renewable energy and hydrogen vehicle storage systems.....	191
8.1.5 Summary of peer-to-peer energy trading of the net-zero energy community with renewable energy systems integrating hydrogen vehicle storage.....	204
8.2 Peer-to-peer trading optimizations on the net-zero energy community integrated with energy storage of hydrogen and battery vehicles	206
8.2.1 Framework of peer energy trading optimizations on the net-zero energy community integrated with energy storage of hydrogen and battery vehicles	206
8.2.2 System modelling of hybrid renewable energy systems for the net-zero energy community integrated with hydrogen vehicles or battery vehicles	209
8.2.3 Peer-to-peer energy trading optimization and improved peer energy management of the net-zero energy community with both hydrogen vehicles and battery vehicles.....	212
8.2.4 Comparison results of hydrogen vehicles-integrated and battery vehicles-integrated renewable energy systems for the net-zero energy community	217

8.2.5 Multi-objective optimization results on the net-zero energy community integrated with both hydrogen vehicles and battery vehicles	225
8.2.6 Improved peer trading management results of the net-zero energy community integrated with both hydrogen vehicles and battery vehicles	229
8.2.7 Summary of peer-to-peer trading optimizations on the net-zero energy community integrated with energy storage of hydrogen and battery vehicles	233
CHAPTER 9 CONCLUSIONS AND RECOMMENDATIONS FOR FUTURE WORK	236
9.1 Summary of research findings and contributions.....	236
9.1.1 System modelling and preliminary experiments of hybrid renewable energy and storage systems.....	237
9.1.2 Design optimization of photovoltaic and battery systems for a low-energy building	238
9.1.3 Energy planning of renewable energy and hybrid storage systems for a high-rise building	239
9.1.4 System optimization of renewable energy and storage systems for a diversified net-zero energy community	240
9.1.5 Peer-to-peer energy trading optimization of a net-zero energy community with renewable energy and storage systems	241
9.2 Recommendations for future research.....	243
REFERENCES	245

LIST OF FIGURES

Fig. 1.1 Share of final energy use (left) and carbon emissions (right) in the world	2
Fig. 1.2 Share of final energy use (left) and carbon emissions (right) in Hong Kong.....	2
Fig. 1.3 Overall study framework on hybrid RE-EES systems for power supply to buildings and communities in urban areas	16
Fig. 3.1 Framework on system modelling and evaluation methodology of hybrid systems	36
Fig. 3.2 Time-of-use grid penalty cost model of renewable energy systems	42
Fig. 3.3 Uniform peer energy trading price model	44
Fig. 3.4 Individual peer energy trading price model.....	46
Fig. 4.1 Experiments on the PV-battery storage system in Hunan University (a) testing building platform (b) rooftop Poly-Si PV (c) inverter and lithium-ion battery	61
Fig. 4.2 Schematic of the grid-connected PV-battery system in the testing platform	63
Fig. 4.3 Energy management flow of the maximizing self-consumption strategy	63
Fig. 4.4 Energy management flow of the time-of-use strategy.....	64
Fig. 4.5 PV power output during six experimental days.....	64
Fig. 4.6 Power flow under the maximizing self-consumption strategy in 15th Dec.	65
Fig. 4.7 Power flow under the time-of-use strategy in 18th Dec.....	66
Fig. 5.1 Design optimization framework of the PV-battery system in the low-energy building..	69
Fig. 5.2 Low-energy building installed with the PV-battery system in Shenzhen	70

Fig. 5.3 Simulation model of the PV-battery system in TRNSYS environment	73
Fig. 5.4 Energy management strategy of the PV-battery system in the low-energy building	75
Fig. 5.5 Optimization objectives of the PV-battery system	77
Fig. 5.6 Pareto-optimal solutions of the multi-criterion optimization case	81
Fig. 5.7 Power flow in week 3 of June in Case 7 (overall optimum case)	82
Fig. 5.8 Power flow in week 3 of December in Case 7 (overall optimum case)	83
Fig. 5.9 Comparison of PV self-consumption, PV efficiency and load cover ratio	83
Fig. 5.10 Comparison of battery state of health and cycling aging	84
Fig. 5.11 Comparison of standard deviation of net grid power and exceeded load.....	85
Fig. 5.12 Annual net grid power in Case 5 (a, grid optimum) and Case 7 (b, overall optimum) .	87
Fig. 5.13 Comparison of net present value and levelized cost of energy of studied cases	88
Fig. 5.14 Comparison of carbon emissions of studied cases	90
Fig. 5.15 Local sensitivity analysis of battery number on optimization objectives.....	91
Fig. 5.16 Local sensitivity analysis of grid import limit on optimization objectives	92
Fig. 5.17 Local sensitivity analysis of grid export limit on optimization objectives	93
Fig. 5.18 Global sensitivity analysis of the optimization study on the PV-battery system	95
Fig. 6.1 Floor layout of the typical high-rise residential building	100
Fig. 6.2 Framework of renewable energy applications for the high-rise building.....	103
Fig. 6.3 Pareto frontier of technical and economic criteria in Case 4 (optimum case).....	107

Fig. 6.4 Impact of battery capacity on optimization indicators	108
Fig. 6.5 Impact of wind turbine number on optimization indicators	109
Fig. 6.6 Power flow of the PV system in the typical week (Case 1)	110
Fig. 6.7 Power flow of the PV-wind system in the typical week (Case 2)	111
Fig. 6.8 Power flow of the PV-wind-battery system in the typical week (Case 3).....	111
Fig. 6.9 Power flow of the optimum PV-wind-battery system in the typical week (Case 4)	112
Fig. 6.10 Energy flow and load matching in Case 1 (a), Case 2 (b), Case 3 (c), Case 4 (d)	115
Fig. 6.11 Annual average load cover ratio of four cases	116
Fig. 6.12 Annual average renewable energy self-consumption ratio of four cases	116
Fig. 6.13 Lifetime present value of four typical renewable application scenarios	118
Fig. 6.14 Framework of the PV-wind-battery-hydrogen system for the high-rise building	122
Fig. 6.15 Schematic of the PV-wind-battery-hydrogen system for the high-rise building	124
Fig. 6.16 Flow chart of the hybrid system under two management strategies.....	127
Fig. 6.17 Pareto optimal and final optimum results of four decision-making strategies	131
Fig. 6.18 Projection distribution of Pareto optimal and final optimum results.....	132
Fig. 6.19 Sensitivity analysis of design variables on optimization objectives.....	134
Fig. 6.20 Distribution of sizing variables of EMS 1 and EMS 2 of Pareto optimal solutions....	135
Fig. 6.21 Results of optimum solutions of four DMSs of the hybrid system	136
Fig. 6.22 Monthly energy flow and system technical performance in DMS 2 (end-user priority)	137

Fig. 6.23 Lifetime present value of four optimum cases of the hybrid system.....	139
Fig. 6.24 Impact of storage technology prices on the system net present value	140
Fig. 6.25 Impact of HV lifetime and FiT mode on the system net present value	141
Fig. 6.26 Monthly carbon emissions of four DMSs of the hybrid system.....	142
Fig. 7.1 Framework of renewable energy and storage system for the community	147
Fig. 7.2 Electrical load of campus buildings, office buildings and residential buildings	149
Fig. 7.3 Schematic of renewable energy and storage system for the community.....	150
Fig. 7.4 Energy management strategy of renewable energy system for the community	153
Fig. 7.5 Pareto optimal and final optimum solution of four net-zero energy scenarios	157
Fig. 7.6 Supply performance of net-zero energy scenarios with battery storage.....	159
Fig. 7.7 Grid penalized energy of buildings and community under three systems.....	162
Fig. 7.8 Grid integration performance of buildings and community under three systems	163
Fig. 7.9 Lifetime net present value of buildings and community under three systems	165
Fig. 7.10 Carbon emissions and equivalent carbon emission cost under three systems	168
Fig. 7.11 Impact of grid import estimation ratio and grid export estimation ratio on grid penalty cost of the community with battery storage	171
Fig. 7.12 Impact of penalty factor ratio on grid penalty cost of the community with battery	172
Fig. 8.1 Framework of peer energy trading of the net-zero energy community.....	177
Fig. 8.2 Hybrid renewable energy and HV systems for the net-zero energy community.....	179
Fig. 8.3 Schematic of energy trading in the net-zero energy community of five cases.....	180

Fig. 8.4 Energy management strategy of Case 1 (a) simplified diagram (b) renewable generation flow priority of group 1 (c) load matching flow priority of group 1	182
Fig. 8.5 Detailed energy management strategy of Case 1 (only P2G).....	182
Fig. 8.6 Energy management strategy of Case 2 and Case 3 (a) simplified diagram (b) renewable generation flow priority of group 1 (c) load matching flow priority of group 1	183
Fig. 8.7 Energy management strategy of Case 2 (P2P trading in uniform price mode)	185
Fig. 8.8 Energy management strategy of Case 3 (P2P trading in individual price mode).....	186
Fig. 8.9 Energy management strategy of Case 4 and Case 5 (a) simplified diagram (b) renewable generation flow priority of group 1 (c) load matching flow priority of group 1	189
Fig. 8.10 Annual renewable energy flow and load matching in Case 2 (P2P in uniform price)	192
Fig. 8.11 P2P trading energy and cost in Case 2 (a, P2P trading in uniform price) and Case 3 (b, P2P trading in individual price)	194
Fig. 8.12 P2P trading cost saving in Case 2 (a, P2P trading in uniform price) and Case 3 (b, P2P trading in individual price).....	196
Fig. 8.13 Renewable energy self-consumption and load coverage of five cases.....	197
Fig. 8.14 Annual energy trading of five cases	199
Fig. 8.15 Time-of-use grid penalty cost of five cases.....	200
Fig. 8.16 Annual electricity cost of five cases	201
Fig. 8.17 Annual equivalent carbon emissions of five cases	201
Fig. 8.18 Lifetime NPV of five cases in current and future cost scenarios	203

Fig. 8.19 Framework of peer trading optimizations on the net-zero energy community integrated with HVs and BVs	206
Fig. 8.20 Schematic of HV-integrated renewable energy systems with P2G (Case 1) and P2P trading (Case 3) of the diversified net-zero energy community	210
Fig. 8.21 Schematic of BV-integrated renewable energy systems with P2G (Case 2) and P2P trading (Case 4) of the diversified net-zero energy community	211
Fig. 8.22 Multi-objective optimization on renewable energy systems with both HVs and BVs	213
Fig. 8.23 Flowchart of renewable energy and vehicle systems with time-of-use P2P trading ...	215
Fig. 8.24 Flowchart of improved P2P strategy of the community with both HVs and BVs	217
Fig. 8.25 Comparison of renewable energy self-consumption of four cases with HVs or BVs.	219
Fig. 8.26 Comparison of on-site load coverage of four cases with HVs or BVs	220
Fig. 8.27 Grid integration and carbon emissions of four cases with HVs or BVs.....	221
Fig. 8.28 Annual electricity bill of four cases with HVs or BVs.....	222
Fig. 8.29 System lifetime net present value of four cases with HVs or BVs.....	223
Fig. 8.30 Pareto optimal and final optimum results of hybrid PV-wind-HV-BV systems under TOU and non-TOU management strategies.....	225
Fig. 8.31 Projection distribution of Pareto optimal and final optimum results.....	226
Fig. 8.32 Distribution of sizing vehicle numbers of Pareto optimal and final optimum solutions under TOU and non-TOU management strategies	227

Fig. 8.33 Projection distribution of sizing vehicle numbers under TOU and non-TOU strategies
..... 228

Fig. 8.34 Renewable energy consumption and load coverage of optimum and improved cases 229

Fig. 8.35 Annual grid power exchange and carbon emissions of the optimum and improved cases
..... 231

Fig. 8.36 Annual electricity bill and lifetime NPV of the optimum and improved cases..... 232

LIST OF TABLES

Table 1.1 Comparison of characteristics of electrical energy storage technologies	7
Table 2.1 Summary of feasibility studies on hybrid RE-EES systems for buildings	23
Table 2.2 Summary of optimization studies on hybrid RE-EES systems for buildings	27
Table 2.3 Summary of studies on peer-to-peer energy trading in communities.....	31
Table 3.1 Decision matrix of DMSs based on the analytical hierarchy process method.....	50
Table 4.1 Specification of the PV-battery system in the testing platform	61
Table 4.2 Battery SOC error analysis of two tested strategies	66
Table 5.1 Thermal properties of the low-energy building	71
Table 5.2 Specification of the PV-battery system in the low-energy building.....	72
Table 5.3 Parameters for economic analysis of the PV-battery system.....	78
Table 5.4 Electricity price of the utility grid in different periods	78
Table 5.5 Optimization criteria of optimization cases of PV-battery systems	79
Table 5.6 Optimization results of studied cases with PV-battery systems	80
Table 5.7 Lifetime NPV and LCOE comparison of studied cases	89
Table 6.1 Thermal properties of the typical high-rise residential building.....	100
Table 6.2 Load demand modelling results of the typical high-rise residential building.....	102
Table 6.3 Parameters of renewable energy systems for the high-rise building	104
Table 6.4 Parameters for economic assessment on renewable energy systems.....	106

Table 6.5 System sizing results of four renewable application scenarios.....	109
Table 6.6 PRV and LCOE of four typical renewable energy scenarios	118
Table 6.7 Sizing results of four decision-making strategies for the hybrid system	132
Table 6.8 Economic analysis of four optimum cases of the hybrid system.....	139
Table 7.1 Optimization variables of net-zero energy building and community systems.....	156
Table 7.2 Sizing results of renewable energy systems for four net-zero energy scenarios	158
Table 7.3 Supply performance of net-zero energy scenarios with and without battery storage .	159
Table 7.4 Grid integration improvement of net-zero energy buildings and the community	164
Table 7.5 Economic analysis of buildings and community under three systems	167
Table 7.6 Decarbonisation potential of net-zero energy buildings and the community	169
Table 8.1 Four community cases with different storage vehicles and energy trading strategies	212

NOMENCLATURE

Abbreviations

ABS	absolute value
AHP	analytical hierarchy process
BES	battery energy storage
BIPV	building-integrated photovoltaics
BV	battery vehicle
CEa	annual equivalent carbon emission
DHW	domestic hot water
DMS	decision-making strategy
DR	demand ratio
EES	electrical energy storage
EFF	application efficiency
EMS	energy management strategy
EXL	exceeded load
FAST	Fourier amplitude sensitivity test
FC	fuel cell
FiT	feed-in tariff
FSOC	fractional state of charge
HES	hydrogen energy storage
HRE	heat recovery efficiency
HSE	hydrogen system efficiency

HV	hydrogen vehicle
LCOE	levelized cost of electricity
LCR	load cover ratio
LPSP	loss of power supply probability
MDUP	minimum distance to the utopia point
MOOC	multi-objective optimization coefficient
NBa	annual net electricity bill
NGE	net grid exchange
NPV	net present value
NSGA-II	Non-dominated Sorting Genetic Algorithm-II
PC	penalty cost
PEMFC	proton exchange membrane fuel cell
PRV	present value
PV	photovoltaic
P2G	peer-to-grid
P2P	peer-to-peer
RE	renewable energy
SCR	self-consumption ratio
SDR	supply-demand ratio
SR	surplus ratio
SOC	state of charge
SOH	state of health
STD	standard deviation

TOU time-of-use
WT wind turbine

Symbols

c_{car} societal cost of carbon
 c_{ele} local electricity price
 c_{fit} feed-in tariff rate
 C_{ini} initial cost
 d annual cost degradation rate
 f_{car} local carbon intensity of electricity
 f_{mai} proportion of maintenance cost to initial cost
 i annual real discounted rate
 j a specific replacement number
 J total replacement number
 l component lifetime
 l_{res} residual lifetime of a component
 n a specific year
 N system lifetime
 δ_{PV} annual degradation rate of the photovoltaic system
 δ_{WT} annual degradation rate of the wind turbine system
 γ annual price increasing rate of electricity

CHAPTER 1 INTRODUCTION

Global efforts are observed to develop a sustainable energy framework with clean energy sources, carriers and end-users towards carbon neutrality in the near future, where renewable energy is expected to be a prominent contributor. This thesis conducts a systematic study on hybrid renewable energy and electrical energy storage systems for power supply to buildings and communities in urban areas. It mainly aims to promote and guide renewable energy applications in high-density urban cities with advantageous renewable energy resources and growing electricity demands. This chapter firstly introduces the research background, including the significance of developing renewable energy applications for carbon mitigations and energy sustainability, and the importance of integrating energy storage technologies in renewable energy systems for energy flexibility and efficiency advances. Then, the global development status and prospects of widely used renewable energy and storage technologies are introduced, including the global installation status and anticipation, cost variation and expectation, worldwide policy and finance plans. The main research aims and objectives of the present thesis are then explained, followed by the research framework and organizations.

1.1 Research background

The global energy-related CO₂ emissions grew 1.7% in 2018 to a record high of 33.1 GT due to the increasing fossil fuel consumption, and nearly two-thirds of the growth is attributed to the power sector [1]. The world is still not on track to limit global warming to well below 2°C stipulated by the Paris agreement, although the CO₂ emissions remained relatively stable in 2019 [2]. It is estimated that the building sector accounts for 30% of the global final energy use and 28% of energy-related carbon emissions in 2018 as the largest contributor, followed by the transport

sector contributing to 28% of the global final energy use and 23% of carbon emissions as per Fig. 1.1 [3]. Similar high shares of carbon emissions are also observed in the building sector (over 60%) and transport sector (16%) in high-density cities like Hong Kong, as the second largest carbon emitter in China, as shown in Fig. 1.2 [4]. Therefore, the building and transport sectors should be targeted as major sources for carbon emission mitigation efforts. About 13% of the global energy use and 50% of global carbon emissions need to be reduced in the building sector between 2018 and 2040, to achieve the sustainable development scenario expected by the International Energy Agency [5].

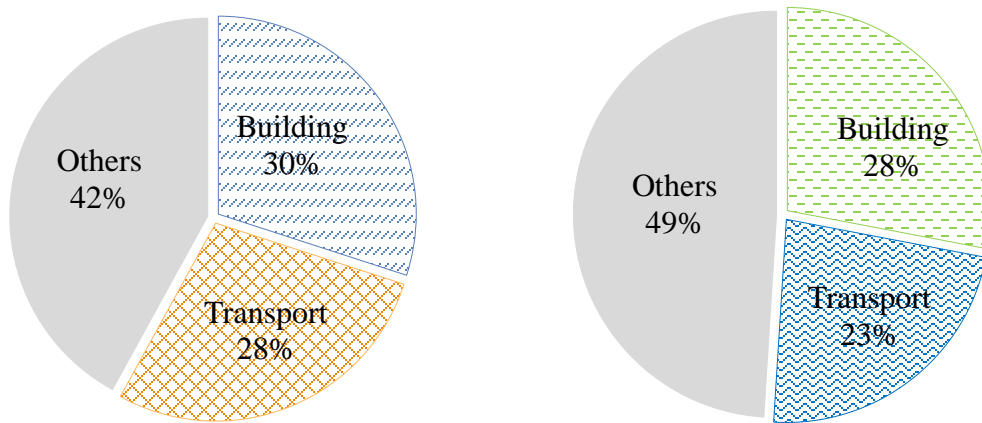


Fig. 1.1 Share of final energy use (left) and carbon emissions (right) in the world

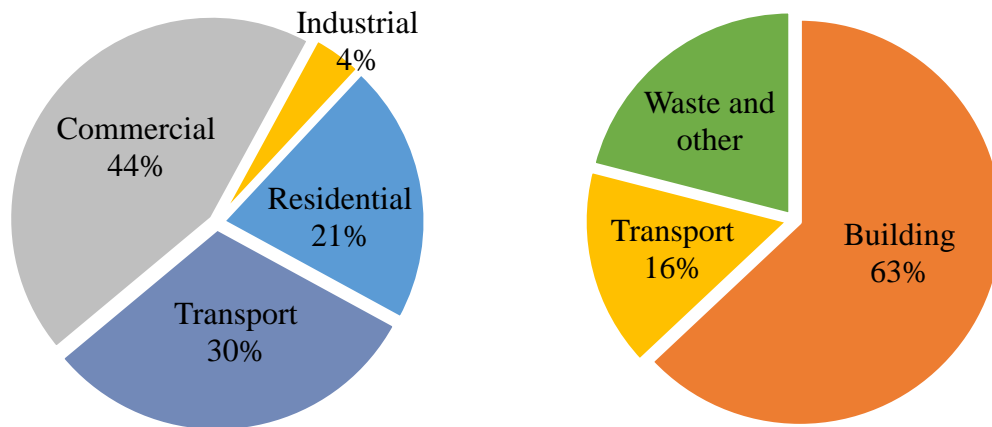


Fig. 1.2 Share of final energy use (left) and carbon emissions (right) in Hong Kong

A compound reduction rate of 3.8%/year in CO₂ emissions is anticipated to keep the expected temperature rise well below 2°C reaching 9.5 GT CO₂ by 2050. And over half of the necessary CO₂ emission reductions are expected from renewable energy, predicting to share up to 86% of total electricity generation by 2050 [6]. And 2019 saw a faster increase in renewable electricity generation than in electricity demand, with falling fossil-fuel electricity generation for the first time [7]. Renewable energy is widely adopted as a prominent solution for the building and transport sectors to provide green power to buildings and electric vehicles, given its sustainability and environmental friendliness [8]. The renewable energy accounts for about 13.6% of total final energy consumption in the building sector in 2017 as the fastest growing source, while it only contributes 3.3% of total final energy consumption in the transport sector in the same year [2]. While it is projected that all buildings must adopt renewable energy strategies by 2050 to meet net-zero energy and net-zero carbon requirements [5].

Renewable energy sources, such as solar and wind power, highly depend on weather conditions, which are intermittent, unstable and unmatched with the fluctuating building load. Electrical energy storage technologies (e.g. battery storage, hydrogen storage) are therefore required to store surplus renewable energy, to assure a reliable power supply to buildings. Energy storage can allow for flexible dispatch of renewable electricity at times of demand, and also can enable surplus or otherwise curtailed variable renewable electricity to be applied to end-uses, such as heating and cooling load, mobility and electricity generation. Therefore, it is significant to study hybrid renewable energy and electrical energy storage (RE-EES) applications for power supply to buildings and communities integrating clean transportations (e.g. battery vehicles and hydrogen vehicles), to achieve carbon neutrality in the integrated building and transport sectors within urban contexts.

1.2 Global development status and prospects of renewable energy and electrical energy storage systems

The global development status and prospects of the most widely used renewable energy technologies in buildings (i.e. solar photovoltaic (PV) and wind turbine systems) are reported, including the global installation status and anticipation, cost variation and prediction, worldwide policy and finance plans. Then, electrical energy storage (EES) technologies for renewable energy integrations are introduced, in terms of the global installation market, detailed characteristic comparison, global development of battery and hydrogen storage as the main adopted EES technologies in this study.

1.2.1 Global development status and prospects of solar photovoltaic and wind power

An accelerating development potential in renewable energy, especially solar and wind power, is observed driven by rapid cost reductions and technology advances. The global solar PV installations grew 12% in 2019, accumulating to 627 GW dominated by the Chinese market at over 200 GW [2]. It is anticipated that the total solar PV capacity would rise over thirteen-fold in 2050 to 8519 GW based on 2019, with 60% for utility scale and 40% for distributed installations [9]. Dramatic decline in the total installed cost of solar PV is observed of about 74% between 2010 and 2018 to about 1210 US\$/kW, with a competitive levelized cost of electricity (LCOE) over all fossil fuel sources, driven by lower solar module prices and ongoing reductions in balance-of-system costs. The solar PV project is expected to enjoy continuous cost reduction in next three decades to about 165 - 481 US\$/kW by 2050, with a LCOE of 0.014 - 0.05 US\$/kWh [10]. The global wind power installations expanded 19% in 2019, accumulating to about 651 GW with 621 GW onshore and the rest offshore [2]. It is predicted that the total onshore and offshore wind

installation capacity would rise to 5044 GW and 1000 GW respectively by 2050, promising to be the prominent source to generate about 35% of total electricity needs [11]. The onshore wind is one of the most competitive sources of new power generation capacity, experiencing an average installation cost reduction of 22% between 2010 and 2018 reaching 1497 US\$/kW. And it is expected to further drop to 650 - 1000 US\$/kW by 2050, with a LCOE of only 0.02 - 0.03 US\$/kWh, becoming the cheapest power source [10]. The installed cost of offshore wind systems decreased by about 5% since 2010 and would decrease greatly in the coming decades, with the shift to deeper waters and sites further from shore, reaching 1400 - 2800 US\$/kW by 2050. The offshore wind system is expected to be globally competitive with fossil fuels by 2030, with a LCOE of 0.05 - 0.09 US\$/kWh [10].

Ambitious policy and finance plans are launched globally to accelerate the clean energy transition from the fossil fuel leading market to the renewable energy leading market, to reduce carbon emissions and mitigate the climate change. Specifically, nearly 10000 cities and local governments agreed to jointly reduce carbon emissions, to achieve the Paris Agreement of limiting global warming to 1.5°C above pre-industrial levels [12]. 77 countries, ten regions and over 100 cities promised to achieve net-zero carbon emission by 2050, and increasing finance supports of US\$ 1.7B, 100M and 6M are attracted from France, Qatar and Hungary, respectively [13]. A strategic roadmap is issued to make Europe the first carbon-neutral continent by 2050 as the frontrunner in climate-friendly industries, green technologies and green financing. It is reported that up to EUR 100B is planned for most vulnerable sectors and regions, and totally EUR 260B is required to achieve the climate and energy policy targets in 2030 [14]. At least US\$ 1T will be invested to support building decarbonisation in developing countries by 2030, to meet goals of the Paris Agreement under which all buildings must be net-zero carbon by 2050. Although less than

1% of buildings meet the requirement at present [15]. Significant efforts in carbon mitigation are observed in China, as the world's biggest source of carbon emissions, achieving a carbon emission intensity reduction of 45% since 2005, and sharing a quarter of newly afforested lands globally [13]. Moreover, China provides an ambitious blueprint to reach the carbon emission peak before 2030 and achieve carbon neutrality before 2060 [16]. Globally, at least 57 carbon-pricing initiatives, including direct taxation and trading schemes, were implemented or scheduled, to reduce carbon footprints in significant sectors across 47 countries covering 20% of global greenhouse gas emissions [17].

1.2.2 Global development status and prospects of electrical energy storage technologies

Advanced electrical energy storage (EES) technology is an important contributor to promote renewable energy applications in the future energy framework to improve the energy dispatch flexibility and utilization efficiency. The EES technologies can be sorted into three categories, including mechanical, electrochemical and electric storage according to their working mechanism, all of which can play an important role in renewable energy system integrations. The mechanical storage technologies generally include the pumped hydro energy storage, flywheel energy storage, and compressed air energy storage. The electrochemical storage technologies cover the battery energy storage, electric vehicle energy storage and hydrogen energy storage [18]. And the electric storage technology here refers to the supercapacitor energy storage. The global market for all types of energy storage reached 183 GW in 2019, where the pumped hydro storage accounts for more than 86% of 158 GW [2], as the most mature EES. About 30 GWh of stationary storage and 200 GWh of mobile vehicle storage are installed globally, which would be expanded to over 9000 GWh and 14145 GWh respectively by 2050 [19].

The detailed characteristics of EES technologies are compared in Table 1.1, covering the technical, economic, environmental indicators, main advantages and disadvantages. It is shown that pumped hydro storage and compressed air storage technologies have larger storage capacity, longer life time and relatively lower capital cost than other EES technologies. The storage capacity of flywheel storage and lithium-ion battery storage technologies is smaller, while their capital cost is higher. The supercapacitor and flywheel storage technologies have superior energy efficiency with fastest response time. The hydrogen storage technology has the lowest energy storage efficiency but its capital cost is favorable. The lifetime of mechanical and electric storage technologies is generally longer than electrochemical storage technologies. The environmental impact of flywheel and lithium-ion battery storage technologies is the lowest.

Table 1.1 Comparison of characteristics of electrical energy storage technologies

EES technology	Capacity [20] (MW)	Efficiency [20] (%)	Capital cost [20] (\$/kWh)	Life time [20] (years)	Life time (cycles)	Response time [20]	Environmental impact [21]	Advantages [22]	Disadvantages [22]
Pumped hydro	100-5000	75-85	5-100	40-60	10000-30000 [23]	fast (ms)	high	mature technology high energy capacity high power capacity flexible response low cost and long life	site limitation high environmental impact long construction time
Flywheel	0.25	93-95	1000-5000 [24]	20+ [24]	20000+ [25]	very fast	no	high power density fast response low environmental impact	low energy density space requirement high standing losses [26]
Compressed air	3-400	50-89	2-100	20-60	8000-12000 [23]	fast	high	long duration low capital cost low environmental impact	site limitation need gas fuel input long construction time

EES technology	Capacity [20] (MW)	Efficiency [20] (%)	Capital cost [20] (\$/kWh)	Life time [20] (years)	Life time (cycles)	Response time [20]	Environmental impact [21]	Advantages [22]	Disadvantages [22]
Lithium-ion battery	0.1	75-97 [27]	1000-2000 [28]	5-30 [27] 5-15 [25]	1500+[22], 1000-10000 [29]	fast	very low	long cycle life high efficiency high depth of discharge [28]	higher initial cost less recyclability [28]
Lead-acid battery	0-40	70-90 [30], 65-80 [29]	300-600 [30], 150-500 [29]	3-15 [27] 5-15 [25]	500-1000 [30], 200-1800 [29]	fast	medium	mature technology relatively cheap readily recyclable [28]	limited depth of discharge require regular checks [28] require venting
Hydrogen	0-50	20-50	10-20	5-15	1000+ [25]	good (<1s)	low	high energy density	high initial cost low efficiency
Super-capacitor	0.3	90-95	2000	20+	100000+ [24]	very fast	low	high power density long cycle life high efficiency	short term power high initial cost low energy density

Battery and hydrogen energy storage in both stationary storage and mobile vehicle forms are widely applied in renewable energy integrations for building power supply, given their applicable storage capacity, fast response and carbon-free characteristics. The detailed global application status and future prospects of these two typical energy storage technologies are explicated as below, as the main utilized energy storage technologies in this thesis.

(1) Battery energy storage

Battery technology has been widely adopted for renewable electricity storage in buildings, given its fast response, high efficiency and low environmental impact. The accumulated global battery storage capacity, excluding small-scale installations, reached over 3 GW in early 2019 [31]. The top installation markets for battery storage in 2019 are found in Korea, China, the U.S. and Germany, where the U.S. experienced a record high for new additions of 523 MW [32]. And the

Chinese battery market saw about 520 MW of new installations in the same year [2]. Germany was the leading European market for residential battery storage in 2019 with 369 MWh [33]. The renewables-plus-storage is emerged as a major driver of battery market growth in recent years, with rising coupled solar PV/wind and battery storage projects in the U.S., Australia, China and the U.K. The U.S. is a leading market for the stand-alone utility-scale battery storage planning for renewable energy integration and demand response maintenance. The solar-plus-storage for residential installations in the U.S. doubled between 2017 and 2019, and a 20 MW storage system aggregated from around 5000 households is approved for connecting to the utility grid for the first time [34]. A home battery scheme in South Australia is launched to secure 5500 installations of about 62 MWh by 2020. Australia is a leading market of residential battery capacity with an addition of 233 MWh of new home batteries in 2019 with an accumulation of up to 1 GWh. About 143 MWh of grid-scale battery capacity is installed at the same time, more than double the amount in 2018 [35].

The lithium-ion battery experienced an 85% reduction in the average cost between 2010 and 2018 [36] and a 50% reduction in LCOE between 2018 and early 2020 [37]. The integration of lithium-ion battery and renewable energy sources has become competitive with traditional fossil fuel sources in providing flexible power. The global manufacturing capacity of lithium-ion batteries expanded from 14 GWh in 2010 [36] to 316 GWh in early 2019, where China taking over 86%, followed by Australia, India, South Africa and the U.S. [38]. Increasing amounts of investment are attracted globally for battery storage, with up to US\$ 1.36B from venture capital firms [39]. The declining cost of lithium-ion batteries contributes to the increasing competitiveness of battery vehicles (BVs), compared with traditional fossil fuel-based vehicles. 46 countries set renewable transport targets and over 18 jurisdictions issued 100% electric vehicle targets or

targeted bans on internal combustion engine vehicles by the end of 2019 [2]. The global electrical vehicle continues to grow quickly in 2019, with a total stock reaching 259M with majority for two- and three-wheelers, followed by around 7.2M of electric cars, 0.5M of electric buses and 0.4M of light commercial vehicles. The electric cars increased by 40% in 2019 with over 2M additions from 2018, where majority of the global stock is sold in China (47%), followed by Europe (25%) and the U.S. (20%). About 2M electric vehicle charging points (both private and public, fast and slow chargers) were installed in 2019 globally, accumulating to a total stock of up to 7.5M [40].

(2) Hydrogen energy storage

Renewable hydrogen is experiencing an unprecedented momentum as a clean energy carrier available for a variety of sectors, such as transport, heating and industrial raw materials. It is promising to shape a sustainable energy future, when renewable power generation becomes sufficiently cheap and widespread to create low-carbon hydrogen. The lower heating value of hydrogen is about 120 MJ/kg (3 times of gasoline), which makes it an attractive transport fuel. But hydrogen needs to be compressed or liquefied, as the energy intensity of hydrogen is relatively low at 0.01 MJ/L (1/3 of natural gas) [41]. The compressed hydrogen storage is the most economic storage option at the discharge duration longer than 20 - 45 hours in terms of the cost of storage electricity [41]. It is estimated that about 160 Mt of renewable hydrogen could be produced annually by 2050 rising from 1.2 Mt in 2018, and the production cost is expected to be decreased from 4.0 - 8.0 US\$/kg to 0.9 - 2.0 US\$/kg [6]. The installation capacity of electrolyzers would also rise from 0.04 GW in 2016 to 1700 GW in 2050 to support the large-scale development of renewable hydrogen [6]. The alkaline electrolyzer has been used since the 1920s, as a commercial and mature technology with a relatively low initial cost (500 - 1400 US\$/kW), compared with other electrolyzers, such as the proton exchange membrane electrolyzer (1100 - 1800 US\$/kW)

and solid oxide electrolyzer (2800 - 5600 US\$/kW) [42]. The electrical efficiency of alkaline electrolyzer at the lower heating value is about 63% - 70% depending on the technology performance and supply power, and it is projected to be increased to 70% - 80% in the long-term development. The hydrogen fuel cell costs 1600 US\$/kW for a 1 MW proton exchange membrane fuel cell unit with an electrical efficiency of 50% - 60%, and it is predicted to be reduced to about 425 US\$/kW by 2030 [43].

Recently, hydrogen vehicles (HVs) have experienced an unprecedented development as a promising alternative for the clean energy solution. Over 12900 fuel cell electric cars are registered worldwide by the end of 2018 with an 80% increment in the year, although still small compared with the accumulated 5.1M BVs. Nearly half of HVs are sold in the U.S., followed by 23% in Japan and 14% in China, while most HVs are manufactured by Toyota, Honda and Hyundai. There are 376 publicly available hydrogen refueling stations with 100 in Japan, followed by 60 in Germany and 44 in the U.S. [44], but the number is still small compared with the 5.2M charging points (90% private chargers) for BVs by the end of 2018 [45]. HVs can be refueled in 3 - 5 minutes, much shorter than that of BVs (can be 3 - 6 hours), and fuel cells could have a lower material footprint than lithium batteries. The cruise range of HVs can be over 400 km, longer than that of BVs with a global average around 250 km [41].

A promising global development of HVs is anticipated in the near future to achieve a low-carbon transport sector. The Korean government aims to achieve 6.2M HVs and 1200 refueling stations by 2040, and make hydrogen economy a driving force of innovation growth [46]. About 20000 - 50000 HVs and 400 - 1000 refueling stations are projected in France by 2028, and 1000 refueling stations will be constructed in Germany [44]. Up to 1M fuel cell electric vehicles and 1000 hydrogen refueling stations will be developed by 2030 in China, to launch the hydrogen

transport in ten cities following existing BVs [47]. A similar plan is outlined to encourage the development of low-carbon hydrogen in California [48]. Japan also planned to have 0.2M HVs and 320 refueling stations by 2025, with accumulated HVs of 0.8M by 2030 [49]. Hydrogen Council anticipates more than 400M hydrogen cars, 15 - 20M hydrogen trucks and 5M hydrogen buses all over the world by 2050 [50].

1.3 Research aims and objectives

This thesis aims to study hybrid renewable energy and electrical energy storage systems for power supply to both a single building and communities in urban regions for achieving carbon neutrality in the near future. Applications of typical electrical energy storage technologies are investigated, including stationary battery storage, mobile battery vehicle storage, mobile hydrogen vehicle storage and their hybrids, by practical experiments, transient system simulations (TRNSYS), coupled multi-objective optimizations (jEplus+EA), techno-economic-environmental assessments and sensitivity analyses. The main research aims and objectives of the present thesis are summarized as follows:

(1) To develop novel energy management strategies, flexible grid integration models, robust system planning optimization approaches, systematic peer-to-peer energy trading management and optimization platforms of hybrid renewable energy and storage systems for applications in the integrated building and transport sectors for achieving carbon neutrality in Hong Kong and similar high-density urban regions.

(2) To develop robust energy planning and optimization approaches for hybrid renewable energy systems integrated with stationary battery and mobile hydrogen vehicle storage, for a typical high-rise residential building in Hong Kong, considering different vehicle-to-building

schedules. Two energy management strategies with different priorities of battery and hydrogen storage operations are proposed. The optimal system size configurations and optimal energy management strategy solutions of key stakeholders with different preferences (i.e. end-user, transmission system operator and investor) are determined, with multi-objective optimizations and decision-making strategies based on the minimum distance to the utopia point and analytical hierarchy process methods.

(3) To propose novel time-of-use grid penalty cost business models for hybrid renewable energy and storage systems to improve the power flexibility and economy between net-zero energy community systems and the utility grid. The net-zero energy building and net-zero energy community simulation models with hybrid renewable energy systems integrated with stationary batteries and hydrogen vehicle groups are developed, subject to multi-objective optimizations considering renewable self-consumption, on-site load coverage and grid penalty cost. And the actual annual energy use data and simulations on the university campus, commercial office and high-rise residential building groups in Hong Kong are adopted for the system techno-economic-environmental feasibility analysis.

(4) To develop novel dynamic peer-to-peer energy trading optimization platforms for a diversified net-zero energy community with hybrid renewable energy and green vehicle (i.e. battery vehicle, hydrogen vehicle) storage systems, by proposing innovative peer-to-peer energy trading price models and time-of-use peer energy trading management and optimization strategies, for high system economy and grid flexibility. The detailed techno-economic-environmental superiority of peer-to-peer energy trading cases are demonstrated in comparison with baseline peer-to-grid energy trading cases, for both battery vehicle-integrated renewable energy systems and hydrogen vehicle-integrated renewable energy systems.

(5) To develop effective design optimization approaches to improve the techno-economic-environmental performances of a photovoltaic-battery storage system in a practical low-energy building in an urban city (Shenzhen), by proposing novel energy management strategies considering battery cycling aging, grid relief and time-of-use pricing. The optimal system configurations and grid operations from perspectives of the energy supply, battery storage, utility grid and whole system are provided, based on the coupled dynamic simulations and single-criterion/multi-criterion optimizations.

(6) To propose improved technical and economic evaluation criteria for hybrid renewable energy and storage systems as the optimization objectives to achieve optimum solutions for typical applications in a standard high-rise residential building in a high-density urban city (Hong Kong). A technical system evaluation criterion is developed integrating the energy supply, battery storage, building demand and grid relief indicators. And the system levelized cost of energy is improved considering detailed renewable energy benefits, including the feed-in tariff, transmission loss saving, network expansion saving, and carbon reduction benefits. The detailed technical and economic feasibility of typical renewable energy system applications is analyzed and compared, including photovoltaic systems, hybrid photovoltaic-wind systems and hybrid photovoltaic-wind-battery systems.

(7) To conduct experiments on a test building platform with an actual photovoltaic-battery storage system to study the system performance under typical energy management strategies (e.g. maximizing self-consumption strategy, time-of-use strategy). The experimental results are then used to validate the energy balance based battery and energy management models in transient system simulations.

This comprehensive study on hybrid renewable energy and storage systems for applications in both a single building and large-scale building communities in urban areas, can help researchers and policy makers to evaluate the system technical, economic and environmental feasibility, regarding the energy demand, energy supply, energy storage, energy management and grid integration aspects. The systematic research methodology and framework on the hybrid renewable energy and storage systems, involving the building and transport sectors, can provide significant guidance for relative stakeholders to develop renewable energy applications and accelerate the progress towards carbon neutrality within urban contexts.

1.4 Research framework and organization

Succeeding to the above introduction on the research background and global development status of hybrid RE-EES systems, **Chapter 2** presents a detailed literature review on hybrid RE-EES systems covering the techno-economic-environmental feasibility research, design optimization study, and peer-to-peer energy trading analysis. And the specific research gaps are identified.

The overall framework of the main context of this thesis (Chapters 3 - 8) on hybrid RE-EES systems for power supply to buildings and communities in urban areas is shown in Fig. 1.3. It includes three main parts, i.e. system models and preliminary experiments (Chapters 3 - 4), hybrid RE-EES systems for a single building (Chapters 5 - 6), and hybrid RE-EES systems for building communities (Chapters 7 - 8).

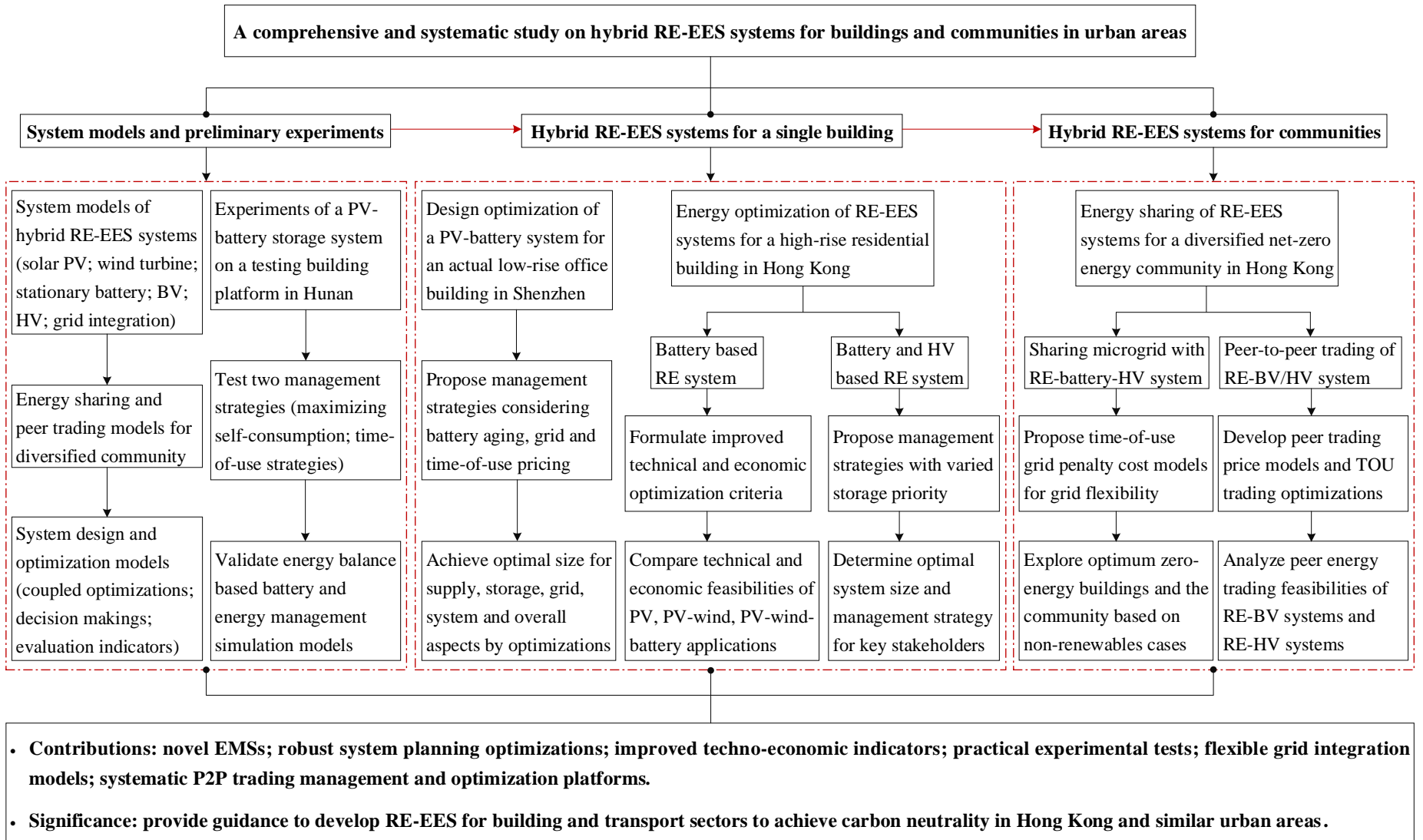


Fig. 1.3 Overall study framework on hybrid RE-EES systems for power supply to buildings and communities in urban areas

Specifically, **Chapter 3** firstly introduces the system modelling of main components of hybrid RE-EES systems, including energy supply (solar PV system, wind turbine system), energy storage (stationary battery storage, battery vehicle, hydrogen vehicle), grid integration (power interaction limits, time-of-use grid penalty cost business model), and peer-to-peer trading price models (uniform and individual price models). The energy demand and energy management aspects are also studied, which are varied with specific cases as explained in each chapter. This chapter also explains the system design optimization methods, based on the Non-dominated Sorting Genetic Algorithm-II with the coupled TRNSYS and jEPlus+EA platform. Various decision-making strategies are also adopted to determine the final optimum solution out of the obtained Pareto optimal set of multi-objective optimizations, including the weighted sum method, minimum distance to the utopia point method and analytical hierarchy process method. And key assessment indicators are formulated to evaluate the technical (supply, energy storage, grid integration), economic (lifetime net present value, improved LCOE) and environmental (annual equivalent carbon emissions and corresponding costs) performances of hybrid RE-EES systems.

Chapter 4 presents the preliminary experiments on a practical PV-battery storage system based on a testing building platform in Hunan University. Two basic energy management strategies (i.e. maximizing self-consumption strategy and time-of-use strategy) are developed and realized in the testing platform to control the system operation and compare the system performances. The tested PV-battery system models are also established in the TRNSYS environment to validate the battery and energy management strategy models based on the energy balance mechanism.

Following the experimental study on the PV-battery system in Chapter 4, **Chapter 5** studies the design optimization of an actual PV-battery system installed in a low-energy office building in

Shenzhen to improve the system performances. A novel energy management strategy considering the battery cycling aging, grid relief and local time-of-use pricing is proposed. Single-criterion optimizations with the weighted sum method are performed, focusing on four major aspects of the PV-battery system including the energy supply, battery storage, utility grid and whole system. Meanwhile, the multi-criterion optimization is performed with the minimum distance to the utopia point method, focusing on the overall performance of above four aspects for a comprehensive technical, economic and environmental evaluation. Moreover, both local sensitivity analyses based on the optimal solution and global sensitivity analyses with the Fourier Amplitude Sensitivity Test are conducted to further quantify the significance and impact of selected design parameters.

In addition to study RE-EES system applications in the low-rise office building in Chapter 5, **Chapter 6** investigates the energy planning approaches of hybrid RE-EES systems for a single high-rise residential building in Hong Kong, including battery storage based RE systems and hybrid battery and HV based RE systems. For the battery storage based RE systems, typical renewable application scenarios (PV, PV-wind, PV-wind-battery) are investigated through coupled modelling and optimizations with TRNSYS and jEPlus+EA. A comprehensive technical optimization criterion is developed integrating the energy supply, battery storage, building demand and grid relief indicators, and the LCOE considering detailed renewable energy benefits is formulated including the feed-in tariff, transmission loss saving, network expansion saving and carbon reduction benefits. While for the hybrid battery and HV based RE systems, two energy management strategies are developed with different operation priorities of the battery and hydrogen storage. Multi-objective optimizations are conducted to select the optimum management strategy and configuration of the hybrid PV-wind-battery-hydrogen system. Techno-economic

indicators are developed for the multi-objective optimizations, and four decision-making strategies are applied to search the final optimum solution for major stakeholders with different preferences.

Following the research on hybrid RE-EES systems for the single building, **Chapter 7** further studies the design optimization of hybrid renewable energy systems integrated with stationary battery and mobile HV storage for a diversified net-zero energy community, consisting of university campus, commercial office and high-rise residential buildings based on practical energy use data and simulations. A time-of-use grid penalty cost model, evaluating grid import and export during on-peak and off-peak periods, is proposed to achieve the power grid flexibility and economy. Multi-objective optimizations are conducted to size net-zero energy buildings and the net-zero energy community, considering the renewable energy self-consumption, on-site load coverage and grid penalty cost.

Furthermore, **Chapter 8** explores the peer-to-peer energy trading management and optimization of the diversified net-zero energy community with hybrid renewable energy systems integrated with BV and HV storages. An individual peer trading price model is proposed for the diversified community, consisting of building groups with different energy distributions and grid pricing schemes. The time-of-use peer trading management strategies are developed for both uniform and individual trading price modes, to improve the power flexibility and economy of the utility grid. Typical net-zero energy community models are developed and compared with different energy storage vehicle types (HV/BV) and energy trading modes (peer-to-grid/peer-to-peer). Multi-objective peer-to-peer trading optimizations of the net-zero energy community integrated with both HVs and BVs are conducted to find optimal configurations of vehicle numbers and time-of-use management operations. An improved peer-to-peer trading management strategy is further

proposed considering the peer trading priority and complementary operations of hybrid vehicle storages, to enhance the grid integration, decarbonisation and economy.

Finally, **Chapter 9** concludes the key findings and contributions of the present thesis, and provides recommendations for future work.

In all, this thesis conducts a comprehensive and systematic study on hybrid RE-EES systems by conducting practical experimental tests, proposing novel energy management strategies, formulating improved technical and economic assessment indicators, developing robust system planning and optimization approaches, establishing flexible grid integration models, and developing systematic peer-to-peer energy trading management and optimization platforms. This thesis makes significant contributions on helping researchers and policy makers to design and evaluate hybrid RE-EES systems for both a single building and communities. And it provides major stakeholders with clear guidance to develop renewable energy applications towards carbon neutrality of integrated building and transport sectors within urban contexts.

CHAPTER 2 LITERATURE REVIEW

This chapter conducts a detailed literature review on hybrid renewable energy and storage systems for power supply to both a single building and communities, including the techno-economic-environmental feasibility research, system design optimization research, and peer-to-peer energy trading research. Research gaps on hybrid renewable energy and storage system applications are identified based on the summary table on each aspect.

2.1 Feasibility analysis of hybrid renewable energy and storage systems for a single building and communities

The techno-economic-environmental feasibility of employing hybrid renewable energy and electrical energy storage (RE-EES) systems for power supply to both a single building and building communities has been widely investigated in the academia. On the one hand, the system feasibility for single building applications has been explored based on case studies and parametric analyses. For example, a standalone plug-in hybrid electric vehicle charging station powered by solar photovoltaic (PV) and wind energy with fuel cells is tested. The research results show that the lifetime and cost of the fuel cell system are more favorable than that of the battery system [51]. A demonstration project with the solar PV and fuel cell electric vehicle in a residential building was set up in the Netherlands to study the net-zero energy and vehicle-to-grid operations. It is found that the annual grid imported electricity can be reduced by 71% with the integration of the fuel cell vehicle [52]. The technical and economic performances of a PV-wind system with vehicle integrated hydrogen storage are analyzed for a zero-emission single family house in Finland, considering the system net present value and operational carbon emissions [53]. The vehicle integrated hydrogen storage and battery storage are designed for solar and wind systems in a

practical office center of the Netherlands. This study validated the feasibility of using electric vehicles as the power backup, as well as the flexibility and cost-effectiveness of fuel cell vehicles over battery vehicles [54]. The impact of vehicle-to-building interactions and vehicle charging strategies on the performance of zero-emission office buildings is analyzed. The author reports that the matching capability and building-vehicle interactions can be significantly improved by expanding the vehicle charging boundary to remote parking sites [55].

Additionally, many types of RE-EES systems have been developed to achieve sustainable power supply to building communities for technical [56], economic [57-59] and environmental [60, 61] feasibility studies. The efficiency and economic feasibility of using renewable hydrogen and biogas is analyzed for the power and fuel supply to a 10000 resident community in California. It is shown that 80% of net-zero community electricity can be fulfilled by renewable energy. The authors also report that electrolysis and solid oxide fuel cell technologies can be economically competitive with the natural gas and utility grid for community-scale energy systems in the next one or two decades [56]. A local renewable energy community is studied by developing poly-generation, electric and hydrogen storage systems for the optimal total life cycle cost. The results indicate that the battery storage with a high roundtrip efficiency of 90% is more effective than the power-to-gas hydrogen storage with an efficiency of 23%, while the battery storage alone is not economical for community renewable energy systems [57]. Novel business models are proposed for renewable community microgrids, considering the optimal sizing and energy management of the renewable energy system by minimizing the customer electricity cost. Case studies are conducted for seventeen locations in Chile with varied renewable resources and electricity tariffs, showing that community microgrids are generally more profitable than single-dwellings [58]. A 100% renewable energy network model is proposed for electrified and hydrogen cities by

optimizing the total annual cost. Case studies in Korean rural and urban communities indicate that the energy carrier and energy demand structure are significant factors for the system configuration and economy [59]. The stochastic operation of multiple distributed energy systems with renewable energy is studied through a Markovian process, by minimizing the expected net energy and carbon emission cost in a local energy community [60]. The power generation planning of isolated microgrids with diesel and renewable energy sources is presented, considering the integration of electric vehicles and cooking systems. The economic and environmental benefits of the renewable energy system for a remote community in Ecuador are demonstrated based on the HOMER analysis [61].

Table 2.1 Summary of feasibility studies on hybrid RE-EES systems for buildings

Hybrid system	Software	Application site	Important findings	Reference
Feasibility analysis of hybrid RE-EES systems for a single building				
PV-wind-stationary hydrogen	--	A standalone hybrid vehicle charging station	Lifetime and cost of fuel cell systems are more favorable than battery systems	Fathabadi. 2020 [51]
PV-mobile hydrogen vehicle	MATLAB	Vehicle-to-grid, the Netherlands	Annual grid imported electricity can be reduced by 71% using fuel cell vehicle	Robledo et al. 2018 [52]
PV-wind-mobile hydrogen vehicle	TRNSYS	An on-grid single family house, Finland	Techno-economic feasibility of using HV in a net-zero energy building is explained	Cao et al. 2018 [53]
PV-wind-mobile hydrogen vehicle	MATLAB	An on-grid office center, the Netherlands	Fuel cell vehicles are more economic and flexible than battery vehicles	Farahani et al. 2020 [54]
PV-wind-mobile battery vehicle	TRNSYS	An on-grid office building, Hong Kong	Matching capability and building-vehicle interactions are improved by expanding the mobile boundary	Cao 2019 [55]

Hybrid system	Software	Application site	Important findings	Reference
Feasibility analysis of hybrid RE-EES systems for building communities				
PV-hydrogen	AFLEET	A 10000 resident community, California	80% of net-zero community electricity can be fulfilled by renewable energy	Silverman et al. 2020 [56]
PV-battery-hydrogen	Calliope	A 1000 households community, Texas	Battery storage with a high roundtrip efficiency of 90% is more effective than power-to-gas hydrogen storage with an efficiency of 23%	Bartolini et al. 2020 [57]
PV-wind-battery	MATLAB	Seventeen diverse locations, Chile	Community microgrids are generally more profitable than single-dwellings	Avilés et al. 2019 [58]
PV-wind-battery-hydrogen	CPLEX	Rural and urban communities, Korea	Energy carrier and energy demand structure are significant factors for the system configuration and economy	You et al. 2020 [59]
PV-battery	CPLEX	Local energy communities, U.S.	Potential benefits can be achieved for the community through optimal management of local energy resources	Yan et al. 2020 [60]
PV-wind-mobile battery vehicle	HOMER	An island community microgrid, Ecuador	Economic and environmental benefits can be obtained integrating renewables and electric vehicles in island microgrids	Clairand et al. 2019 [61]

These studies on the techno-economic-environmental feasibility of hybrid RE-EES systems for power supply to a single building and communities are summarized in Table 2.1. It can be identified that most existing feasibility studies on hybrid renewable energy systems integrated with HV storage are limited to single building applications, and few of them consider different cruise schedules of HV groups. And the community-scale renewable energy and storage systems are

rarely integrated with HV groups following different schedules as both commuting tools and shared storage technologies, as most existing feasibility studies for building community applications are limited to stationary hydrogen storage. Furthermore, the economic performance and decarbonisation potential of hybrid RE-EES systems are seldom clarified for the net-zero energy single building and net-zero energy communities integrated with green vehicles.

2.2 Design optimization of hybrid renewable energy and storage systems for a single building and communities

Recently, a large number of studies have been conducted on the design optimization of RE-EES systems for power supply to a single building and communities in both urban and remote regions. In terms of the single building applications in urban areas, the grid-connected PV-wind systems with and without battery storage are studied for power supply to a residential building in an Italian city with TRNSYS 17. The Pareto-front and energy reliability-constrained methods are used to achieve the optimum energy reliability of the renewable energy system [62]. The lifecycle cost and carbon emissions of a one-floor building in The Bahamas are investigated, by optimizing the building envelope and energy supply from the PV-battery system. In this study, the Percentage of Persons Dissatisfied of building occupants is treated as a constraint in the optimization process with the co-simulation and optimization platform of EnergyPlus and jEPlus+EA. It clarifies the feasibility of developing renewable energy systems for residential buildings in The Bahamas [63]. The PV system is also developed as one of the energy retrofit measures to achieve the optimal performance on the energy demand, cost and carbon emissions for a low-density residential building located in 19 selected European cities. The Active Archive Non-dominated Sorting Genetic Algorithm (aNSGA-II type) is adopted to realize the optimization process in the joint

simulation and optimization environment of EnergyPlus and Python. This study concludes that the application of solar energy is the most convenient solution for building retrofitting [64].

In addition to applying RE-EES systems to a single building, urban community application optimizations are also studied by researchers. The building envelope and renewable supply systems of a residential complex with five buildings in Italy are optimized to minimize the global cost and air-conditioning load [65]. Waibel et al. investigated the influence of building geometry on the cost and carbon emissions for four office blocks with PV-battery systems in Switzerland [66]. A hybrid PV-wind-battery system is developed for a municipality building with six blocks in Portugal, by optimizing the total cost of energy considering various feed-in tariff schemes. It is indicated that the developed mixed integer linear programming is feasible for evaluating renewable energy systems in zero energy buildings [67]. A systematic and integrative decision-making method is also presented to find the cost-optimal solution for a microgrid PV-wind-battery-fuel cell-diesel system installed in an urban community of Egypt [68].

Furthermore, optimization work is also conducted on RE-EES systems for buildings and communities in remote area without grid power access. An off-grid PV-wind-battery system is optimized to achieve the minimum total present cost and loss of power supply probability (LPSP) for a house in Tehran. The study adopts the genetic algorithm with particle swarm optimization (GA-PSO) and multi-objective particle swarm optimization (MOPSO) methods to achieve an optimum LCOE of 0.508 US\$/kWh [69]. An improved crow search algorithm (CSA) is proposed to size an off-grid PV-diesel-FC system, to achieve the minimum total net present cost with the LPSP and renewable energy portion as constraints. It indicates that the hybrid system is reliable and economic to meet the electrical load of a remote building in Kerman [70]. The PV-wind-battery system for a remote island with ten houses is sized with a novel mathematical model,

introducing a saturation factor of each renewable energy resource. This study shows that a 2 kW wind turbine is the most cost-effective installation for the island, and the wind-alone system performs better than the solar-alone system [71]. An off-grid PV system coupled with the hydrogen storage and retired electric vehicle (EV) is developed for power supply to a small neighborhood of ten houses in China on the HOMER platform. It is found that the Non-dominated Sorting Genetic Algorithm-II method is superior to the multi-objective evolutionary algorithm based on decomposition (MOEA/D), for minimizing the loss of power supply, economic cost and potential energy waste [72].

Table 2.2 Summary of optimization studies on hybrid RE-EES systems for buildings

Renewable system	Application site	Optimization method	Simulation platform	Optimization objective	Reference
On-grid PV-wind-battery	An urban residential building, Italy	Pareto-front method, energy reliability-constrained method	TRNSYS	Energy reliability	Mazzeo et al. 2018 [62]
On-grid PV-battery	A one-floor home, The Bahamas	NSGA-II	EnergyPlus, jEPlus+EA	Lifecycle cost, carbon emission	Bingham et al. 2019 [63]
On-grid PV	A residential building, 19 Europe cities	aNSGA-II type	EnergyPlus, Python	Demand, costs, carbon emission	Salata et al. 2020 [64]
On-grid PV	Residential complex (five buildings), Italy	PSO	TRNSYS, GenOpt	Global cost, heating/cooling demand	Ferrara et al. 2019 [65]

Renewable system	Application site	Optimization method	Simulation platform	Optimization objective	Reference
On-grid PV-battery	Four office buildings, Switzerland	Radial basis function optimization	EnergyPlus, Rhinoceros 3D, Grasshopper	Operational cost, carbon emission	Waibel et al. 2019 [66]
On-grid PV-wind-battery	Six building blocks, Portugal	Mixed integer linear programming model	General Algebraic Modeling System	Total economic cost	Rosa et al. 2018 [67]
Microgrid PV-wind-battery-FC-diesel	Urban community, Egypt	Systematic and integrative decision-making method	HOMER Pro	Total net present cost	Elkadeem et al. 2020 [68]
Off-grid PV-wind-battery	A house in Tehran, Iran	GAPSO	HOMER	Total present cost, LPSP	Ghorbani et al. 2018 [69]
Off-grid PV-diesel-FC	A remote building in Kerman, Iran	Crow search algorithm	MATLAB	Total net present cost	Ghaffari, Askarzadeh. 2020 [70]
Off-grid PV-wind-battery	Ten-house remote island, China	Mathematical model	MATLAB	Net present cost, simple payback time, LPSP	Ma et al. [71]
Off-grid PV-FC-EV	Ten-house neighborhood, China	NSGA-II, MOEA/D	HOMER	Loss of power supply, cost, energy waste	Huang et al. 2019 [72]

These studies on design optimization on hybrid RE-EES systems for a single building and communities in urban and rural areas are summarized in Table 2.2 indicating detailed optimization methods and objectives. It is found that the system cost is a primary objective adopted by many researchers, and the energy reliability of renewable supply systems is also widely concerned. The

environmental impact, as evaluated by carbon emissions, has attracted increasing attention given the contribution of renewable energy to the sustainable energy development as a promising alternative fuel.

2.3 Peer-to-peer energy trading in communities with hybrid renewable energy and storage systems

The peer-to-peer (P2P) energy trading in communities with hybrid RE-EES systems has aroused increasing attention in recent years to accelerate distributed renewable energy developments, especially in regions with large-scale household PV and battery storage applications such as Australia, Germany, America and England. The cost optimization, participant motivation and system improvement are widely investigated by researchers on the P2P trading management in renewable energy communities.

Much attention from researchers is paid on the cost saving potential in renewable community with P2P trading studied by various optimization models [73-77]. Specifically, the total cost of a community with 68 homes installed with rooftop PV systems in Portugal is optimized, by adopting the mixed integer liner programming model. The study results show that 28% and 55% of economic savings can be achieved for consumers and prosumers, respectively [73]. The similar optimization model is also adopted to study the P2P trading cost saving potential of a 500 households community with rooftop PV and private battery storage systems in Australia. The authors reported that a maximum of 28% cost saving can be obtained by households with large PV-battery installations on weekdays [74]. However, the cost saving is not always in a linear increase with the renewable energy and storage penetration rate, where a saturation point is observed by a case study of a 40 smart homes community with PV and private battery storage

systems in Canada [75]. A two-stage aggregated control method is developed to optimize the P2P energy trading in a community with 100 homes installed with PV and private battery storage in the U.K. The results indicate that a 30% reduction in the energy bill can be achieved, together with improvements on the PV self-consumption by 10% - 30% and self-sufficiency by about 20% [76]. And a bi-level optimization model is also proposed to manage the peer and storage revenue for a 10-home community with rooftop PV and central battery storage units in Australia. It is shown that the grid pricing scheme is an important factor affecting the peer sharing revenue in the community [77].

In addition to the cost optimization on the renewable energy community with P2P trading, researchers also investigate the participant motivation [78, 79] and system improvement [80-84] of P2P trading management. For example, the P2P trading preferences in energy communities of 301 German homeowners are studied by the experimental survey, showing that the community electricity prices and private storage charging state are key factors affecting the trading behavior [78]. The questionnaire survey is also carried out on 4742 German homeowners with PV and private battery storage installations to learn their participation motivations for P2P trading in communities. The survey results show that the ability to share electricity and high independence are main motivations for the participants [79]. The ancillary service provision is developed for a P2P energy trading community to create benefits for customers and power utility. The case study on a 20-home community in the Great Britain indicates that higher ancillary service prices and more electric vehicles achieve higher revenue for consumers [80]. A three-layer P2P trading framework is proposed for a 36-home community with distributed PV systems, indicating that the PV self-consumption ratio can be improved with the P2P trading scheme [81]. A motivational psychology framework of P2P trading in communities installed with PV systems is proposed by

game-theoretic methods. The authors reported that about 18.38% and 9.82% of daily carbon emissions in Summer and Winter can be reduced by the proposed energy trading model, compared with the feed-in-tariff scheme in a household community in Australia [82]. The Blockchain technology is also widely developed to establish the P2P energy trading platform for communities. Its effectiveness in automation, security and time response is validated by a home community case with PV and battery or electric vehicle units in the U.S. [83]. The P2P energy transaction with real-time double auction market is investigated for a diversified community with 90 homes and 4 enterprises in China, to maintain the energy and economic effectiveness without sacrificing privacy preservation and robustness [84].

Table 2.3 Summary of studies on peer-to-peer energy trading in communities

Community and location	Supply system	Focus and methodology	Main findings	References
Cost optimization on P2P trading				
68 homes (Portugal)	PV	Total cost minimization by mixed integer linear programming model	Achieving 28% and 55% economic saving for consumers and prosumers	Neves et al. 2020 [73]
500 homes (Australia)	PV and private battery storage	Net energy cost minimization by mixed integer linear programming model	A maximum of 28% saving can be achieved by households with large PV-battery systems	Nguyen et al. 2018 [74]
40 smart homes (Canada)	PV and private battery storage	Total energy cost optimization by CPLEX	Cost saving may decrease with increasing renewables and storage after a saturation point	Alam et al. 2019 [75]

Community and location	Supply system	Focus and methodology	Main findings	References
100 homes (the U.K.)	PV and private battery storage	A two-stage aggregated control for P2P sharing by MATLAB	30% reduction in electricity bills is achieved by P2P sharing	Long et al. 2018 [76]
10 homes (Australia)	PV and central battery storage	Optimize peer and storage revenue by a bi-level optimization model	Grid pricing scheme is a key factor affecting the peer sharing revenue	Fernandez et al. 2021 [77]
Participant motivation and system improvement on P2P trading				
301 homes (Germany)	PV and private battery storage	Peer trading preferences by experimental survey	Community electricity prices and private storage charging state are key factors	Hahnel et al. 2020 [78]
4742 homes (Germany)	PV and private battery storage	P2P trading participation motivations of consumers by questionnaire survey	Sharing electricity and being independent are main motivations	Hackbarth et al. 2020 [79]
20 homes (Great Britain)	PV and/or electric vehicle	Ancillary service provision from P2P trading by MATLAB	Higher ancillary service prices and more electric vehicles achieve higher revenue for consumers	Zhou et al. 2020 [80]
36 homes (China)	PV	A three-layer P2P trading framework	PV self-consumption ratio can be improved with P2P trading	Li et al. 2020 [81]
Homes (Australia)	PV	A motivational psychology framework of P2P trading by game-theoretic method	18.38% and 9.82% of daily carbon emissions in Summer and Winter can be reduced	Tushar et al. 2019 [82]

Community and location	Supply system	Focus and methodology	Main findings	References
Home community (the U.S.)	PV and battery/electric vehicle	P2P energy trading platform with Blockchain technology	High level of automation, security and fast real-time settlements are maintained	Esmat et al. 2021 [83]
90 homes and 4 enterprises (China)	PV and battery/electric vehicle	P2P energy transaction with real-time double auction market	Energy and economic effectiveness can be achieved without sacrificing privacy preservation and robustness	Wang et al. 2020 [84]

These studies on peer energy trading in communities with hybrid RE-EES systems are summarized in Table 2.3, regarding to the cost optimization, participant motivation and system improvement aspects. It can be found that most existing research on the P2P energy trading management focuses on household communities, whereas few studies focus on net-zero energy communities integrating large-scale building groups with fundamental units in high-density cities. In addition, most of the research investigates the P2P sharing in communities installed with household solar PV and battery/electric vehicle units, while few studies investigate the hybrid renewable energy and storage systems. District community-based P2P energy sharing with hybrid renewable energy and HV storage systems is worthy to be investigated, especially with the ongoing increments on the HV market, renewable energy deployment and utility grid power pressure.

2.4 Research gaps on hybrid renewable energy and storage systems for a single building and communities

This chapter reviews the recent literatures on hybrid RE-EES systems for buildings and communities, concerning the techno-economic-environmental feasibility, system design optimization, and peer-to-peer energy trading aspects. Based on the literature review as

summarized in Tables 2.1-2.3, detailed research gaps on hybrid RE-EES systems can be identified as follows:

(1) Field experiments on hybrid RE-EES systems are seldom conducted to study the system operational performances and validate the simulation models of energy balanced based battery and energy management strategies.

(2) Few design optimization studies on hybrid RE-EES systems consider the robust energy planning and energy management approaches integrating the energy supply, storage, demand and grid integration aspects. Moreover, few studies have considered the potential renewable energy benefits when evaluating the cost of energy for renewable applications in buildings within urban contexts.

(3) Most of existing studies on hybrid renewable energy and hydrogen storage systems are limited to stationary hydrogen storage, and the integrations of HVs are limited to single building applications. Few studies focus on hybrid renewable energy systems integrated with multiple HV groups in different cruise schedules for net-zero energy community applications.

(4) Few studies on grid integration with hybrid RE-EES systems propose grid power exchange limits and time-of-use grid penalty cost business models in the system management and optimizations to achieve high power flexibility and economy for the utility grid, especially in large-scale community applications.

(5) Most of existing research on the P2P energy trading management focuses on home community applications with household solar PV and battery/electric vehicle units. While few of them focuses on net-zero energy communities with large-scale fundamental building groups in high-density cities. And hybrid renewable energy and green vehicle storage systems (e.g. hybrid

solar PV and wind turbine systems integrated with HV and BV storage) are seldom involved in the P2P trading research.

(6) Most of previously developed peer trading pricing schemes are not suitable for studying P2P trading of diversified communities with building groups who want to set individual peer selling/buying prices, rather than co-determined by the community peers. Peer energy trading price models for large-scale communities with diversified building groups, hybrid RE-EES systems, and different grid price schemes need to be developed. Additionally, the time-of-use P2P energy trading management and optimization is seldom investigated to maintain the power flexibility and economy of the utility grid. Moreover, the lifetime economic analysis on RE-EES systems for power supply to net-zero energy communities with P2P trading in the future cost scenario is seldom conducted for an economic reference to potential stakeholders.

CHAPTER 3 SYSTEM MODELING AND EVALUATION

METHODOLOGY OF HYBRID RENEWABLE ENERGY AND STORAGE SYSTEMS FOR BUILDINGS

This chapter specifies the detailed system modelling and evaluation methodology of hybrid renewable energy and electrical energy storage systems for power supply to a single building and communities with urban contexts, with the framework shown in Fig. 3.1.

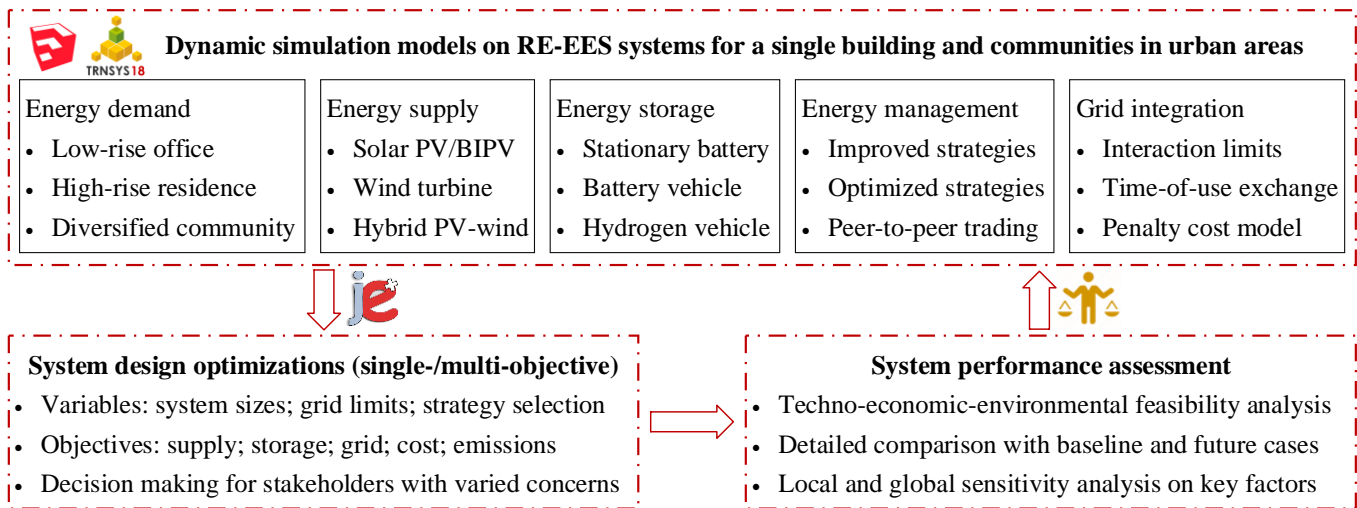


Fig. 3.1 Framework on system modelling and evaluation methodology of hybrid systems

Firstly, the dynamic simulation models on hybrid renewable energy and storage systems are presented covering five main components (i.e. energy demand, energy supply, energy storage, grid integration and energy management), based on the SketchUp and TRNSYS 18 platforms. Then, design optimizations on hybrid renewable energy and storage systems are conducted to find the optimum system sizes, grid limits and management strategy, with the coupled simulation and optimization platform of TRNSYS 18 and jEplus+EA. Both single-objective and multi-objective optimizations are conducted focusing on the performance of system supply, energy storage, grid

integration, system cost and carbon emissions. The decision-making strategies are also explained to determine the final optimum solution from the Pareto optimal set for key stakeholders with different preferences. Finally, the system performances of optimum solutions are assessed, including techno-economic-environmental feasibility analyses, detailed comparison with baseline and future scenarios, and sensitivity analyses on key factors.

3.1 System modelling of renewable energy and storage systems for a single building and communities

3.1.1 Solar photovoltaic modelling

Solar photovoltaic (PV) panels can be installed on both the rooftop and façade of buildings according to the application cases. The rooftop PV panels are modelled by TRNSYS Type 103 at a tilted angle close to the latitude of the location [85]. The model determines the current-voltage characteristics of the PV array using the empirical equivalent circuit model [86]. The power generation of the PV system is the product of the current and voltage under the maximum power point tracking mode to achieve higher energy efficiency. The façade PV modules are modelled by TRNSYS Type 567 integrated with the multi-zone building model Type 56, according to the empirical equivalent circuit model and algorithm developed by Duffie and Beckman [87], considering different azimuths of installed facades. An adjacent shading factor of 76.64% is considered for façade PV panels applied in high-density urban environment like Hong Kong compared with a standalone baseline building [88].

3.1.2 Wind turbine modelling

Wind turbine systems can be developed for power supply to buildings and communities especially in coastal areas like Hong Kong, with advantageous wind resources and complementary

power characteristics with PV power [89]. The wind turbine is simulated by TRNSYS Type 90, and external operation parameters from wind turbine manufactures are adopted to provide power and wind speed characteristics [90]. The transmission loss of the wind power [91] is considered when used for power supply to buildings in urban areas far away from the wind power plant.

3.1.3 Stationary battery storage and battery vehicle storage modelling

The stationary battery model is developed based on the energy balance mechanism with the state of charge (SOC) as the iteration indicator shown in Eq. (3.1) [92]:

$$SOC_i = SOC_0 + \frac{\int P_{bat_{net}}}{Bat_{rated} \cdot SOH} \quad (3.1)$$

where SOC_0 is the initial battery state of charge. $P_{bat_{net}}$ is the net power flow through the battery bank including charging and discharging power in opposite values, kW. Bat_{rated} is the rated capacity of the battery bank, kWh. SOH is the battery state of health considering the battery degradation. The cycling aging of the battery tank is considered as shown in Eq. (3.2) [93, 94]:

$$cycling\ aging_i = aging_0 + 0.5 \cdot \frac{\int |P_{bat_i}|}{Bat_{rated}} \cdot \frac{1}{Equ_{lifecycle}} \quad (3.2)$$

where $aging_0$ is the initial battery aging. P_{bat_i} is the charging or discharging power throughout the battery bank, kW. $Equ_{lifecycle}$ is the equivalent life cycle number of the battery bank, degrading from its initial full usable capacity at 100% SOH to the end of its life at 80% SOH . The lead-acid battery and lithium-ion battery have 1000 [18] and 6000 [95] cycles respectively in the service life. It is assumed that battery SOH is at 80% when battery aging arrives at 1, so the battery SOH can be formulated as Eq. (3.3) [93, 94]:

$$SOH_i = SOH_{i-1} - aging_i \cdot 0.2 \quad (3.3)$$

The battery storage units can be charged by surplus renewable energy or discharged to meet the electrical load by controlling the fractional battery state of charge (FSOC) with an operational limit (0.25 - 0.9 for the lead-acid battery [96] and 0.15 - 0.98 for the lithium-ion battery [97]). The maximum charging and discharging rate of the battery are also considered according to the battery characteristics (i.e. 0.2C for the lead-acid battery [98] and 1C for the lithium-ion battery [99]).

The battery vehicle (BV) is modeled by the TRNSYS Type 47a based on the energy balance mechanism according to the commercial product of “Tesla Model S 75”, with an equivalent storage capacity with the hydrogen vehicle (HV) for performance comparison for integration with the renewable energy systems. A maximum electricity storage state of charge at 0.95 is set for the BV, and a minimum state of charge at 0.39 is set to cover one-day cruise and keep above the minimum vehicle storage level.

3.1.4 Hydrogen vehicle storage modelling

The HV model is developed from a commercialized product “2019 Toyota Mirai” with the maximum power output of 114 kW and maximum hydrogen storage tank mass of 5 kg at a maximum pressure of 700 bars. It is tested that the “Toyota Mirai” with full hydrogen storage can cover a cruise range of about 502 km [100]. HVs can meet the building load by consuming hydrogen in the proton exchange membrane fuel cell (PEMFC) when they are parked at home. The hydrogen consumption of HVs on the road is considered in the simulation, by calculating the FSOC of hydrogen storage tanks in HVs. Thermal heat can be recovered from the electrolyzers, compressors and PEMFCs when HVs are parked at home, to meet the air-conditioning reheat and domestic hot water demand of residential buildings, thereby increasing the overall hydrogen system efficiency.

The hydrogen energy storage system consists of electrolyzers, primary compressors carrying hydrogen from electrolyzers to stationary hydrogen storage tanks, secondary compressors transporting hydrogen from stationary hydrogen storage tanks to mobile hydrogen storage tanks, and PEMFCs. The electrolyzer is modelled by TRNSYS Type 160a based on an advanced alkaline electrolyzer product “PHOEBUS” [101]. The cell number varies in different cases dependent on the supply power entering the electrolyzer, to keep the current density between 40 - 400 mA/cm² [102]. TRNSYS Type 167 is adopted to model the multistage polytropic compressor, which is turned on when the pressure of entering hydrogen is lower than that of the targeted storage tank. The hydrogen storage tanks are simulated by Type 164b to store compressed hydrogen at a high efficiency of around 99% with a maximum pressure of 700 bars, based on the van der Waals equation of state for real gas [41]. The fuel cell is simulated by Type 170d for PEMFC, showing the electrochemical process of converting the chemical energy of hydrogen and oxygen to electrical currents.

3.1.5 Grid integration with power interaction limits and time-of-use grid penalty cost business model

(1) Grid integration with power interaction limits

In terms of the grid integration of hybrid renewable energy and storage systems, the standard deviation (STD) of the net grid power can be firstly derived to show the average grid stress as per Eq. (3.4) [103]:

$$Average\ grid\ stress_{year} = STD(P_{grid\ to\ load} + P_{grid\ to\ battery} - P_{RE\ to\ grid})_{step} \quad (3.4)$$

where $P_{grid\ to\ load}$ is the power flow from the utility grid to meet the load, kW. $P_{grid\ to\ battery}$ is the power flow from the utility grid to charge the battery bank, kW. $P_{RE\ to\ grid}$ is the feed-in power from the renewable energy sources to the utility grid, kW.

In order to further consider the grid integration with the renewable energy system, both grid export and import limits are introduced. The grid import limit ($Grid_{import}$) is set to regulate the grid to meet the load and battery demand, while the exceeded load over the $Grid_{import}$ in Eq. (3.5) is still to be met by the utility grid. Exceeded battery demand, however, is not addressed.

$$P_{exceeded\ load} = P_{load} - P_{RE\ to\ load} - P_{battery\ to\ load} - Grid_{import} \quad (3.5)$$

where P_{load} is the building load demand, kW. $P_{RE\ to\ load}$ is the power from renewable energy sources to meet the load, kW. $P_{battery\ to\ load}$ is the power from the battery bank to the building load, kW.

The grid export limit ($Grid_{export}$), which is the ratio of the rated renewable energy power, is set to limit surplus renewable energy power feeding into the utility grid, so that any power over the $Grid_{export}$ is dumped. These grid integration indicators can be subject to design optimizations of hybrid RE-EES systems as an original contribution.

(2) Time-of-use grid penalty cost business model for renewable energy systems

The installation of renewable energy for power supply to buildings and communities may impose extra burden on the existing utility grid especially in large-scale applications. A business model of the grid penalty cost is proposed to integrate the building community microgrid with the utility grid, based on the local time-of-use electricity pricing mode, counting both imported power from grid and exported power to grid. It is assumed that the on-peak period is the daily period between 9:00 and 21:00 and the off-peak period comprises all other hours according to the power grid company in Hong Kong [104]. The time-of-use penalty cost of renewable energy systems

includes four parts, namely grid import of off-peak time and grid import of on-peak time as per Fig. 3.2(a), grid export of off-peak time and grid export of on-peak time as per Fig. 3.2(b).

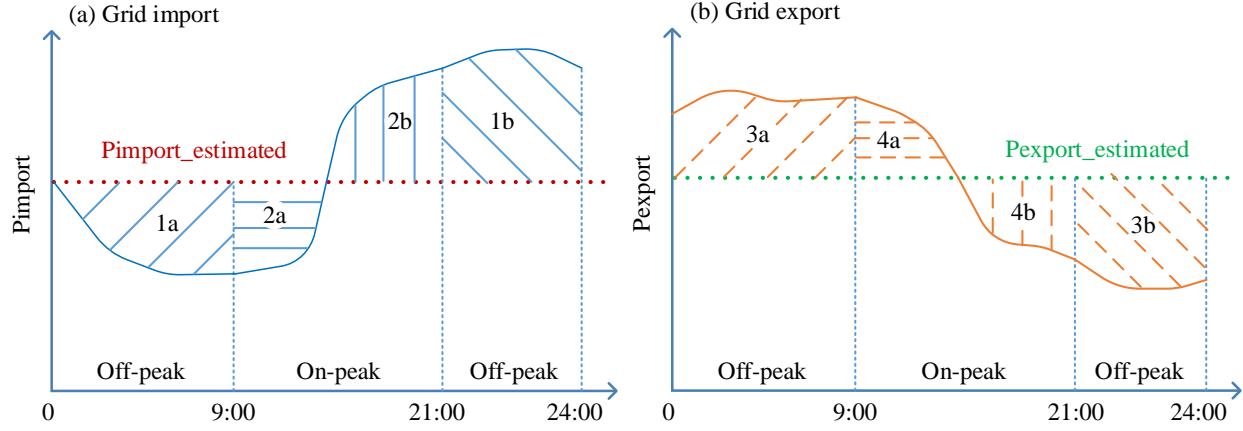


Fig. 3.2 Time-of-use grid penalty cost model of renewable energy systems

The formulation of penalty cost of grid import in off-peak time is shown in Eq. (3.6).

$$PC_{import_offpeak} = \left(\int P_{import_estimated} - \int P_{import_offpeak} \right) \cdot PF_{offpeak} \quad (3.6)$$

where $PC_{import_offpeak}$ is the penalty cost of imported power from grid during off-peak hours as indicated by area $1a$ ($PC > 0$ with a fine when $P_{import_offpeak} < P_{import_estimated}$), and area $1b$ ($PC < 0$ with a bonus when $P_{import_offpeak} > P_{import_estimated}$) in US\$, as excess import is encouraged by grid during off-peak periods. $P_{import_estimated}$ is the grid import estimation defined as the ratio of peak electrical load of buildings in kW. $P_{import_offpeak}$ is the dynamic imported power from grid during off-peak hours, kW. $PF_{offpeak}$ is the penalty factor during off-peak hours, US\$/kWh.

The formulation of penalty cost of grid import during on-peak time is shown in Eq. (3.7).

$$PC_{import_onpeak} = \left(\int P_{import_onpeak} - \int P_{import_estimated} \right) \cdot PF_{onpeak} \quad (3.7)$$

where PC_{import_onpeak} is the penalty cost of imported power from grid during on-peak hours, as indicated by area $2a$ ($PC < 0$ when $P_{import_onpeak} < P_{import_estimated}$) and area $2b$ ($PC > 0$ when

$P_{import_onpeak} > P_{import_estimated}$) in US\$, as extra import during on-peak periods is not preferred by grid. P_{import_onpeak} is the dynamic imported power from grid during on-peak hours, kW. PF_{onpeak} is the penalty factor during on-peak hours, US\$/kWh.

The formulation of penalty cost of grid export in off-peak time is shown in Eq. (3.8).

$$PC_{export_offpeak} = \left(\int P_{export_offpeak} - \int P_{export_estimated} \right) \cdot PF_{offpeak} \quad (3.8)$$

where $PC_{export_offpeak}$ is the penalty cost of exported power from grid during off-peak hours as indicated by area 3a ($PC > 0$ when $P_{export_offpeak} > P_{export_estimated}$) and area 3b ($PC < 0$ when $P_{export_offpeak} < P_{export_estimated}$) in US\$, as excess export in off-peak periods is not encouraged by grid. $P_{export_offpeak}$ is the dynamic exported power to grid during off-peak hours, kW. $P_{export_estimated}$ is the grid export estimation defined as the ratio of rated renewable energy capacity in kW.

The formulation of penalty cost of grid export in on-peak time is shown in Eq. (3.9).

$$PC_{export_onpeak} = \left(\int P_{export_estimated} - \int P_{export_onpeak} \right) \cdot PF_{onpeak} \quad (3.9)$$

where PC_{export_onpeak} is the penalty cost of exported power to grid during on-peak hours as indicated by area 4a ($PC < 0$ when $P_{export_onpeak} > P_{export_estimated}$) and area 4b ($PC > 0$ when $P_{export_onpeak} < P_{export_estimated}$), as residual grid export is welcomed during on-peak periods. P_{export_onpeak} is the dynamic exported power from grid during on-peak hours, kW.

Therefore, the time-of-use grid penalty cost (PC_{TOU}) can be formulated as per Eq. (3.10):

$$PC_{TOU} = PC_{import_offpeak} + PC_{import_onpeak} + PC_{export_offpeak} + PC_{export_onpeak} \quad (3.10)$$

3.1.6 Uniform and individual peer energy trading price models of hybrid renewable energy and storage systems

(1) Uniform peer energy trading price model

The uniform peer energy trading price model for the building community with three different functional building groups is developed, based on the total supply-demand ratio (SDR) of the community, assuming that the relationship between price and SDR is inverse-proportional [105] as per Fig. 3.3.

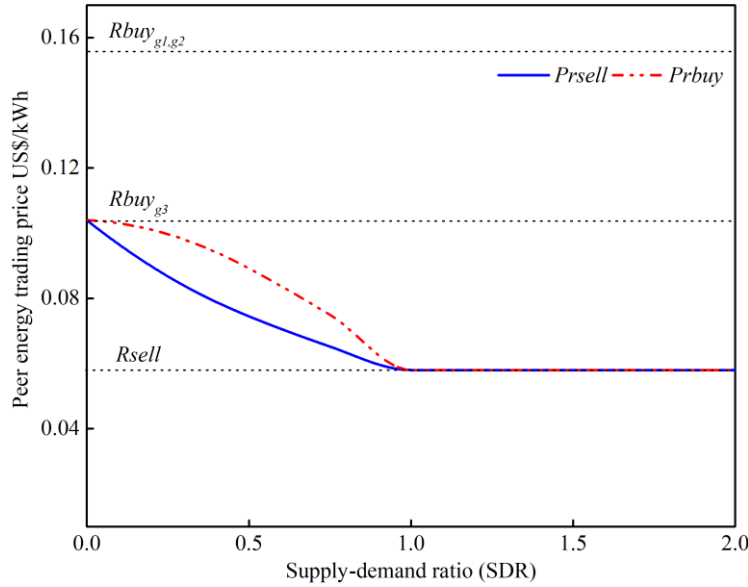


Fig. 3.3 Uniform peer energy trading price model

The dynamic energy supply available for peer energy selling of the community is the sum of surplus renewable energy after the self-consumption of the building groups. And the dynamic demand needing peer energy buying of the community is the sum of electrical load shortage after the self-sufficiency of the building groups. So the *SDR* is formulated by Eq. (3.11) as shown below.

$$SDR = \frac{\sum P_{REgi_sur}}{\sum P_{Loadgi_shor}} \quad (3.11)$$

where P_{REgi_sur} is the surplus renewable energy after the self-consumption of building group i , kW.

P_{Loadgi_shor} is the electrical load shortage after the self-sufficiency of building group i , kW.

The P2P energy selling price (Pr_{sell}) in the community can be formulated as the piecewise function of SDR as Eq. (3.12) [105].

$$Pr_{sell} = f(SDR) = \begin{cases} \frac{R_{sell} \cdot R_{buy_{g3}}}{(R_{buy_{g3}} - R_{sell}) \cdot SDR + R_{sell}}, & 0 \leq SDR \leq 1 \\ R_{sell} & , 1 < SDR \end{cases} \quad (3.12)$$

where R_{sell} is the grid feed-in tariff rate of renewable energy and it is the same for all building groups, 0.058 US\$/kWh [98]. $R_{buy_{gi}}$ is the grid electricity buying rate of group i in US\$/kWh which is different with building types (e.g. 0.154 US\$/kWh for non-residential buildings and 0.104 US\$/kWh for residential buildings in Hong Kong [106]). Here a lower electricity rate of $R_{buy_{g3}}$ is adopted for the uniform trading price model to ensure the peer energy selling price lower than the grid energy selling price.

The P2P energy buying price (Pr_{buy}) in the community is also formulated as the piecewise function of SDR as per Eq. (3.13), and it is dependent on the selling price considering the economic balance [105].

$$Pr_{buy} = f(SDR) = \begin{cases} Pr_{sell} \cdot SDR + R_{buy_{g3}} \cdot (1 - SDR), & 0 \leq SDR \leq 1 \\ R_{sell} & , 1 < SDR \end{cases} \quad (3.13)$$

(2) Individual peer energy trading price model

An individual peer energy trading price model allocating an individual trading price to each building group is proposed, to study the P2P energy trading behavior of the diversified community consisting of building groups with different energy distributions and grid pricing schemes. The peer selling price of each building group is determined by its intrinsic surplus renewable energy with an inverse-proportional relation, and the peer buying price of each building group is determined by its intrinsic demand shortage with a proportional relation as per Fig. 3.4.

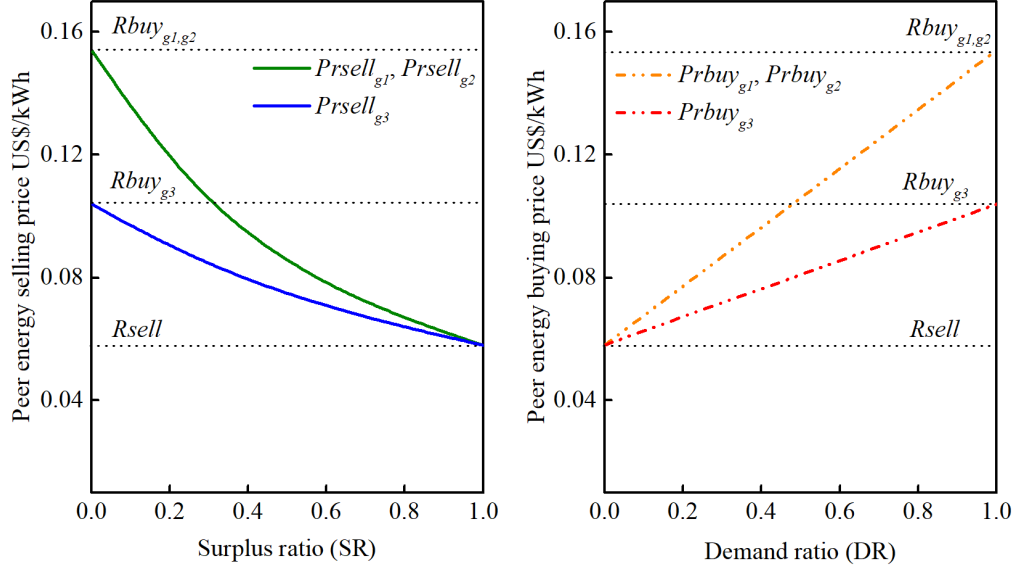


Fig. 3.4 Individual peer energy trading price model

The surplus renewable energy of an individual building group for peer trading is indicated by the surplus ratio (SR) as per Eq. (3.14).

$$SR_{gi_sur} = \frac{P_{REgi_sur}}{P_{REgi}} \quad (3.14)$$

where P_{REgi} is the dynamic renewable energy generation of building group i , kW.

The demand shortage of an individual building group for peer trading is indicated by the demand ratio (DR) as per Eq. (3.15).

$$DR_{gi_shor} = \frac{P_{Loadgi_shor}}{P_{Loadgi}} \quad (3.15)$$

where P_{Loadgi} is the dynamic electrical load of building group i , kW.

The peer selling price and peer buying price of each building group are developed as Eqs. (3.16-3.17) dependent on the SR and DR . It should be noted that the peer selling price and peer buying price of an individual building group are independent, as its renewable energy surplus and

demand shortage could be not positive values at the same time. And the peer energy trading prices vary with the dynamic renewable energy generation and electrical load of the building group.

$$Prsell_{gi} = f(SR_{gi_sur}) = \frac{R_{sell} \cdot R_{buy_{gi}}}{(R_{buy_{gi}} - R_{sell}) \cdot SR_{gi_sur} + R_{sell}} \quad (3.16)$$

$$Prbuy_{gi} = f(DR_{gi_shor}) = (R_{buy_{gi}} - R_{sell}) \cdot DR_{gi_shor} + R_{sell} \quad (3.17)$$

3.2 System design optimization methods, decision-making strategies and evaluation indicators

3.2.1 Optimization methods and decision-making strategies

Both single-criterion and multi-criterion optimizations of hybrid RE-EES systems are conducted considering the system technical, economic and environmental performances, based on the coupled TRNSYS and jEPlus+EA platform. This optimization tool has been widely used with high adaptability and flexibility integrating the integer-based encoding scheme, constrained multi-objective ranking and pareto archived global elitism [107]. The Non-dominated Sorting Genetic Algorithm-II (NSGA-II) is adopted to solve the multi-objective optimization problem, given its robustness and versatility as one of the best known algorithms for multi-objective optimizations, with a high efficiency in ranking competing objectives. It generates the first set of solutions with random sampling, and ranks them according to the optimization criteria. Better solutions are then selected to reproduce offspring generations using a high crossover rate (0.9) and a low mutation rate (0.05) for a reasonable convergence speed and acceptable accuracy [108]. The NSGA-II program improves the adaptive fit of candidate populations based on the sorting method of Pareto dominance with a set of constrains and objectives. The parent and offspring generations are combined to form the next-generation population with all solutions sorted into amounts of non-

dominated fronts. The evolution cycle ends with a set of pareto optimal solutions once the termination criteria are met, and the tournament selection between all solutions is adopted to find the optimal front as the Pareto front [109]. The population size and maximum generation are set as 10 and 200 respectively, to secure the search of global optima in the system optimizations [110]. A typical desktop computer is adequate to carry out the computing work, and one optimization scenario takes about 5 days or more.

Decision-making strategies (DMSs) are required to determine a final optimum solution out of the obtained Pareto optimal set obtained by the multi-objective optimizations. Various decision-making strategies are applied focusing on different preferences of major stakeholders of the hybrid RE-EES systems, including the weighted sum method, minimum distance to the utopia point method and analytical hierarchy process method.

(1) DMS with the weighted sum method

The weighted sum method is one of best known multi-objective DMS approaches, by combing the multiple objectives into one single objective, by summing the normalized objective functions as the multi-objective optimization coefficient (*MOOC*) as shown in Eq. (3.18) as below.

$$MOOC = \sum \omega_i \frac{Obj_i - Obj_{min}}{Obj_{max} - Obj_{min}} \quad (3.18)$$

where ω_i is the sum weighting coefficient of objective i . Obj_i is the original value of the optimization objective. Obj_{min} and Obj_{max} are the minimum and maximum values of corresponding objectives.

(2) DMS with the minimum distance to the utopia point (MDUP) method

The utopia point of the multi-objective optimization is an ideal optimum solution, supposing all objectives to be minimized simultaneously. The MDUP method obtains the optimum solution

by calculating the distance to the utopia point as the MOOC as per Eq. (3.19), whose minimum value is adopted to identify the final optimum solution [109]. An equivalent weighting is applied to all optimization objectives in the MDUP method.

$$MOOC = \|P_i - P_u\| \quad (3.19)$$

where P_i is the Pareto optimal solutions and P_u is the utopia point.

(3) DMS with the analytical hierarchy process (AHP) method

The AHP method obtains the weights of different optimization criteria via structuring a decision matrix $D_{m \times m}$ consisting of all concerned objectives with different levels of importance valued by decision-makers. A pairwise comparison among optimization criteria is established by defining D_{ij} , which is larger than 1 if objective i is prioritized over j ($D_{ji} = 1/D_{ij}$). D_{ij} is an integer varying between 1 - 9 defined by Saaty, showing that 1 means objective i and j is equally important, and 9 means objective i is extremely important than j [111]. The consistency ratio of the decision matrix should be kept lower than 0.1 by calculating the principal eigenvalue, to ensure the reasonability of the established matrix of optimization criteria [112]. The scale of weights can be then derived by solving and normalizing the principal eigenvector of the decision matrix. The AHP method can be adopted to derive the weights of optimization objectives, considering the preferences of three major stakeholders of the hybrid RE-EES system (i.e. the end-user, transmission system operator and investor). Specifically, the system end-user prioritizes the supply performance indicator integrating *SCR*, *LCR* and *HSE*. The transmission system operator values the grid integration most, while the investor's major concern is the net present cash flow. The decision matrix of these DMSs based on the AHP method is shown in Table 3.1.

Table 3.1 Decision matrix of DMSs based on the analytical hierarchy process method

End-user priority				Transmission system operator priority				Investor priority			
	<i>Supply</i>	<i>NGE</i>	<i>NPV</i>		<i>Supply</i>	<i>NGE</i>	<i>NPV</i>		<i>Supply</i>	<i>NGE</i>	<i>NPV</i>
<i>Supply</i>	1	9	5	<i>Supply</i>	1	1/5	2	<i>Supply</i>	1	2	1/5
<i>NGE</i>	1/9	1	1/2	<i>NGE</i>	5	1	9	<i>NGE</i>	1/2	1	1/9
<i>NPV</i>	1/5	2	1	<i>NPV</i>	1/2	1/9	1	<i>NPV</i>	5	9	1
Weight	0.761	0.082	0.158	Weight	0.158	0.761	0.082	Weight	0.158	0.082	0.761
consistency ratio=0.1%				consistency ratio=0.1%				consistency ratio=0.1%			

The evaluating criterion (i.e. MOOC) to select a final optimum solution out of the Pareto solutions with the AHP method is shown in Eq. (3.20).

$$MOOC = WT_{Supply} \cdot Supply_{nor} + WT_{NGE} \cdot NGE_{nor} + WT_{NPV} \cdot NPV_{nor} \quad (3.20)$$

where WT_{Supply} , WT_{NGE} , WT_{NPV} are the weights of optimization objectives *Supply*, *NGE* and *NPV* obtained by the decision matrix. $Supply_{nor}$, NGE_{nor} , NPV_{nor} are the normalized values of optimization criteria *Supply*, *NGE* and *NPV*.

3.2.2 Techno-economic-environmental evaluation indicators of hybrid renewable energy and storage systems

The technical, economic and environmental indicators are formulated to evaluate the performances of hybrid RE-EES systems for applications in a single building and communities. The technical indicators mainly evaluate the performance of the system supply, energy storage, and grid integration aspects. The economic indicators mainly include the lifetime net present value,

levelized cost of energy and annual electricity bills. The environmental indicators mainly include annual equivalent carbon emissions and annual equivalent carbon emission cost.

(1) Technical performance evaluation indicators

1) Supply performance evaluation

The annual average renewable energy self-consumption ratio (*SCR*) of hybrid RE-EES systems is formulated as Eq. (3.21) to evaluate the utilization efficiency of renewable power supply:

$$SCR = \frac{\text{on-site RE consumption}}{\text{total RE generation}} = \frac{E_{RE \text{ to load}} + E_{RE \text{ to storage}}}{E_{RE}} \quad (3.21)$$

where $E_{RE \text{ to load}}$ is the total annual electricity from solar PV panels and wind turbines to meet the on-site building load, kWh. $E_{RE \text{ to storage}}$ is the charging energy from solar PV and wind sources to the energy storage units (e.g. batteries and electrolyzers), kWh. E_{RE} is the total annual energy generation of solar PV panels and wind turbines, kWh.

The annual average load cover ratio (*LCR*) is developed to estimate the on-site coverage of the building electrical load by hybrid RE-EES systems as per Eq. (3.22):

$$LCR = \frac{\text{on-site supply}}{\text{total electrical load}} = \frac{E_{RE \text{ to load}} + E_{storage \text{ to load}}}{E_{load}} \quad (3.22)$$

where $E_{storage \text{ to load}}$ is the energy discharged from storage units (e.g. batteries and fuel cells) to meet the electrical load, kWh. E_{load} is the total electrical load including building demand and energy required for hydrogen compression, kWh.

Since some renewable energy power may be dumped when exceeds the grid export limit in the case of setting grid exchange power limits, the renewable energy utilization efficiency (*EFF*) is also assessed as per Eq. (3.23):

$$EFF = \frac{\text{utilized RE electricity}}{\text{total electricity generation from RE}} = \frac{E_{RE \text{ to load}} + E_{RE \text{ to storage}} + E_{RE \text{ to grid}}}{E_{RE}} \quad (3.23)$$

where $E_{RE \text{ to grid}}$ is the feed-in energy from renewable energy resources to the utility grid, kWh.

2) Energy storage evaluation

The hydrogen system efficiency (HSE) of hybrid RE-EES systems with integrated hydrogen vehicles is formulated as Eq. (3.24):

$$HSE = \frac{H_2 \text{ system supply}}{H_2 \text{ system consumption}} = \frac{E_{FCs \text{ to road}} + E_{FCs \text{ to load}} + E_{HR \text{ to reheat}} + E_{HR \text{ to DHW}}}{E_{RE \text{ to electro}} + E_{grid \text{ to electro}} + E_{comp} + E_{H_2 \text{ tank}}} \quad (3.24)$$

where $E_{FCs \text{ to road}}$ is the energy from fuel cells to drive the motor of HVs when travelling, kWh. $E_{FCs \text{ to load}}$ is the energy from fuel cells to cover the electrical load when HVs are parked at buildings, kWh. $E_{HR \text{ to reheat}}$ is the heat recovered from the hydrogen system to meet the air-conditioning reheat demand, kWh. $E_{HR \text{ to DHW}}$ is the heat recovered from the hydrogen system to meet the domestic hot water (DHW) load, kWh. $E_{grid \text{ to electro}}$ is the refueled energy from the utility grid to drive the electrolyzer to generate hydrogen for HVs' daily cruise, when FSOCs of H_2 storage tanks in HVs are lower than minimum thresholds, kWh. E_{comp} is the energy consumption of compressors in the hydrogen system, kWh. $E_{H_2 \text{ tank}}$ is energy change of the H_2 storage tanks during the evaluation period, kWh.

For the battery storage side, the annual cycling aging is calculated as explained in Eq. (3.2).

3) Grid integration evaluation

The hybrid RE-EES system exchanges power with the utility grid by exporting surplus renewable energy and importing power for unmet demands, which may impose much burden on the power transmission system in the long-term and large-scale operations. It is therefore significant to control and optimize the grid integration for the hybrid system. The absolute net

power exchange between the utility grid and hybrid system is developed as a grid integration evaluation indicator as Eq. (3.25).

$$NGE = ABS(\text{grid supply} - \text{grid feed-in}) = ABS(E_{\text{grid to load}} + E_{\text{grid to storage}} - E_{RE \text{ to grid}}) \quad (3.25)$$

where NGE is the absolute value of the difference in grid supply and grid feed-in energy, kWh. $E_{RE \text{ to grid}}$ is the surplus energy from PV and wind sources to the utility grid, kWh.

In addition to assessing the net grid exchange power, the standard deviation of the net grid power as per Eq. (3.4) and the time-of-use grid penalty cost as per Eq. (3.10) are also developed for the grid integration evaluation when connected with hybrid RE-EES systems.

(2) Economic performance evaluation indicators

1) Lifetime net present value (NPV)

To evaluate the economic performance of hybrid RE-EES systems for power supply to buildings and communities, the lifetime net present value (NPV) is formulated including the investment cost of renewable energy systems, grid feed-in tariff (FiT) and electricity bill as shown in Eq. (3.26).

$$NPV = PRV_{\text{investment}} - PRV_{\text{FiT}} + PRV_{\text{bill}} \quad (3.26)$$

where $PRV_{\text{investment}}$ is the present value of investment of hybrid systems, US\$. PRV_{FiT} is the present value of feed-in tariff, US\$. PRV_{bill} is the present value of electricity bill for grid import energy, US\$.

The present value of investment of hybrid systems includes the present value of initial cost (PRV_{ini}), present value of operation and maintenance cost ($PRV_{O\&M}$), present value of replacement cost (PRV_{rep}) and present value of residual cost (PRV_{res}) as per Eq. (3.27). The system components

include PV panels, wind turbines, inverters, battery units, electrolyzers, compressors, hydrogen storage tanks and HVs.

$$\begin{aligned}
PRV_{investment} &= PRV_{ini} + PRV_{O\&M} + PRV_{rep} - PRV_{res} \\
&= C_{ini} + \sum_{n=1}^N \frac{f_{mai} \cdot C_{ini}}{(1+i)^n} + \sum_{j=1}^J C_{ini} \left(\frac{1-d}{1+i} \right)^{j \cdot l} - C_{ini} \frac{l_{res}}{l} \cdot \frac{(1-d)^N}{(1+i)^N}
\end{aligned} \tag{3.27}$$

where C_{ini} is the initial cost of hybrid systems, US\$. i is the annual real discounted rate. n is the specific year, and N is the system lifetime. f_{mai} is the proportion of the operation and maintenance cost to the initial cost including insurance [113]. j is the specific replacement number, and J is the total replacement number. d is the annual cost degradation rate. l is the lifetime, and l_{res} is the residual lifetime.

Renewable energy applications in Hong Kong can get a favorable amount of FiT subsidy at 3 HK\$/kWh for a 200 - 1000 kW system until end 2033, while the renewable generation thereafter would be owned by the system investor. It can then be assumed that FiT subsidy after 2033 can be obtained at the rate of the local electricity price for renewable energy generation as shown in Eq. (3.28).

$$PRV_{FiT} = \sum_{n=1}^{13} \frac{(E_{PV} \cdot (1-\delta_{PV})^{n-1} + E_{WT} \cdot (1-\delta_{WT})^{n-1}) \cdot c_{fit}}{(1+i)^n} + \sum_{n=14}^{20} \frac{(E_{PV} \cdot (1-\delta_{PV})^{n-1} + E_{WT} \cdot (1-\delta_{WT})^{n-1}) \cdot c_{ele} \cdot (1+\gamma)^{n-1}}{(1+i)^n} \tag{3.28}$$

where E_{PV} is the annual energy production of the PV system, kWh. δ_{PV} is the degradation rate of the PV system. E_{WT} is the annual energy production of the wind system, kWh. δ_{WT} is the degradation rate of the wind system. c_{fit} is the feed-in tariff in the first 13 years issued by the government, US\$/kWh. c_{ele} is the local electricity price of residential buildings, US\$/kWh. And γ is the annual price increasing rate of the electricity.

When assuming all renewable generation gets the FiT subsidy at the local FiT rate, the present value of FiT is formulated as shown in Eq. (3.29), and the on-site used renewable electricity is charged at the time-of-use tariff rate counted in the electricity bill item according to the local FiT scheme [114].

$$PRV_{FiT} = \sum_{n=1}^{n=N} \frac{(E_{PV} \cdot (1-\delta_{PV})^{n-1} + E_{WT} \cdot (1-\delta_{WT})^{n-1}) \cdot c_{fit}}{(1+i)^n} \quad (3.29)$$

2) Levelized cost of energy (LCOE)

To evaluate the economic feasibility of hybrid RE-EES systems for power supply to buildings, an improved LCOE is formulated considering the investment costs and detailed benefits according to local regulations as per Eq. (3.30).

$$LCOE = \frac{(PRV_{investment} - PRV_{benefits})}{\sum_{n=1}^{n=N} \frac{E_{PV} \cdot (1-\delta_{PV})^{n-1}}{(1+i)^n} + \sum_{n=1}^{n=N} \frac{E_{WT} \cdot (1-\delta_{WT})^{n-1}}{(1+i)^n}} \quad (3.30)$$

where $PRV_{benefits}$ is the present value of potential benefits of renewable energy systems, including the FiT subsidy, transmission loss saving, network expansion saving and carbon reduction benefit as shown in Eq. (3.31).

$$PRV_{benefits} = PRV_{fit} + PRV_{tra} + PRV_{exp} + PRV_{car} \quad (3.31)$$

where PRV_{fit} is the FiT present value of the renewable system based on local regulations, US\$. PRV_{tra} is the present value of transmission loss saving, US\$. PRV_{exp} is the present value of network expansion saving, US\$. PRV_{car} is the present value of carbon reduction benefit, US\$.

The current fuel mix in Hong Kong mainly consists of coal, natural and nuclear energy, which generate electricity in remote plants far away from populated regions. So electricity supplied to buildings in urban areas needs to be transmitted and distributed via underground cables and

overhead lines. It is reported that the average transmission loss in Hong Kong during 2010 to 2014 is about 13.541% of the electricity output [91], and this part of the energy loss can be saved using the building integrated PV systems as shown in Eq. (3.32).

$$PRV_{tra} = \sum_{n=1}^{n=20} \frac{f_{tra} \cdot c_{ele} \cdot E_{PV} \cdot (1 - \delta_{PV})^{n-1} \cdot (1 + \gamma)^{n-1}}{(1 + i)^n} \quad (3.32)$$

where f_{tra} is the proportion of the transmission loss to the generated electricity.

In order to meet the increasing demand of electricity consumption in different sectors, extra investment is needed to expand the utility network and infrastructure. It is reported by China Light and Power Hong Kong Limited that: 24% of the capital investment is spent on meeting the electricity demand of new developments and corresponding infrastructures; 38% of the capital investment is on maintaining the supply reliability; another 30% is on carbon emission reduction projects; and the remaining 8% is on smart city and digital technologies [115]. The development of renewable energy systems for building applications can save such network expansion costs as shown in Eq. (3.33).

$$PRV_{exp} = \sum_{n=1}^{n=20} \frac{f_{exp} \cdot c_{ele} \cdot (E_{PV} \cdot (1 - \delta_{PV})^{n-1} + E_{WT} \cdot (1 - \delta_{WT})^{n-1}) \cdot (1 + \gamma)^{n-1}}{(1 + i)^n} \quad (3.33)$$

where f_{exp} is ratio of cost on the network expansion to the total electricity investment.

A climate action plan has been launched in Hong Kong to keep pace with the Paris Agreement to control the carbon emission. It is projected to decrease the carbon footprint to about 3.3 - 3.8 tonnes/capita by 2030, leading to a reduction by 65% - 70% compared with that in 2005 [4]. The electricity consumption by the building sector in Hong Kong contributes to over 60% of carbon emissions, which can be significantly reduced by using renewable energy as calculated by Eq. (3.34).

$$PRV_{car} = \sum_{n=1}^{n=20} \frac{f_{car} \cdot c_{car} \cdot (E_{PV} \cdot (1 - \delta_{PV})^{n-1} + E_{WT} \cdot (1 - \delta_{WT})^{n-1})}{(1+i)^n} \quad (3.34)$$

where f_{car} is the local carbon intensity of electricity, kgCO₂/kWh. c_{car} is the societal cost of carbon, US\$/kgCO₂.

3) Annual electricity bill

The electricity bill for grid imported energy in Hong Kong includes the demand charge, energy charge, fuel cost adjustment, rent and rates special rebate, according to the local time-of-use tariff for buildings with large power demand [116] as per Eq. (3.35).

$$PRV_{bill} = \sum_{n=1}^{n=N} \frac{(Bill_{demand} + Bill_{energy} + Bill_{fuel} - Bill_{rebate}) \cdot \varepsilon}{(1+i)^n} \quad (3.35)$$

where $Bill_{demand}$ is the annual demand charge of time-of-use electricity tariff, HK\$. $Bill_{energy}$ is the annual energy charge, HK\$. $Bill_{fuel}$ is the annual fuel cost adjustment, HK\$. $Bill_{rebate}$ is the annual rent and rates special rebate, HK\$. ε is the exchange rate of HK\$ and US\$. The detailed formulation of these electricity bill items is shown as Eqs. (3.36-3.39).

$$Bill_{demand} = \text{MIN}(5000 \cdot 12, P_{max_on} \cdot 12) \cdot 120.3 + \text{MAX}(0, P_{max_on} \cdot 12 - 5000 \cdot 12) \cdot 115.3 \\ + \text{MAX}(0, P_{max_off} \cdot 12 - P_{max_on} \cdot 12) \cdot 33.9 \quad (3.36)$$

$$Bill_{energy} = \text{MIN}(E_{sum_on}, 200 \cdot P_{max_on} \cdot 12) \cdot 0.567 + \text{MAX}(0, E_{sum_on} - 200 \cdot P_{max_on} \cdot 12) \cdot \\ 0.547 + E_{sum_off} \cdot 0.469 \quad (3.37)$$

$$Bill_{fuel} = (E_{sum_on} + E_{sum_off}) \cdot 0.298 \quad (3.38)$$

$$Bill_{rebate} = (E_{sum_on} + E_{sum_off}) \cdot 0.012 \quad (3.39)$$

where P_{max_on} is the annual maximum imported power during on-peak time, kW. P_{max_off} is the annual maximum imported power during off-peak time, kW. E_{sum_on} is the total annual imported

energy during on-peak time, kWh. E_{sum_off} is the total annual imported energy during off-peak time, kWh.

The annual net electricity bill (NB_a) of the community with P2P trading can be formulated in Eq. (3.40), counting the electricity bill of buying energy from peers and utility grid of building groups, and electricity profit of selling surplus energy to peers and utility grid of building groups.

$$NB_a = \sum E_{Grid\ import\ gi} \cdot R_{buy\ gi} + \sum E_{peer\ buy\ gi} \cdot Pr_{buy\ gi} - \sum E_{Grid\ export\ gi} \cdot R_{sell} - \sum E_{peer\ sell\ gi} \cdot Pr_{sell\ gi} \quad (3.40)$$

where $E_{Grid\ import\ gi}$ is the total grid imported energy of group i including grid imported energy to electrical load ($E_{Grid\ to\ Load\ gi}$) and to electrolyzers ($E_{Grid\ to\ E\ gi}$), kWh. $E_{peer\ buy\ gi}$ is the energy buying from peers' renewable sources and storage for the electrical load and storage of group i including $E_{RE\ gi\ to\ Load\ gi}$, $E_{RE\ gj\ to\ E\ gi}$ and $E_{FC\ gj\ to\ Load\ gi}$, kWh. $Pr_{buy\ gi}$ is the electricity buying price group i in US\$/kWh varied with the dynamic energy surplus and demand. $E_{Grid\ export\ gi}$ is grid exported energy from renewable sources of group i , kWh. $E_{peer\ sell\ gi}$ is the energy from renewable sources and storage of group i selling to its peers for the electrical demand and storage including $E_{RE\ gi\ to\ Load\ gj}$, $E_{RE\ gi\ to\ E\ gj}$ and $E_{FC\ gi\ to\ Load\ gj}$, kWh. $Pr_{sell\ gi}$ is the electricity selling price of group i in US\$/kWh dependent on the dynamic energy surplus and demand.

(3) *Environmental performance evaluation indicators*

The annual equivalent carbon emissions (CE_a) is also calculated to assess the decarbonisation potential of renewable energy systems compared with baseline scenarios without renewable energy applications as shown in Eq. (3.41) [55].

$$CE_a = (E_{grid\ import} - E_{grid\ export}) \cdot CEF_{eq} \quad (3.41)$$

where $E_{grid\ import}$ is the total annual electricity imported from the utility grid, kWh. $E_{grid\ export}$ is the total annual electricity exported to the utility grid, kWh. CEF_{eq} is the equivalent CO₂ emission factor (e.g. 0.572 kgCO₂/kWh in Hong Kong [55]), and the equivalent carbon emission cost subject to the local social cost of carbon (e.g. 0.024 US\$/kgCO₂ in Hong Kong [117]) is also evaluated.

CHAPTER 4 EXPERIMENTAL TEST AND MODEL VALIDATION OF SOLAR PHOTOVOLTAIC AND BATTERY STORAGE SYSTEMS FOR BUILDINGS

This chapter conducts preliminary experiments on a solar photovoltaic and battery storage system based on a practical testing building platform in Hunan University. Two basic energy management strategies (i.e. maximizing self-consumption strategy, time-of-use strategy) are developed and realized in the testing platform, to control the system operation and compare the system performances. The tested solar photovoltaic and battery storage system models are also established in the TRNSYS environment to validate the battery and energy management strategy models based on the energy balance mechanism.

4.1 Experiment design of the solar photovoltaic and battery storage system

An experiment of a solar photovoltaic (PV) and battery storage system is carried out in a testing platform in Hunan, China as shown in Fig. 4.1. Rooftop PV is installed with rated capacity of 9.15 kW, and a 12 kWh battery storage unit is matched. Two basic energy management strategies, i.e. maximizing self-consumption strategy and time-of-use strategy, are developed and realized in the testing platform to control the system operation for model validation.



(a)



(b)



(c)

Fig. 4.1 Experiments on the PV-battery storage system in Hunan University (a) testing building platform (b) rooftop Poly-Si PV (c) inverter and lithium-ion battery

The specific parameters of the PV-battery are shown in Table 4.1.

Table 4.1 Specification of the PV-battery system in the testing platform

Solar module	SK6612P-305(Poly-Si)
Rated maximum power	305 W
Voltage at Pmax	36.5 V
Current at Pmax	8.35 A

Solar module	SK6612P-305(Poly-Si)
Open-circuit voltage	45.3 V
Short-circuit current	8.94 A
Normal operating cell temperature	47±2°C
Maximum system voltage	1000 V
Dimension	1957*992 mm
Rooftop module number	30
PV initial cost	4000 US\$
Battery	MINIES-P90B12-E-R2 (LiFePO ₄)
Rated capacity	12 kWh
Maximum on-grid power	9 KVA
Operational SOC	15%-98%
Size	738(W)*598(D)*1070.5(H) mm
Battery initial cost	10000 US\$

Fig. 4.2 shows the schematic of the grid connected PV-battery system. Two inverters (GW5000-DT) are connected to the rooftop PV panels at the converting efficiency of 95%. A two-way grid meter is installed to measure the power flow from the utility grid (positive: power out from grid, negative: power feed into grid). The inverter signal and grid signal are collected by Hall sensors and connected to the power distribution plate, which are also connected with the battery bank. The target active power of the battery is controlled according to the difference of dynamic PV and load power.

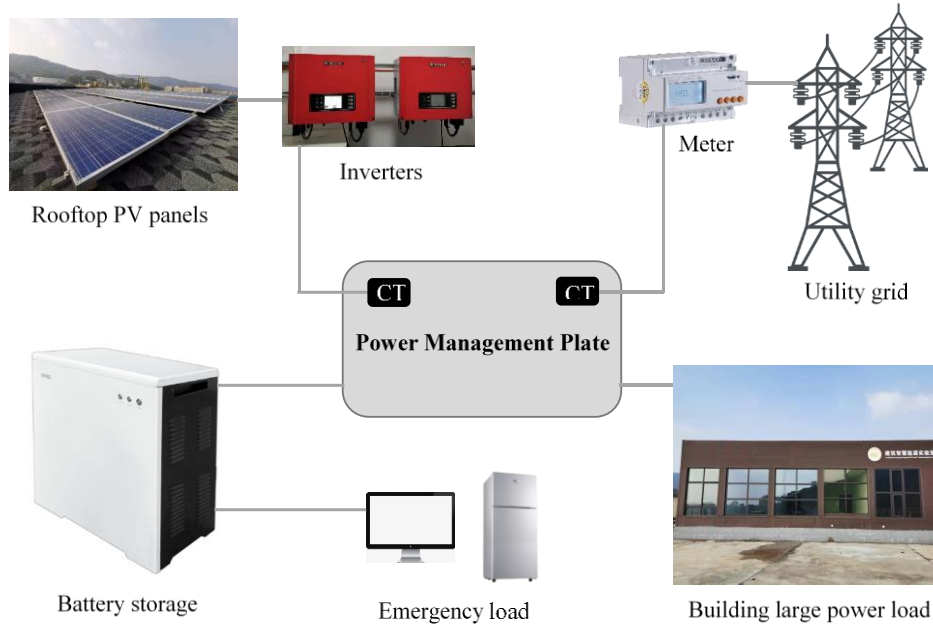


Fig. 4.2 Schematic of the grid-connected PV-battery system in the testing platform

The first realized energy management strategy aims to maximize the self-consumption ratio of the PV-battery system as shown in Fig. 4.3. Three days (15, 16, 17 December) with different weather conditions were chosen to operate the maximizing self-consumption strategy. The dynamic PV generation, load power, grid power and battery SOC were collected for data analysis.

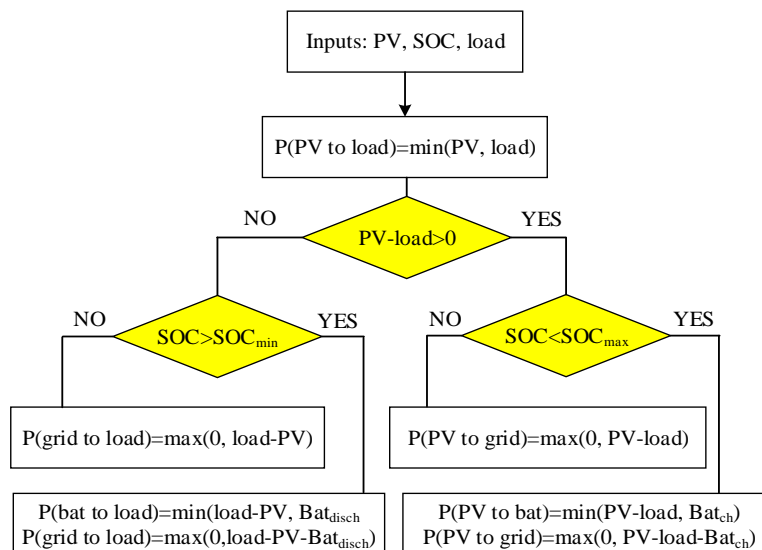


Fig. 4.3 Energy management flow of the maximizing self-consumption strategy

The second realized strategy is time-of-use strategy operated in 18, 19, 20 December as shown in Fig. 4.4.

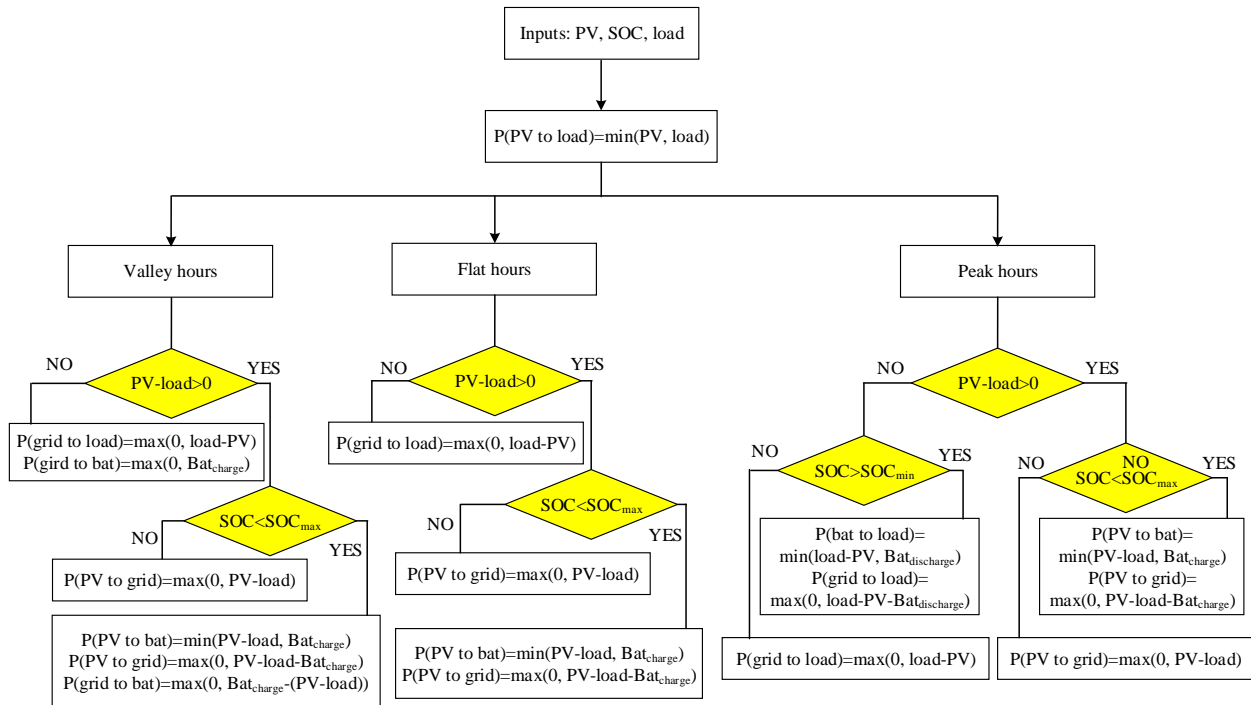


Fig. 4.4 Energy management flow of the time-of-use strategy

The dynamic PV power output during these six testing days is shown in Fig. 4.5.

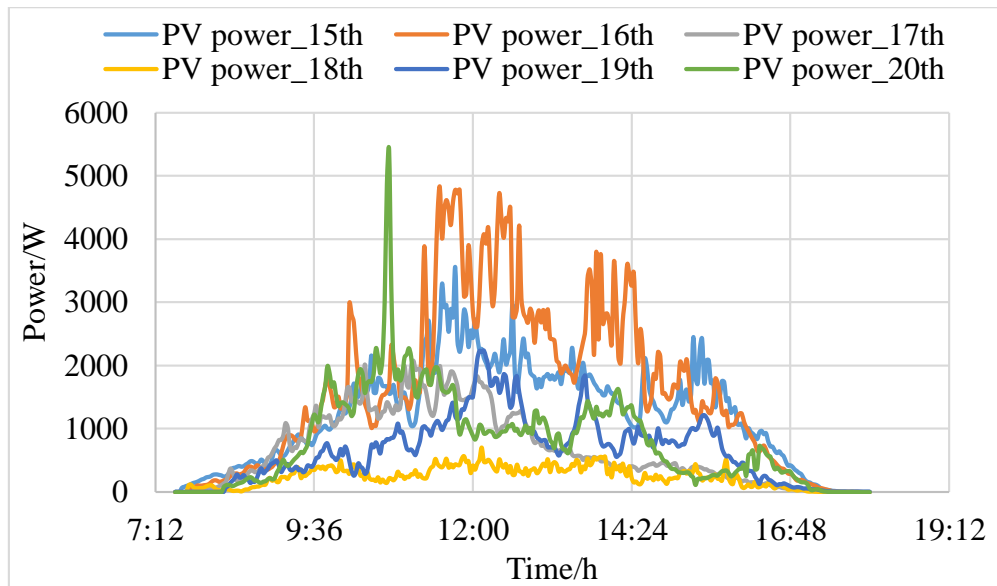


Fig. 4.5 PV power output during six experimental days

4.2 Experimental results and model validation

The PV battery system under these two basic energy management strategies are further established in TRNSYS to compare the simulation and experiment results. The power flow under the maximizing self-consumption strategy (in 15 Dec.) and time-of-use strategy (in 18 Dec.) are shown in Figs. 4.6-4.7, and the battery SOC is compared to show the case validation.

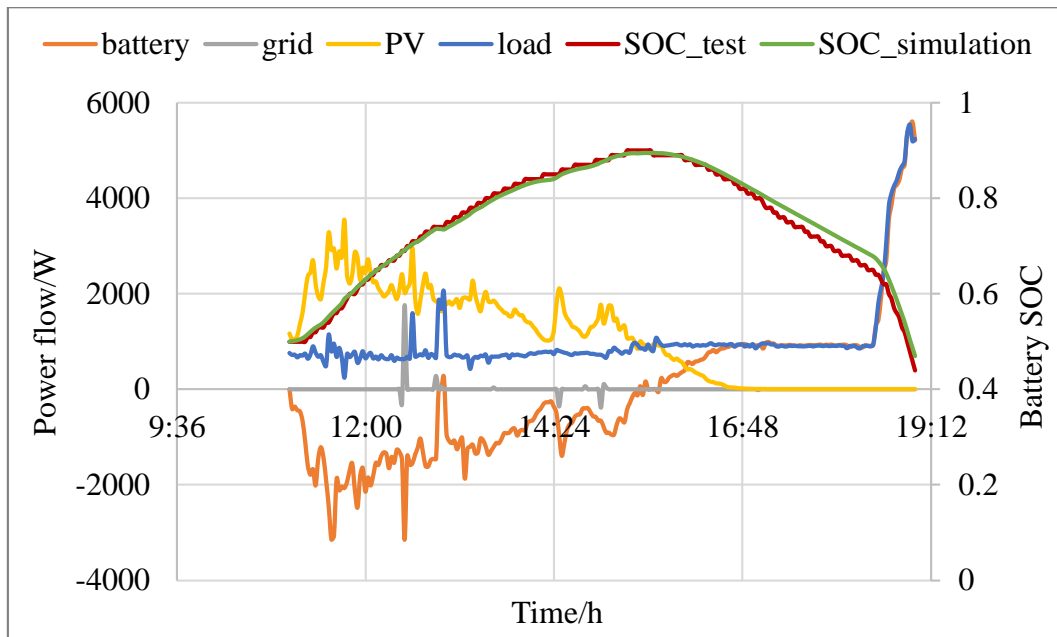


Fig. 4.6 Power flow under the maximizing self-consumption strategy in 15th Dec.

The PV self-consumption ratio and load self-sufficiency are 0.985 and 0.993 in the maximizing self-consumption strategy, while these ratios decrease to 0.698 and 0.625 respectively if there is no battery storage under the same power input and strategy. It indicates that the battery storage is important to improve on-site PV power consumption and system self-sufficiency. The grid feed-in energy would increase from 0.365 kWh to 4.768 kWh if battery storage is not used in the system, and the imported energy from grid would also rise from 0.58 kWh to 4.683 kWh when battery is absent from the system. The root mean square deviation and mean bias error

between the simulated values from the tested values under the maximizing self-consumption strategy in 15th December are 1.49% and 0.99% respectively as per Table 4.2. The maximum error deviation between testing SOC and simulated SOC is 0.0349 (relative error 6.8%) which happens between 17:00 to 18:30, since the Hall sensors collecting the inverter power signal and grid power signal has internal equipment error when both PV and load power is relatively low during this period.

Table 4.2 Battery SOC error analysis of two tested strategies

Strategy	Root mean square error	Mean bias error	Maximum relative error
Maximizing self-consumption	1.49%	0.99%	6.80%
Time-of-use	0.94%	0.84%	3.93%

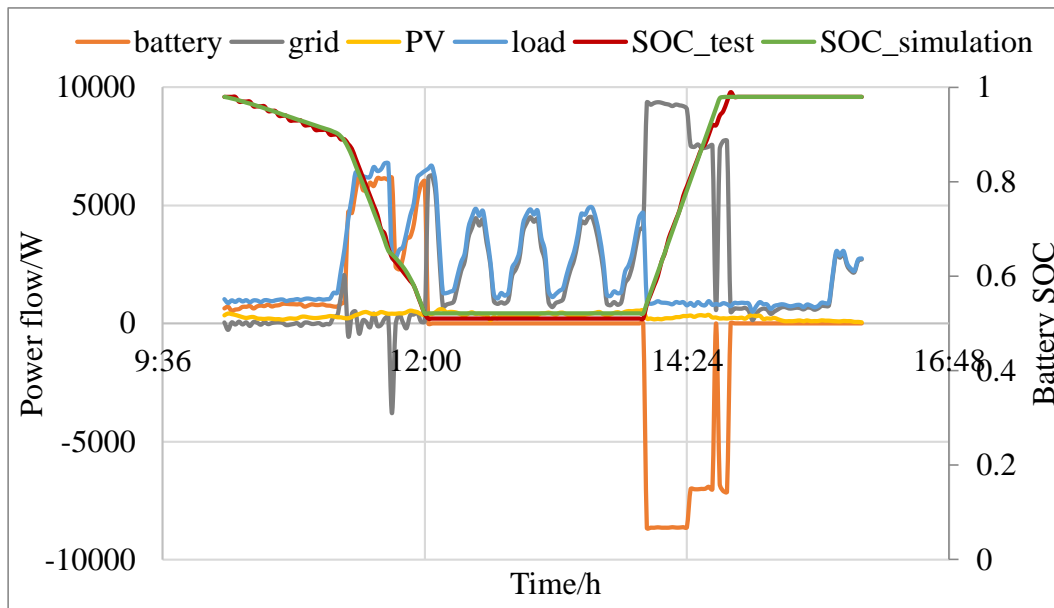


Fig. 4.7 Power flow under the time-of-use strategy in 18th Dec.

The PV self-consumption ratio is 100% even there is no battery storage in 18th, since the generated PV power is limited. But the load sufficiency can be increased from 0.197 in the case of

no battery storage to 0.44 with battery, since the battery is charged by grid in the low-price period under the time-of-use strategy. The root mean square deviation and mean bias error between the simulated values from the tested values under the maximizing PV self-consumption strategy are 0.94% and 0.84% respectively as per Table 4.2. The maximum error deviation between testing SOC and simulated SOC is 0.0369 (relative error 3.93%) when the battery SOC approaches to its maximum, since the actual battery SOC is not theoretically accurate when the battery is almost being fully charged.

CHAPTER 5 DESIGN OPTIMIZATION OF A SOLAR PHOTOVOLTAIC AND BATTERY STORAGE SYSTEM FOR A SINGLE LOW-ENERGY BUILDING

Based on the experimental study on the solar photovoltaic and battery storage system in Chapter 4, this chapter aims to study the design optimization of an actual solar photovoltaic and battery storage system installed in a low-energy building in Shenzhen to improve the system performances. A novel energy management strategy considering the battery cycling aging, grid relief and local time-of-use pricing is proposed. Single-criterion optimizations are performed focusing on four major aspects of the solar photovoltaic and battery storage system, including the energy supply, battery storage, utility grid and whole system. Meanwhile, the multi-criterion optimization is performed focusing on the overall performance of above four aspects for a comprehensive technical, economic and environmental evaluation. And both local sensitivity analyses and global sensitivity analyses are conducted to further quantify the significance and impact of selected design parameters.

5.1 Framework of design optimization of the solar photovoltaic and battery storage system for the single low-energy building

This study aims to analyze and optimize the solar photovoltaic (PV) and battery storage system installed in a real low-energy building in an urban city of China, with the study framework shown in Fig. 5.1. Optimum energy management strategies for the PV-battery system need to be explored, as the existing management strategy (see Case 1) cannot make full use of the energy conversion and storage system. The PV energy utilization is limited with a high system cost,

because surplus PV power is not fed into the utility grid to gain the local PV feed-in tariff (FiT) incentive and a fixed grid pricing scheme is applied to the existing building. The existing operation scenario is therefore modelled as the baseline case for comparison.

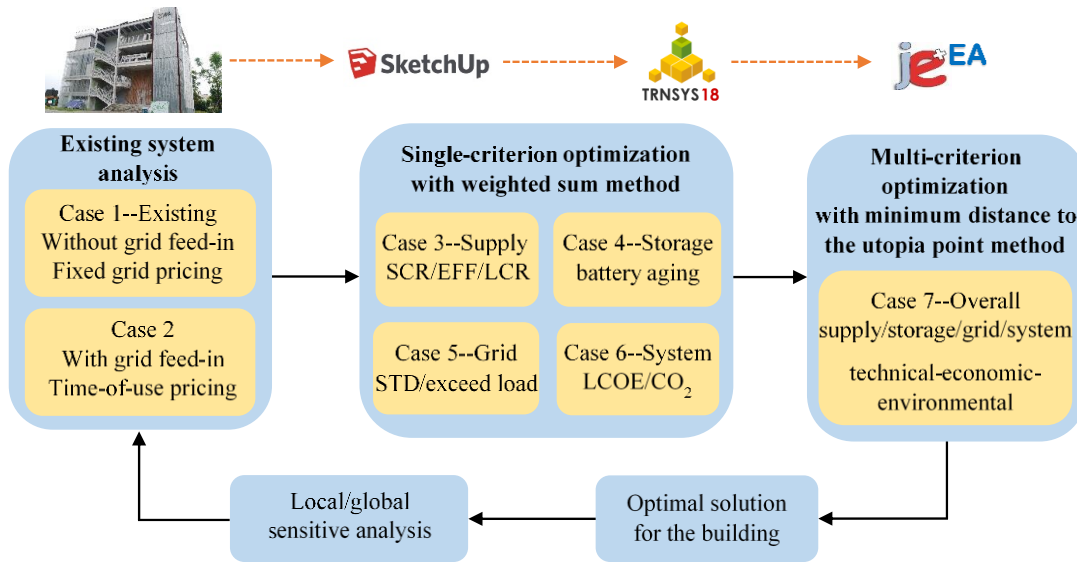


Fig. 5.1 Design optimization framework of the PV-battery system in the low-energy building

In order to improve the existing system performance, Case 2 is firstly proposed based on the same system configuration with Case 1 but a new control strategy considering the grid feed-in and time-of-use pricing. On top of Case 2, both single-criterion and multi-criterion optimizations are conducted with three optimization variables: the battery cell number, grid export limit, and grid import limit. The optimization analyses are conducted on the joint modeling and optimization platform of TRNSYS and jEPlus+EA with the Non-dominated sorting genetic algorithm (NSGA-II) at a simulation time step of 0.125 h. Regarding the optimization design and objectives, single-criterion optimizations (Cases 3-6) with the weighted sum method are performed, focusing on four major aspects of the PV-battery system including the energy supply, battery storage, utility grid and whole system. Case 3 aims to optimize the supply performance with a combined objective of three indicators, including the PV self-consumption ratio (SCR), PV power utilization efficiency

(EFF) and load cover ratio (LCR). Case 4 focuses on the battery health by minimizing the battery cycling aging. Case 5 explores the grid relief potential to minimize the standard deviation (STD) of the net grid power and reduce the exceeded load. Case 6 intends to achieve good economic and environmental system performances considering the levelized cost of energy (LCOE) and CO₂ emissions. Then, the multi-criterion optimization is performed with the minimum distance to the utopia point method in Case 7, focusing on the overall performance of above four aspects for a comprehensive technical, economic and environmental evaluation of the PV-battery system. Finally, local sensitivity analyses based on the optimal solution and global sensitivity analyses with the Fourier Amplitude Sensitivity Test (FAST) are conducted to further quantify the significance and impact of selected design parameters.

5.2 Low-energy building with the solar photovoltaic and battery storage system in Shenzhen



Fig. 5.2 Low-energy building installed with the PV-battery system in Shenzhen

The low-energy building is located in Shenzhen of China with a hot and humid climate, and it is mainly designed for office and exhibition functions. Fig. 5.2 shows the appearance of the building installed with the PV-battery system and energy management center.

The total building area is 658.15 m² with 3 floors and the detailed as-built parameters are shown in Table 5.1.

Table 5.1 Thermal properties of the low-energy building

Building	Parameter	Value
Roof	Heat transfer coefficient	0.30 W/(m ² ·K)
	Thermal inertia index	1.07
External-wall	Heat transfer coefficient	0.43 W/(m ² ·K)
	Thermal inertia index	2.78
External-window	Window-wall ratio	East: 0.47; South: 0.59; West: 0.45; North: 0.40
	Heat transfer coefficient W/(m ² ·K)	East: 2.64; South: 2.38; West: 2.14; North: 2.51
	Shading coefficient	East: 0.30; South: 0.22; West: 0.16; North: 0.26
Lighting	Office power density	5.80 W/m ²
	Laboratory power density	7.70 W/m ²
	Corridor power density	2.50 W/m ²
	Convective heat transfer ratio	0.33 [118]
	Radiant heat transfer ratio	0.67 [118]
Occupant [118]	Sensible heat	66 W/person
	Latent heat	68 W/person
	Convective heat transfer ratio	0.4
	Radiant heat transfer ratio	0.6
Equipment [118]	Office power density	15 W/m ²
	Laboratory power density	15 W/m ²
	Corridor power density	5 W/m ²
	Convective heat transfer ratio	0.3
	Radiant heat transfer ratio	0.7

In terms of the PV-battery system, thin-film PV panels are used with a total rated capacity of 13.12 kW, and a battery bank with a rated capacity of 45.6 kWh is installed. The detailed specification of the PV-battery system is shown in Table 5.2.

Table 5.2 Specification of the PV-battery system in the low-energy building

Solar panel	ASP-S1-80W (CdTe)
Maximum power	80 W
Open circuit voltage	118.5 V
Short circuit current	1.01 A
Voltage at max. power point	92 V
Current at max. power point	0.88 A
Maximum system voltage	1000 V
Rooftop cell number	149
Façade PV cell number	15
Battery	NP100-12FR (Lead-Acid)
Nominal capacity	100 Ah/12 V
Number in series	38
Operational SOC (SOC_{min} - SOC_{max})	25%-90% [96]
Max. charging/discharging rate	0.2C
Charging efficiency	0.9
Life cycle	1000 cycles [18]

5.3 System modelling and management of the solar photovoltaic and battery storage system

Fig. 5.3 shows the schematic of the developed PV-battery model based on the TRNSYS platform, where five main components, namely the building load, PV panel, battery storage, utility grid, and energy management strategy are integrated. A SketchUp model of the building is firstly established according to practical building dimensions, and then imported into TRNSYS to define internal building properties. According to the practical building configuration, the load is calculated with submodules of the building envelope, ventilation, air conditioning, indoor occupant, equipment and lighting based on Type 56, Type 117, Type 752, Type 655, Type 648 and other auxiliary components in the TRNSYS library [119]. The typical meteorological year weather data of Shenzhen is connected to the building and PV generators [120].

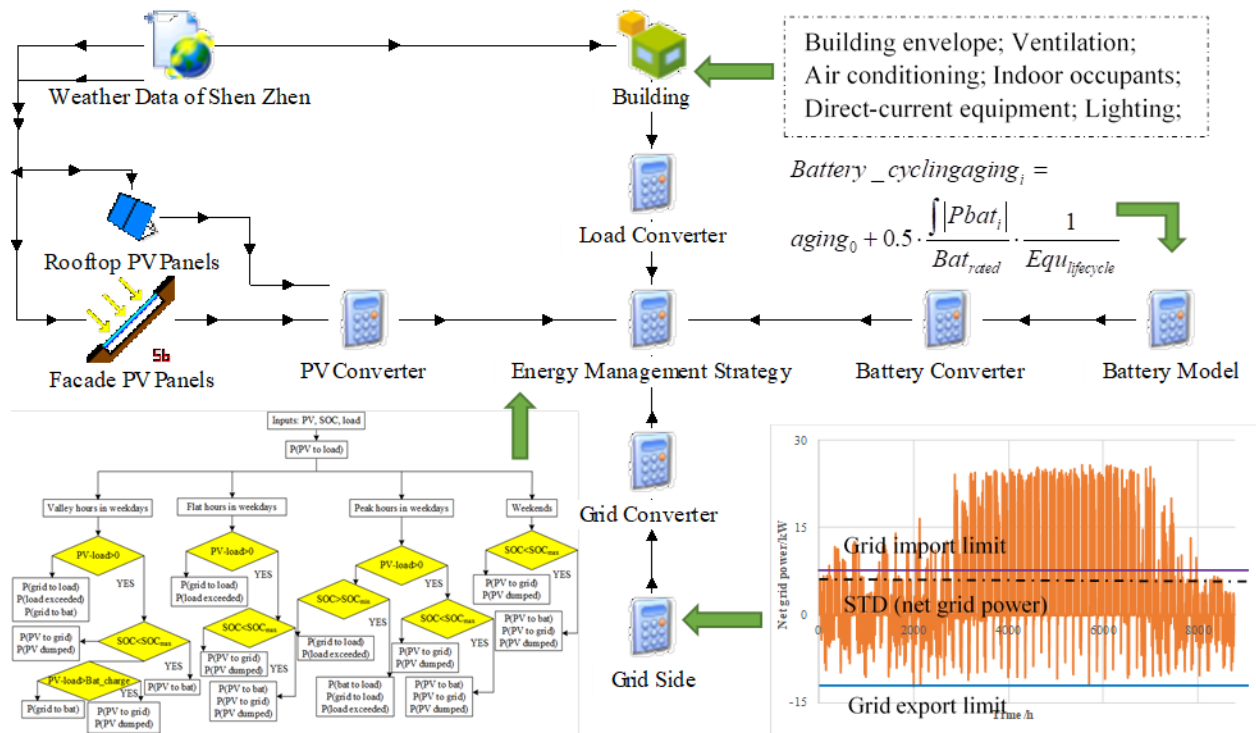


Fig. 5.3 Simulation model of the PV-battery system in TRNSYS environment

This study aims to improve the overall performance of the PV-battery system considering the supply efficiency, battery health, grid integration and system economic-environmental impact by developing a new energy management strategy as shown in Fig. 5.4. When the PV power is available, it is firstly supplied to meet the building load as shown in Eq. (5.1):

$$P_{PV\ to\ load} = \min(P_{PV}, P_{load}) \quad (5.1)$$

where P_{PV} is the generated power of PV panels considering an inverter efficiency of 0.95, kW; P_{load} is the building load demand, kW.

Then the power flow is directed according to peak-valley hours in the day. During valley hours in weekdays, surplus PV power after meeting the load is used to charge the battery as shown in Eq. (5.2) with a charging efficiency of 0.9:

$$P_{PV\ to\ battery} = \min((P_{PV} - P_{load}), Bat_{charge}) \quad (5.2)$$

where Bat_{charge} is the available charge capacity of the battery bank formulated as Eq. (5.3):

$$Bat_{charge} = \max((SOC_{max} - SOC) \cdot Bat_{rated} \cdot SOH/step, Charge_{max} \cdot Bat_{rated} \cdot SOH) \quad (5.3)$$

where Bat_{rated} is the rated capacity of the battery bank, kWh. $step$ is the simulation time step (0.125 h). $Charge_{max}$ is the maximum charge rate of the lead-acid battery in the targeted building (0.2C).

Then surplus PV power after meeting the load and battery is fed into the utility grid and gets FiT allowance as shown in Eq. (5.4):

$$P_{PV\ to\ grid} = \min(Grid_{export} \cdot PV_{rated}, P_{PV} - P_{load} - Bat_{charge}) \quad (5.4)$$

where $Grid_{export}$ is the grid export limit as a ratio of rated PV power PV_{rated} . If surplus PV power exceeds the grid export limit, the exceeded part is dumped as per Eq. (5.5):

$$P_{PV\ dumped} = \max(0, P_{PV} - P_{load} - Bat_{charge} - Grid_{export} \cdot PV_{rated}) \quad (5.5)$$

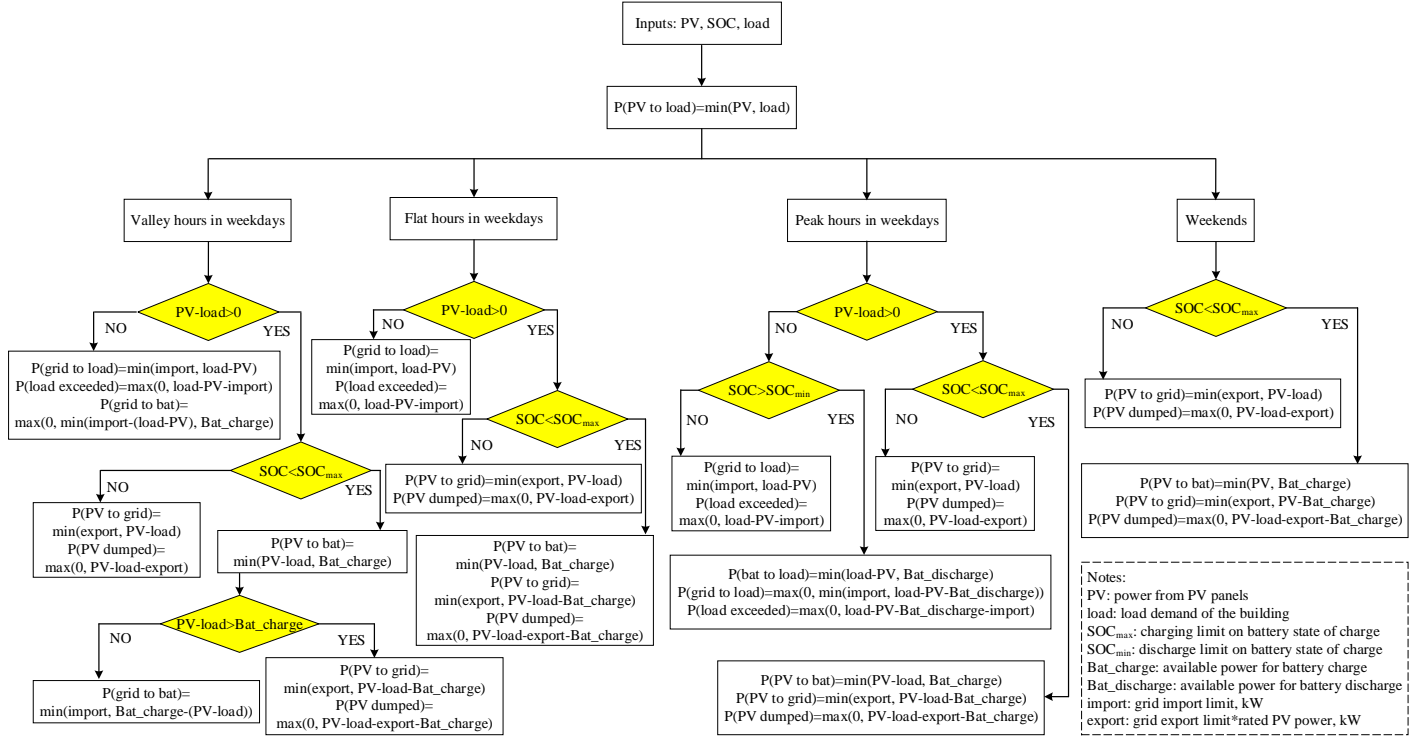


Fig. 5.4 Energy management strategy of the PV-battery system in the low-energy building

If PV power is not enough for the building load or battery, the utility grid can meet both the load and battery demand given the low grid price in valley hours as per Eqs. (5.6-5.8):

$$P_{grid\ to\ load} = \min(Grid_{import}, P_{load} - P_{PV}) \quad (5.6)$$

where $Grid_{import}$ is the power import limit from the utility grid, kW. It should be noted that the exceeded load with reference to $Grid_{import}$ are still met by the grid, but the exceeded battery demand is not met by the grid.

$$P_{exceeded\ load} = \max(0, P_{load} - P_{PV} - Grid_{import}) \quad (5.7)$$

$$P_{grid\ to\ battery} = \min(Grid_{import} - (P_{load} - P_{PV}), Bat_{charge}) \cdot LT(P_{PV}, P_{load}) + \min(Grid_{import}, Bat_{charge} - (P_{PV} - P_{load}) \cdot GE(P_{PV}, P_{load})) \quad (5.8)$$

where $LT(P_{PV}, P_{load})$ means that the PV power is lower than the building load and the grid is used to meet both the unsatisfied load and battery. And $GE(P_{PV}, P_{load})$ means the PV power is not lower than the building load so that the battery can be charged by both PV and grid.

During flat hours with a relatively high grid electricity price, the grid is not used to charge the battery even when surplus PV power after meeting the building load is not enough for charging the battery. And during peak hours with the highest grid electricity price, the battery takes precedence over the grid to meet the unsatisfied load from PV power as shown in Eq. (5.9):

$$P_{battery\ to\ load} = \min(P_{load} - P_{PV}, Bat_{discharge}) \quad (5.9)$$

where $Bat_{discharge}$ is the available discharge capacity of the battery as per Eq. (5.10):

$$Bat_{discharge} = \max((SOC - SOC_{min}) \cdot Bat_{rated} \cdot SOH/step, Discharge_{max} \cdot Bat_{rated} \cdot SOH) \quad (5.10)$$

where $Discharge_{max}$ is the maximum discharge rate of the lead-acid battery in the building (0.2C).

As the building is not in operation during weekends, the PV power is firstly used to charge the battery and then fed into the utility grid. And the residual PV power over the grid export limit is dumped.

5.4 System design optimization of the solar photovoltaic and battery storage system

Single-criterion and multi-criterion optimizations are conducted considering the technical, economic and environmental performances of the PV-battery system with the joint TRNSYS and jEPlus+EA platform. Three optimization variables are adopted in the system design optimization including the battery cell number, grid export limit and grid import limit. The search range of the battery cell number is 2 - 100 at an increment of 2 cells. The grid import limit varies between 0 -

30 kW at the step of 1 kW, while the grid export limit is expressed as the ratio of rated PV power changing within the range of 0 - 1 at an increment of 0.1. Eight optimization objectives are established under four major aspects of the PV-battery system, including the energy supply, battery storage, utility grid and whole system as shown in Fig. 5.5. For the energy supply aspect, three indicators including SCR, EFF and LCR are combined as the performance criterion. For the battery storage aspect, the annual battery cycling aging is the only focus. And for the utility grid aspect, two indicators including STD of net grid power and the exceeded load are integrated as the criterion. And for the whole system aspect, LCOE and CO₂ emission are synthesized as the whole system performance criterion.

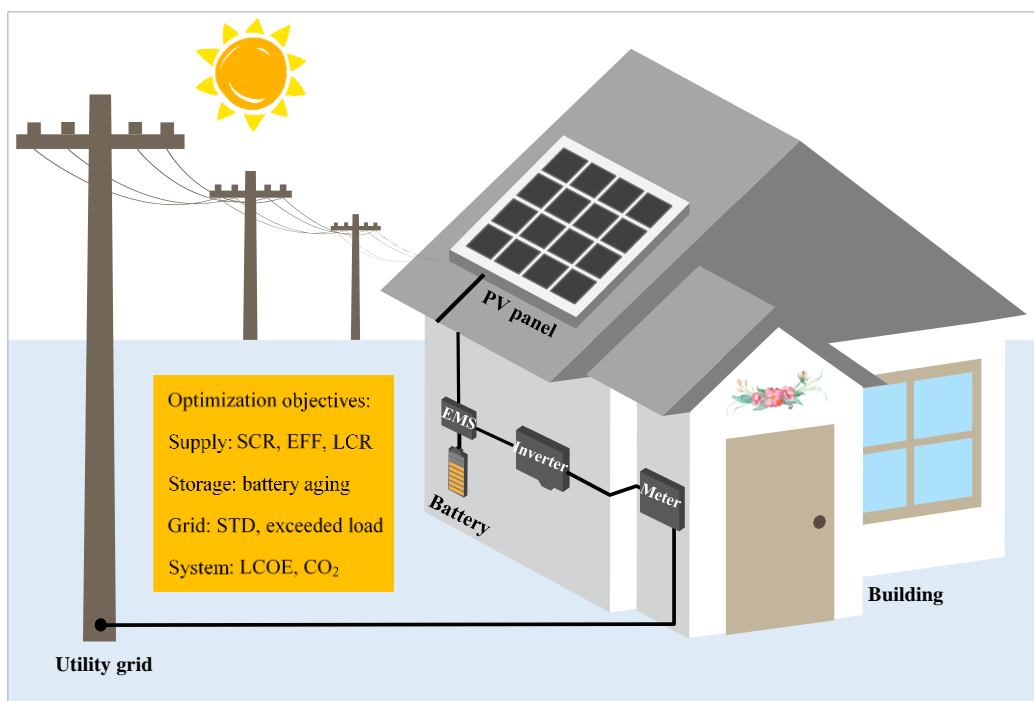


Fig. 5.5 Optimization objectives of the PV-battery system

Table 5.3 shows detailed parameters for the economic analysis of the PV-battery system in the building.

Table 5.3 Parameters for economic analysis of the PV-battery system

Parameter		Value
PV system	Initial cost ($c_{pv_initial}$)	1400 US\$/kW
	Life time (l_{pv})	20 years
Battery system	Initial cost ($c_{bat_initial}$)	150 US\$/kWh
	Life time ($l_{battery}$)	5 years
Inverter	Initial cost ($c_{inverter_initial}$)	90 US\$/kW
	Life time ($l_{inverter}$)	10 years
Grid FiT (c_{fit})		0.058 US\$/kWh [121]
Governmental subsidy (c_{sub})		0.014 US\$/kWh [121]
Discount rate (d)		4.5%/year [63]
Interest rate (i)		5.8%/year [63]
Electricity price (c_{ele})		See Table 5.4
Electricity price rising rate (i_{ele})		1.85%/year [122]
Life time of PV-battery system (l_{sys})		20 years

Table 5.4 Electricity price of the utility grid in different periods

Price mode [123]	Time	Hours	Price (\$/kWh)
Time-of-use pricing	Valley period	23:00-7:00	0.04
	Flat period	7:00-9:00, 11:30-14:00, 16:30-19:00, 21:00-23:00	0.10
	Peak period	9:00-11:30, 14:00-16:30, 19:00-21:00	0.15
Fixed pricing	All period	0:00-24:00	0.10

In order to obtain a single-criterion optimum solution in Cases 3-6 focusing on the energy supply, battery storage, utility grid, and whole system performance criterion respectively, the weighted sum method [124] is used by allocating the same weighting to corresponding objectives in these cases. In Case 7, all normalized criteria are subject to a multi-criterion optimization to find the final optimum solution, determined by the minimum distance to the utopia point method [125]. And the optimization criteria of Cases 3-7 are shown in Table 5.5.

Table 5.5 Optimization criteria of optimization cases of PV-battery systems

Optimization case		Optimization criterion
Single-criterion optimization	Case 3:	$Supply_{optimal} = \frac{1}{3} \frac{SCR - SCR_{min}}{SCR_{max} - SCR_{min}} + \frac{1}{3} \frac{EFF - EFF_{min}}{EFF_{max} - EFF_{min}} + \frac{1}{3} \frac{LCR - LCR_{min}}{LCR_{max} - LCR_{min}}$
	Case 4:	$Storage_{optimal} = \frac{aging - aging_{min}}{aging_{max} - aging_{min}}$
	Case 5:	$Grid_{optimal} = \frac{1}{2} \frac{STD - STD_{min}}{STD_{max} - STD_{min}} + \frac{1}{2} \frac{EXL - EXL_{min}}{EXL_{max} - EXL_{min}}$
	Case 6:	$System_{optimal} = \frac{1}{2} \frac{LCOE - LCOE_{min}}{LCOE_{max} - LCOE_{min}} + \frac{1}{2} \frac{CO_2 - CO_{2\ min}}{CO_{2\ max} - CO_{2\ min}}$
Multi-criterion optimization	Case 7:	$Overall_{optimal} = \left[Supply_{optimal}, Storage_{optimal}, Grid_{optimal}, System_{optimal} \right]^T$

Table 5.6 shows the targeted optimization criteria and corresponding design solutions of the studied cases. Case 1 is the existing case in the building under fixed grid electricity pricing without grid feed-in as the baseline for comparison. Case 2 introduces time-of-use electricity pricing and allows grid feed-in from the PV system without limitations. Cases 3-6 individually optimizes each aspect of the PV-battery system, including the energy supply, battery storage, utility grid and whole system economic-environmental performance. Case 7 simultaneously optimizes technical,

economic and environmental performances in all four aspects of the PV-battery system with a robust decision-making method.

Table 5.6 Optimization results of studied cases with PV-battery systems

Case	Case 1 (building existing)	Case 2 (grid feed-in and TOU)	Optimization				
			Case 3 (supply)	Case 4 (storage)	Case 5 (grid)	Case 6 (system)	Case 7 (overall)
Time-of-use pricing (TOU)	--	√	√	√	√	√	√
Supply optimal (max. SCR, EFF and LCR)	--	--	√	--	--	--	√
Storage optimal (min. battery aging)	--	--	--	√	--	--	√
Grid optimal (min. STD and exceeded load)	--	--	--	--	√	--	√
System optimal (min. LCOE and CO ₂ emission)	--	--	--	--	--	√	√
Optimization parameters							
Battery cell number	38	38	100	100	28	2	90
Grid import limit/kW	30	30	5	0	30	1-30	5
Grid export limit (ratio of PV rated power)	0	1	1	0-1	0	1	0.8

The Pareto-optimal solutions in Case 7 are shown in Fig. 5.6, which demonstrates the trade-off among four major aspects, including the energy supply, battery storage, utility grid and whole system. The final optimal solution highlighted as the red triangle is obtained using the decision-making strategy of the minimum distance to the utopia point [125].

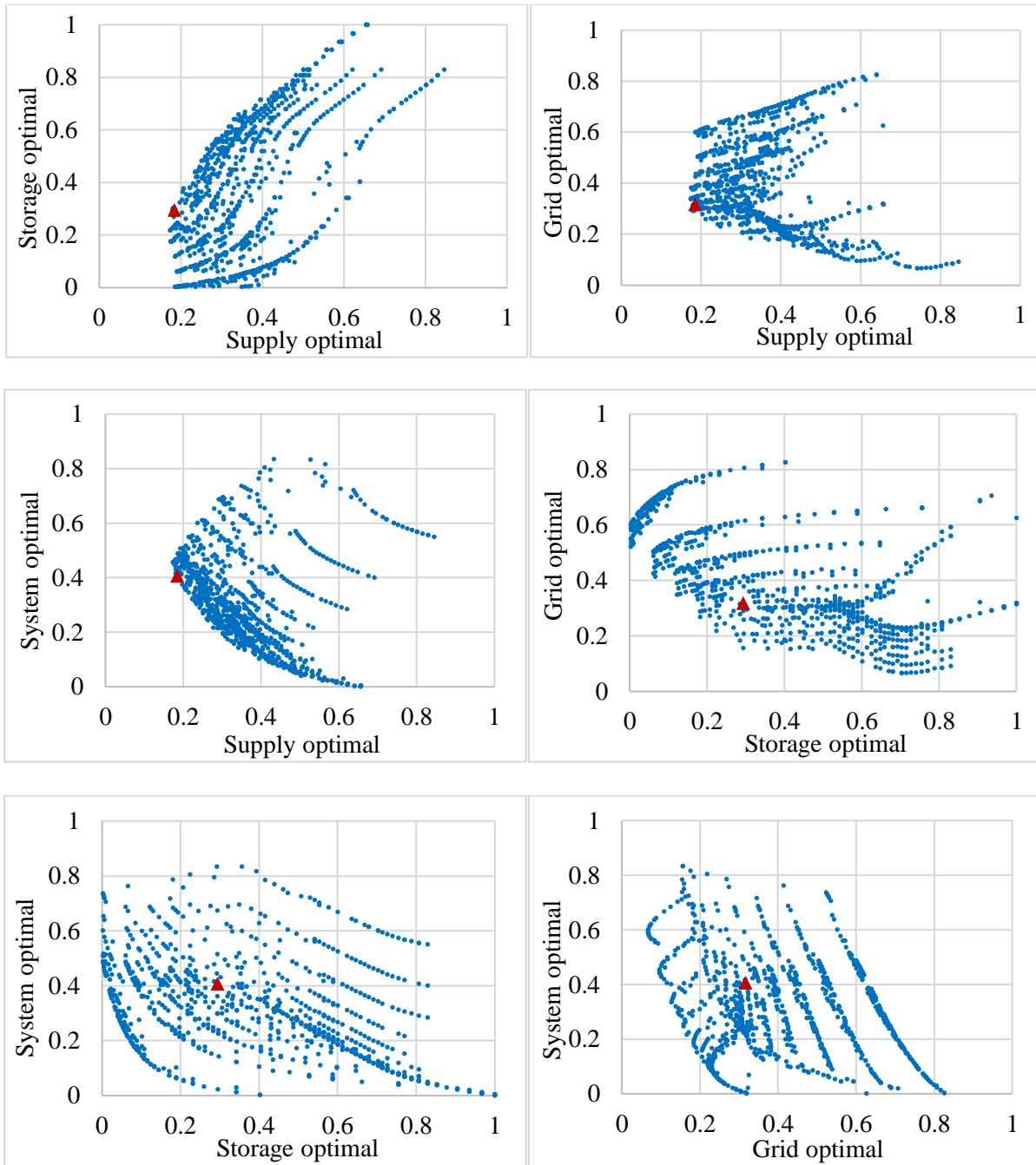


Fig. 5.6 Pareto-optimal solutions of the multi-criterion optimization case

5.5 Techno-economic-environmental performances of the solar photovoltaic and battery storage system

The PV-battery system performances in the four focused aspects, i.e. energy supply, battery health, grid relief, and system economic-environmental impact, are compared in this section across studied cases, to discuss the improvement potential of the novel energy management strategy.

5.5.1 Energy supply performance analysis

Figs. 5.7 and 5.8 show the power flow of the PV-battery system in the third week of June and December for Case 7. It shows that the building load generally exceeds the PV generation on typical weekdays in summer, when the battery is discharged to meet the unsatisfied load during peak hours and charged by the utility grid during valley hours. The power flow in winter differs with that in summer, as the building load is generally smaller with reduced air-conditioning load. Surplus PV power is then used to charge the battery and be fed into the grid with a lower frequency of battery discharge.

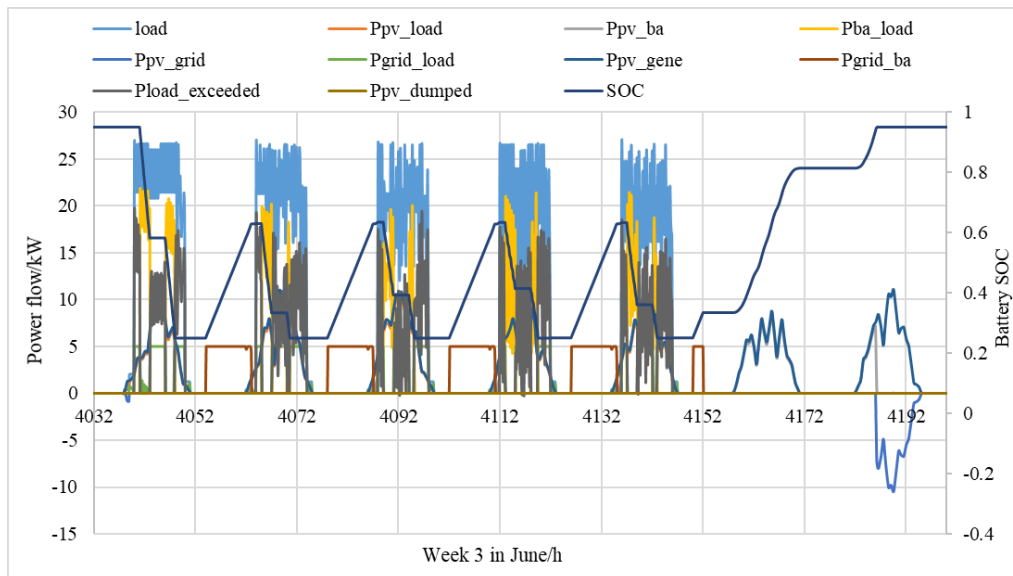


Fig. 5.7 Power flow in week 3 of June in Case 7 (overall optimum case)

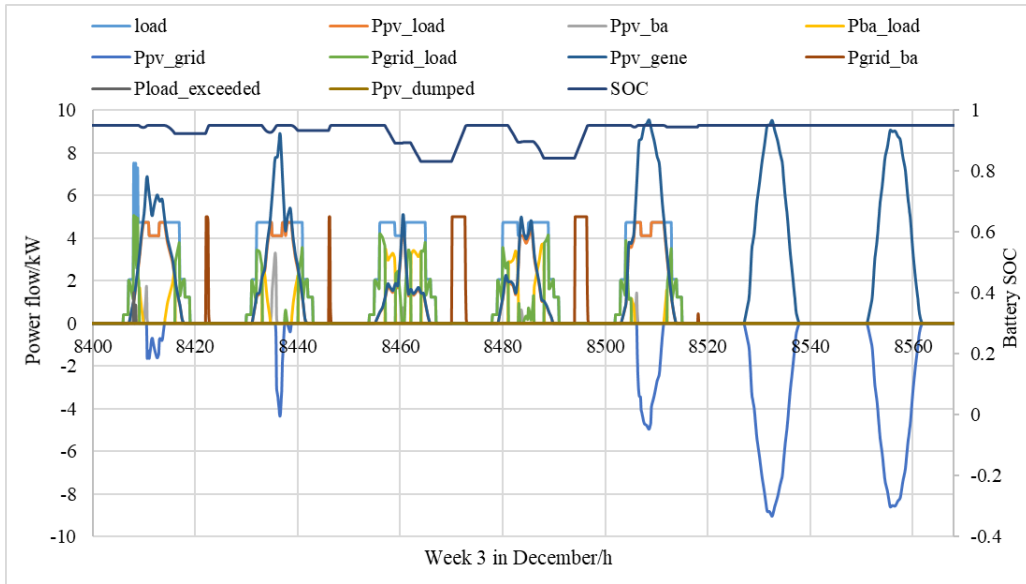


Fig. 5.8 Power flow in week 3 of December in Case 7 (overall optimum case)

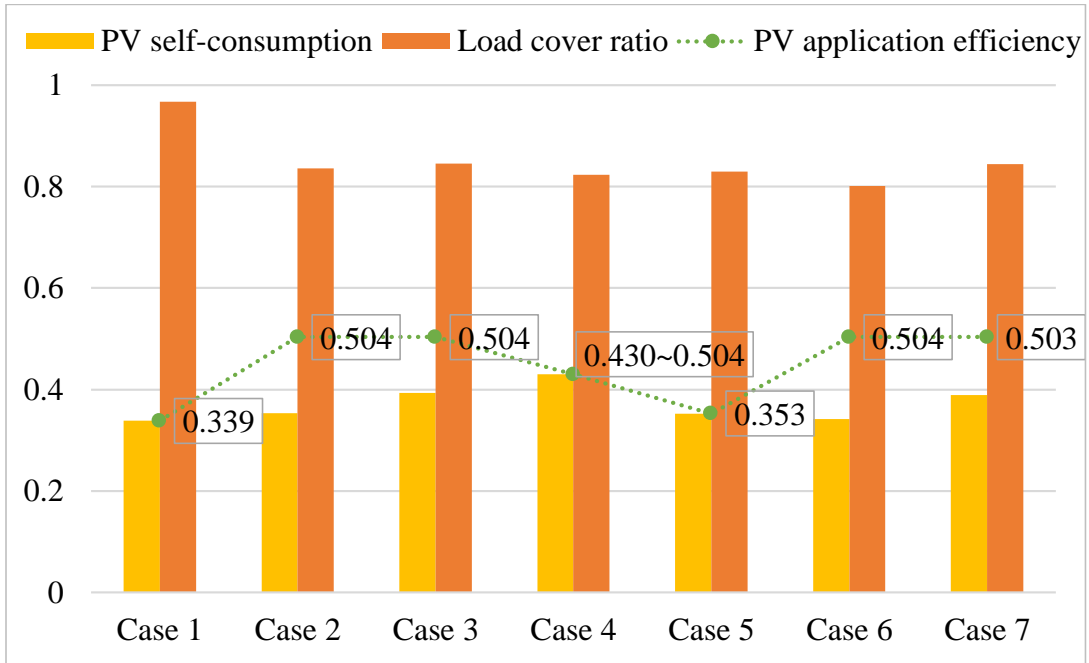


Fig. 5.9 Comparison of PV self-consumption, PV efficiency and load cover ratio

(Note: Case 1 is the existing case in the building, Case 2 allows grid feed-in and TOU, Case 3 optimizes the supply aspect, Case 4 optimizes the storage aspect, Case 5 optimizes the grid aspect, Case 6 optimizes the system aspect, Case 7 optimizes overall aspects.)

In addition to introducing the hourly power flow of typical weeks in Case 7, the yearly results of three optimized energy supply indicators under the seven focused cases are also studied to make a comprehensive case comparison as shown in Fig. 5.9. Case 1 has the maximum annual average LCR, as the power from PV or battery is directed to meet the building load whenever available under the fixed grid pricing mode. However, Case 1 performs worst in SCR and EFF due to the strict limitation on grid export power. Compared with Case 1, EFF in Case 2 is increased by nearly 48.6% with the grid feed-in permission. Case 3 achieves the best overall performance in these three energy supply performance indicators, as a result of the judicious mono-criterion optimization. Case 4 has the maximum SCR because battery charging by grid is controlled by a grid import limit of 0 kW and the battery can only be charged by PV. In addition, EFF varies between 0.430 and 0.504 as the grid export limit is not a significant factor for Case 4. SCR and EFF of Case 7 are increased by 15.0% and 48.6% than that of Case 1.

5.5.2 Battery health performance analysis

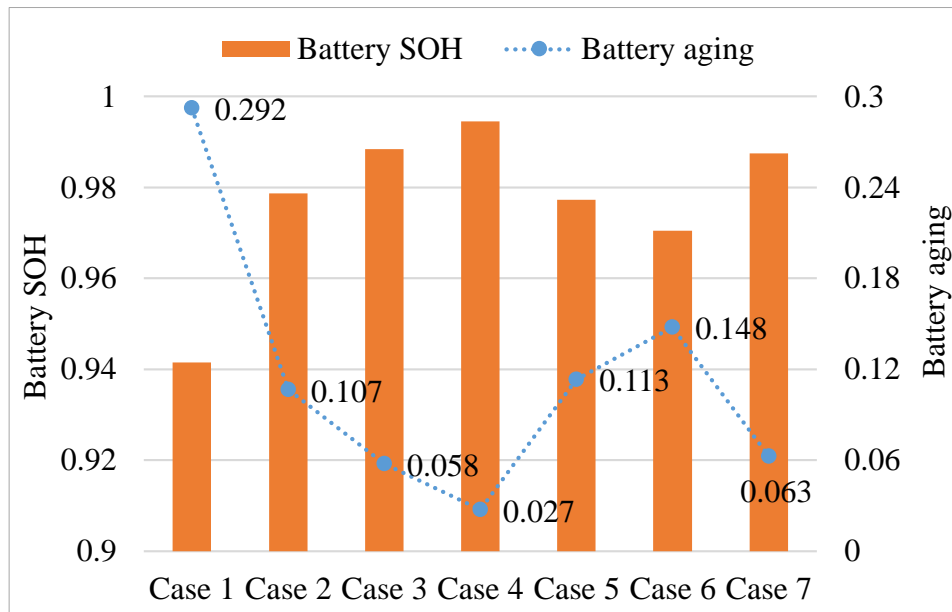


Fig. 5.10 Comparison of battery state of health and cycling aging

(Note: Case 1 is the existing case in the building, Case 2 allows grid feed-in and TOU, Case 3 optimizes the supply aspect, Case 4 optimizes the storage aspect, Case 5 optimizes the grid aspect, Case 6 optimizes the system aspect, Case 7 optimizes overall aspects.)

Fig. 5.10 compares battery cycling aging and SOH of studied cases. The annual cycling aging of the battery bank in Case 4 with the rated capacity at 120 kWh is the minimized by single-criterion optimization to about 0.027, leading to a high usable battery capacity of about 99.5% of its rated capacity after one-year operation. The calculated battery cycling aging is generally consistent with the result of an existing literature reporting a 0.124 cycling degradation of the lead-acid battery with the capacity of 165.6 kWh during four-year operation [93]. The maximum cycling aging is about 0.292 in Case 1 with a smaller battery number of 38 and unrestricted battery charging. The annual battery cycling aging of Case 7 is smaller than that of Case 1 by 78.5%, resulting in the extension on the battery SOH from 94.2% in the baseline case to 98.7%. It is therefore proved significant to consider the battery health management in PV-battery systems.

5.5.3 Grid relief performance analysis

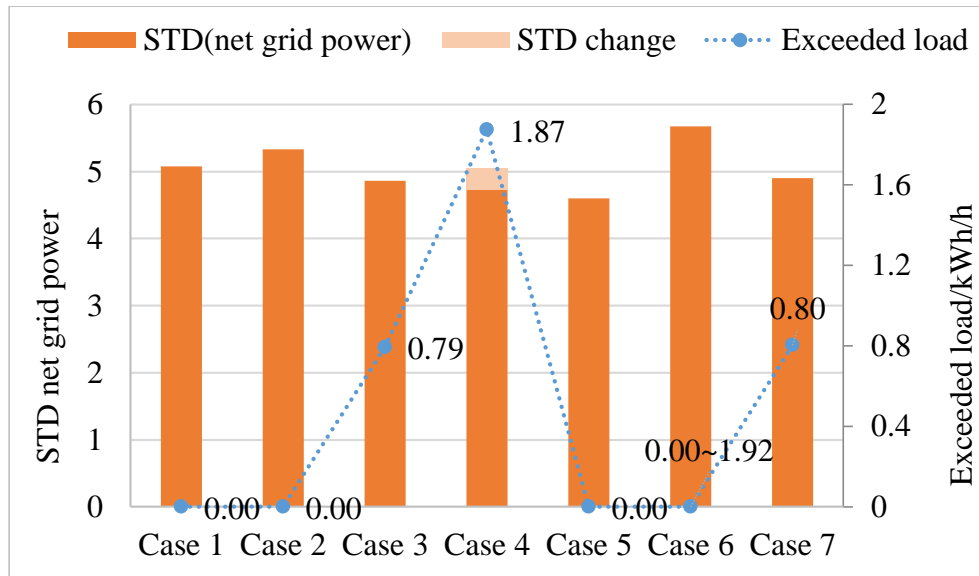
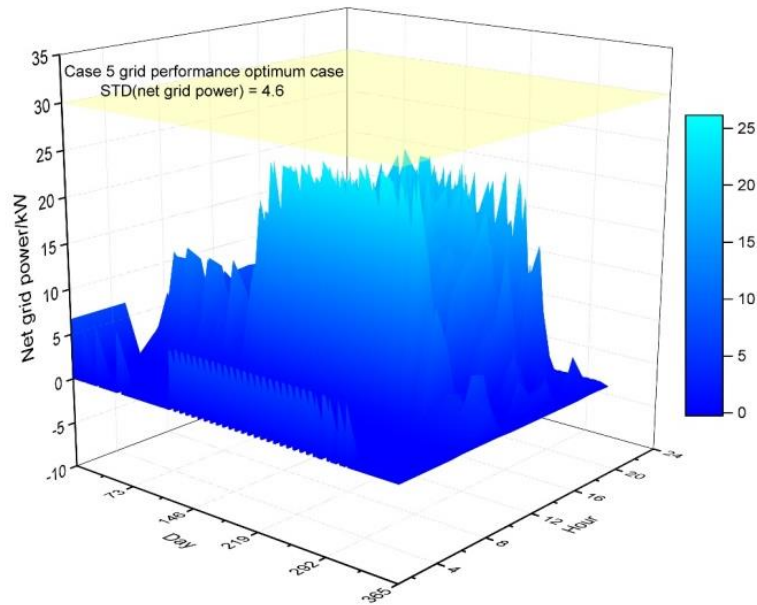


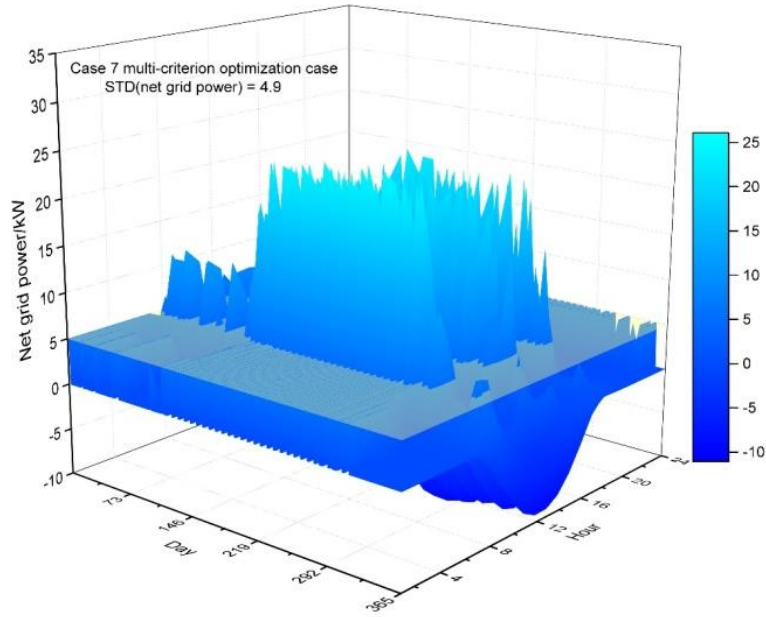
Fig. 5.11 Comparison of standard deviation of net grid power and exceeded load

(Note: Case 1 is the existing case in the building, Case 2 allows grid feed-in and TOU, Case 3 optimizes the supply aspect, Case 4 optimizes the storage aspect, Case 5 optimizes the grid aspect, Case 6 optimizes the system aspect, Case 7 optimizes overall aspects.)

Fig. 5.11 compares the annual STD of the net grid power and exceeded load of these studied cases. Case 5 achieves the minimum average grid stress among all cases with the lowest STD of about 4.60 under 28 battery cells and strict limitation for grid power export. The annual average exceeded load in Case 5 is 0 due to the high grid import limit. The STD of net grid power in Case 6 reaches the maximum of 5.68 with a minimum battery cell number and no grid export limitation. The STD of net grid power in Case 4 changes from 4.72 to 5.05 given an optimized grid export limit ranging between 0 - 1, and the STD of Case 7 is smaller than that of Case 1 by 3.4%.



(a)



(b)

Fig. 5.12 Annual net grid power in Case 5 (a, grid optimum) and Case 7 (b, overall optimum)

The annual distribution of net grid power in the grid performance optimum case (Case 5) and multi-criterion optimization case (Case 7) is shown in Fig. 5.12, where grid import power is presented by positive values and grid export power is in negative values. The flow distribution in Case 5 is more centralized than that in Case 7 with a smaller STD by about 6.5%. The cross section in yellow is the grid import limit optimized to be 30 kW in Case 5 and 5 kW in Case 7. The average load exceeding the grid import limit is determined to be 0 in Case 5 and 0.8 kWh/h in Case 7, as a useful reference for grid operators to maintain the network stability.

5.5.4 System economic and environmental performances analysis

Fig. 5.13 compares the NPV and LCOE of the PV-battery system including the initial cost, maintenance cost, electricity bill, renewable energy subsidy and grid FiT within a 20-year operation. Case 6 has the minimum LCOE of about 0.124 US\$/kWh, which is lower than that of Case 1 of 0.170 US\$/kWh with a cost saving of nearly 26.8%. Case 4 has the maximum LCOE,

because of the high initial cost and electricity bill resulting from the large battery cell number and strict restriction on battery charging by the grid. Since the optimized grid export limit varies from 0 to 1 in Case 4, the present value of FiT changes from 0 to 2520 US\$ and the LCOE ranges between 0.228 to 0.235 US\$/kWh. The calculated LCOE value agrees with the result reported in a previous literature indicating that LCOE of current PV-battery systems is around the range of 0.15 to 0.21 US\$/kWh [126].

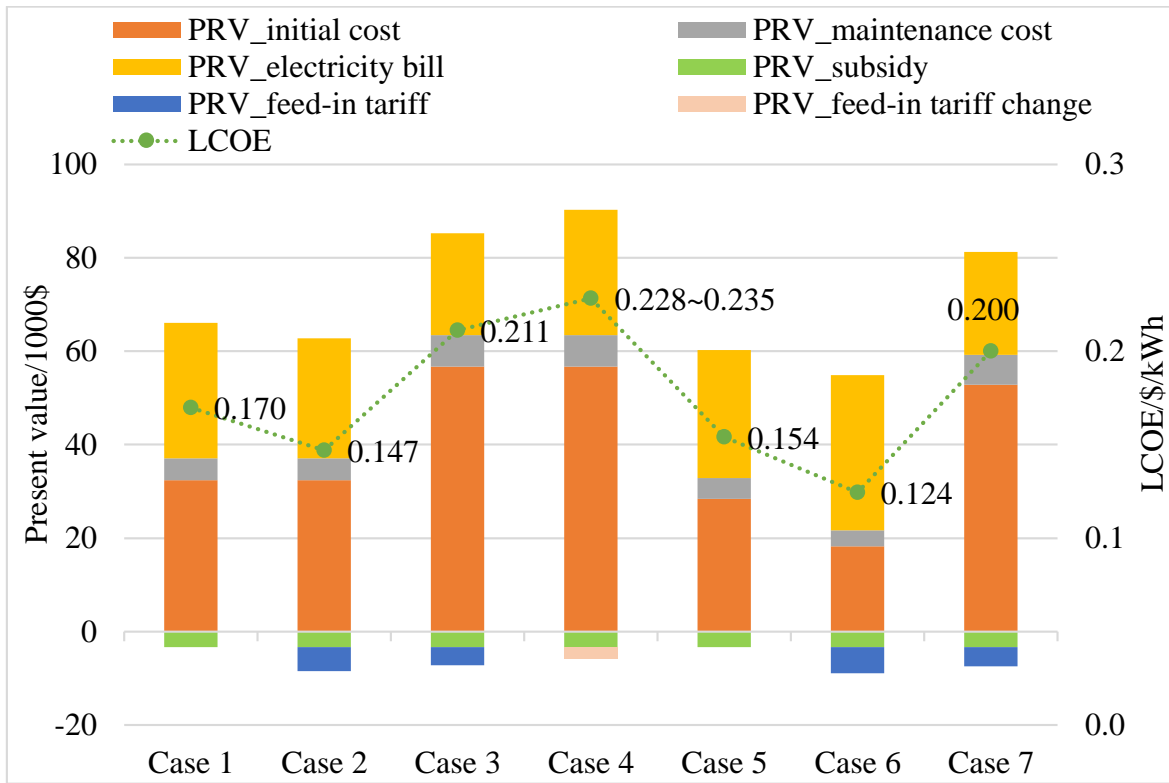


Fig. 5.13 Comparison of net present value and levelized cost of energy of studied cases

(Note: Case 1 is the existing case in the building, Case 2 allows grid feed-in and TOU, Case 3 optimizes the supply aspect, Case 4 optimizes the storage aspect, Case 5 optimizes the grid aspect, Case 6 optimizes the system aspect, Case 7 optimizes overall aspects.)

Table 5.7 Lifetime NPV and LCOE comparison of studied cases

Lifetime NPV (1000US\$) and LCOE (US\$/kWh)	Case 1	Case 2	Case 3	Case 4	Case 5	Case 6	Case 7
	Existing in building	Grid feed-in and TOU	Supply optimal	Storage optimal	Grid optimal	System optimal	Overall optimal
Initial cost PRV	32.37	32.37	56.71	56.71	28.44	18.24	52.78
Maintenance cost PRV	4.70	4.70	6.78	6.78	4.36	3.49	6.44
Electricity bill PRV	29.03	25.72	21.75	26.73	27.42	33.10	22.07
Subsidy PRV	-3.37	-3.37	-3.37	-3.37	-3.37	-3.37	-3.37
FiT PRV	0.00	-5.10	-3.87	-2.52~0.00	0.00	-5.52	-4.01
Total NPV	62.72	54.31	77.99	84.32~86.84	56.85	45.94	73.91
Total NPV saving	--	8.41	-15.27	-21.60~-24.12	5.87	16.78	-11.19
LCOE	0.170	0.147	0.211	0.228~0.235	0.154	0.124	0.200
LCOE saving	--	0.023	-0.041	-0.058~-0.065	0.016	0.046	-0.030

A detailed breakdown of NPV and LCOE calculations for studied cases is summarized in Table 5.7. It reveals that simply adding the grid feed-in permission and time-of-use pricing control (Case 2) can bring 5100 US\$ reimbursement from the grid feed-in and save 3310 US\$ electricity bills, compared with the existing operation case during the 20-year service time. As for Case 3 focusing on optimizing the energy supply performance, initial and maintenance costs are increased but the electricity bill is reduced and FiT is earned compared with the baseline case. When comparing Case 4 with the baseline case, LCOE is increased with the battery number rising from 38 to 100 while the battery is completely restricted from being charged by the grid. Case 5 has lower LCOE than the baseline case, mainly due to lower initial and maintenance costs with less battery cells. Case 6 achieves the best economic performance with a saving of about 16780 US\$ in total NPV and 0.046 US\$/kWh in LOCE. Case 7 has higher NPV and LCOE compared with the

baseline case, due to a balanced optimization of the energy supply, battery storage, utility grid and whole system covering technical, economic and environmental performances.

Fig. 5.14 compares the annual CO₂ emission of studied cases. The CO₂ emission in Case 1 and Case 5 is relatively high as the PV power is strictly restricted from feeding into the grid. Case 6 has the minimum annual CO₂ emission, because of a full permission on grid export power and less power loss in battery storage. The CO₂ emission in Case 7 is about 0.33 tCO₂/year, which is much lower than that of the baseline case (0.50 tCO₂/year) by nearly 34.7%.

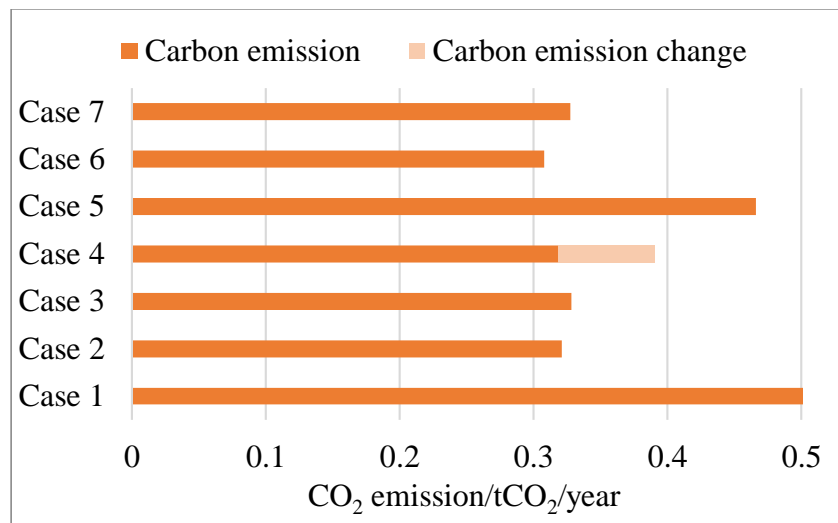


Fig. 5.14 Comparison of carbon emissions of studied cases

(Note: Case 1 is the existing case in the building, Case 2 allows grid feed-in and TOU, Case 3 optimizes the supply aspect, Case 4 optimizes the storage aspect, Case 5 optimizes the grid aspect, Case 6 optimizes the system aspect, Case 7 optimizes overall aspects.)

5.6 Post-optimization sensitivity analysis of the solar photovoltaic and battery storage system

In order to further quantify the impact of system design and management parameters on technical, environmental and economic performances of the PV-battery system, both local and

global sensitivity analyses are conducted as future design references for relevant stakeholders of on-grid renewable energy and storage systems in low-energy buildings.

5.6.1 Local sensitivity analysis

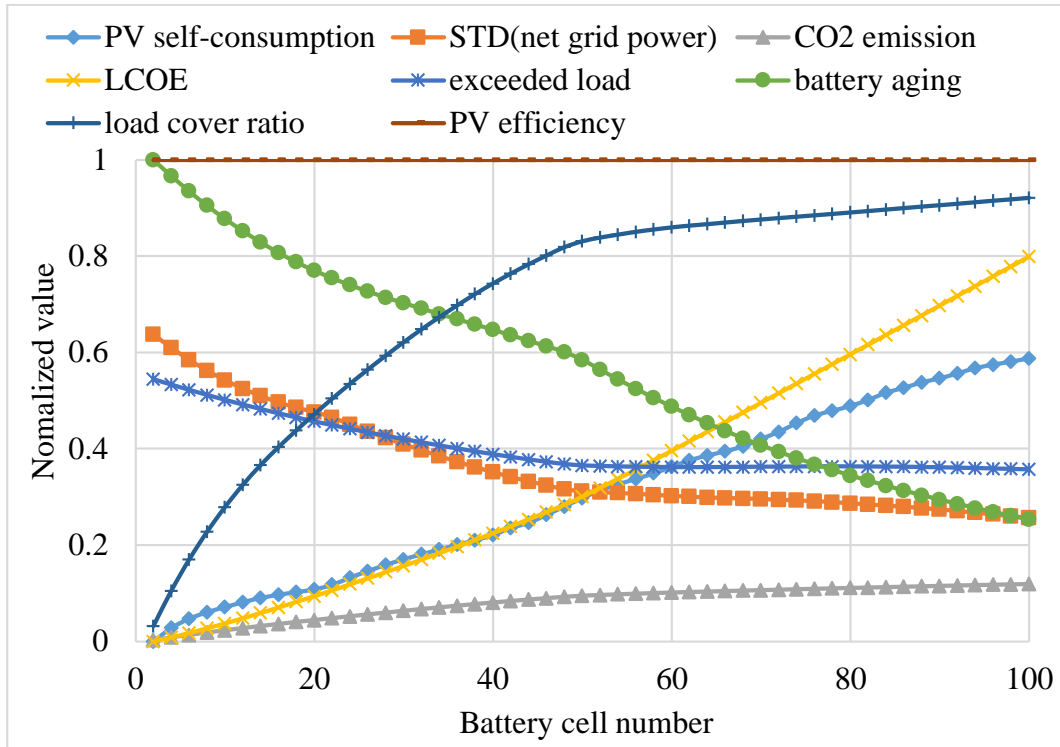


Fig. 5.15 Local sensitivity analysis of battery number on optimization objectives

This part analyzes the sensitivity of optimization objectives by changing one design parameter at a time while keeping the other two fixed. The optimization result of Case 7 is taken as the reference, with the battery cell number at 90, grid import limit at 5 kW and grid export limit at 80% of rated PV power. Fig. 5.15 shows the impact of the battery number on optimization objectives, and the optimization objectives are normalized for a clearer comparison. The battery cell number has a positive impact on SCR and LCR, as more PV power can be utilized with increased storage capacity. The system LCOE and CO₂ emission also increase with the battery number, due to a higher initial cost and higher battery charging loss. On the contrary, cycling aging

of the battery bank, STD of net grid power and exceeded load are reduced with the increasing battery number and storage capacity.

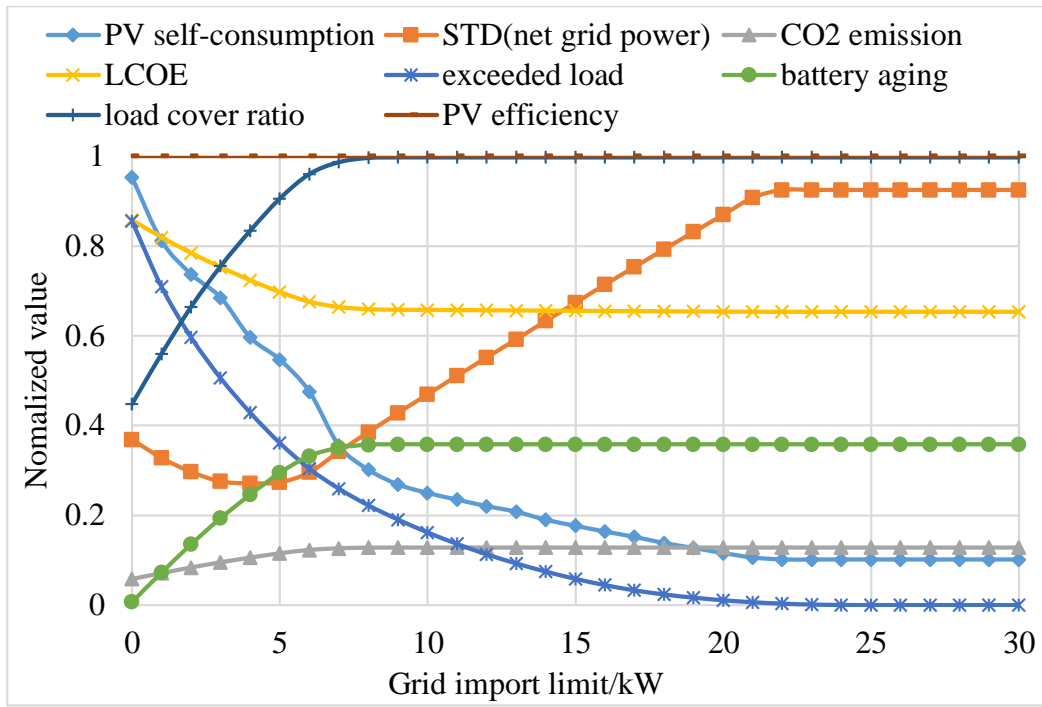


Fig. 5.16 Local sensitivity analysis of grid import limit on optimization objectives

Fig. 5.16 shows the impact of the grid import limit on normalized optimization objectives. It is shown that the LCR rises with the increasing grid import limit, as more grid power is accessible to charge the battery which can meet the load in return. Higher grid import limits also result in a higher battery cycling aging and CO₂ emission while a lower SCR. Furthermore, the electricity bill is reduced due to an increased utilization of valley-price electricity. And the variation of these four objectives gradually levels off, because the power flow from the battery bank to charge the load is directed after the PV supply. The STD of net grid power shows a decreasing trend at the beginning and an increasing trend later with the rising grid import limit. A minimum STD is achieved when the limit is around 5 kW, which agrees well with the optimization results.

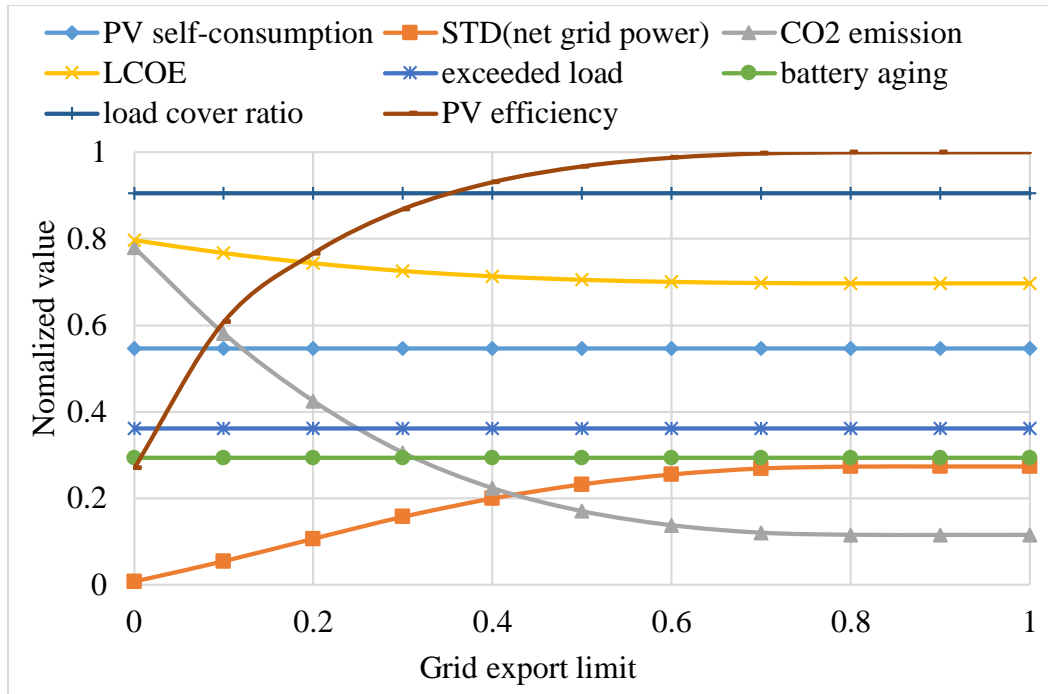
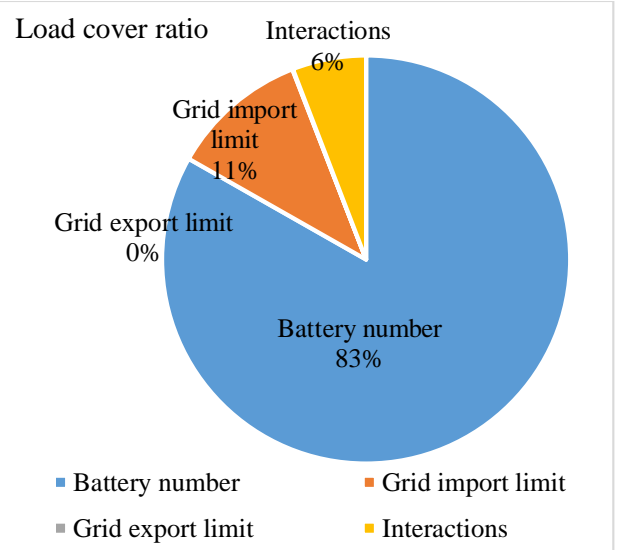
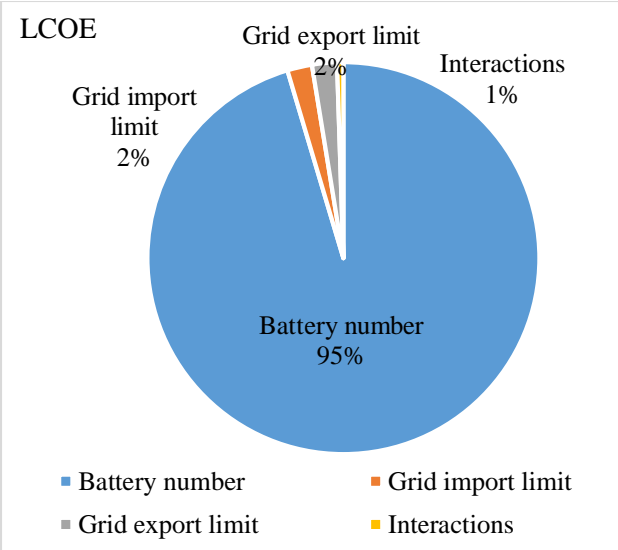
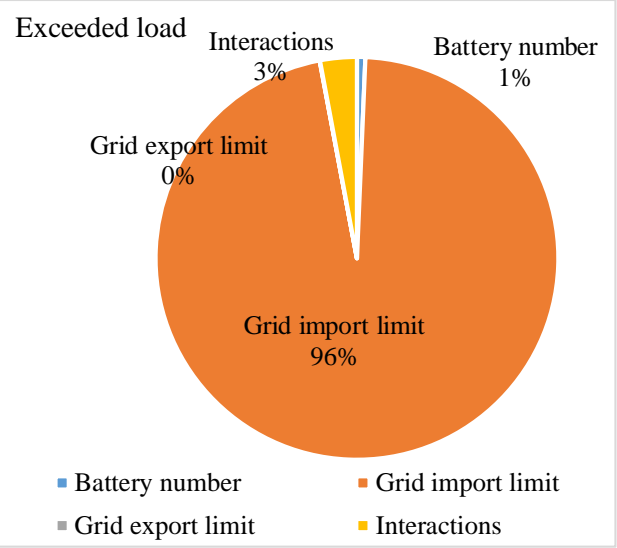
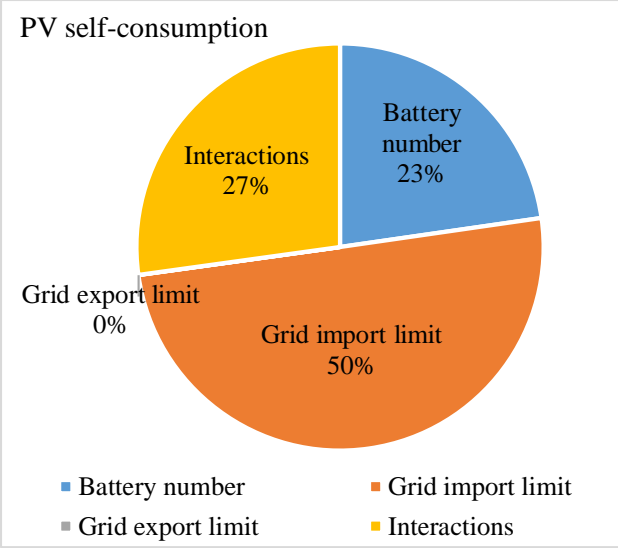


Fig. 5.17 Local sensitivity analysis of grid export limit on optimization objectives

Fig. 5.17 shows the impact of the grid export limit (ratio of rated PV power) on normalized optimization objectives. The PV efficiency and STD of net grid power increase with the rising grid export limit, as more surplus PV power can be delivered into the grid. The CO₂ emission and LCOE decrease with more grid export power, because of the lower electricity bill and higher FiT. However, the grid export limit has a relatively small influence on SCR, exceeded load, battery aging and LCR. The specific impact of optimization parameters on these objectives is further explained by the global sensitivity analysis.

5.6.2 Global sensitivity analysis

To further validate the local sensitivity results and quantify the exact contribution of each design parameter, global sensitivity analyses based on FAST first-order indices [88] are conducted. Fig. 5.18 shows the major impact of three design parameters on eight optimization objectives, concerning the technical, economic and environmental performances of the PV-battery system.



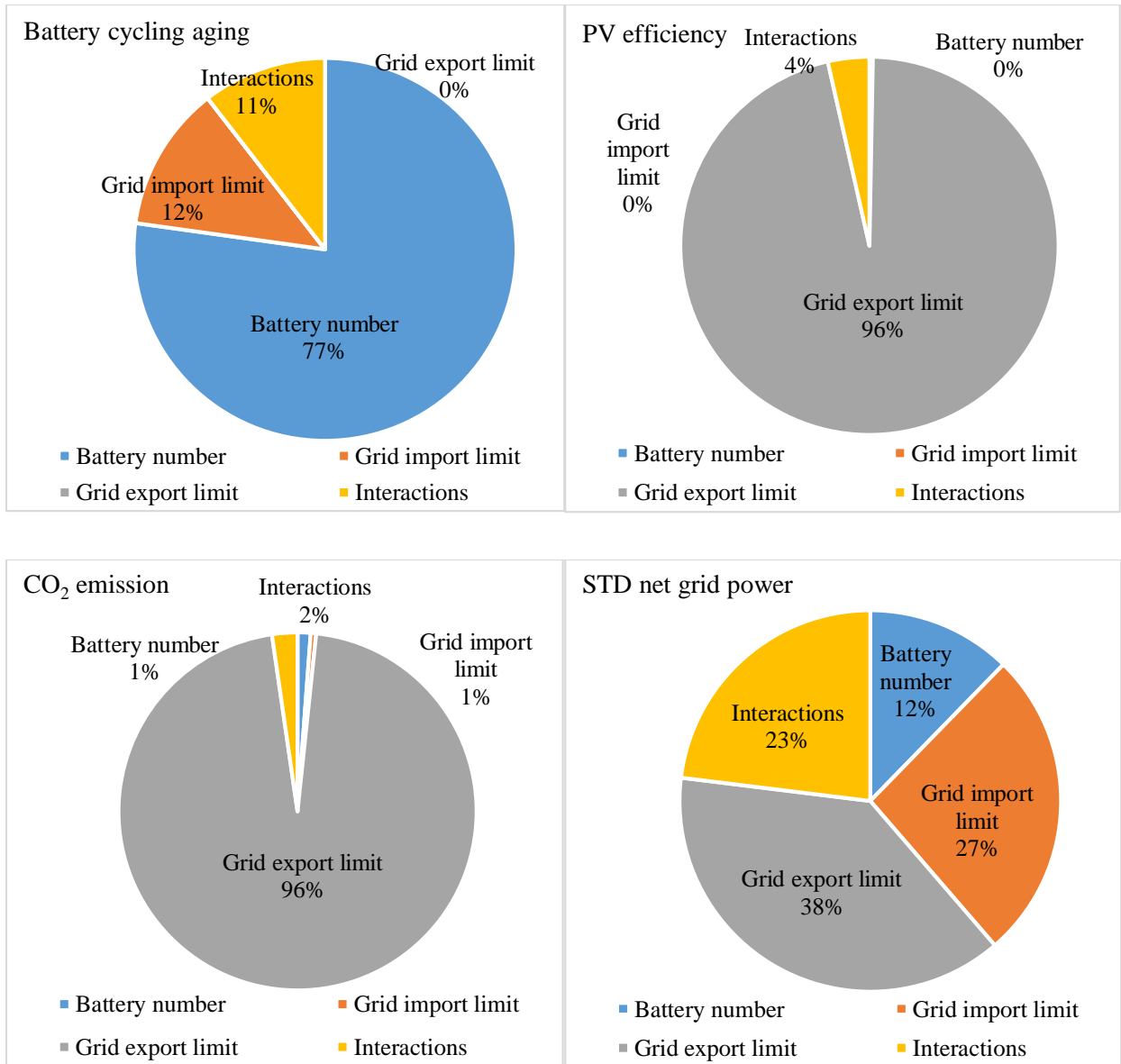


Fig. 5.18 Global sensitivity analysis of the optimization study on the PV-battery system

It is shown that the grid import limit has the major contribution of 50% to SCR variation, followed by the 23% contribution of the battery number. The grid export limit is identified to be not significant to SCR variation, and interactions of these three parameters account for 27% of the variation. Moreover, the grid import limit also accounts for 96% variation of the exceeded load. The battery number contributes to the major variation in LCOE, LCR and battery cycling aging

for 95%, 83% and 77%, respectively. It can be found that the grid export limit has a major impact of 96% on the PV efficiency and CO₂ emission. The variation of the net grid power standard deviation is however comparatively evenly attributed to the grid export limit for 38%, the grid import limit for 27% and the battery number for 12%. It can be indicated that these three optimized parameters are significant to achieve a balanced optimum performance in technical, economic and environmental aspects of the PV-battery system. A suitable design of the energy storage and management system should consider both unique and interactive contributions from these parameters.

5.7 Summary of design optimization of solar photovoltaic and battery storage systems for the single low-energy building

This chapter proposed a novel energy management control algorithm for the photovoltaic-battery system for a practical low-energy building in a typical hot summer and warm winter city of China. System design and management parameters are subject to both single-criterion and multi-criterion optimizations, based on the coupled TRNSYS and jEPlus+EA modeling platform with different decision-making approaches. The sensitivity of technical, economic and environmental performance indicators to these optimization parameters are further investigated, with robust local and global parametric analyses. Important findings are drawn as follows:

(1) A novel energy management strategy is proposed to improve the current operation condition of the photovoltaic-battery system without grid feed-in and time-of-use pricing (Case 1). The photovoltaic self-consumption and utilization efficiency can be increased by 4.5% and 48.6% by introducing the grid export and peak-valley electricity pricing into the new control algorithm (Case 2). Battery cycling aging through the one-year operation can be reduced by 63.5%. The

present value of the electricity bill during the 20-year service time is reduced by 3310 US\$ with the 5100 US\$ income from the grid feed-in tariff, leading to the reduction on the levelized cost of energy from 0.170 US\$/kWh to 0.147 US\$/kWh.

(2) Single-criterion optimization based design solutions are obtained for each performance criterion with the weighted sum method. The photovoltaic self-consumption, utilization efficiency and load cover ratio can reach 0.39, 0.50 and 0.85 respectively with the optimum energy supply performance in Case 3. The annual battery cycling aging in the battery performance optimum case (Case 4) is about 0.027, and the battery state of health after one-year operation can be prolonged from 94.2% in the baseline case to 99.5%. Remarkable impacts on relieving the utility grid can be achieved by setting the grid export limit and grid import limit (Case 5), where the standard deviation of net grid power can be reduced by 9.3% compared with the baseline case. Total net present value and levelized cost of energy can be reduced by 16780 US\$ and 0.046 US\$/kWh in the whole system performance optimum case (Case 6), while the CO₂ emission can be reduced by 38.6% compared with the existing case in the target building.

(3) The optimum design configuration of the photovoltaic-battery system considering the simultaneous optimization of the energy supply, battery storage, utility grid and whole system for the target building is determined to be with 90 battery cells, a 5 kW grid import limit and 80% of rated photovoltaic power as the grid export limit. The minimum distance to the utopia point method is proved to be efficient and robust in determining the final optimum solution from the trade-off between different performance criteria. Compared with the baseline case, the photovoltaic self-consumption and utilization efficiency can be increased by 15.0% and 48.6% respectively, while the standard deviation of net grid power, battery cycling aging and CO₂ emission is reduced by 3.4%, 78.5% and 34.7% respectively. A balance between technical, environmental and economic

performance aspects has been achieved to deliver an overall optimum design and energy management solution.

(4) Both local and global sensitivity analyses are conducted to further quantify the unique and interactive impact of system design and management parameters on different performance indicators. The grid import limit has the major contribution to the photovoltaic self-consumption and exceeded load variation. The battery number contributes to the major variation in levelized cost of energy, load cover ratio and battery cycling aging. The grid export limit has a major impact on the PV efficiency and CO₂ emission. And the variation of the net grid power standard deviation is comparatively evenly attributed to these three optimization parameters. Findings from post-optimization sensitivity analyses can provide important references for the system design and management to further expand renewable energy applications in urban areas, for achieving a carbon neutral energy framework in the near future.

CHAPTER 6 ENERGY PLANNING OF RENEWABLE ENERGY SYSTEMS WITH BATTERY AND HYDROGEN VEHICLE STORAGE FOR A SINGLE HIGH-RISE BUILDING

In addition to study hybrid renewable energy and storage system applications in a low-rise office building in Chapter 5, this chapter investigates the energy planning approaches of hybrid renewable energy and storage systems for a typical high-rise residential building in Hong Kong, including battery storage based renewable energy systems, and hybrid battery and hydrogen vehicle based renewable energy systems.

For the battery storage based renewable energy systems, typical renewable application scenarios (solar photovoltaic, solar photovoltaic-wind, solar photovoltaic-wind-battery) are investigated. A comprehensive technical optimization criterion is developed integrating the energy supply, battery storage, building demand and grid relief indicators, and the levelized cost of energy considering detailed renewable energy benefits is formulated including the feed-in tariff, transmission loss saving, network expansion saving and carbon reduction benefit.

For the hybrid battery and hydrogen vehicle based renewable energy systems, two energy management strategies are developed with different storage operation priorities. Multi-objective optimizations are conducted to select the optimum management strategy and configuration of the hybrid photovoltaic-wind-battery-hydrogen system. Techno-economic indicators are developed for the multi-objective optimizations and four decision-making strategies are further applied to search the final optimum solution for major stakeholders with different preferences.

6.1 Load profile of a typical high-rise residential building in Hong Kong

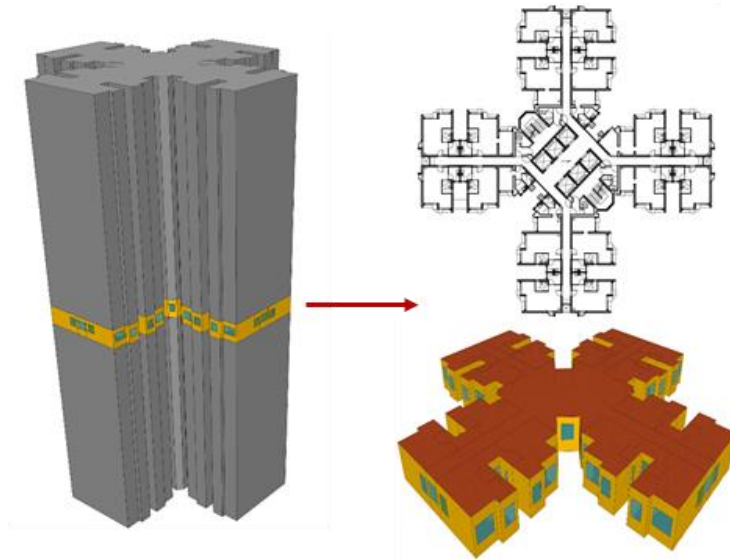


Fig. 6.1 Floor layout of the typical high-rise residential building

A high-rise residential building of 30 floors is constructed with a typical floor layout of the New Harmony One design from the public housing in Hong Kong. It is reported that about 30% of the population in Hong Kong live in the public rental housing, which widely adopts this standard design plan in new developments [127]. There are eight one-bedroom units designed for two occupants and eight two-bedroom units designed for four occupants in each floor as shown in Fig. 6.1. The building is firstly established in SketchUp and then imported to TRNSYS 18 to generate the load profile. The detailed parameters of the building envelope are shown in Table 6.1 according to the local design code [128, 129].

Table 6.1 Thermal properties of the typical high-rise residential building

Building envelope	Material	Thickness (m)	Thermal conductivity (W/m K)
External wall	Gypsum plastering	0.01	0.38
	Heavy concrete	0.1	2.16

Building envelope	Material	Thickness (m)	Thermal conductivity (W/m K)
	Cement/sand plastering	0.01	0.72
	Mosaic tiles	0.005	1.5
Internal wall	Gypsum plastering	0.02	0.38
	Heavy concrete	0.13	2.16
	Gypsum plastering	0.02	0.38
Floor	Heavy concrete	0.1	2.16
	Cement screed	0.025	0.72
	Plastic tiles	0.005	1.5
Roof	Gypsum plaster	0.01	0.38
	Heavy concrete	0.15	2.16
	Expanded polystyrene	0.05	0.034
	Cement/sand screed	0.05	0.72
	Asphalt	0.02	1.15
	Concrete tiles	0.025	1.1
Window	Tinted glass	0.006	1.05

The ventilation, air conditioning, occupancy, equipment and lighting profiles are set, based on the local design code published by Hong Kong Electrical and Mechanical Services Department [130]. The detailed load is modeled by internal components of the TRNSYS library including Type 56, Type 648, Type 667, Type 752, Type 655 and other auxiliary units. Type 15 is used to provide weather data of a typical meteorological year for the building load estimation. The simulation of the high-rise residential building is conducted at a time step of 0.125 h, and the load results of the whole year and July are shown in Table 6.2. It is found that the average air-conditioning load of the building is 43.99 kWh/m² and the average hot water load is about 46.51 kWh/m² comparable

to that of air conditioning. The modelled building results agree with the survey results reported by Wan et.al, showing that the reliable ranges of the average annual air-conditioning and hot water electricity consumption in standard public rental housing blocks in Hong Kong are 40 - 45 kWh/m² and 41 - 50 kWh/m² [131]. The total building load in the typical year and seventh month is 129.33 kWh/m² and 13.66 kWh/m² respectively.

Table 6.2 Load demand modelling results of the typical high-rise residential building

Building load	Annual	July
Internal gain load, kWh	559,506.67	47,534.66
Internal gain load per unit area, kWh/m ²	38.84	3.30
Air conditioning load, kWh	633,699.28	104,041.23
Air conditioning load per unit area, kWh/m ²	43.99	7.22
Hot water load, kWh	670,055.50	45,290.16
Hot water load per unit area, kWh/m ²	46.51	3.14
Building total load, kWh	1,863,261.46	196,866.05
Building total load per unit area, kWh/m ²	129.33	13.66

6.2 Development of battery storage based renewable energy systems for the high-rise building

6.2.1 Framework of battery storage based renewable energy systems for the high-rise building

The framework of renewable energy applications for the high-rise building is shown in Fig. 6.2. The building-integrated photovoltaic (BIPV) system with both rooftop and façade installations is firstly developed for the typical high-rise building as Case 1. BIPV is combined with wind power

in Case 2 to achieve the annual energy balance of the supply and demand, as PV power alone cannot cover the total building demand. The battery is introduced and optimized in Case 3 to improve the power match of PV-wind power with the residential electrical load. The wind power and battery capacity are jointly sized and optimized in Case 4 to find a techno-economic optimum solution for the high-rise building. An integrated technical optimization criterion is developed for technical feasibility assessment, focusing on the energy supply, building demand, battery storage and grid relief performance. And a comprehensive LCOE covering detailed benefits of the renewable system is formulated for economic feasibility assessment, including the FiT subsidy, transmission loss saving, network expansion saving and carbon reduction benefit. The final optimum solution is solved by the minimum distance to the utopia point method on top of the obtained Pareto Frontier from a multi-criterion design optimization.

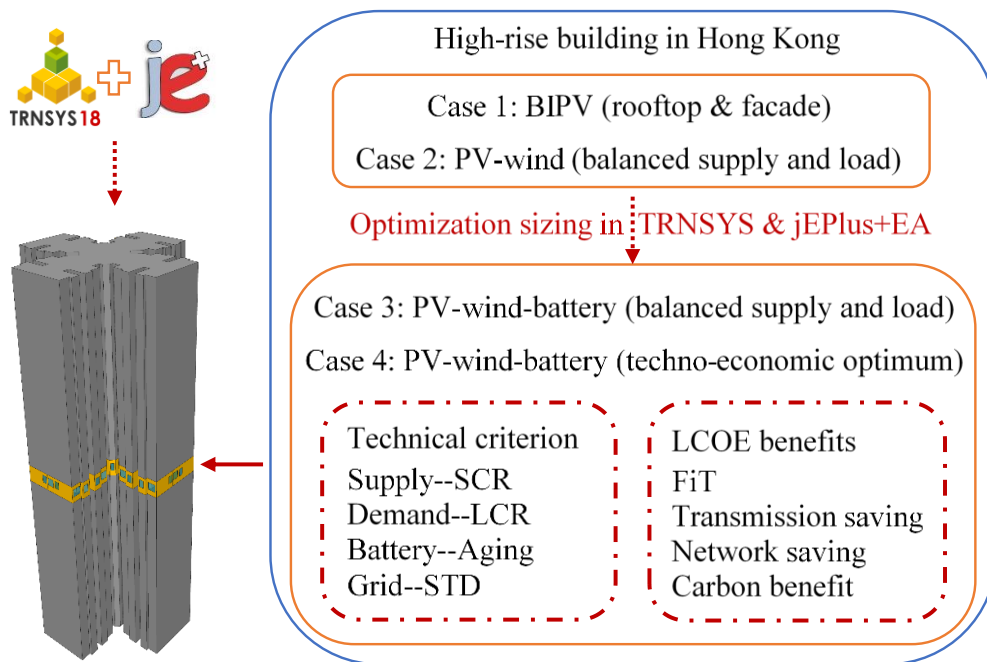


Fig. 6.2 Framework of renewable energy applications for the high-rise building

6.2.2 System modelling and multi-objective optimization of battery storage based renewable energy systems for the high-rise building

The renewable energy systems are connected to the utility grid to import electricity to meet the unsatisfied load or export surplus renewable power into the grid. The maximizing self-consumption strategy as validated by the experiment is adopted as the energy management method of all studied cases. When surplus renewable energy is available after meeting the building demand, it is controlled to charge the battery until reaching the maximum SOC and then be fed into the grid. When the electrical load in the building cannot be satisfied by renewable sources, the battery is discharged to cover the load until reaching the minimum SOC, and then the utility grid is used to meet the load. Design parameters of the renewable systems are shown in Table 6.3.

Table 6.3 Parameters of renewable energy systems for the high-rise building

System component	Rooftop PV	Facade PV	Wind turbine	Battery storage	Inverter
Installed capacity	70.76 kW	805.95 kW	Case determined	Case determined	--
Annual output per unit power kWh/W	1.215	0.461	--	--	--
Annual output per unit area kWh/m ²	218.019	69.114	--	--	--
Initial cost (cover installation)	3500 US\$/kW	3500 US\$/kW	4000 US\$/kW	1000 US\$/kWh	700 US\$/kW
Maintenance (ratio of initial cost) [132]	2%	2%	1%	1%	1%
Lifetime, year	20	20	20	5	10

It shows that 70.76 kW PV panels can be installed on the rooftop of the high-rise building excluding the required area for roof maintenance. And the annual output of the rooftop PV installation is 1.215 kWh/W and 218.019 kWh/m². PV panels are also installed on four façades of the high-rise building, considering an adjacent shading factor of 76.64% with a standalone building as the baseline [88], leading to much lower annual power generation of about 0.461 kWh/W.

To size the battery capacity in Case 3 and optimize the wind and battery capacity in Case 4, the multi-objective optimization method is adopted to find techno-economic optimum solutions, based on the coupled simulation and optimization platform of TRNSYS and jEPlus+EA. An integrated technical optimization criterion is developed covering the performance of the energy supply, battery storage, building demand and grid relief. And the LCOE is evaluated as the economic criterion, considering detailed benefits of applying renewables in urban areas, including the FiT subsidy, transmission loss saving, network expansion saving and carbon reduction benefit. The battery capacity is the only optimization variable in Case 3, as the building-integrated rooftop and façade PV capacity are fixed by the building geometry, while wind power is determined by the annual energy balance between the renewable power generation and building electrical load. Both the battery capacity and wind power capacity are selected as optimization variables in Case 4 to find a comprehensive optimum solution for the hybrid PV-wind-battery system applied in the high-rise building. The variation range of the battery capacity installed in the building is 120 - 2400 kWh (4 - 80 kWh/floor). And the increment of the battery capacity is 120 kWh (4 kWh for each floor with four units). The number of wind turbines at a rated capacity of 100 kW each is selected as the other optimization variable, with a changing range of 1 - 20 at an increment of 1. The detailed economic parameters for the cost feasibility assessment are shown in Table 6.4.

Table 6.4 Parameters for economic assessment on renewable energy systems

Parameter	Value
Real discount rate (i)	5.8%/year [63]
Price degression rate (d)	4.5%/year [63]
PV degradation (δ_{PV})	1%/year [133]
Wind turbine degradation (δ_{WT})	1.5%/year [134]
Electricity tariff (c_{ele})	0.145 US\$/kWh [135]
Electricity price rising rate (γ)	1.4%/year [115]
Feed-in tariff (c_{fit})	0.3846 US\$/kWh [114]
Transmission loss ratio (f_{tra})	13.54% [91]
Network expansion ratio (f_{exp})	24% [115]
Carbon intensity of electricity (f_{car})	0.66 kgCO ₂ /kWh [136]
Societal cost of carbon (c_{car})	0.024 US\$/kgCO ₂ [117]

The number of wind turbines in Case 2 and Case 3 based on the annual demand-supply balance is calculated to be 6. The optimum battery capacity in Case 3 is then obtained from a trade-off between the integrated technical and economic criteria. And an optimum solution of 1080 kWh is derived from the minimum distance to the utopia point method [125]. To optimally size the wind and battery capacity of the hybrid PV-wind-battery system in Case 4, the multi-objective optimization work with the integrated technical criterion and economic criterion (LCOE) are developed to achieve the Pareto frontier (Fig. 6.3). It indicates an obvious trade-off conflict where the integrated technical criterion increases as the economic criterion decreases. The optimum solution as highlighted with the blue triangle is obtained by the minimum distance to the utopia point method with a battery capacity of 1680 kWh and 10 wind turbines. It can achieve the optimum performance in both integrated technical criterion (considering the energy supply, battery

storage, building demand and grid integration) and the economic criterion (LCOE with detailed benefits). Sensitivity analyses on the battery and wind turbine capacities are further conducted to examine their impact on each system performance indicator.

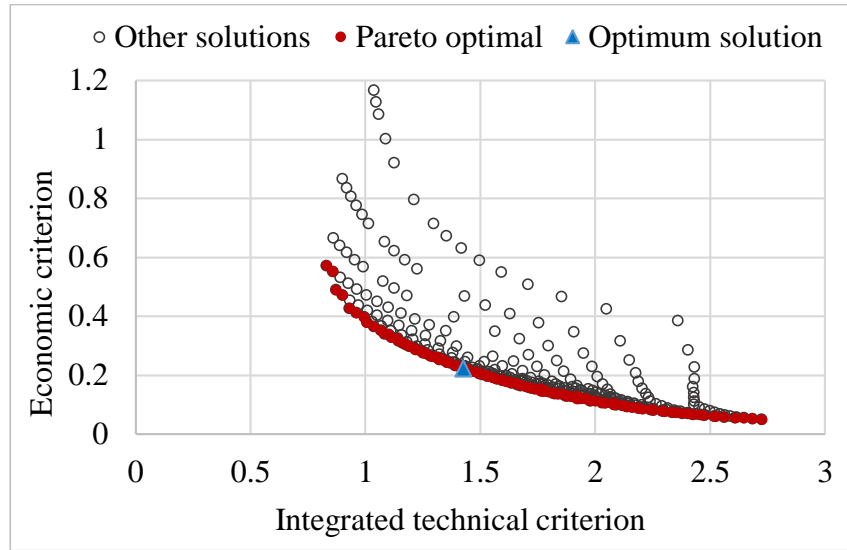


Fig. 6.3 Pareto frontier of technical and economic criteria in Case 4 (optimum case)

The impact of the battery capacity on the economic indicator (LCOE) and technical indicators, including the load cover ratio (LCR), renewable energy self-consumption ratio (SCR), battery cycling aging (Aging), and standard deviation of net grid power (STD) is illustrated in Fig. 6.4. The wind turbine number is kept at the optimum value obtained in Case 4 (i.e. 10). Both SCR and LCR show increasing trends with the increased battery capacity as the magnitude of energy from renewable sources to the battery and energy from the battery to the load increases, while the renewable energy generation and building load do not change with the battery capacity. Battery cycling aging decreases with growing battery capacity and the net grid power exchange is more stabilized with the rising batteries. The LCOE also increases with the rising battery capacity for higher investment.

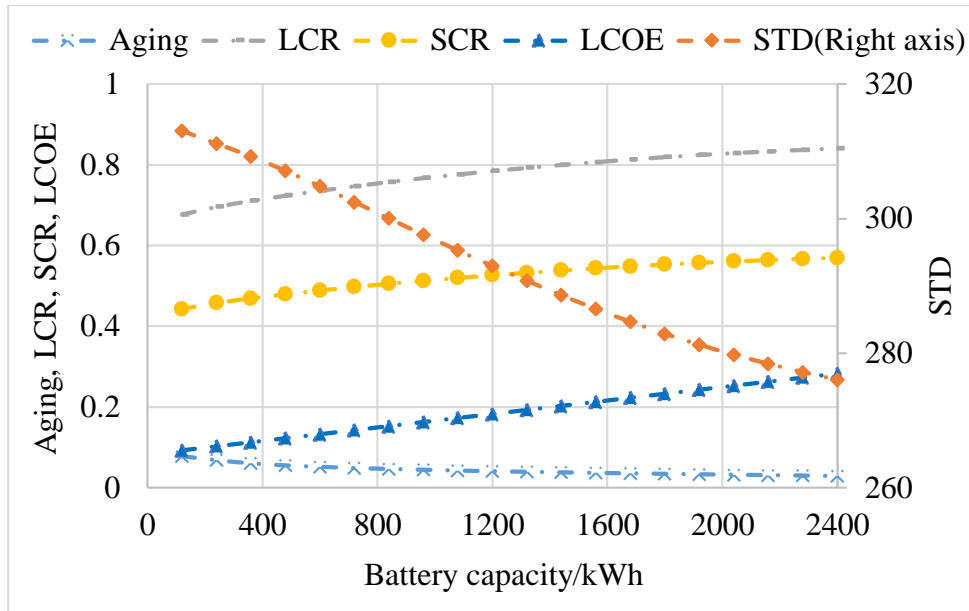


Fig. 6.4 Impact of battery capacity on optimization indicators

The impact of the wind turbine number on the five optimization indicators with a fixed battery capacity of 1680 kWh (the optimum solution in Case 4) is shown in Fig. 6.5. Both LCR and STD are positively related to the wind turbine number with larger renewable energy generation. The SCR decreases with the rising number of wind turbines with more available renewable energy generation, and the LCOE also decreases with the increasing wind turbines, as wind power requires lower investment than PV [85, 137]. The battery cycling aging is firstly positively and then negatively related to the wind turbine number, because both charging and discharging affect the battery cycling aging performance.

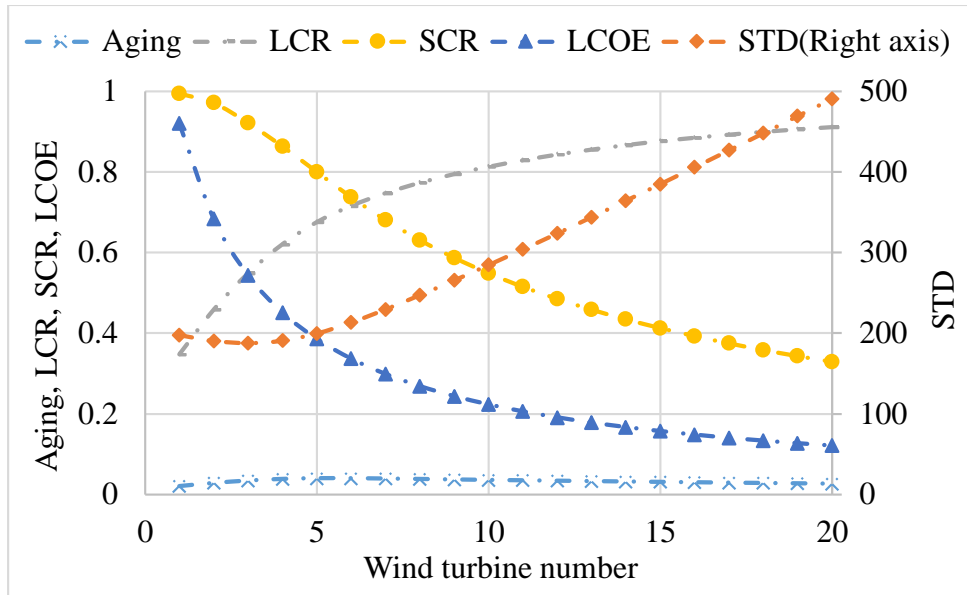


Fig. 6.5 Impact of wind turbine number on optimization indicators

The sizing and optimization results of all four application scenarios are summarized in Table 6.5. The PV capacity of these cases keeps at 876.71 kW, which is determined by the building layout with a maximum availability assumption.

Table 6.5 System sizing results of four renewable application scenarios

System sizing	Case 1	Case 2	Case 3	Case 4
Wind turbine /number	0	6 (energy balance)	6 (energy balance)	10 (optimized)
Battery/kWh	0	0	1080 (optimized)	1680 (optimized)

6.2.3 Techno-economic feasibility results of renewable energy applications for the high-rise building

(1) Technical analysis of renewable energy applications

The technical performance of four application scenarios in the high-rise residential building is analyzed in this section. The power flow distributions of the renewable energy systems in a typical week (the third week in June) and each month are presented for each case, while the annual load cover and renewable energy self-consumption performance are compared among four cases.

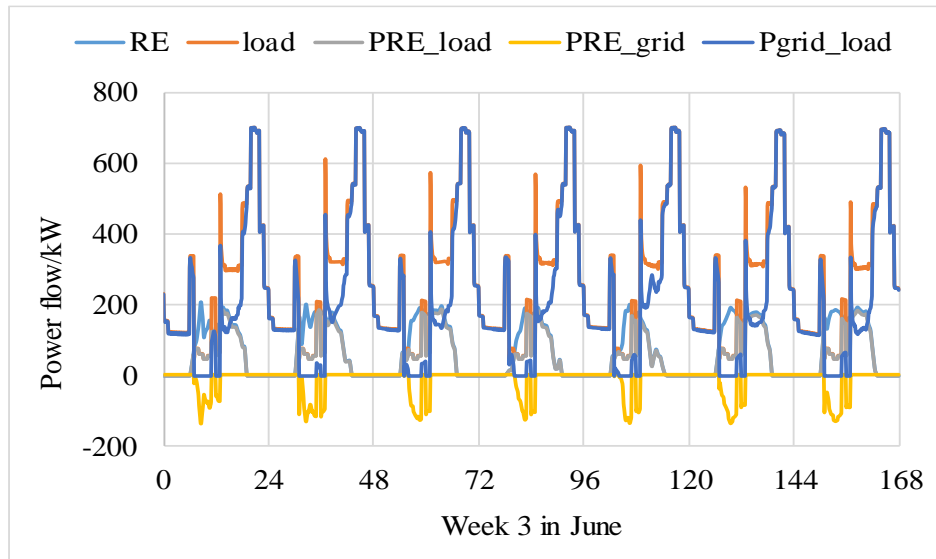


Fig. 6.6 Power flow of the PV system in the typical week (Case 1)

The power flow of the PV system (Case 1) for building applications in the third week of June is presented in Fig. 6.6. The total weekly electrical load of the high-rise building is about 44514.35 kWh, while the PV generation in this week is 11171.15 kWh with its 74.92% for the building load. The remaining 25.08% of renewable energy is fed into the grid, even though the building load cannot be fully covered. The observed mismatch between the renewable generation and building electrical load echoes with findings in an existing research study [138]. The PV supply can only cover 18.80% of the weekly load in the typical high-rise building, so that the grid undertakes the left burden with a maximum grid transmission power of 699.97 kW.

When the PV is combined with wind power to keep an energy balance between the annual demand and supply (Case 2), more renewable energy is available with a weekly renewable energy

generation of 40585.03 kWh covering 57.41% of the weekly load as shown in Fig. 6.7. The average renewable energy self-consumption ratio in this week is about 62.97% and more renewable energy is fed into the utility grid. The grid covers much less weekly electrical load (for 42.59%) compared with Case 1, with a maximum grid transmission power of 676.82 kW.

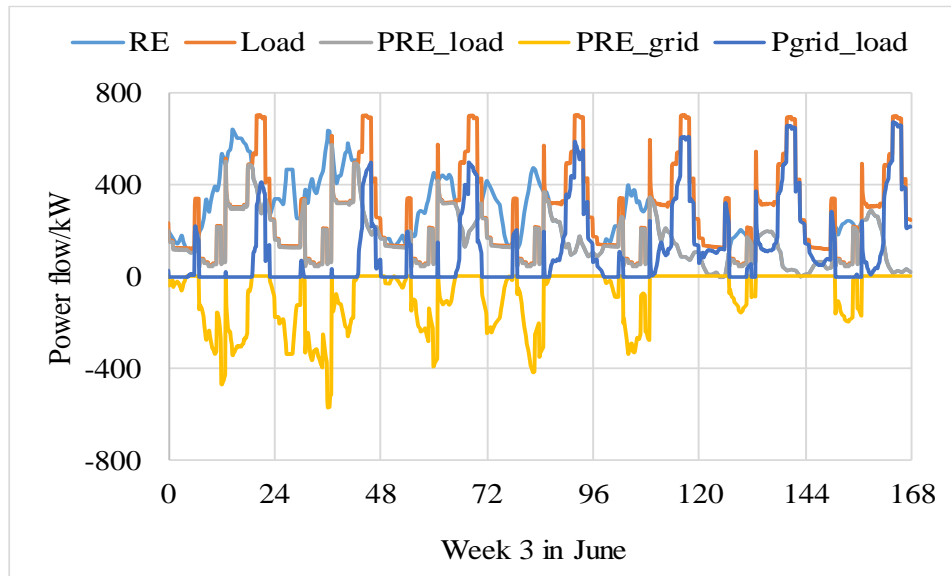


Fig. 6.7 Power flow of the PV-wind system in the typical week (Case 2)

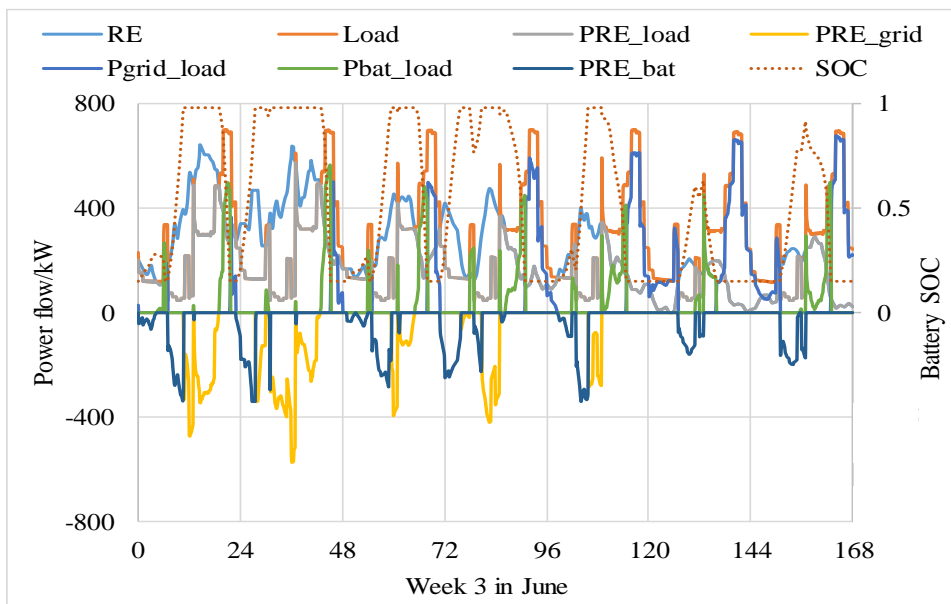


Fig. 6.8 Power flow of the PV-wind-battery system in the typical week (Case 3)

When battery storage is included in Case 3 for the energy-balanced scenario with an optimum techno-economic performance, the PV-wind-battery system can cover 69.68% of the electrical load in this typical week, which is higher than that in Case 1 and Case 2 as shown in Fig. 6.8. The battery storage undertakes 12.27% of the weekly load, which needs to be covered by the grid in Case 2 (battery discharging as positive power and battery charging as negative power). The utility grid covers the remaining 30.32% weekly load with the maximum grid transmission power of 676.82 kW. The maximum grid transmission power in Case 2 and Case 3 is the same, as the renewable energy generation in these two cases is the same and the grid is controlled to cover the unsatisfied load when battery discharging is not available. The weekly self-consumption ratio of the system is about 79.12% which is higher than that in Case 2 with 16.15% renewable power charging the battery. It is validated that the battery storage can increase the load matching and self-consumption performance of the system to a large extent as reported in Ref. [98].

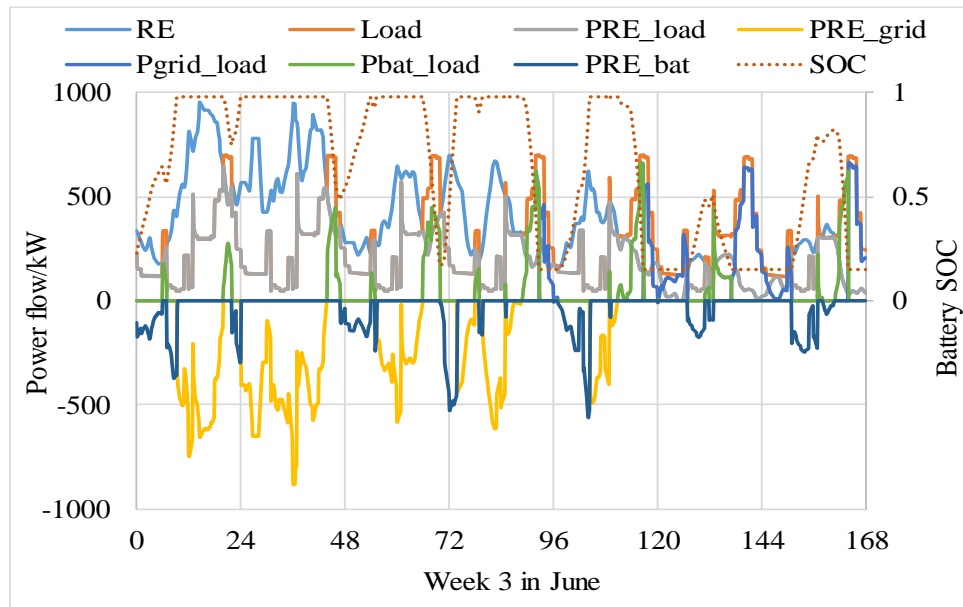
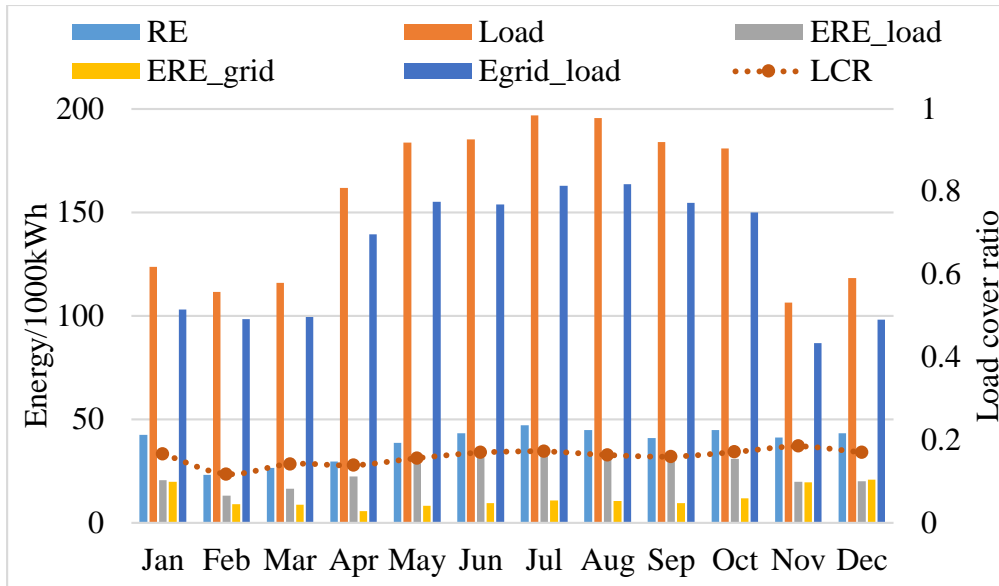


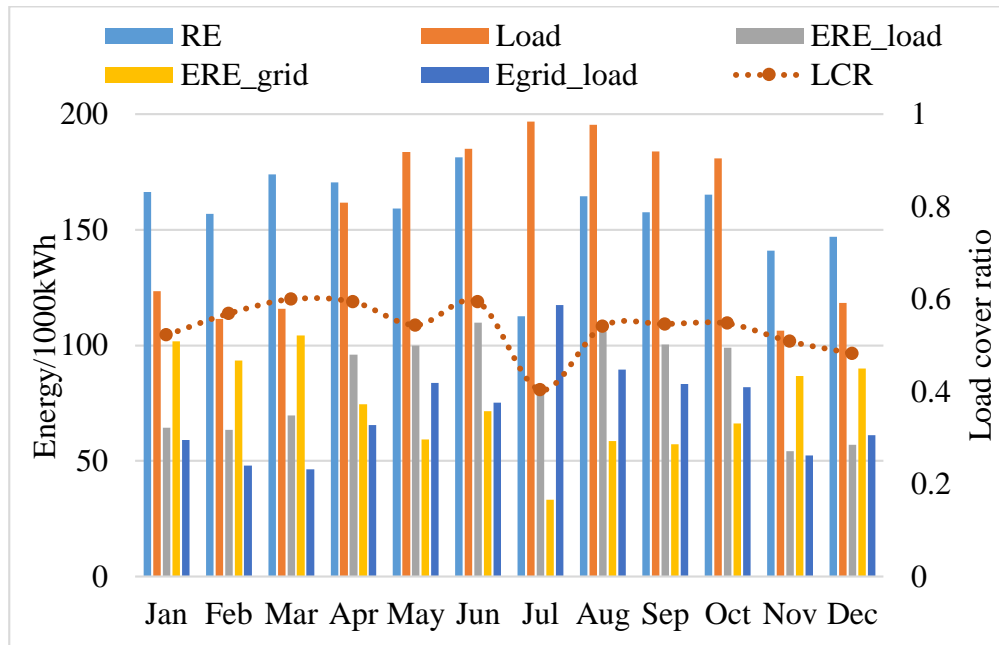
Fig. 6.9 Power flow of the optimum PV-wind-battery system in the typical week (Case 4)

The wind power and battery storage are simultaneously optimized in Case 4 to find a comprehensive techno-economic optimum solution for the high-rise building as shown in Fig. 6.9. It indicates that the hybrid PV-wind-battery system covers the majority (82.57%) of the total load in the typical week with 14.14% from battery storage. And the grid only needs to cover 17.43% of the weekly load with the maximum grid transmission power of -885.15 kW, as a large amount of renewable energy is available in the optimum hybrid system.

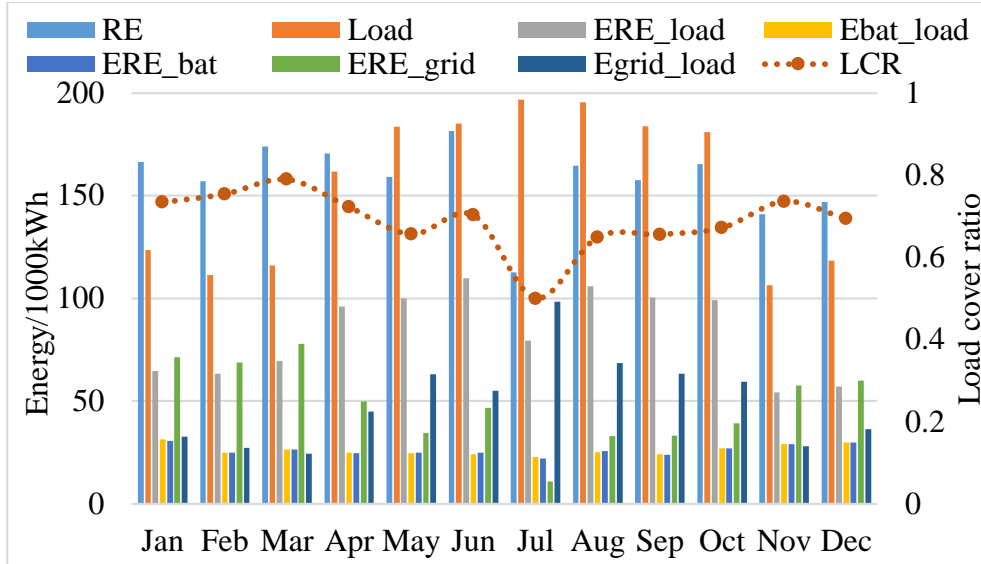
The monthly energy flow and load matching performances of four application cases are illustrated in Fig. 6.10. It is indicated that the building electrical load in summer is relatively higher than that in winter, due to a large cooling load in the hot summer and warm winter region. In Case 1 with the BIPV, both monthly PV generation and building load achieve the maximum value in July for 47.15 MWh and 196.84 MWh and the maximum monthly LCR is 18.47% on November. The monthly LCR significantly increases in Case 2 with the application of wind power and the maximum LCR is about 60.04% in March. With the application of battery storage in Case 3, the monthly LCR can be further increased on top of Case 2 reaching a maximum of 79.03% in March. The monthly LCR shows a rising trend in Case 4 with increased wind turbines and batteries compared with Case 3 and the maximum LCR reaches up to 90.32% in March. An obvious seasonal difference on LCR can be observed when wind turbines are introduced in Cases 2, 3 and 4 with a minimum value in July and maximum value in March as dependent on the wind power generation.



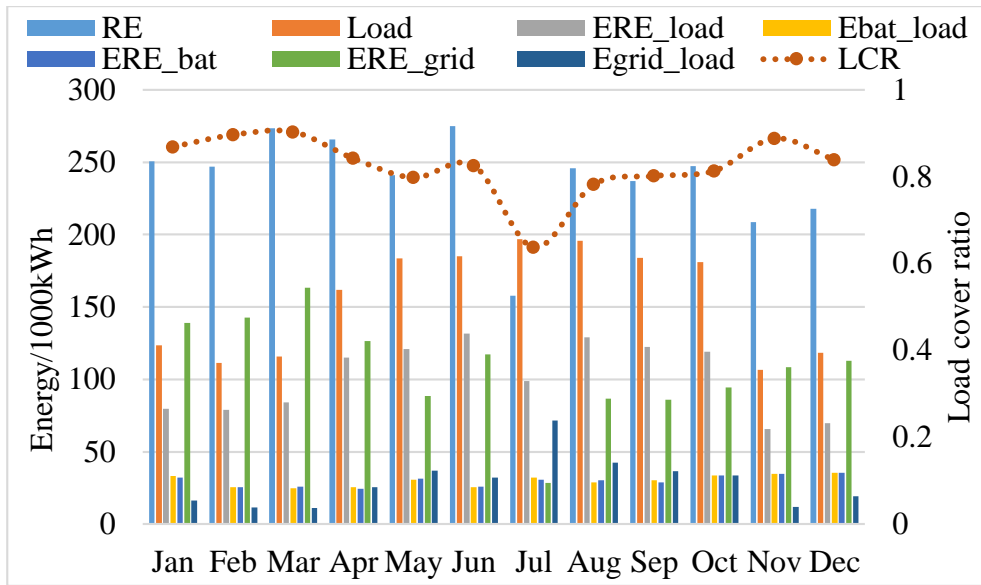
(a)



(b)



(c)



(d)

Fig. 6.10 Energy flow and load matching in Case 1 (a), Case 2 (b), Case 3 (c), Case 4 (d)

(Note: Case 1 with only PV system, Case 2 with PV-wind system, Case 3 with PV-wind-battery system, Case 4 with optimized PV-wind-battery system.)

The annual average LCR of these four cases is compared in Fig. 6.11. The annual average LCR can be increased from 16.02% in Case 1 to 53.65% in Case 2 when wind power is introduced

to the system. The mismatch between the renewable power generation and the building load is obvious as shown in Case 2, where 46.35% of the annual load is taken by the grid. The battery storage can therefore help cover another 14.08% of the annual load in Case 3, further reducing the reliance on the grid. Finally, the comprehensive optimum scenario as studied in Case 4 covers the majority of the annual load of 81.29%.

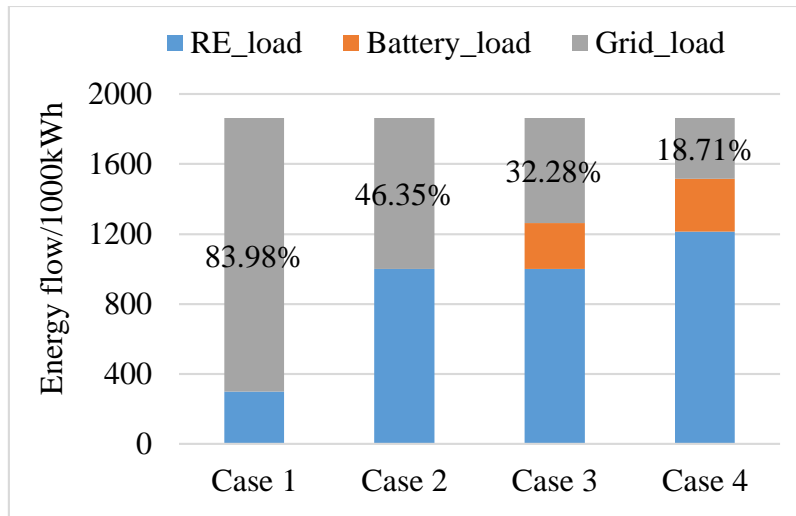


Fig. 6.11 Annual average load cover ratio of four cases

(Note: Case 1 with only PV system, Case 2 with PV-wind system, Case 3 with PV-wind-battery system, Case 4 with optimized PV-wind-battery system.)

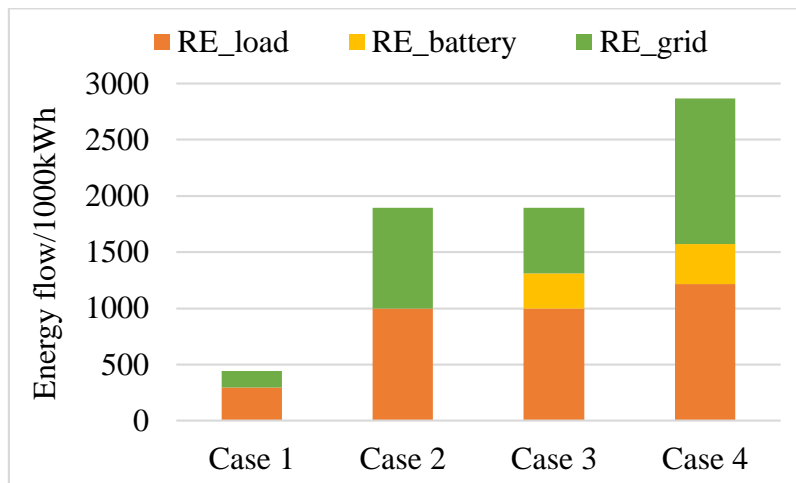


Fig. 6.12 Annual average renewable energy self-consumption ratio of four cases

(Note: Case 1 with only PV system, Case 2 with PV-wind system, Case 3 with PV-wind-battery system, Case 4 with optimized PV-wind-battery system.)

Fig. 6.12 compares the annual average renewable energy self-consumption ratio across four studied cases. It is indicated that 67.59% of the PV generation is directed to meet the building load with the other 32.41% fed into the grid in Case 1. With the increase of renewable energy generation, the exported energy into the grid increases as shown in Case 2 and Case 4. And batteries store about 16.56% of renewable generation in Case 3 which is originally fed into the grid in Case 2. The self-consumption ratio of the optimum PV-wind-battery system in Case 4 is 54.89% with the other 45.11% of renewable energy fed into the grid.

Battery aging after one-year operation in Case 3 is about 4.85% and the battery state of health is about 99.03% of rated capacity. Battery aging in Case 4 is further reduced to 3.568% since a larger battery capacity is employed and the battery state of health is improved to about 99.28% of the rated capacity. As for the grid integration performance, the standard deviation of net grid power increases with more renewable energy generation, while the battery storage contributes to reducing the standard deviation as compared between Case 2 and Case 3.

(2) Economic analysis of renewable energy applications

The economic performance of four renewable energy systems is further analyzed in this section. The lifetime present value considering the investment costs and detailed benefits is compared in Fig. 6.13. The investment of the renewable energy systems increases from Case 1 to Case 4 as wind turbines are installed in Case 2 and batteries are matched for Case 3, while the optimized wind turbine and battery capacity are the maximum in Case 4. The initial cost ratios of the major investment for four cases are 77.34%, 80.18%, 69.18% and 68.09% respectively. The benefits of the renewable application in Case 2 and Case 3 are the same as per renewable energy

generation. The FiT subsidy of the renewable application dominates the total gained benefits with 81.42%, 76.59%, 76.59% and 75.70% respectively in the four cases.

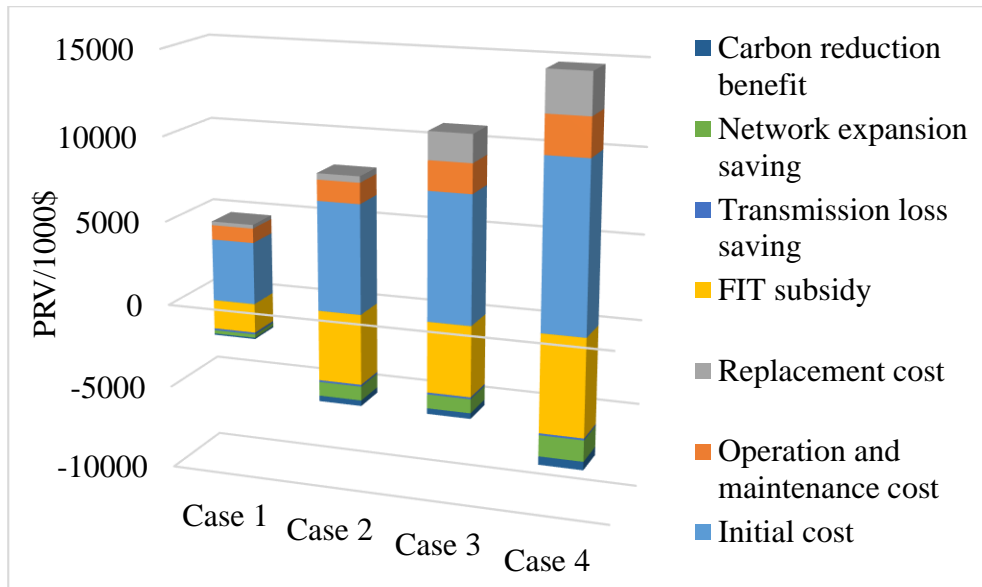


Fig. 6.13 Lifetime present value of four typical renewable application scenarios

(Note: Case 1 with only PV system, Case 2 with PV-wind system, Case 3 with PV-wind-battery system, Case 4 with optimized PV-wind-battery system.)

Table 6.6 PRV and LCOE of four typical renewable energy scenarios

PRV and LCOE	Case 1	Case 2	Case 3	Case 4
Initial cost US\$	3,682,182	6,502,182	7,582,182	10,062,182
Operation and maintenance cost US\$	858,574	1,236,309	1,739,956	2,271,584
Replacement cost US\$	220,359	371,168	1,638,497	2,443,109
FiT subsidy US\$	-1,727,839	-4,200,066	-4,200,066	-5,848,217
Transmission line saving US\$	-113,484	-113,484	-113,484	-113,484

Network expansion saving US\$	-201,139	-838,104	-838,104	-1,262,747
Carbon reduction benefit US\$	-79,592	-332,370	-332,370	-500,888
System LCOE US\$/kWh	0.5252	0.1251	0.2610	0.2230

The detailed PRV and LCOE of the four typical renewable application scenarios are summarized in Table 6.6. It shows that the LCOE of the PV system in Case 1 is 0.5252 US\$/kWh, which is higher than the reported result of PV applications in Hong Kong for 0.2609 US\$/kWh [85], as the energy generation of the façade PV is impaired by adjacent shading. The LCOE of the PV-wind system in Case 2 is 0.1251 US\$/kWh as wind power requires lower investment than PV applied in Hong Kong [85, 137]. The LCOE in Case 3 increases to 0.2610 US\$/kWh with the application of batteries at a relatively higher cost. And the LCOE of the optimum PV-wind-battery system in Case 4 is about 0.2230 US\$/kWh, which is lower than the reported result of 0.42 US\$/kWh conducted in Korea [132], as a large amount of FiT subsidies available in Hong Kong and other renewable energy benefits are considered in this study. Furthermore, the LCOE of PV-wind-battery systems is expected to be further reduced, as the lithium battery cost is showing a steady decreasing trend in recent years [31].

6.2.4 Summary of battery storage based renewable energy systems for the high-rise building

This section analyzes the techno-economic feasibility of four typical scenarios of renewable energy applications for power supply to a high-rise residential building in Hong Kong. The integrated technical optimization criterion focusing on the performance of four major system components (energy supply, battery storage, building demand and grid relief) and the improved levelized cost of energy considering detailed renewables benefits (feed-in tariff subsidy,

transmission loss saving, network expansion saving and carbon reduction benefit) are developed for design optimizations of renewable energy systems. Important findings are concluded as below:

(1) The technical feasibility of four typical renewable application scenarios for high-rise residential buildings is clarified. The photovoltaic system in Case 1 can cover 16.02% of the annual building electrical load, while the photovoltaic-wind system with balanced annual supply and demand in Case 2 covers 53.65% of the annual load. The photovoltaic-wind-battery system with balanced annual supply and demand in Case 3 can further satisfy 69.26% of the annual load and relieve the utility grid stress. The battery storage can improve the annual average load cover and self-consumption ratios by 14.08% and 16.56% as compared in Case 2 and Case 3. The optimum PV-wind-battery system in Case 4 can cover the majority of total annual load of 81.29% with a simultaneous consideration of the battery health protection and grid relief.

(2) The levelized cost of energy of the photovoltaic system in Case 1 is about 0.5252 US\$/kWh, as the adjacent shading impairs the energy generation of façade photovoltaic. The levelized cost of energy of the photovoltaic-wind system (0.1251 US\$/kWh) with a balanced annual supply and demand in Case 2 is the lowest in four scenarios, while it increases to 0.2610 US\$/kWh after battery storage is coupled with the renewable system in Case 3. The levelized cost of energy of the optimum hybrid photovoltaic-wind-battery system in Case 4 is predicted to be 0.2230 US\$/kWh, which can be further reduced with the declining price of the lithium-ion battery.

(3) It is suggested that the application of photovoltaic-wind systems in high-rise residential buildings in Hong Kong is feasible with a low levelized cost of energy, while the photovoltaic-wind-battery systems can contribute to higher building energy autonomy with an affordable cost. The techno-economic feasibility of these typical renewable application scenarios can provide relative stakeholders critical references to facilitate the renewable penetration into high-density

urban areas, and therefore accelerating the realization of carbon neutrality for the power sector in Hong Kong and other similar high-density regions.

6.3 Development of battery and hydrogen vehicle storage based renewable energy systems for the high-rise building

6.3.1 Framework of battery and hydrogen vehicle storage based renewable energy systems for the high-rise building

The framework of the battery and HV storage based renewable energy systems for the single high-rise building is shown in Fig. 6.14. The hybrid renewable energy and storage system is first established in TRNSYS 18 [139] for power supply to a typical high-rise residential building in Hong Kong, with two groups of HVs following different cruise schedules. The hybrid renewable energy supply adopts a combination of solar PV and wind power systems given their good complementary characteristics [140]. Solar PV panels are assumed to be installed on the rooftop and three vertical facades. The hybrid storage technologies consisting of lithium-ion battery energy storage (BES) and vehicles integrated hydrogen energy storage (HES) are utilized to match with the hybrid renewable energy supply. The battery technology is widely adopted for renewable energy storage in buildings given its fast response, high efficiency and low environmental impact [18], while the hydrogen vehicle technology meets well with the low-carbon development plan in the building and transport sectors of Hong Kong [4]. The batteries equipped in the building can be charged by available renewable energy and discharged to meet the electrical load. The hydrogen system includes the electrolyzers, compressors, stationary hydrogen (H₂) storage tank fixed in the building and two groups of mobile HVs with a H₂ storage tank and proton exchange membrane fuel cell (PEMFC) in each HV. The two groups of mobile HVs with different cruise schedules can

be discharged to meet the electrical load when parking at home. And the heat release of the hydrogen system is recovered from the electrolyzers, compressors and PEMFCs for the air-conditioning reheat and domestic hot water demand to enhance the overall efficiency of the HES system. The utility grid is connected to the hybrid PV-wind-battery-hydrogen system to take in surplus renewable generation, cover the unmet electrical load and supply power to the hydrogen system for necessary daily cruise consumption.

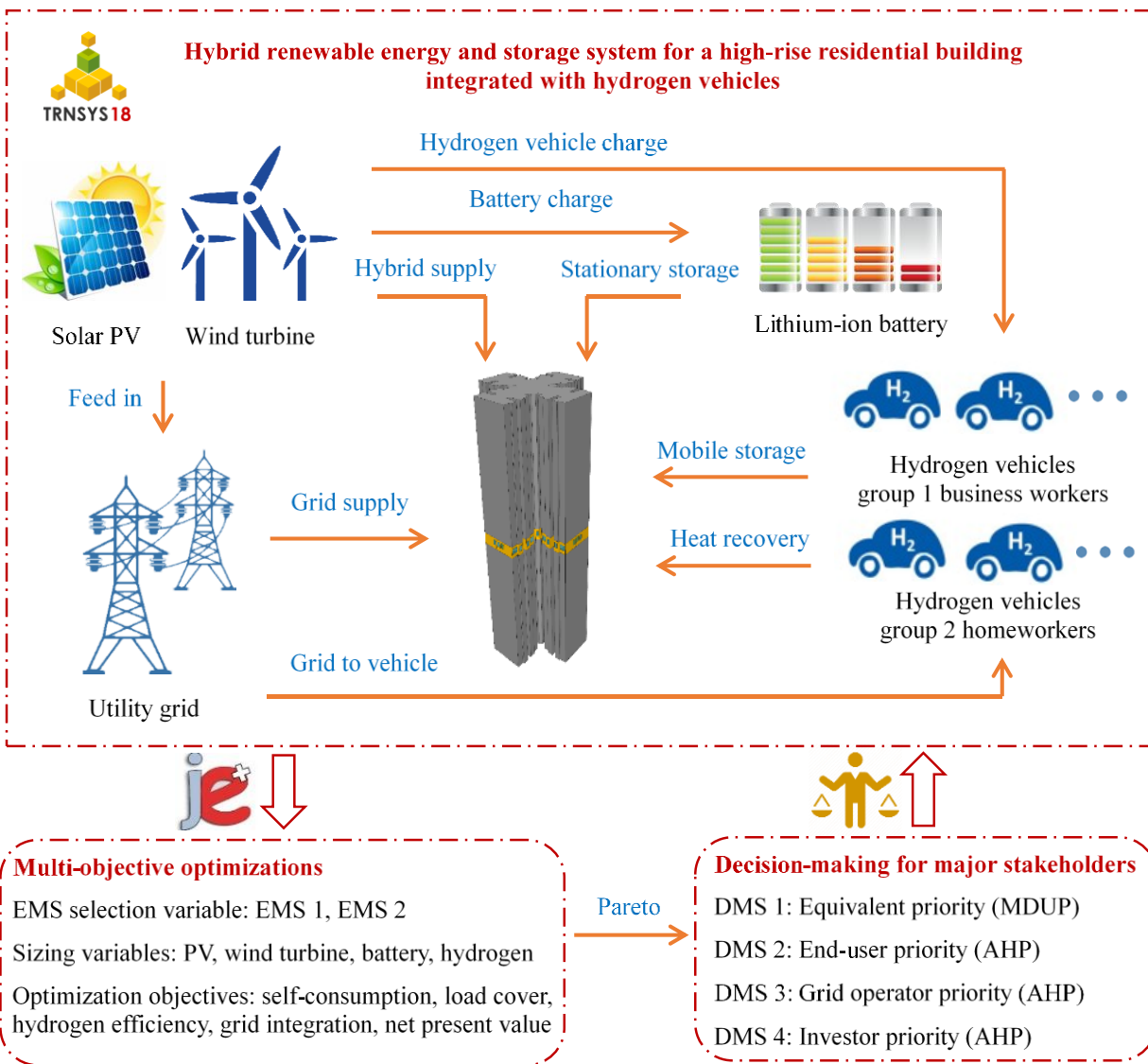


Fig. 6.14 Framework of the PV-wind-battery-hydrogen system for the high-rise building

Two energy management strategies (EMSs) are developed with different operation priorities of the storage technologies, where BES is prioritized over HES in EMS 1 and HES is prioritized in EMS 2. Multi-objective optimizations are conducted with the joint simulation and optimization platform of TRNSYS and jEplus+EA, to select the optimum EMS and configuration of the hybrid PV-wind-battery-hydrogen system, regarding the façade PV area, wind turbine number, battery capacity and stationary H₂ storage tank volume. Techno-economic indicators are developed for the multi-objective optimization, covering the self-consumption of renewable energy, on-site cover of the electrical load, overall efficiency of the hydrogen system, absolute value of net grid exchange and lifetime net present value. Four decision-making strategies (DMSs) are adopted to find the final optimum solution, focusing on different concerns of major stakeholders from Pareto optimal solutions. Specifically, DMS 1 assigns equivalent priority to all design criteria, based on the minimum distance to the utopia point (MDUP) method. DMSs 2 - 4 focus on the preference of the end-user, transmission system operator and investor respectively based on the analytical hierarchy process (AHP) method.

6.3.2 System modelling of battery and hydrogen vehicle storage based renewable energy systems for the high-rise building

Fig. 6.15 shows the schematic of the hybrid PV-wind-battery-hydrogen system for the HVs integrated building. Detailed information of the hybrid supply, battery energy storage (BES), hydrogen energy storage (HES) and energy management strategy (EMS) is explained as below.

Hybrid supply: Rooftop PV panels are modelled by TRNSYS Type 103 with a tilted angle of 22° close to the local latitude and a capacity of about 70.76 kW. Façade PV panels are simulated by TRNSYS Type 567 and assumed to be installed on three building façades excluding North. The installation capacity is a design variable in sizing the hybrid system considering techno-economic

indicators from the perspective of different stakeholders. An adjacent shading factor of 76.64% is introduced to model the façade PV power generation within the urban context [88]. Wind turbines are also modelled by TRNSYS Type 90, based on the tested power-speed characteristic curve from manufacturers as the supplementary power supply [141]. The installation capacity of wind power is also subject to further optimizations considering different stakeholders' concerns, assuming a power transmission loss rate of 13.541% for the residential building in populated regions [91].

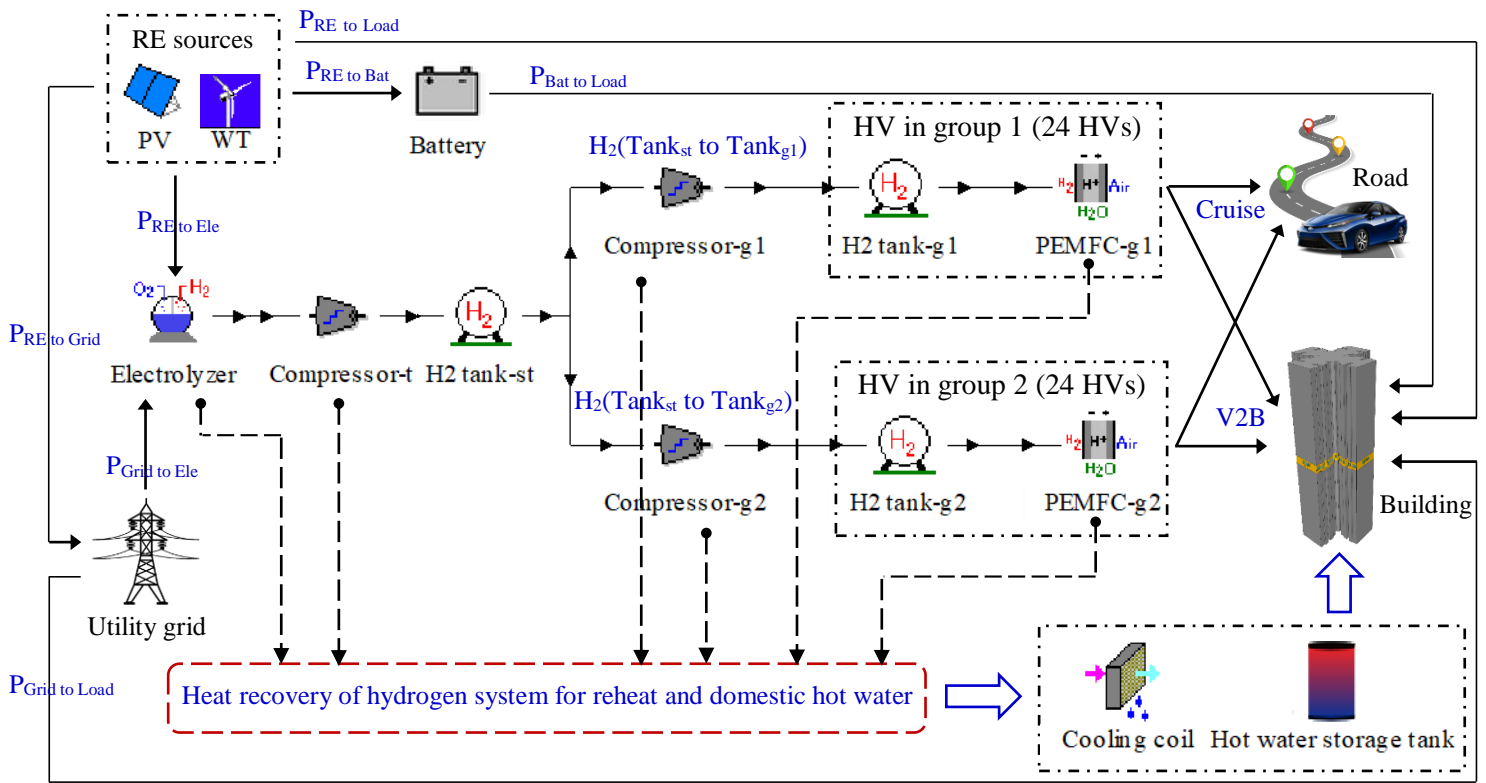


Fig. 6.15 Schematic of the PV-wind-battery-hydrogen system for the high-rise building

Battery energy storage (BES): The batteries are assumed to be installed in the building and subject to design optimization considering preferences of different stakeholders. It can be charged by surplus renewable energy or discharged to meet the electrical load, by controlling the fractional battery state of charge (FSOC) with an operational limit between $FSOC_{Bat_min}$ - $FSOC_{Bat_max}$ (0.15

- 0.98). The maximum charging and discharging rate of the battery is also considered according to the battery characteristic (i.e. 1C for the lithium-ion battery) [99].

Hydrogen energy storage (HES): 48 hydrogen vehicles (HVs) are assumed for the 30-floor residential building with 480 households of 1440 residents, based on a local survey showing that the car owner ratio in public housing of Hong Kong is about 9.9% [142]. The hydrogen vehicle model is developed from a commercialized product “2019 Toyota Mirai” with the maximum power output of 114 kW and maximum hydrogen storage tank mass of 5 kg at a maximum pressure of 700 bars. It is tested that the “Toyota Mirai” with full hydrogen storage can cover a cruise range of about 502 km [100]. 48 HVs are divided equally into two groups: the business worker group (group 1) and homemaker group (group 2) in different driving schedules. The average daily driving distances of the business worker and homemaker group are about 53.45 km and 36.75 km respectively [143], and the daily leaving home periods of these two groups are 8:00 - 19:00 on weekdays and 8:00 - 12:00 on every day respectively. HVs can meet the building load by consuming hydrogen in PEMFC when they are parked at home. The hydrogen consumption of HVs on the road is calculated but the detailed operation of HVs during the cruise is not the main focus of this study. Thermal heat is recovered from the electrolyzers, compressors and PEMFCs when HVs are parked at home, to meet the air-conditioning reheat and domestic hot water demand of the building, thereby increasing the overall hydrogen system efficiency.

The hydrogen energy storage system consists of electrolyzers, compressor (*Com-t*) transporting hydrogen from the electrolyzers to a stationary hydrogen (H_2) storage tank (*Tank-st*) installed in the building, and two groups of hydrogen vehicles (*HV-g1*, *HV-g2*). A mobile H_2 storage tank (*Tank-g1*, *Tank-g2*) and proton exchange membrane fuel cell (*PEMFC-g1*, *PEMFC-g2*) are included in each HV, and a compressor (*Com-g1*, *Com-g2*) is allocated to each vehicle

group to convey hydrogen from the stationary H₂ storage tank to each mobile H₂ tank when parked at home. The electrolyzer is modelled by TRNSYS Type 160a based on the advanced alkaline electrolyzer Phoebus [101]. The cell number varies in different cases based on the supply power entering the electrolyzer to keep the current density between 40 - 400 mA/cm² [102]. TRNSYS Type 167 is adopted to model the multistage compressor, which is turned on when the pressure of entering hydrogen is lower than that of the targeted storage tank. The H₂ storage tanks are simulated by Type 164b to store compressed hydrogen at a high efficiency of around 99% with a maximum pressure of 700 bars, based on the van der Waals equation of state for real gas [41]. The fuel cell is simulated by Type 170d for PEMFC, showing the electrochemical process of converting the chemical energy of hydrogen and oxygen to electrical currents. The hydrogen storage tanks of HVs are checked over the night on each travelling day (0:00 - 8:00), and the utility grid drives the electrolyzer to generate hydrogen to secure the minimum FSOC level of mobile tanks for one-day cruise. The volume of the stationary H₂ storage tank needs to be optimized for system sizing.

Energy management strategy (EMS): Two energy management strategies with different operation priorities of the storage technologies are studied, as the charging and discharging orders of the battery tank and hydrogen vehicle have a significant impact on the technical and economic performances of the system. EMS 1 prioritizes battery storage over hydrogen storage when charging by surplus renewable energy or discharging for unsatisfied load, while EMS 2 performs in a reversed priority. Detailed control logics of EMS 1 and EMS 2 are illustrated in Fig. 6.16. Specifically, the available renewable power (P_{RE}) from PV panels and wind turbines is first used to meet the electrical load (P_{Load}) in the building under both strategies.

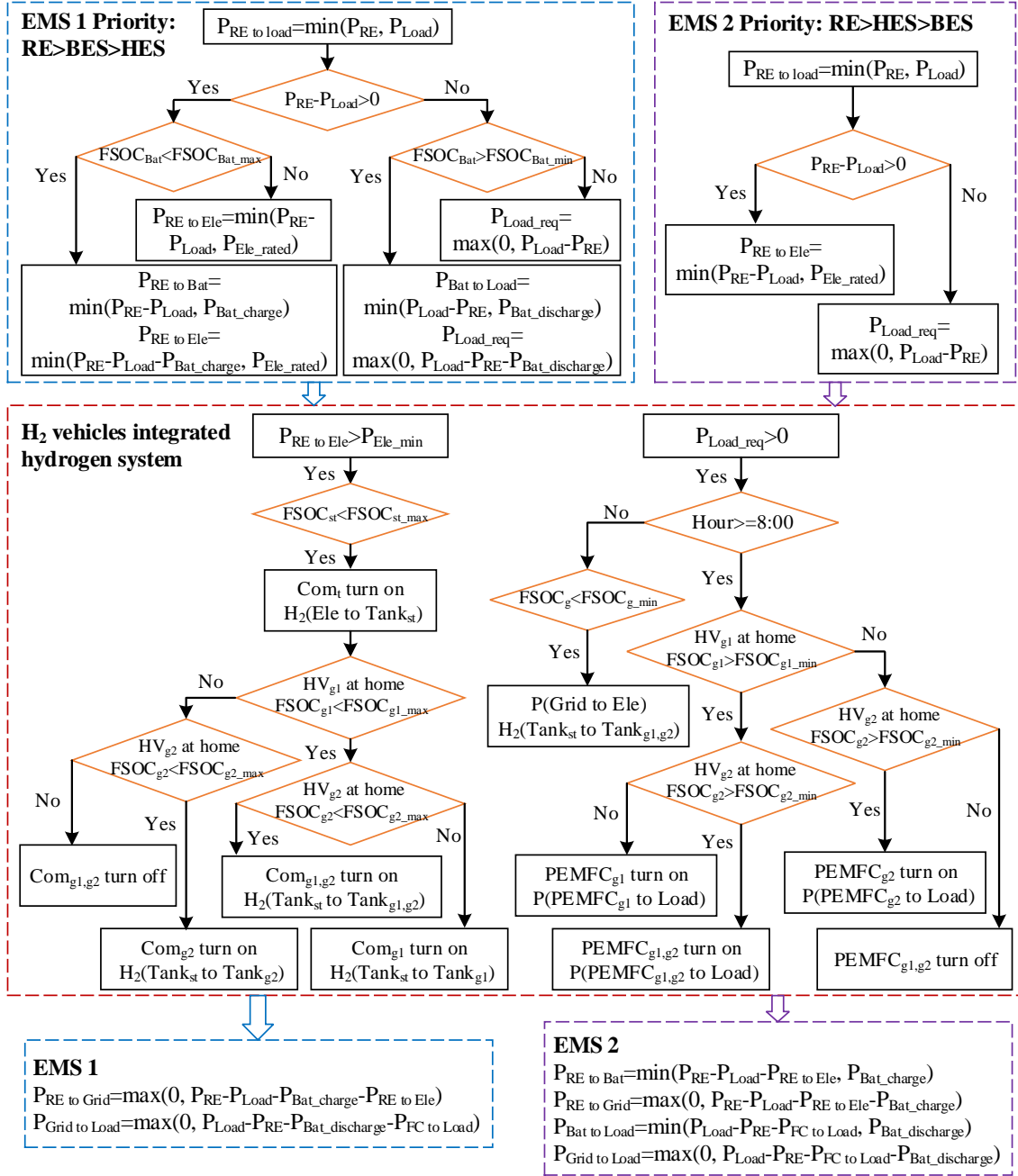


Fig. 6.16 Flow chart of the hybrid system under two management strategies

In EMS 1, surplus renewable energy is controlled to charge the battery considering its maximum charging rate and available charging state as calculated by P_{Bat_charge} . Then, remaining renewable energy is used to drive the electrolyzer to generate hydrogen and store it in the stationary H₂ storage tank via the compressor (Com_t) according to its fractional state of charge ($FSOC_{st}$)

which is also limited by the rated power of the electrolyzer (P_{Ele_rated}). The residual renewable energy is lastly fed into the utility grid, when both the battery and H₂ storage tank are fully charged. The battery is operated to meet the load when renewable energy is not enough for the building demand, and its operation is limited by the maximum discharging rate and accessible discharging state of the battery as calculated by $P_{Bat_discharge}$. The unmet load (P_{Load_req}) then needs to be covered by HVs parked at home with available hydrogen. Finally, the utility grid meets the remaining electrical load. While in EMS 2, the electrolyzer is charged by surplus renewable energy prior to the battery and HVs are discharged to meet the electrical demand before the battery. The selection signal of these two EMSs is set as one concerned variable in the multi-objective optimizations, to determine the optimum EMS for major stakeholders (i.e. the end-user, transmission system operator and investor) with different preferences.

The operation of the hydrogen energy storage system is determined by the two groups of HVs with different driving schedules. Compressed hydrogen is supplied from the stationary H₂ storage tank ($Tank_{st}$) to the mobile H₂ storage tanks of HVs parking at home according to the storage FSOC. Specifically, available hydrogen is delivered from $Tank_{st}$ to the mobile tanks of HVs in group 1 ($Tank_{g1}$) via the compressor of group 1 (Com_{g1}), or to those of HVs in group 2 ($Tank_{g2}$) via the compressor of group 2 (Com_{g2}) when only one group of mobile tanks can be charged (the other group is either not at home or fully charged even though at home). And hydrogen in $Tank_{st}$ is equally supplied into $Tank_{g1}$ and $Tank_{g2}$, when both HV groups are parked at home with H₂ storage FSOC values lower than the maximum (0.95). HVs are operated to consume hydrogen in PEMFC to discharge power for the unmet electrical load when parked at home excluding the night time with a low electrical demand (0:00 - 8:00). Namely, the PEMFC of HVs parked at home in group 1 ($PEMFC_{g1}$) and group 2 ($PEMFC_{g2}$) is turned on, when its H₂ storage tank FSOC is larger than

its minimum to cover the one-day cruise (0.10647 in group 1, 0.07321 in group 2) and stay above the atmospheric pressure level (0.0024). During the night time period, the utility grid supplies power to drive the electrolyzer and charge H₂ storage tanks of HVs to secure its minimum FSOC level ($FSOC_{g1_min}$ 0.10887, $FSOC_{g2_min}$ 0.07561) for daytime travelling needs. The initial cost of the electrolyzer and compressor is 1400 US\$/kW [41] and 15000 US\$/Set [144] respectively. The H₂ storage tank costs 50 US\$/N m³ [145] and the HV costs 58500 US\$ according to the official report of the manufacturer [146].

6.3.3 Design optimization of battery and hydrogen vehicle storage based renewable energy systems for the high-rise building

(1) Design optimization settings

Four sizing variables are selected as design parameters of the hybrid PV-wind-battery-hydrogen system, including the façade PV area, wind turbine number, battery capacity and stationary H₂ storage tank volume. The searching space of the installed façade PV area is 300 - 3900 m² at an increment of 600 m², which are installed on three façade areas (South, East and West) of the residential building with an adjacent shading factor of 76.64% [88]. The wind turbine number changes between 1 - 10 with a single turbine capacity of 100 kW and a power transmission loss of 13.541% [91]. The battery capacity is optimized between 240 - 2400 kWh (8 - 80 kWh/floor) at an interval of 240 kWh. The stationary H₂ storage tank volume of the hydrogen storage system is optimized within the range of 1 - 6 m³, as the electrolyzer cell size is determined by the entering power supply to ensure the current density between 40 - 400 mA/cm² [102]. The selection signal of two developed EMSs is also set as an optimization variable for the optimum technical and economic performances of the hybrid system.

Both technical and economic performances of the hybrid PV-wind-battery-hydrogen system are evaluated with the multi-objective optimization. The optimization criteria of the hybrid system comprehensively cover the main concerns of three key stakeholders: the end-user, transmission system operator and investor. The end-user of the hybrid renewable energy and storage system concerns more about the supply performance, which is expressed by a combined criterion integrating the self-consumption ratio of renewable energy, load cover ratio of the electrical demand and overall efficiency of the vehicle-integrated hydrogen storage system. The absolute net power exchange between the utility grid and hybrid system is developed as a decision-making reference for the transmission system operator. The net present value is the difference between the present value of cash outflow and cash inflow of the hybrid system paid by the system investor. The price degeneration rates of main system components are considered, i.e. 5%/year for the battery [147], 10.15%/year for the inverter [148], 4.2%/year for the H₂ storage tank [149], and 4.3%/year for the HV [150].

Decision-making strategies (DMSs) are required to determine a final optimum solution out of the obtained Pareto optimal set. Four decision-making strategies are considered focusing on different concerns of major stakeholders of the hybrid system. The minimum distance to the utopia point method is adopted for DMS 1 with an equivalent priority to all evaluated criteria. The analytical hierarchy process method is adopted for DMS 2: the end-user priority, DMS 3: the transmission system operator priority, and DMS 4: the investor priority.

(2) Design optimization results

The Pareto optimal solutions are obtained through the multi-criterion optimizations by varying the EMS selection and system sizing variables for techno-economic indicators of the hybrid PV-wind-battery-hydrogen system, including *SCR*, *LCR*, *HSE*, *NGE* and *NPV*. These best

solutions are then normalized and the supply performance indicators (i.e. *SCR*, *LCR* and *HSE*) are combined with the weighted sum method as an integrated objective *Supply*.

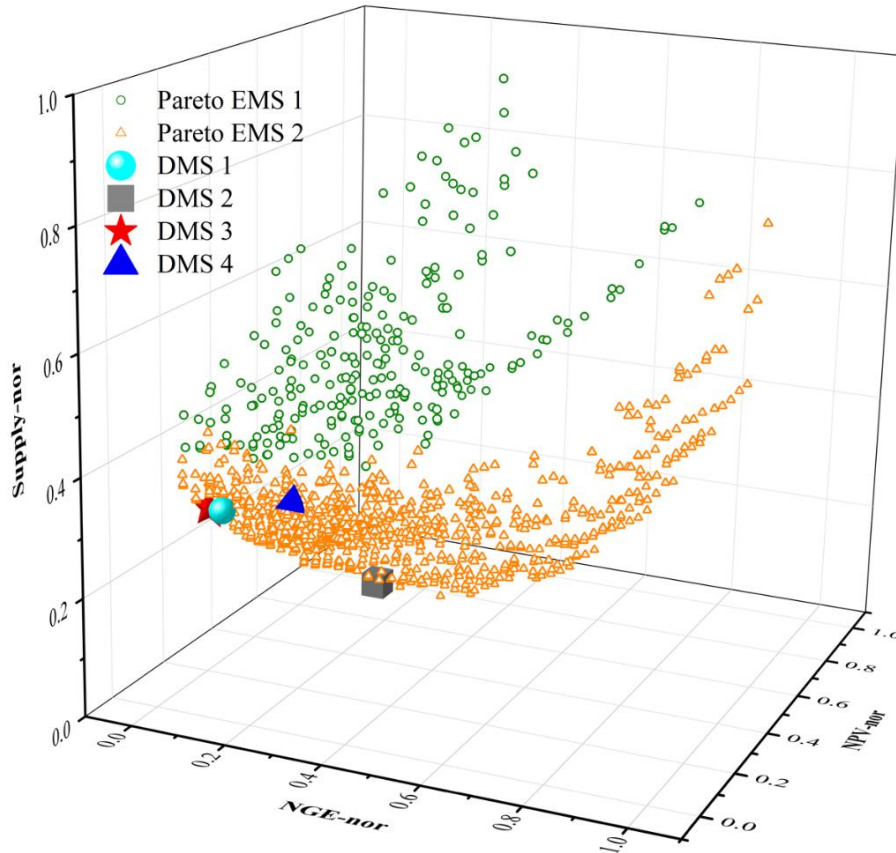


Fig. 6.17 Pareto optimal and final optimum results of four decision-making strategies

The three-dimensional Pareto optimal surface is then demonstrated in Fig. 6.17 consisting of three normalized objectives (i.e. *Supply*, *NGE* and *NPV*). It is indicated that both EMS 1 (BES prioritized over HES) and EMS 2 (HES prioritized over BES) are selected in the Pareto optimal set with different optimization focuses. Four DMSs are further adopted to select the final optimum solution out of the Pareto optimal solutions for key stakeholders. It is found that the optimum solutions of these four DMSs are achieved with EMS 2 where hydrogen storage is prioritized over battery storage.

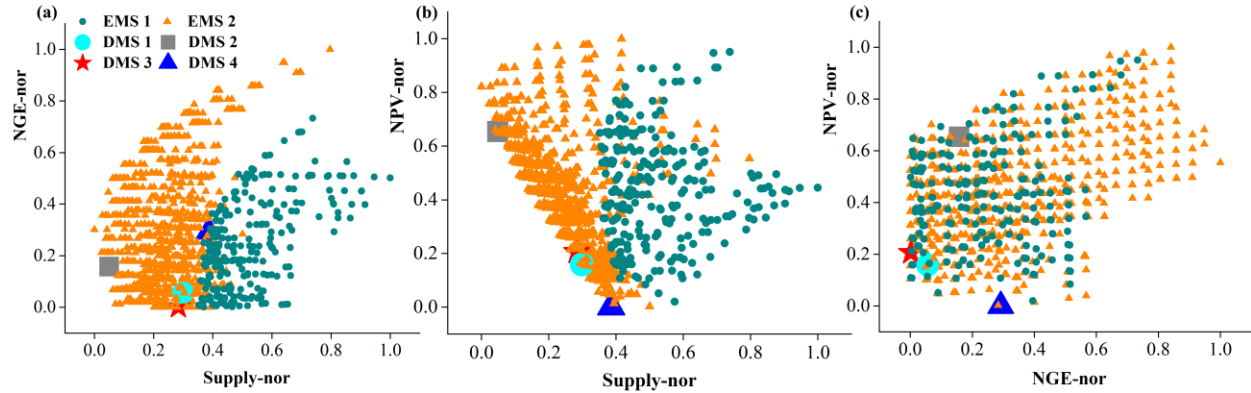


Fig. 6.18 Projection distribution of Pareto optimal and final optimum results

Fig. 6.18 shows the two-dimensional projection of Pareto optimal solutions of EMS 1 and EMS 2 with the highlighted final optimum solutions under four DMSs. It is found that EMS 2 dominates the best solution, when considering objective combinations of *Supply-NGE* and *Supply-NPV* as per Fig. 6.18(a, b), because the indicator *Supply* (integrating *SCR*, *LCR* and *HSE*) achieves better performance under EMS 2, where hydrogen storage is prioritized over battery storage. Namely, EMS 2 should be selected as the energy management scheme of the hybrid system, when focusing on the system supply and grid integration or system supply and economy performance. However, no clear dominance is observed between EMS 1 and EMS 2 when considering the *NGE-NPV* objective combination as shown in Fig. 6.18(c), because the change of EMSs with different operation priorities of storage has minor impact on the system *NGE* and *NPV*. It means that both EMS 1 and EMS 2 are applicable when focusing on the grid integration and system economy performance. The results of optimum solutions under four DMSs are shown in Table 6.7.

Table 6.7 Sizing results of four decision-making strategies for the hybrid system

Optimization results	Facade PV /m ²	Wind turbine number	Battery capacity /kWh	Stationary H ₂ tank /m ³
Equivalent priority (DMS 1)	1500	8	480	5

End-user priority (DMS 2)	3900	5	1920	4
Transmission system operator priority (DMS 3)	900	8	720	5
Investor priority (DMS 4)	900	10	240	6

The sensitivity analysis of four sizing variables for the optimization objectives of the hybrid system is shown in Fig. 6.19 with the optimum solution by DMS 1 as the baseline case. It is indicated that the SCR decreases with the rising façade PV area and wind turbine number given more available renewables power, while the SCR increases with the battery capacity for more on-site renewable energy consumption. The HSE improves with the rising PV and wind capacity, due to more energy storage in the hydrogen system, and it is less sensitive to the changing battery capacity because hydrogen storage is prioritized over battery storage in EMS 2. The LCR shows a steady rise with the larger façade PV area, wind turbine number and battery capacity due to more available power supply from the hybrid system. And the NPV rises sharply with the increasing battery capacity as the initial cost of the battery is relatively high and subject to replacement every five years. The NGE shows a steady drop with the rising battery capacity as more grid exchange can be waived by batteries which can meet the electrical load and consume surplus renewable energy. The stationary H₂ tank volume imposes a relatively lower impact on the optimization objectives compared with the other design variables.

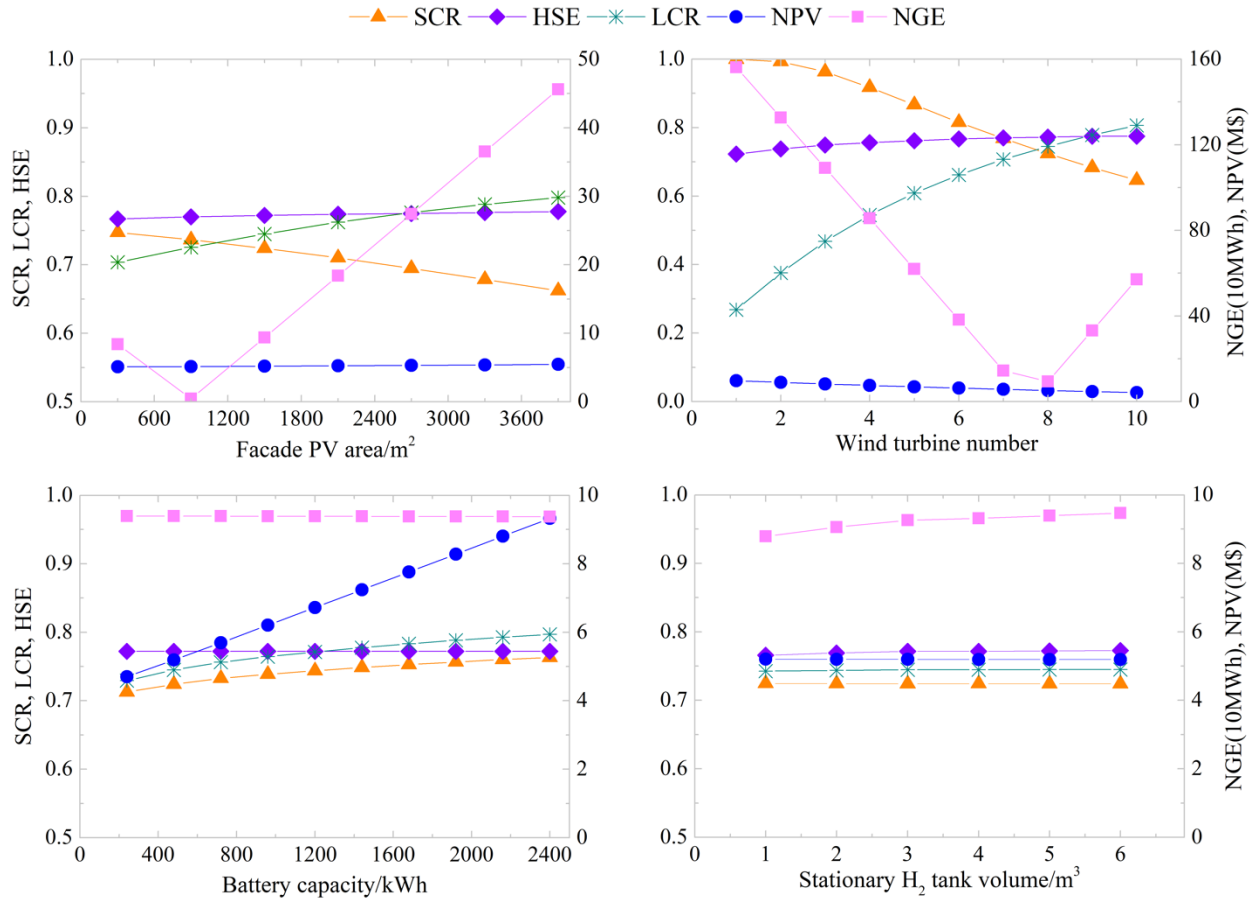


Fig. 6.19 Sensitivity analysis of design variables on optimization objectives

Fig. 6.20 shows the distribution of sizing variables (i.e. the façade PV area, wind turbine number and battery capacity) in the Pareto optimal set of the hybrid system under EMS 1 and EMS 2. These three sizing variables are previously demonstrated to have a greater impact on the optimization objectives compared with the stationary H₂ tank volume (See Fig. 6.19). EMS 2 achieves better performance in terms of the supply performance (integrating *SCR*, *LCR* and *HSE*) compared with EMS 1, and these supply indicators are more sensitive to sizing variables at low magnitudes based on the previous sensitivity analysis. Therefore, the superiority of EMS 2 is more obvious in small-scale systems, while EMS 1 and EMS 2 are comparable in large-scale systems. In summary, EMS 2 has a wider applicability in the hybrid system with different PV, wind and

battery capacities to achieve the optimum techno-economic performances (*Supply*, *NGE* and *NPV*).

While EMS 1 is suitable for the hybrid system with large PV, wind and battery capacities in the multi-objective optimization.

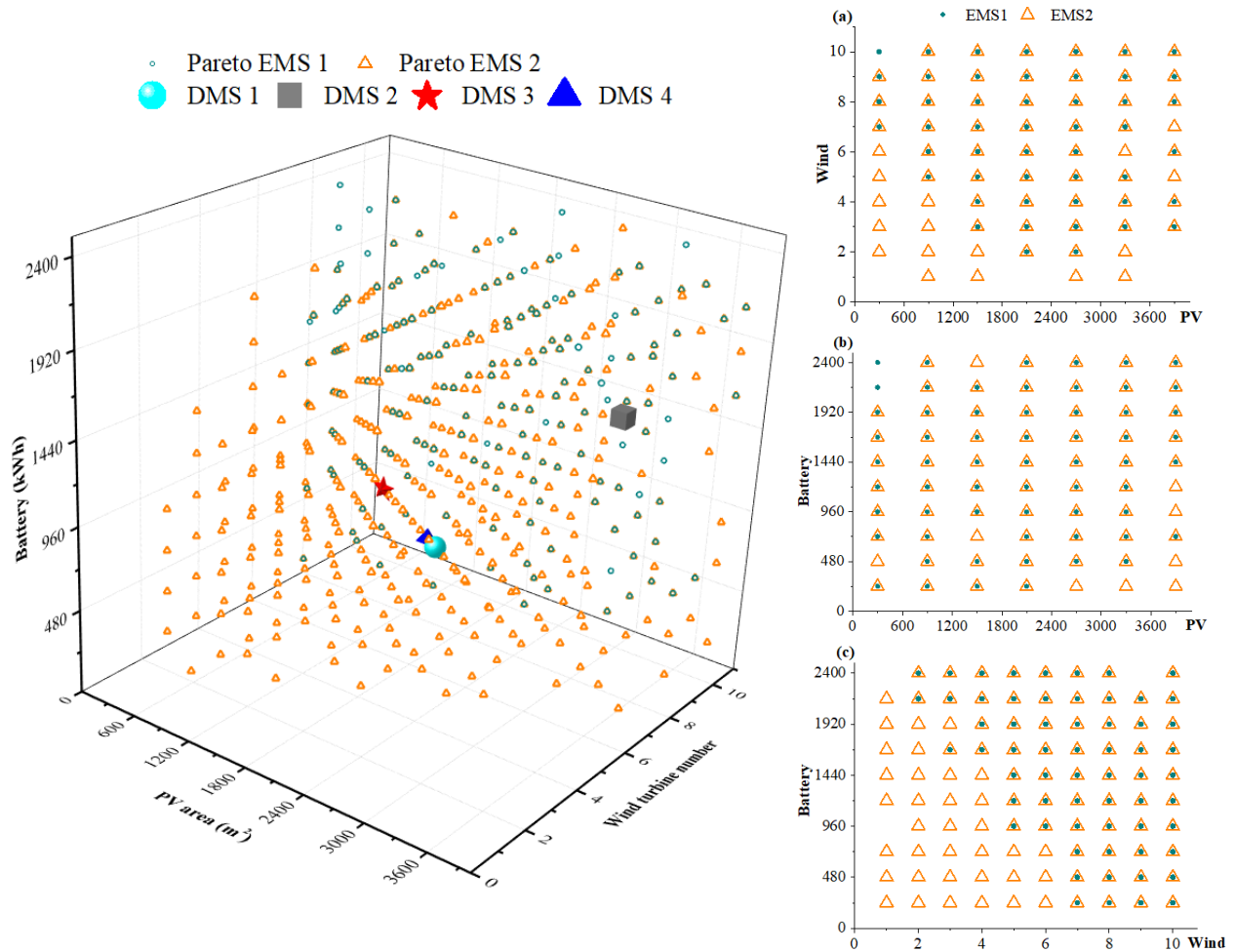


Fig. 6.20 Distribution of sizing variables of EMS 1 and EMS 2 of Pareto optimal solutions

6.3.4 Techno-economic-environmental analysis of battery and hydrogen vehicle storage based renewable energy systems for the high-rise building

(1) Technical analysis of the hybrid PV-wind-battery-hydrogen system

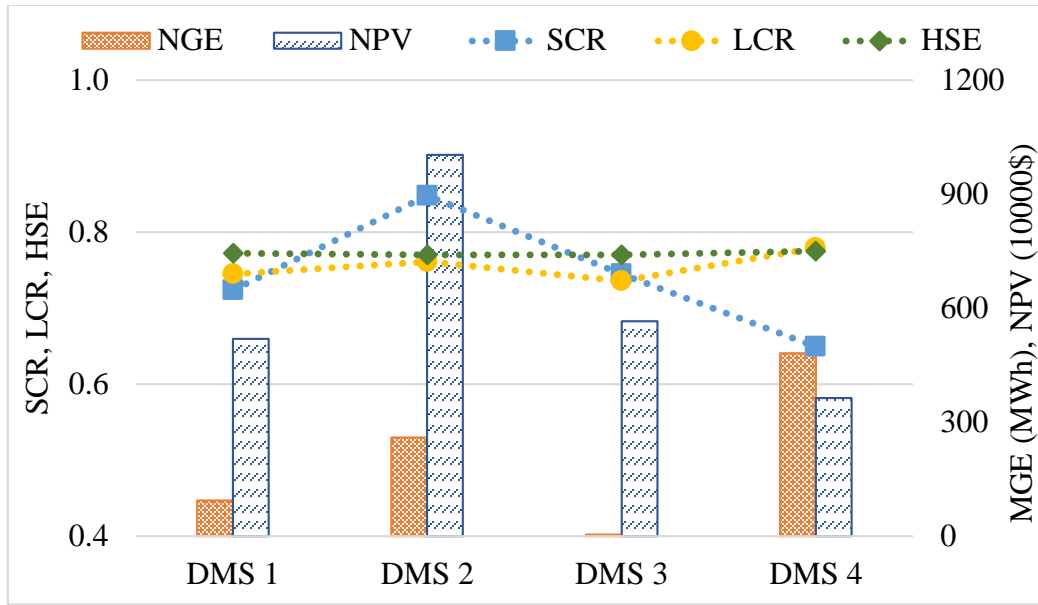


Fig. 6.21 Results of optimum solutions of four DMSs of the hybrid system

(Note: DMS 1: equivalent priority, DMS 2: end-user priority, DMS 3: grid operator priority, DMS 4: investor priority.)

The optimum results of four DMSs of the hybrid system are compared in Fig. 6.21, including the annual average self-consumption of renewable energy (SCR), cover ratio of the electrical load (LCR), overall efficiency of the hydrogen system (HSE), absolute value of the net grid exchange (NGE) and net present value (NPV). The annual average SCR reaches its maximum of 84.79% in DMS 2 with the minimum wind power generation, and a relatively low SCR (64.93%) is observed in DMS 4 with the maximum wind power generation. The LCR shows a minor variation with the maximum of 77.93% under DMS 4. A relatively stable annual average HSE is observed among all DMSs between 77.00% - 77.52%, as hydrogen storage is prioritized over battery storage for energy charging and discharging in EMS 2. Majority of released heat of the hydrogen system can be recovered to cover the air-conditioning reheat and domestic hot water demand in the building with the annual average heat recovery efficiency (HRE) between 95.17% - 95.46%. DMS 1 achieves a

relative balance among all optimization objectives with an equivalent priority. DMS 2 (focusing on the end-user's concern) has the optimum performance on the integrated objective *Supply* with an annual average SCR, LCR and HSE of 84.79%, 76.11% and 77.06% respectively. DMS 3 (focusing on the transmission system operator's concern) has the minimum NGE of 4.55 MWh between the utility grid and the hybrid system compared to the maximum of 482.19 MWh in DMS 4 with the maximum wind energy and minimum battery capacity. DMS 4 (focusing on the investor's concern) achieves a minimum lifetime NPV of about 3.64 M\$ with a detailed breakdown in the economic analysis.

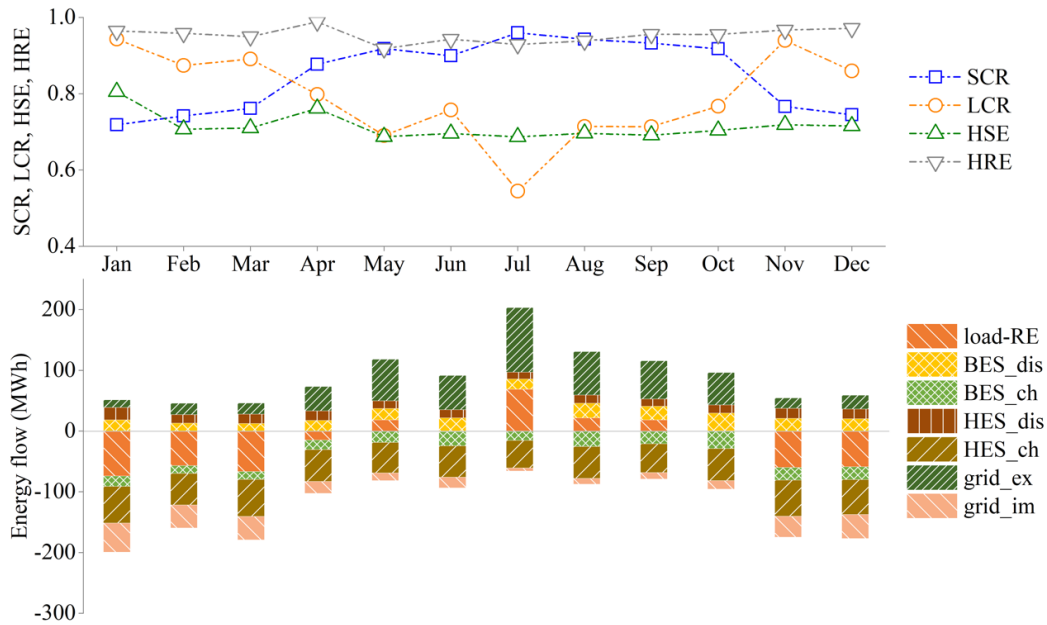


Fig. 6.22 Monthly energy flow and system technical performance in DMS 2 (end-user priority)

The monthly energy flow of major components in the hybrid system and important technical indicators are demonstrated for the final optimum solution of DMS 2 (i.e. supply performance prioritized) as per Fig. 6.22 (power out: positive; power in: negative). An obvious imbalance between the load and supply is observed, with a large renewable energy surplus from November to March and unsatisfied electrical load in July. The charging and discharging energy of battery

storage is relatively balanced, while charging energy of hydrogen storage is notably larger than the discharging energy to the electrical load, due to the large consumption of HVs on road. The monthly average SCR firstly increases and then decreases peaking at 95.96% in July, while the monthly average LCR shows a reversed trend with a maximum of 94.34% in January. The monthly HSE, evaluating the energy storage and heat recovery, also varies with the mismatch between the supply and demand at 68.67% - 80.51%. The majority of released heat from the hydrogen storage system can be recovered for the air-conditioning reheat and domestic hot water demand in the building with a monthly HRE between 91.81% - 98.82%. Over half of total annual electrical load is covered by on-site renewable energy from PV and wind sources, where battery and hydrogen storage undertake 13.86% and 10.34% respectively with the remaining 23.89% from the grid.

(2) Economic analysis of the hybrid PV-wind-battery-hydrogen system

Fig. 6.23 shows the detailed lifetime present value of the hybrid system under four DMSs. The highest investment cost of US\$ 16.40M consisting of the initial cost, operation and maintenance cost (O&M cost) and replacement cost is derived from DMS 2 with the largest PV and battery capacity. The residual cost mainly from hydrogen storage tanks and HVs accounts for a relatively small proportion, and shows a minor difference among all cases at about US\$ 0.19M. A large amount of FiT subsidy can be harvested by the investor in Hong Kong with a maximum of US\$ 9.99M under DMS 4. The detailed breakdown of the NPV is shown in Table 6.8. It is indicated that the lifetime NPV under DMS 4 (investor priority) is the minimum among four DMSs, as the economic performance is prioritized by the system investor. The annual electricity bill of DMS 4 is reduced by 15.44% compared with that of the equivalent priority case (DMS 1), and DMS 4 also gets the maximum amounts of annual FiT subsidy, 14.67% higher than that of DMS 1. The lifetime NPV of DMS 4 is about US\$ 3.64M, which is lower than that of DMS 1 by 29.88%.

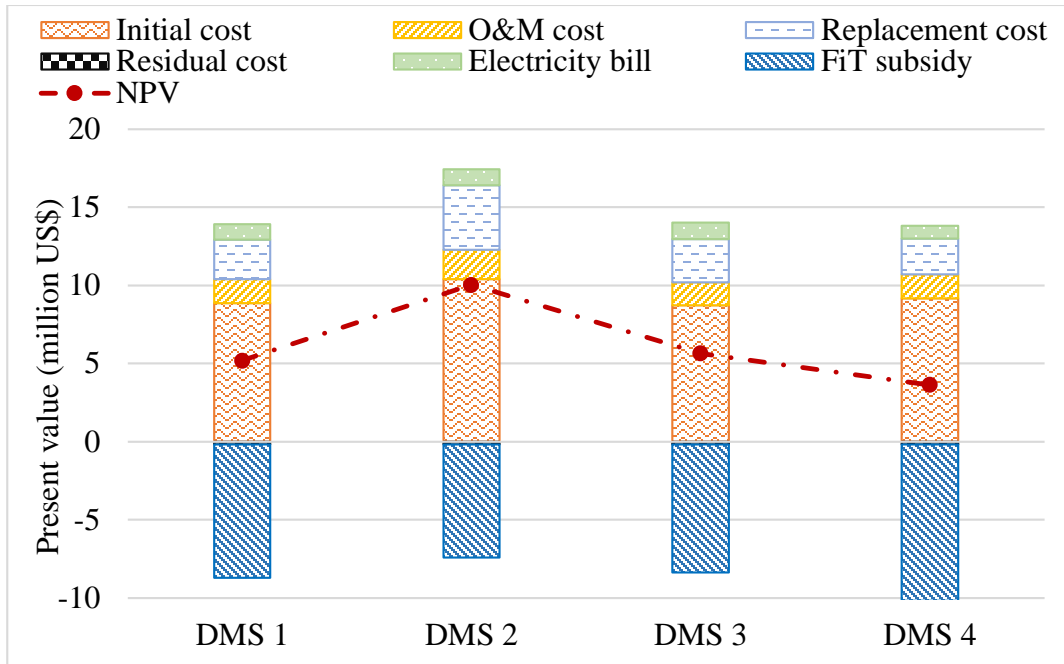


Fig. 6.23 Lifetime present value of four optimum cases of the hybrid system

(Note: DMS 1: equivalent priority, DMS 2: end-user priority, DMS 3: grid operator priority, DMS 4: investor priority.)

Table 6.8 Economic analysis of four optimum cases of the hybrid system

Economic analysis (million US\$)	DMS 1 (equivalent priority)	DMS 2 (end-user priority)	DMS 3 (transmission system operator priority)	DMS 4 (investor priority)
Initial cost	8.85	10.39	8.71	9.17
O&M cost	1.55	1.87	1.49	1.55
Replacement cost	2.51	4.14	2.77	2.26
Residual cost	-0.19	-0.19	-0.19	-0.19
Electricity bill	1.00	1.04	1.03	0.84
FiT subsidy	-8.52	-7.22	-8.17	-9.99
NPV	5.19	10.03	5.65	3.64

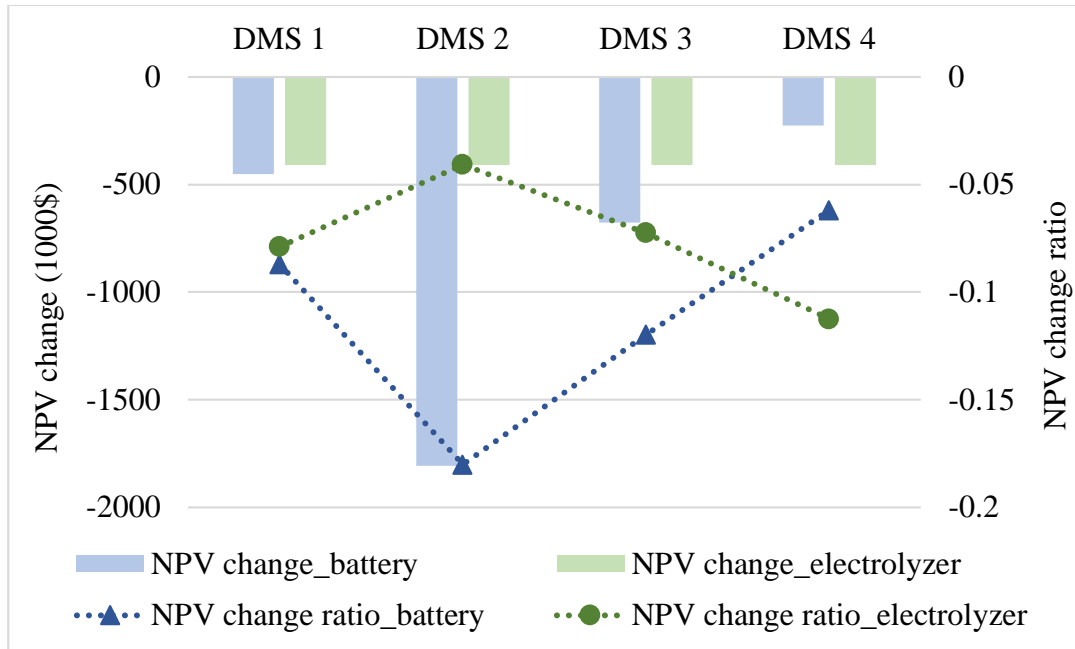


Fig. 6.24 Impact of storage technology prices on the system net present value

(Note: DMS 1: equivalent priority, DMS 2: end-user priority, DMS 3: grid operator priority, DMS 4: investor priority.)

The impact of the initial cost fluctuation of storage technologies (battery and electrolyzer) on the lifetime NPV of the hybrid system is further discussed. The initial cost of storage technologies is varied from a relatively high market price to a low market price. Specifically, the battery price varies from 1000 US\$/kWh [97] to 580 US\$/kWh according to an updated literature [151], and the electrolyzer price varies from 1400 US\$/kW to 500 US\$/kW as estimated by International Energy Agency [152]. The lifetime NPV variation on top of its optimum value under four DMSs is presented in Fig. 6.24. It is indicated that the NPV reduction magnitudes (US\$ 409.55k) caused by the electrolyzer price decrease are the same throughout four cases, given the same calculated maximum electrolyzer cell numbers as determined by the entering power supply from renewable generation or utility grid. While the NPV reduction ratios of the four cases compared with the high market price scenario vary between 4.08% - 11.25%. The NPV magnitude is reduced by 6.20% -

18.01% among four cases, when the battery price decreases to a low market level, with a maximum decline of US\$ 1806.26k in DMS 2 (the maximum battery capacity scenario). It shows that the price fluctuation of storage technologies in the hybrid system has a significant contribution to reducing the lifetime NPV.

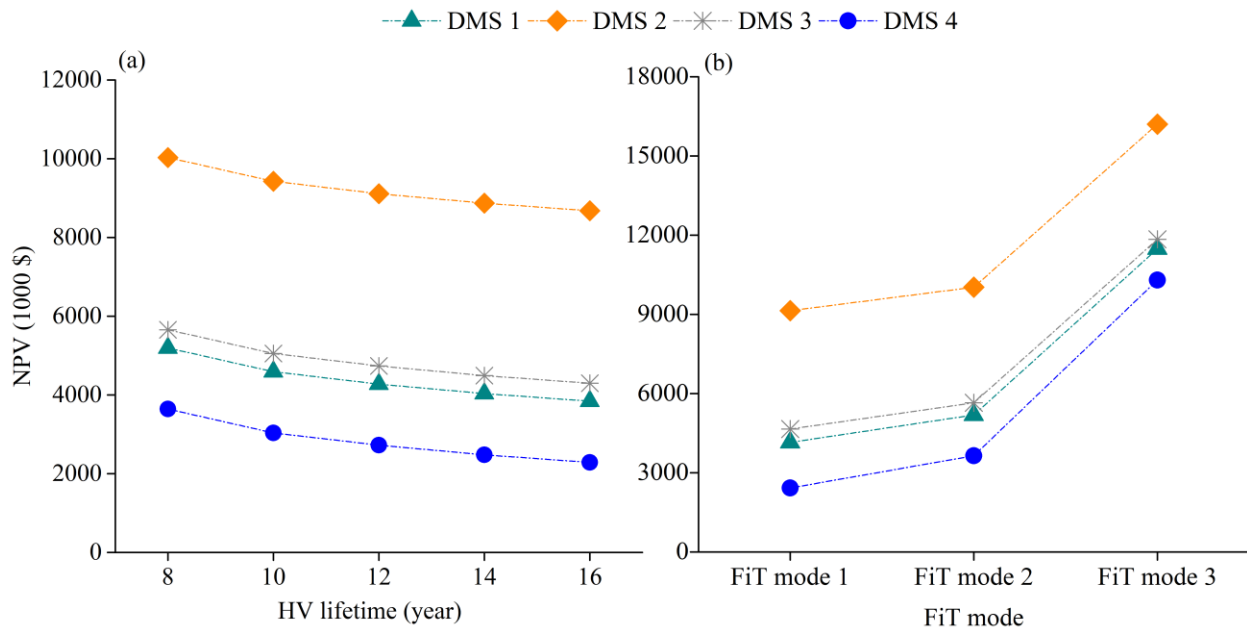


Fig. 6.25 Impact of HV lifetime and FiT mode on the system net present value

(Note: DMS 1: equivalent priority, DMS 2: end-user priority, DMS 3: grid operator priority, DMS 4: investor priority.)

The impact of two important economic parameters (i.e. the HV lifetime and FiT mode) on the system NPV of four DMSs is further discussed in Fig. 6.25(a, b). The system NPV decreases with the rising HV lifetime, due to a lower cost of the hydrogen system. The system NPV is decreased by 13.49% - 37.16% among these four DMSs, when the HV lifetime is changed from 8 years to 16 years. The current renewable energy FiT scheme in Hong Kong provides a subsidy of 3 HK\$/kWh for a 200 - 1000 kW renewable system before 2033, while FiT subsidy after 2033 is not clearly specified. Therefore, three hypothetical FiT modes are discussed for system FiT after

2033: FiT mode 1 - an FiT rate of 3 HK\$ for renewables generation in line with that before 2033; FiT mode 2 - an FiT rate at the local electricity rate for renewable generation as adopted in previous design optimizations; FiT mode 3 - an FiT rate at the local electricity rate for grid exported renewable energy. The system NPV is decreased by 8.92% - 33.52% when the FiT mode is changed from mode 2 to mode 1 following a higher subsidy rate. And a remarkable increase of 61.59% - 182.96% in the system NPV is observed when the FiT mode is changed from mode 2 to mode 3 with less counted renewable generation.

(3) Environmental analysis of the hybrid PV-wind-battery-hydrogen system

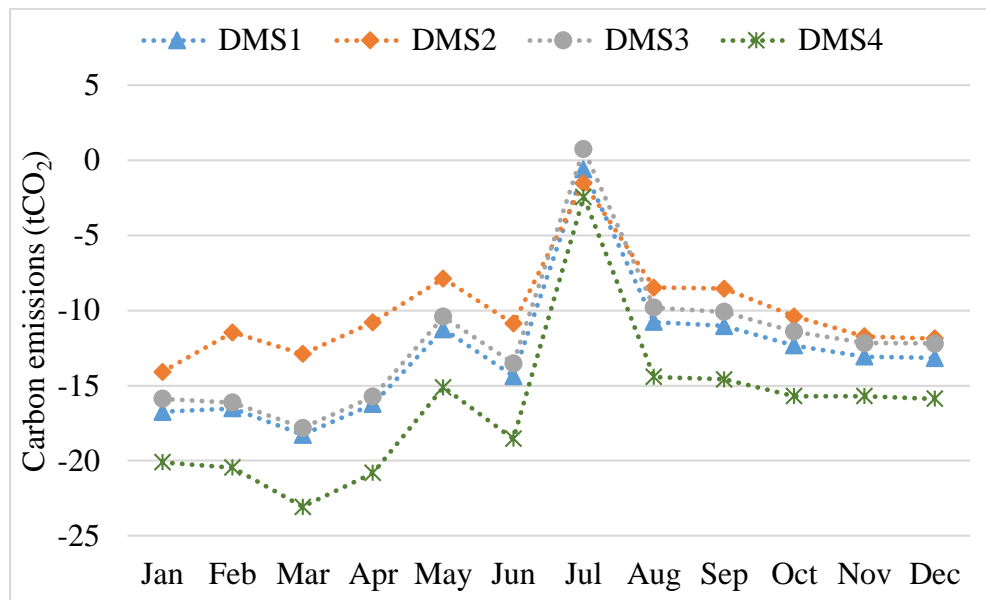


Fig. 6.26 Monthly carbon emissions of four DMSs of the hybrid system

(Note: DMS 1: equivalent priority, DMS 2: end-user priority, DMS 3: grid operator priority, DMS 4: investor priority.)

The monthly carbon emissions of optimum solutions for the hybrid system are determined by the grid imported energy and renewable energy generation as per Fig. 6.26 [63], considering a power transmission loss rate of 0.13541 [91] and local carbon intensity of 0.66 kgCO₂/kWh [136].

The carbon emission can be negative indicating more renewable generation than grid import, or zero indicating carbon neutrality for power supply to the high-rise building. The carbon emission in July under DMS 3 is positive showing that more power needs to be supplied from the utility grid, compared with the generated renewable energy in a high electrical load condition. And the carbon emissions in other months are all negative with a positive impact on the sustainable environment development. The total annual carbon emissions of all four cases are negative with the minimum of -196.82 tCO₂ under DMS 4, indicating that environmental benefits can be achieved together with economic profits.

6.3.5 Summary of battery and hydrogen vehicle storage based renewable energy systems for the high-rise building

This section comprehensively analyzes techno-economic-environmental performances of hybrid photovoltaic-wind-battery-hydrogen systems for power supply to typical high-rise residential buildings with a robust multi-objective design optimization and parametric analysis approach. Two energy management strategies with different priorities of battery and hydrogen storage operations are developed and four decision-making strategies reflecting different stakeholders' concerns are applied to explore the final optimum solutions. Important conclusions are summarized as below:

(1) Two energy management strategies are proposed for the hybrid system with stationary battery storage and two groups of mobile hydrogen vehicles following different cruise schedules, and subject to multi-objective optimizations together with other design variables for a typical high-rise residential building.

(2) It is suggested that both energy management strategy 1 (with battery storage prioritized over hydrogen storage) and energy management strategy 2 (with reversed priority) are suitable for optimizing the grid integration-system economy performance. The Energy Management Strategy 2 should be selected when focusing on the system supply-grid integration or system supply-economy performance. It is also indicated that the Energy Management Strategy 2 has a wider range of applicability in hybrid systems with different photovoltaic, wind and battery installation capacities to achieve the optimum techno-economic performances considering system supply, grid integration and economic indicators. While the Energy Management Strategy 1 is suitable for hybrid systems with large photovoltaic, wind and battery installation capacities in the techno-economic optimization.

(3) The equivalent priority case (Decision-making Strategy 1) can achieve a relatively balanced results among all the optimization objectives, while Decision-making Strategy 2 focusing on the concern of end-users has the optimum supply performance with an annual average self-consumption ratio, load cover ratio and hydrogen system efficiency of 84.79%, 76.11% and 77.06%, respectively. Decision-making Strategy 3 prioritizes the grid integration performance for the transmission system operator, and thus has the minimum absolute net grid exchange of 4.55 MWh, much lower than the maximum of 482.19 MWh in Decision-making Strategy 4. Majority of released heat from the hydrogen system can be recovered to meet the air-conditioning reheat and domestic hot water demand in the building, with an annual average heat recovery efficiency between 95.17% - 95.46% across the four optimum cases.

(4) The system lifetime net present value of the investor priority case (Decision-making Strategy 4) is the most favorable with the minimum electricity bill and maximum feed-in tariff subsidy of about US\$ 3.64M, much lower than that in the equivalent priority case (Decision-

making Strategy 1) by 29.88%. The price fluctuation of battery storage and hydrogen storage technologies from high market to low market price scenarios has a significant impact on reducing the system lifetime net present value. A reduction of 4.08% - 11.25% and 6.20% - 18.01% is derived from the electrolyzer and battery respectively among four decision-making strategies. The system net present value is decreased by 13.49% - 37.16% among four decision-making strategies, when the hydrogen vehicle lifetime is changed from 8 years to 16 years. A remarkable impact of the feed-in tariff mode on the system net present value is also observed, with an 8.92% - 33.52% decrease from mode 2 to mode 1 and 61.59% - 182.96% increase from mode 2 to mode 3. The four optimum cases also achieve negative total annual carbon emissions showing a positive impact on the sustainable environmental development. Especially, the minimum annual carbon emission of -196.82 tCO₂ is obtained from the investor priority case (Decision-making Strategy 4).

(5) This design optimization study on hybrid photovoltaic-wind-battery-hydrogen systems for power supply to typical high-rise residential buildings integrated with hydrogen vehicles provides optimal sizing configurations and energy management schemes for major stakeholders with different concerns. The detailed and in-depth technical, economic and environmental performance analysis offers valuable references for energy planning of hybrid renewable energy and storage systems for future net zero-energy building applications in high-density cities.

CHAPTER 7 SYSTEM OPTIMIZATION OF RENEWABLE ENERGY SYSTEMS WITH BATTERY AND HYDROGEN VEHICLE STORAGE FOR A NET-ZERO ENERGY COMMUNITY

Following the research on hybrid renewable energy and storage systems for a single building in Chapter 5 and Chapter 6, this chapter further studies the design optimization of hybrid renewable energy systems integrated with stationary battery and mobile hydrogen vehicle storage for a diversified net-zero energy community. A time-of-use grid penalty cost model evaluating grid import and export during on-peak and off-peak periods is proposed to achieve the power grid flexibility and economy. Multi-objective optimizations are conducted to size net-zero energy buildings and the community considering the renewable energy self-consumption, on-site load coverage and grid penalty cost.

7.1 Framework of renewable energy systems with battery and hydrogen vehicle storage for the net-zero energy community

The hybrid renewable energy and storage sharing microgrid system is developed in the TRNSYS 18 environment [139] for power supply to a net-zero energy community with the overall framework shown in Fig. 7.1. Three typical building groups of university campus buildings, commercial office and high-rise residential buildings are combined as a community, with on-site collected energy use data and simulations as per local surveys and codes. The load file of the campus building group is obtained from operational data of Phase I - Phase V buildings in the Hong Kong Polytechnic University (PolyU). The load file of the office building group is collected

from the commercial office zone of the International Commerce Center (ICC) in Hong Kong. And the annual load of the high-rise residential building group is obtained from the transient simulation according to local surveys and building codes.

A hybrid renewable energy system of solar photovoltaic (PV) and wind power with complementary characteristics is adopted for the shared power supply to buildings. Stationary battery units are installed in the building community serving as a shared storage among buildings. 1000 hydrogen vehicles (HVs) in three groups following different cruise schedules are developed for the community, serving both as commuting tools and shared storage. A time-of-use grid penalty cost model is proposed optimizing grid import and grid export during on-peak and off-peak periods, to achieve the flexibility and economy of the power grid. An energy management strategy is also established to dynamically control the energy flow among the energy demand, hybrid supply, hybrid storage and utility grid components.

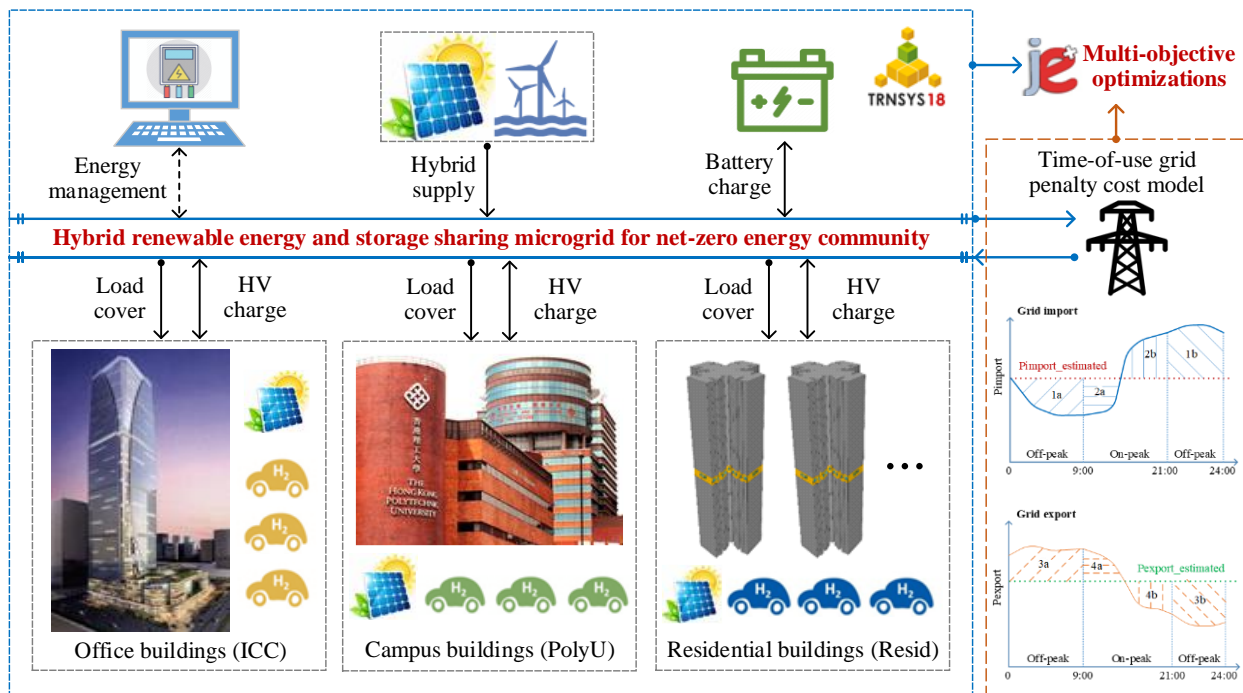


Fig. 7.1 Framework of renewable energy and storage system for the community

Four net-zero energy scenarios are developed and optimized including the net-zero energy community, net-zero energy campus buildings, net-zero energy office buildings and net-zero energy residential buildings, to compare the system performances. Multi-objective optimizations of net-zero energy scenarios are conducted to determine the installation capacity of PV panels, wind turbines and battery units. Three indicators are selected as the optimization criteria, including the self-consumption of renewable generation, on-site coverage of the electrical load and time-of-use grid penalty cost. The impact of battery storage on hybrid renewable energy systems are also quantified, by comparing with four net-zero energy scenarios without battery storage. The energy supply, economic and decarbonisation potential performances of net-zero energy scenarios are further clarified, via the comparison with baseline scenarios without renewable energy supply.

7.2 Load profile of a diversified building community with three building groups

A typical community is established for renewable energy applications covering campus, office and residential buildings in Hong Kong, based on actual energy consumption data and simulations as per local surveys and codes. The dynamic practical electricity consumption of Phase I - Phase V buildings of about 149,260 m² in the Hong Kong Polytechnic University (PolyU) is collected as the campus building load profile. The office building operation data is collected from the International Commerce Center (ICC) in Hong Kong. ICC is a commercial skyscraper with shopping arcades, commercial offices and hotels, but only electricity consumption of commercial offices of about 268,800 m² is adopted for this study. Ten typical high-rise buildings of about 192,095 m² in standard design layouts [127] of public residential buildings (Resid) in Hong Kong are simulated, according to local on-site surveys and building codes [129, 130] as the residential building load profile. The simulated residential building load covers the internal heat gain, air-conditioning load and domestic hot water demand, agreeing well with local survey results [89].

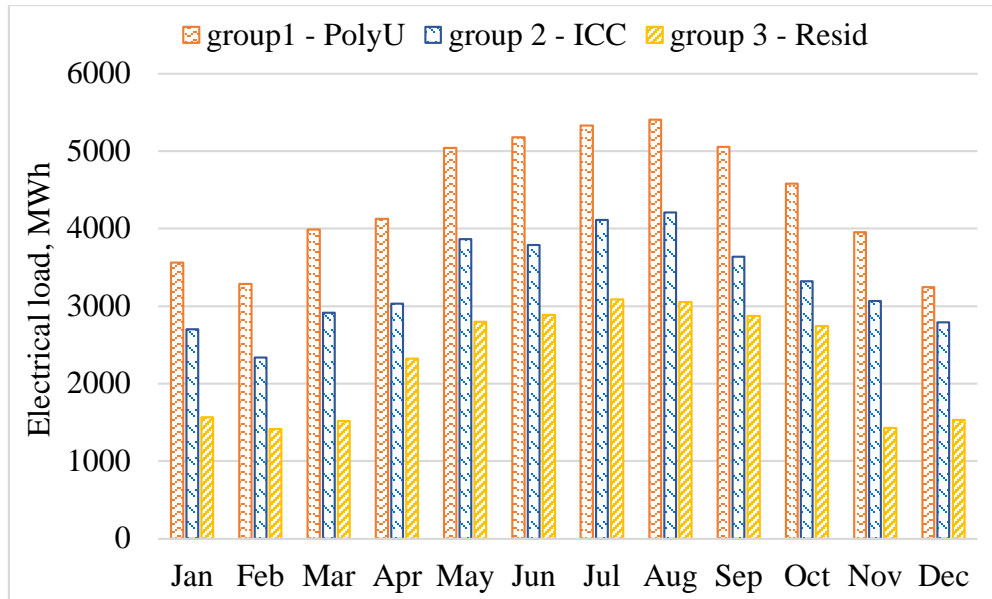


Fig. 7.2 Electrical load of campus buildings, office buildings and residential buildings

The monthly electrical load of these three typical building groups is shown in Fig. 7.2. The monthly electrical load of campus buildings (group 1 - PolyU) varies between 3244 - 5406 MWh, with the minimum in December and maximum in August. The minimum and maximum electrical load of office buildings (group 2 - ICC) is 2336 MWh in February and 4206 MWh in August, respectively. While the electrical load of residential buildings (group 3 - Resid) varies in the range of 1413 - 3086 MWh, with the minimum in February and maximum in July. The specific annual electricity consumption of PolyU is about 353.35 kWh/m²·year (total annual of 52740 MWh), which is higher than 147.94 kWh/m²·year (total annual of 39767 MWh) of ICC and 141.63 kWh/m²·year (total annual of 27206 MWh) of Resid. The total annual electrical load of the community integrating three building groups is about 119,714 MWh and the specific annual load is 196.20 kWh/m²·year.

7.3 System modelling of renewable energy systems with battery and hydrogen vehicle storage for the net-zero energy community

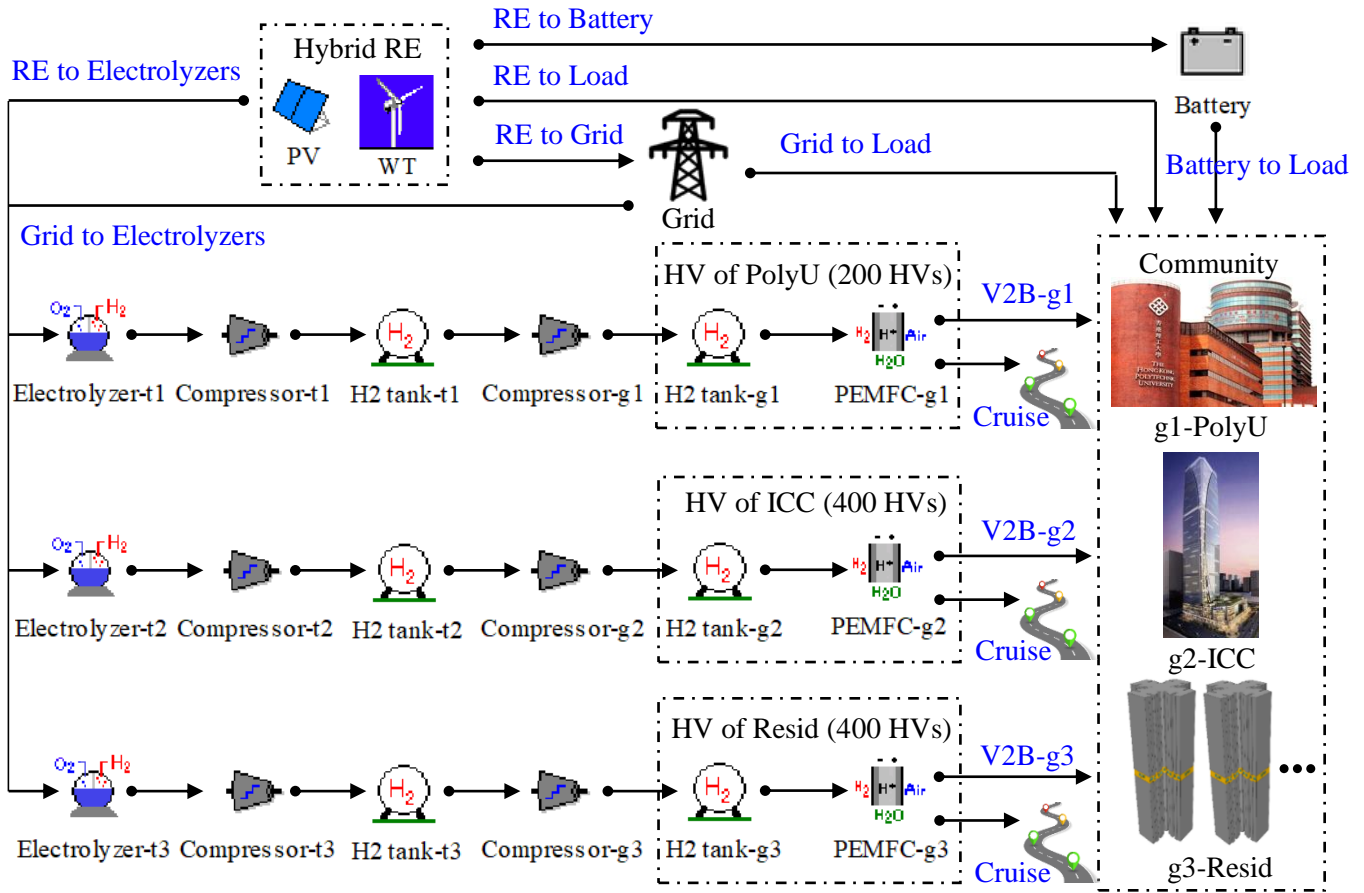


Fig. 7.3 Schematic of renewable energy and storage system for the community

The hybrid renewable energy and storage system for net-zero energy buildings and the community is established in the TRNSYS 18 environment [139] to study the annual operational performance at a timestep of 0.125 h. The schematic of the hybrid system for the net-zero energy community is shown in Fig. 7.3 covering the hybrid supply, stationary battery storage, mobile hydrogen vehicle storage and utility grid integration. The hybrid renewable energy supply and storage is shared in the community microgrid integrating three building groups with different schedules and load distributions.

Hybrid renewable supply: The hybrid solar PV and wind power with complementary generation characteristics are adopted for electricity supply to the net-zero energy building community. The PV panels are simulated by TRNSYS Type 103 with the maximum power point tracked at 22° titled angle close to the latitude of the local geography. The three-blade horizontal-axis wind turbines are also installed for renewable supply modelled by Type 90, according to the tested power-speed characteristic curve of a commercialized product [90]. The installation capacity of PV panels and wind turbines are subject to multi-objective optimizations.

Battery storage: The lithium-ion batteries are installed in the building community shared by three building groups with different operational functions. Batteries can be charged by surplus renewable power or discharged to meet unsatisfied electrical load of the community. The battery charging process is controlled by the battery fractional state of charge (FSOC 0.15 - 0.98), and limited by the maximum battery charging and discharging rate (1C for the lithium-ion battery [98]) at a charging efficiency of 90% [101]. The battery capacity is determined by multi-objective optimizations and the techno-economic-environmental impact of battery storage is further investigated by comparing net-zero energy scenarios with and without battery storage.

Hydrogen vehicle storage: Three groups of HVs are arranged in the community according to occupants' commuting behavior of three building groups. Specifically, 200 HVs are assumed for the PolyU building group with the parking period of 10:00 - 18:00 in weekdays; 400 HVs are assumed for the ICC building group according to its car parking setting and the parking period is 9:00 - 17:00 in weekdays; 400 HVs are assumed for the Resid building group according to a local survey [142] and the parking time is 19:00 - 8:00 from Monday to Saturday and all hours in Sunday. The average daily driving distance of these vehicles is 49.25 km according to a local transport report [153]. The HV is modelled based on a commercialized product "2019 Toyota Mirai", with

a full hydrogen storage of 5 kg at 700 bars and sufficient for a cruise range of up to 502 km [100]. The hydrogen consumption of three HV groups on the road is considered in the simulation, by calculating the FSOC of hydrogen storage tanks of HVs. The parked HVs can also serve as shared energy storage units for the community, to take in surplus renewable energy generation or be discharged for the electrical load. The utility grid is controlled to supply power to HVs, when their residual hydrogen storage is not enough for daily cruise.

Each group of hydrogen system includes electrolyzers (*Electrolyzer-t*), primary compressors (*Compressor-t*) carrying hydrogen from electrolyzers to stationary hydrogen storage tanks (*H₂ tank-t*), secondary compressors (*Compressor-g*) transporting hydrogen from stationary hydrogen storage tanks to mobile hydrogen storage tanks (*H₂ tank-g*) and proton exchange membrane fuel cells (*PEMFC-g*). The electrolyzer is simulated by Type 160a according to an alkaline electrolyzer product “PHOEBUS” [101], and the number of electrolyzer cells is determined by the power supply to keep the electrical current density within 40 - 400 mA/cm² [102]. The multi-stage polytropic compressor is modelled by Type 167 and external electricity is needed to drive the compressor when the entering hydrogen pressure is lower than the desired outlet pressure. The compressed hydrogen storage tank limiting to 700 bars is modelled by Type 164b, based on the van der Waals equation of state for real gases [101]. Type 170d is used to simulate the electrochemical process of PEMFC converting the chemical energy of hydrogen and air to electrical currents. The generated heat accompanied by hydrogen system operations is recovered mainly from electrolyzers, compressors and fuel cells for domestic hot water applications.

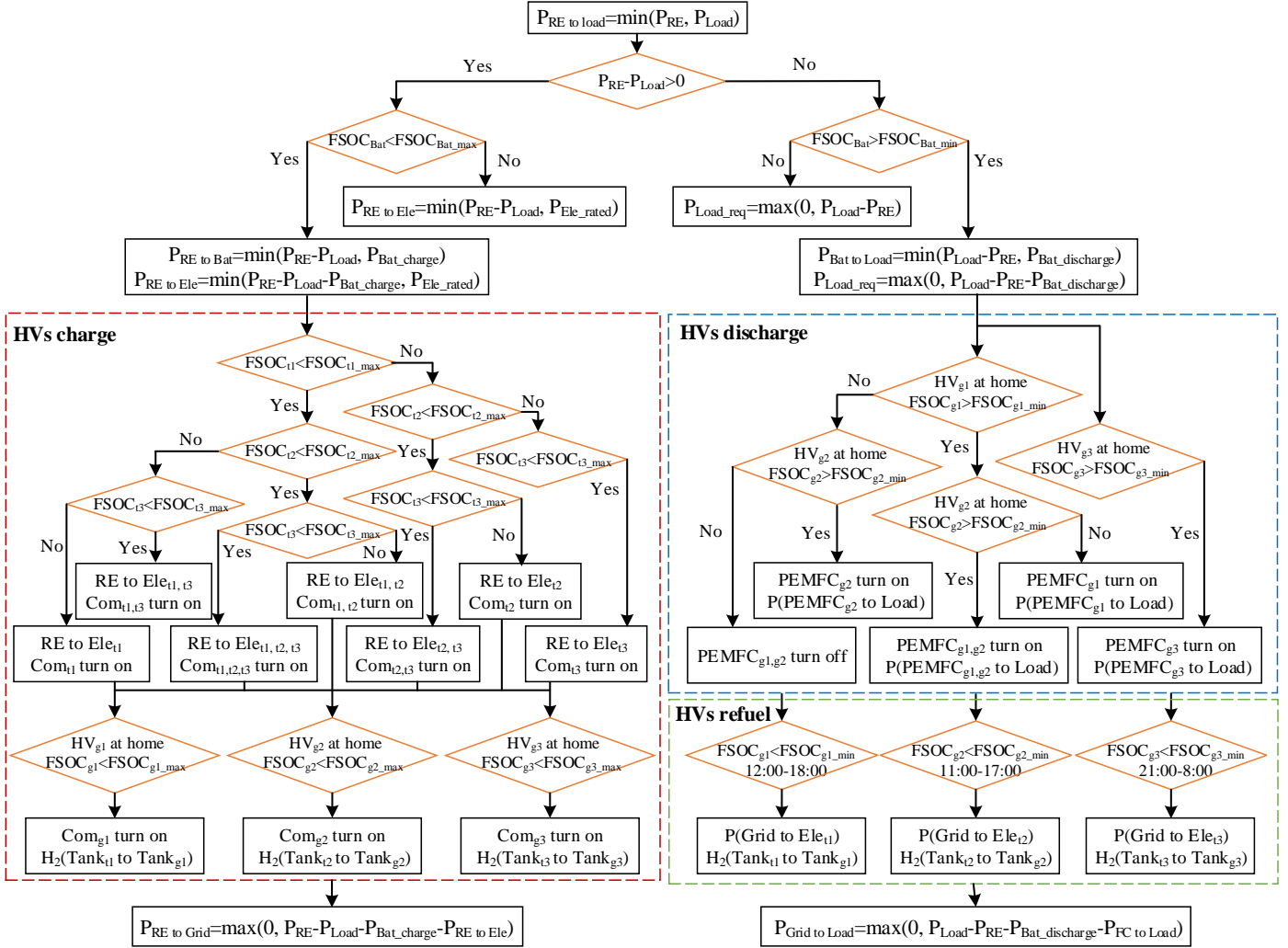


Fig. 7.4 Energy management strategy of renewable energy system for the community

Energy management strategy: The energy management strategy of the hybrid system integrating the stationary battery and three HV groups for the net-zero energy community is shown in Fig. 7.4. The hybrid renewable generation power (P_{RE}) is firstly delivered to meet the electrical load (P_{Load}) of buildings. The surplus renewable energy is used to charge the stationary battery until a full state of charge ($FSOC_{Bat_max}$ 0.98), considering the available charging capacity and charging rate limit. Then renewable energy is controlled to drive three groups of electrolyzers (Ele_t) to produce hydrogen for HVs, considering the available storage state of stationary hydrogen

storage tanks ($FSOC_{t_max}$ 0.95). The corresponding primary compressors (Com_t) are turned on to transport hydrogen from electrolyzers to stationary hydrogen storage tanks ($Tank_t$) when renewable generation is supplied. And secondary compressors (Com_g) are simultaneously turned on to delivery hydrogen from stationary hydrogen storage tanks to mobile hydrogen storage tanks ($Tank_g$), when HV groups are parked at buildings controlled by its maximum storage state ($FSOC_{g_max}$ 0.95). Finally, the residual renewable power is fed into the utility grid.

When renewable energy is not enough for electrical load of buildings, the battery unit is discharged prior to HVs considering the accessible discharging capacity ($FSOC_{Bat_min}$ 0.15) and maximum discharging rate. Then HVs parking at buildings are controlled to consume hydrogen in PEMFCs to provide power according to the charge state of mobile storage tanks. The discharging time of parked HVs of the PolyU group and ICC group is partly overlapped (i.e. 10:00 - 17:00 in weekdays), while the discharging time of parked HVs of the Resid group is totally different with the other two groups. The minimum hydrogen level of mobile storage tanks of three HV groups ($FSOC_{g_min}$ 0.1005) is controlled to cover one-day cruise and stay above the atmospheric pressure during the discharging process. The utility grid serves as the back up to supply power to drive electrolyzers to produce hydrogen for HVs when their storage state is lower than the minimum level. And the utility grid also supplies power for the residual unsatisfied building load.

Four net-zero energy building scenarios with hybrid systems are optimized and analyzed to compare the system supply, economic and decarbonisation potential performance. **Scenario 1:** Net-zero energy community involving three typical building groups integrated with the stationary battery and three groups of HVs following different cruise schedules. The renewable supply and hybrid storage are shared in the community microgrid with three building groups in different operational functions and different load distributions. **Scenario 2:** Net-zero energy campus

buildings integrated with the stationary battery and one group of HVs. *Scenario 3*: Net-zero energy office buildings integrated with the stationary battery and one group of HVs. *Scenario 4*: Net-zero energy residential buildings integrated with the stationary battery and one group of HVs. The installation capacity of PV panels, wind turbines and batteries are optimized for each scenario by multi-objective optimizations. And four net-zero energy scenarios without stationary battery storage and four baseline scenarios without renewable supply are also developed for the techno-economic-environmental performance comparison.

7.4 Design optimization of renewable energy systems with battery and hydrogen vehicle storage for the net-zero energy community

7.4.1 Design optimization variables and objectives of the hybrid system

The installation capacities of the PV panel, wind turbine and stationary battery of four net-zero energy scenarios are sized in the multi-objective optimization process. The PV capacity is dependent on the capacity of wind turbines to achieve a net-zero energy building operation with balanced annual renewable energy generation and annual electricity consumption. So the capacities of wind turbine and battery are selected as the optimization variables with detailed searching range and increment shown in Table 7.1. The searching space of the wind turbine number is 10 - 400 with a single turbine capacity of 100 kW, and the wind power generation at the maximum number almost covers all the electrical load of the community. The optimization ranges of the wind turbine number in the other three net-zero energy scenarios are set, according to the annual load share of the corresponding building group. The searching space of the stationary battery capacity in the net-zero energy community scenario is 5000 - 75000 with the maximum

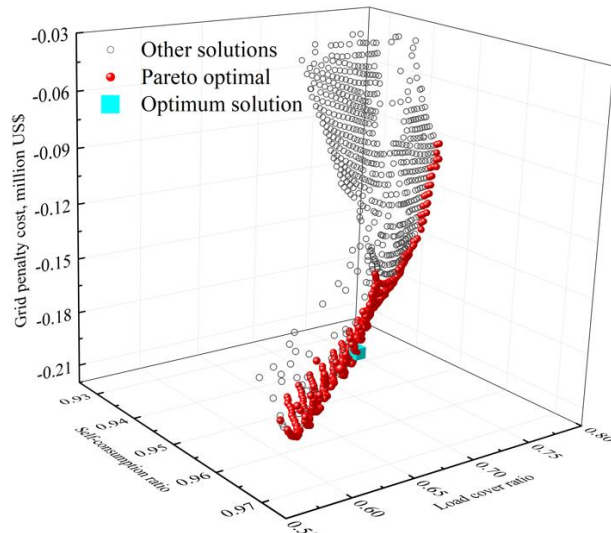
capacity comparable to the storage capacity of HVs. And the search ranges of the other three scenarios are determined according to their HV number.

Table 7.1 Optimization variables of net-zero energy building and community systems

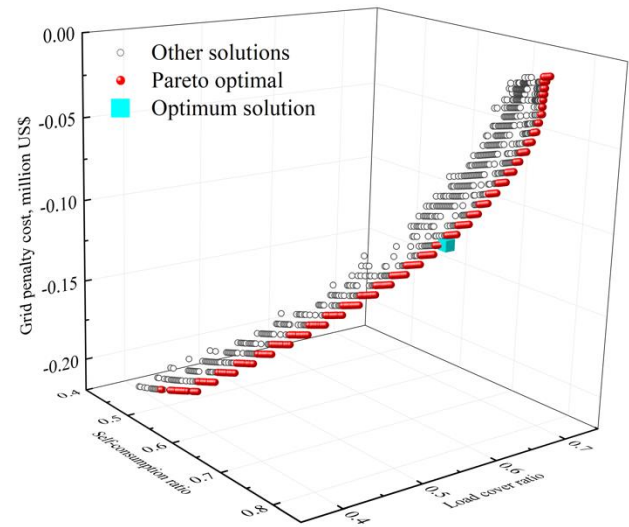
Optimization variables	Wind turbine number		Battery capacity, kWh	
	Range	Increment	Range	Increment
Net-zero energy community	10 - 400	10	5000 - 75000	2000
Net-zero energy campus buildings	10 - 180	5	5000 - 15000	200
Net-zero energy office buildings	10 - 130	3	5000 - 30000	500
Net-zero energy residential buildings	10 - 90	2	5000 - 30000	500

Three optimization criteria are considered in the multi-objective optimization, including the time-of-use grid penalty cost (PC_{TOU}), self-consumption ratio (SCR) and load cover ratio (LCR). The lifetime NPV and annual equivalent carbon emissions are also calculated for the economic and decarbonisation potential of net-zero energy scenarios, compared with baseline scenarios without renewable energy applications. For the grid penalty cost to optimize grid relief potential of net-zero energy buildings and the community compared with baseline scenarios, the grid import estimation ($P_{import_estimated}$) and grid exported estimation ($P_{export_estimated}$) are set as 50% of the peak building load and 20% of the rated renewable capacity respectively in the optimization analysis. And a sensitivity analysis is further conducted to study the impact of grid import and export estimation ratios on the total time-of-use grid penalty cost in Section 7.6. The penalty factors during off-peak time and on-peak time are defined as the ratio of the local off-peak electricity tariff and on-peak electricity tariff of imported energy from utility grid of 0.469 HK\$/kWh and 0.567 HK\$/kWh respectively [116]. The penalty factor ratio is also analyzed in the sensitivity analysis in Section 7.6.

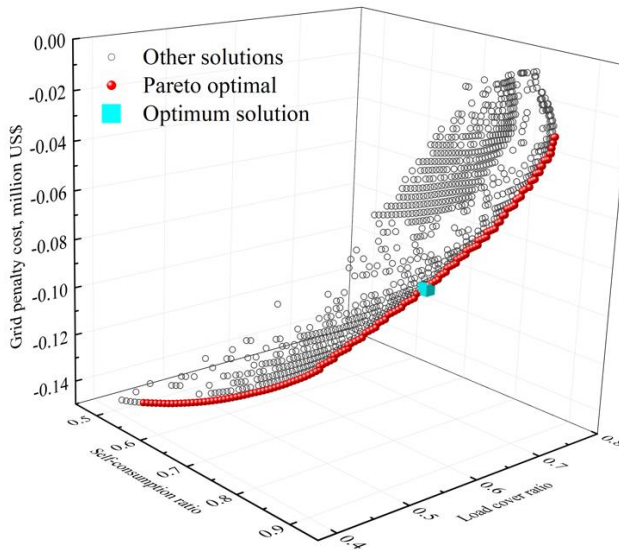
7.4.2 Design optimization results of net-zero energy buildings and community



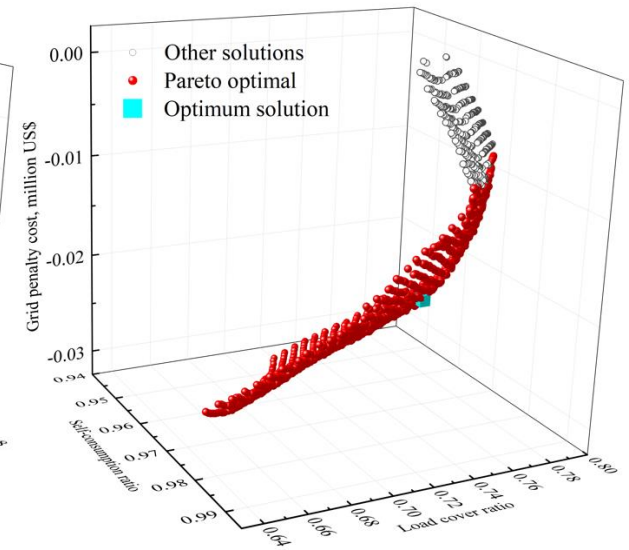
(a) Net-zero energy community



(b) Net-zero energy campus buildings



(c) Net-zero energy office buildings



(d) Net-zero energy residential buildings

Fig. 7.5 Pareto optimal and final optimum solution of four net-zero energy scenarios

Multi-objective optimizations are conducted to size the hybrid systems for four net-zero energy building scenarios. Fig. 7.5 shows the distribution of Pareto optimal solutions among all

searched solutions for optimizing SCR, LCR and PC_{TOU} . It indicates clear trade-off conflicts among the focused optimization criteria in all four net-zero energy scenarios. A final optimum solution is selected from the Pareto optimal set in each scenario as highlighted in cyan cube, according to the minimum distance to the utopia point method [109]. The sizing results of hybrid systems for four net-zero energy building scenarios are shown in Table 7.2.

Table 7.2 Sizing results of renewable energy systems for four net-zero energy scenarios

Sizing results	PV /kW	Wind turbine /kW	Battery /kWh
Net-zero energy community	75095	8000	33000
Net-zero energy campus buildings	21604	8500	15000
Net-zero energy office buildings	23200	3400	30000
Net-zero energy residential buildings	11571	4200	17500

7.5 Techno-economic-environmental results of renewable energy systems with battery and hydrogen vehicle storage for the community

7.5.1 System supply performance of net-zero energy buildings and community

The system supply performance of hybrid systems of four net-zero energy building scenarios with battery and hydrogen vehicle storage is shown in Fig. 7.6. It is found that the maximum SCR and LCR of 97.33% and 75.06% are achieved in the net-zero energy Resid group with the lowest building load and best charging availability of HVs. While the minimum SCR and LCR of 70.70% and 63.14% is achieved in the net-zero energy PolyU group with the highest building load and minimum HV number. The SCR and LCR of the net-zero energy community integrating three building groups outperform the PolyU group and ICC group but are slightly lower than the Resid group. The net-zero energy Resid group has the highest HSE of about 60.92% with a high HV

number and more parking time available for energy exchange with the supply and buildings. And the HSE can be reduced to about 42.66% when the generated heat from electrolyzers, compressors and PEMFCs is not recovered for domestic hot water application. The HSE of the other three net-zero energy building scenarios is comparatively lower between 50.96% - 53.83% with less HVs and lower charging availability.

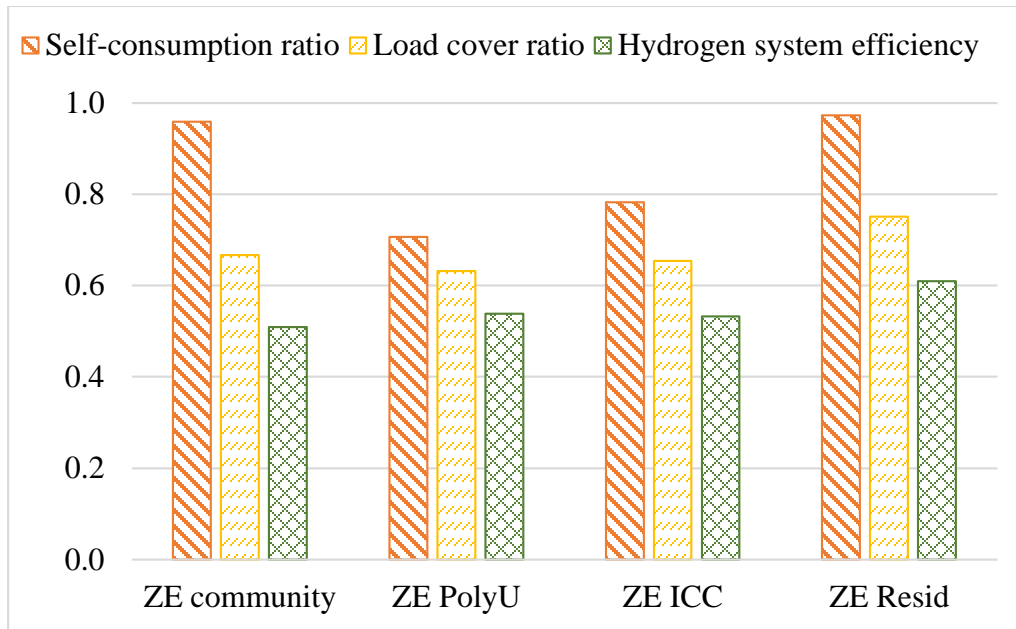


Fig. 7.6 Supply performance of net-zero energy scenarios with battery storage

Table 7.3 Supply performance of net-zero energy scenarios with and without battery storage

System supply performance	Self-consumption ratio (SCR)	Load cover ratio (LCR)	Hydrogen system efficiency (HSE)
ZE community	95.86%	66.62%	50.96%
ZE PolyU	70.70%	63.14%	53.83%
ZE ICC	78.19%	65.39%	53.22%
ZE Resid	97.33%	75.06%	60.92%
ZE community - no battery	95.55% (-0.32%)	62.16% (-6.70%)	50.02% (-1.84%)

System supply performance	Self-consumption ratio (<i>SCR</i>)	Load cover ratio (<i>LCR</i>)	Hydrogen system efficiency (<i>HSE</i>)
ZE PolyU - no battery	61.68% (-12.77%)	55.03% (-12.84%)	56.51% (4.98%)
ZE ICC - no battery	56.10% (-28.25%)	46.45% (-28.96%)	53.78% (1.05%)
ZE Resid - no battery	98.48% (1.19%)	68.94% (-8.15%)	64.77% (6.32%)

Table 7.3 compares the system supply performance of hybrid systems of four net-zero energy building scenarios with and without battery storage indicating their relative difference. It is shown that the SCR of the PolyU group and ICC group is reduced by 12.77% and 28.25% respectively, when battery storage is removed from net-zero energy building scenarios, because less renewable energy is consumed by on-site demand and storage especially during periods when HVs are on cruise. However, the SCR in the Resid group is slightly improved by 1.19% without battery storage, because of higher renewable energy consumption by the large HV group with accessible charging periods. The LCR of all four scenarios is reduced when the battery storage is excluded from net-zero energy buildings. Especially, up to 28.96% decline is observed in the ICC group as less on-site renewable energy is available to meet the building electrical load without batteries. The storage efficiency of hydrogen systems excluding the cruise consumption under all scenarios is slightly improved under the system without batteries, because the battery storage is prioritized over hydrogen storage in original net-zero energy scenarios with battery storage, so that more energy storage is available for hydrogen storage when the battery is absent. While the overall efficiency of hydrogen systems considering the cruise consumption of the net-zero energy community scenario without battery storage is reduced by 1.84% compared with the scenario with battery storage, because the road consumption is relatively large and independent of the battery storage.

It is also indicated that the SCR, LCR and HSE are all improved for the net-zero energy community scenario when battery storage is installed.

7.5.2 Economic performance and decarbonisation potential of net-zero energy buildings and community

The economic performance and decarbonisation potential of net-zero energy buildings and the community with hybrid PV-wind-battery-hydrogen systems are analyzed and compared with baseline scenarios without renewable energy. It is assumed that HV groups are included in baseline scenarios meeting the daily commuting demand of building occupants but refilled in external hydrogen stations at a cost of 16.51 US\$/kg [154]. And net-zero energy scenarios with hybrid PV-wind-hydrogen systems but without battery storage is also developed for comparison to study the impact of battery storage. The grid penalty cost, lifetime NPV and annual carbon emissions of baseline scenarios without renewable energy, net-zero energy scenarios with battery storage and net-zero energy scenarios without battery storage are compared.

(1) Grid penalty cost

The grid penalized energy during on-peak and off-peak periods of the buildings and the community under three systems is compared in Fig. 7.7. The positive penalized energy would result in a grid cost punishment and the negative penalized energy would result in a grid reward to occupants. It is indicated that the grid penalized energy during both off-peak and on-peak time of the community, PolyU and ICC buildings under the baseline scenario are positive with a fine, while it is negative with a bonus during on-peak time for the Resid buildings. Because the grid imported energy during on-peak time for the Resid buildings is relatively small and less than its grid import estimation. Obvious economic reward can be achieved for on-peak grid import and

off-peak grid export for all buildings and the community integrating renewable energy systems with negative penalized energy.

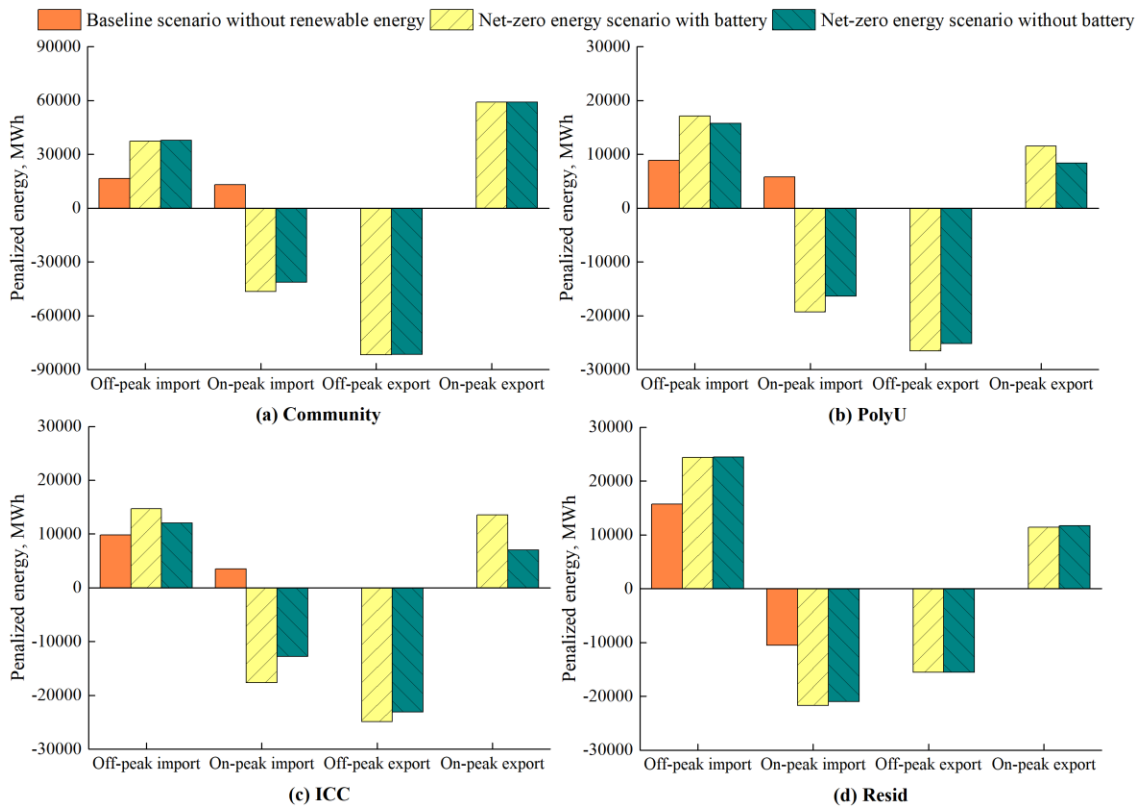


Fig. 7.7 Grid penalized energy of buildings and community under three systems

The annual net grid import energy and grid penalty cost of three buildings and community under three different scenarios are compared in Fig. 7.8. It is indicated that the annual net grid import energy of the Resid group is the minimum (27206.11 MWh) among four baseline scenarios as per Fig. 7.8(a), because the annual electrical load of residential buildings is the minimum. The net grid import energy is significantly reduced in net-zero energy scenarios with battery storage by 71.23% - 90.93%, compared with baseline scenarios without renewable energy. And a net grid import reduction of up to 91.36% is observed in the net-zero energy PolyU group without battery storage (4554.23 MWh) compared with the corresponding baseline scenario, as more renewable generation is fed into the utility grid.

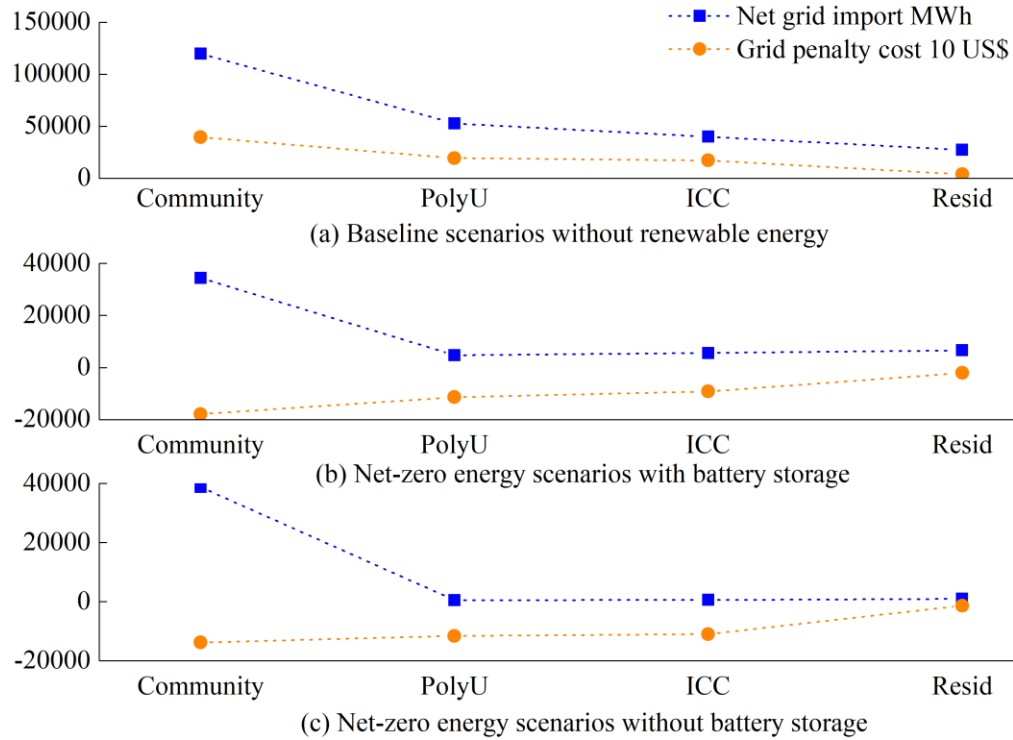


Fig. 7.8 Grid integration performance of buildings and community under three systems

The grid integration improvement of net-zero energy buildings and the community is compared in Table 7.4 indicating the relative difference on top of baseline scenarios. The grid penalty cost of four baseline scenarios ranges from US\$ 37916.41 to US\$ 393649.96 with the minimum achieved in the Resid group for the less building load and energy consumption during on-peak hours. On the contrary, the grid penalty cost of all net-zero energy scenarios is negative as a bonus, contributing to relieving the utility grid with higher operational flexibility and economy performance. Specifically, a reduction of up to 145.36% - 158.92% on the grid penalty cost is achieved in net-zero energy scenarios with battery storage compared with baseline scenarios. And the maximum reduction of 164.41% on the grid penalty cost is observed in the net-zero energy ICC group without battery storage. The PolyU group gets the highest grid bonus compared with the ICC and Resid groups under net-zero energy scenarios, indicating more grid export during on-peak time and less grid import during off-peak time. The community integrating three building

groups with different operational schedules gets more grid reward with higher grid flexibility than three individual building groups in net-zero energy scenarios. The grid penalty cost of the community is about US\$ -178559.85 in net-zero energy scenarios with battery storage, and it is 29.40% lower than that of net-zero energy scenario without battery storage. So the battery storage can significantly contribute to the grid relief of the community.

Table 7.4 Grid integration improvement of net-zero energy buildings and the community

Grid integration	Net grid import MWh	Grid penalty cost US\$
Baseline scenarios without renewable energy		
Community	119714.05	393649.96
PolyU	52740.46	192643.05
ICC	39767.47	170569.33
Resid	27206.11	37916.41
Net-zero energy scenarios with battery storage		
Community	34445.58 (-71.23%)	-178559.85 (-145.36%)
PolyU	4786.04 (-90.93%)	-113500.47 (-158.92%)
ICC	5565.94 (-86.00%)	-92066.53 (-153.98%)
Resid	6645.33 (-75.57%)	-20679.02 (-154.54%)
Net-zero energy scenarios without battery storage		
Community	38821.67 (-67.57%)	-137991.69 (-135.05%)
PolyU	4554.23 (-91.36%)	-115692.02 (-160.06%)
ICC	4777.33 (-87.99%)	-109863.97 (-164.41%)
Resid	7590.23 (-72.10%)	-13336.13 (-135.17%)

(2) Lifetime net present value

The net present value (NPV) of the PolyU, ICC and Resid building groups and the community during a 20-year lifetime under three different scenarios is analyzed as per Fig. 7.9. The lifetime NPV of baseline scenarios without renewable energy mainly covers the electricity bill of the building load and investment of HVs including the initial cost, O&M cost, replacement cost and residual cost. The cost of hydrogen refill by external hydrogen stations is included in the O&M cost. And the lifetime NPV of net-zero energy scenarios includes the investment of renewable energy components, electricity bill and FiT subsidy. The FiT subsidy is obtained in net-zero energy scenarios at an FiT rate of 3 HK\$ for all units of electricity generated by the renewable energy system, and the on-site consumed renewable generation is charged at the electricity rate [114].

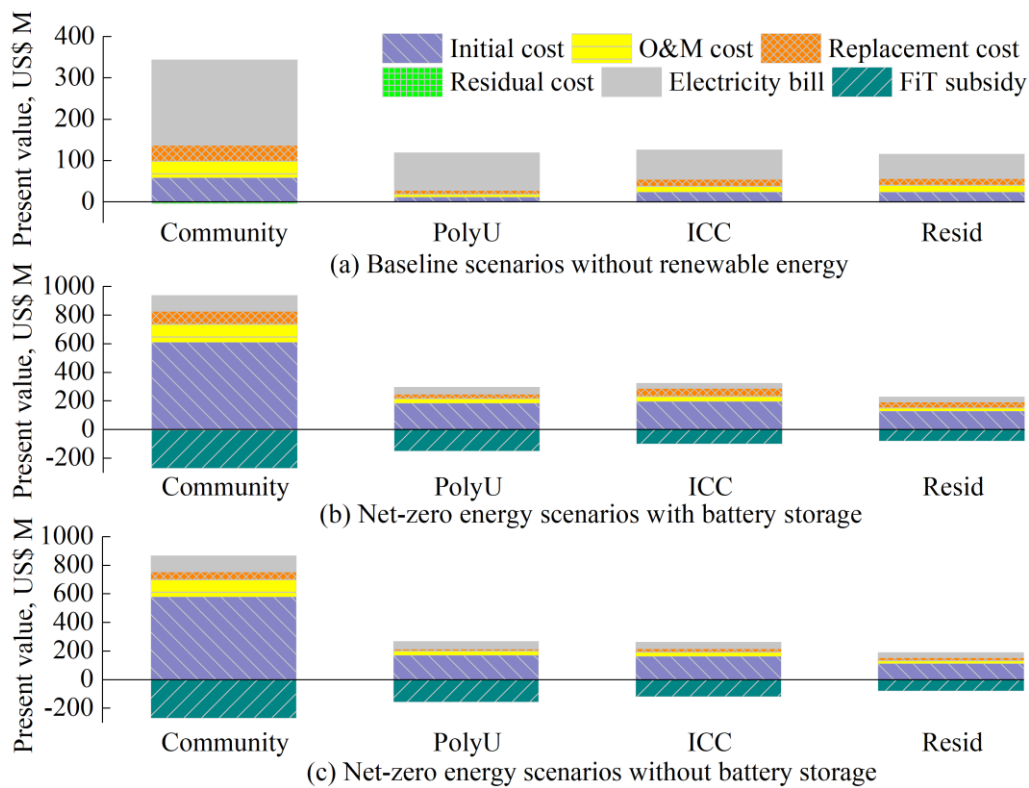


Fig. 7.9 Lifetime net present value of buildings and community under three systems

It is shown that the electricity bill accounts for the majority of the lifetime NPV in baseline scenarios as per Fig. 7.9(a) at about 52.26% - 77.85% for four building scenarios as the electrical

load is totally met by the utility grid. The lifetime electricity bill of the community at about US\$ 207.47M is lower than the sum of electricity bills of three building groups by US\$ 15.90M. The initial cost of the renewable energy system contributes to the main part of lifetime cash outflows (i.e. investment and electricity bill) under all four net-zero energy scenarios with battery storage at 56.79% - 65.41% and four net-zero energy scenarios without batteries at 59.25% - 67.04%. A favorable amount of FiT subsidy can be achieved at US\$ 77.37M - 265.62M for net-zero energy scenarios with battery storage and US\$ 76.47M - 265.79M for net-zero energy scenarios without battery storage. The maximum FiT subsidy is obtained in the community scenario with the maximum renewable energy generation.

Table 7.5 lists detailed items of lifetime NPV of three building groups and their community under three systems. It is indicated that the lifetime NPV of four baseline scenarios varies between US\$ 113.73M - 340.25M including the HV investment and grid electricity bill. The lifetime NPV of four net-zero energy scenarios with battery storage is increased compared with baseline scenarios, due to large investment of renewable energy systems. The net-zero energy community powered by the hybrid PV-wind-battery-hydrogen system shows a 96.17% NPV increment, and a relatively low increment of 22.39% is observed in the net-zero energy PolyU group with batteries. The lifetime NPV of the Reside group is about US\$ 149.32M, which is slightly higher than the PolyU group with more FiT subsidy. It is also highlighted that the lifetime NPV of net-zero energy scenarios without batteries is obviously lower than net-zero energy scenarios with batteries, due to the high initial cost and regular replacement of batteries. The lifetime NPV is lowered by about 6.45% of US\$ 7.62M for the PolyU group without batteries and 1.9% of US\$ 2.16M for the Resid group without batteries compared with baseline scenarios. While the NPV of the community and ICC group without batteries is increased by 75.12% and 15.37% respectively on top of baseline

scenarios. As a result, economic benefits can be obtained by applying hybrid PV-wind-hydrogen systems in the PolyU and Resid groups compared with corresponding baseline scenarios.

Table 7.5 Economic analysis of buildings and community under three systems

Present value million US\$	Initial cost	O&M cost	Replacement cost	Residual cost	Electricity bill	FiT subsidy	Lifetime net present value
Baseline scenarios without renewable energy							
Community	58.50	40.25	37.97	-3.93	207.47	0.00	340.25
PolyU	11.70	7.66	7.59	-0.79	91.97	0.00	118.13
ICC	23.40	15.31	15.19	-1.57	71.97	0.00	124.30
Resid	23.40	17.28	15.19	-1.57	59.43	0.00	113.73
Net-zero energy scenarios with battery storage							
Community	610.29	127.95	86.38	-3.93	112.38	-265.62	667.45 (96.17%)
PolyU	183.44	34.60	28.55	-0.79	48.89	-150.11	144.58 (22.39%)
ICC	195.59	38.35	52.52	-1.57	36.94	-98.10	223.72 (79.99%)
Resid	128.74	24.73	37.00	-1.57	37.79	-77.37	149.32 (31.30%)
Net-zero energy scenarios without battery storage							
Community	577.63	124.18	49.31	-3.93	114.45	-265.79	595.86 (75.12%)
PolyU	168.44	32.86	11.70	-0.79	54.26	-155.96	110.51 (-6.45%)
ICC	161.45	33.89	18.82	-1.57	47.02	-116.21	143.40 (15.37%)
Resid	111.41	22.73	17.34	-1.57	38.12	-76.47	111.57 (-1.90%)

(3) Carbon emissions and equivalent carbon emission cost

The annual carbon emissions and equivalent carbon emission cost of three building groups and their community are compared for the three scenarios as per Fig. 7.10. It is shown that the annual carbon emissions and carbon emission cost of the baseline Resid group (15561.90 tCO₂

and US\$ 373.49k) are less than those of the baseline PolyU group and Resid group, due to lower annual electrical load of the residential buildings. While the carbon emissions and carbon emission cost of the PolyU group are the minimum in net-zero energy building scenarios with the largest amount of renewable energy generation and maximum grid export. The annual carbon emissions of the community integrating three building groups is considerably higher than the sum of carbon emissions of three buildings in net-zero energy scenarios. Because more renewable generation in the community is consumed on-site with a small amount fed into the utility grid, while a relatively large amount imported from the grid although lower than the grid imported sum of three buildings.

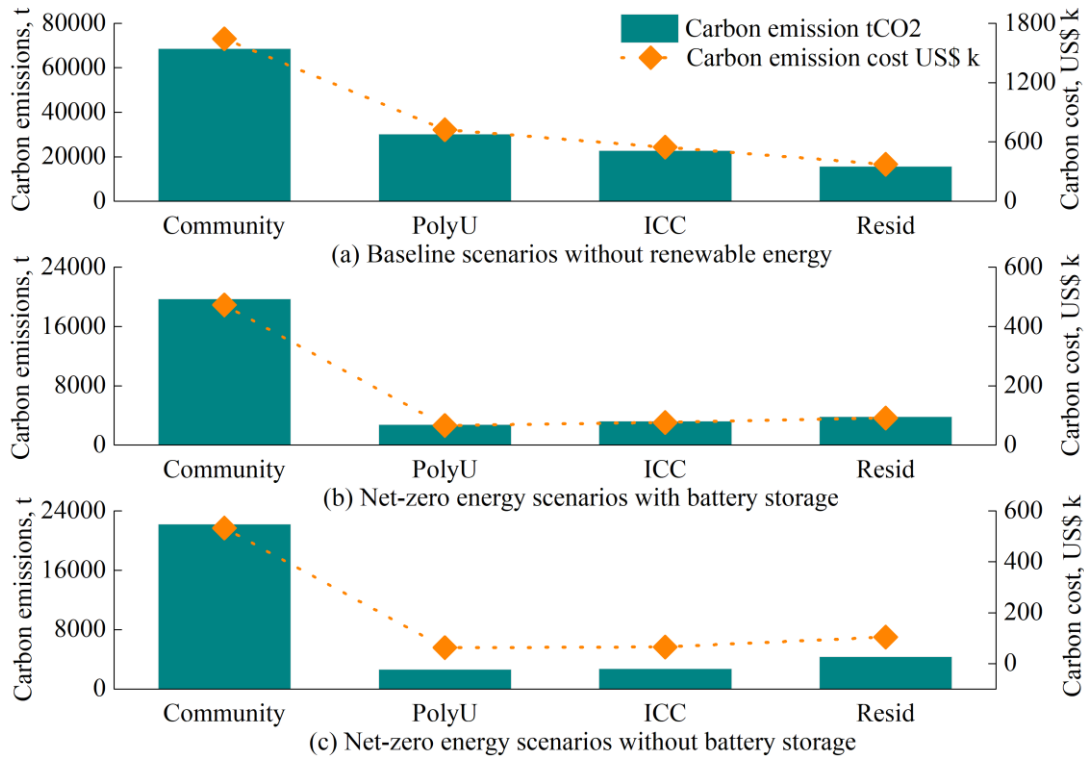


Fig. 7.10 Carbon emissions and equivalent carbon emission cost under three systems

The decarbonisation potential of net-zero energy buildings and community is compared with baseline scenarios as per Table 7.6 with an indication of the relative difference. It is indicated that obvious reductions in carbon emissions and carbon emission cost are achieved for net-zero energy

scenarios, compared with baseline scenarios entirely relying on the utility grid and external hydrogen refill. Specifically, the carbon emissions decline by 71.23% - 90.93% in four net-zero energy scenarios with battery storage with a carbon emission cost saving of US\$ 282.26k - 1170.57k. The carbon emission reduction potential of the community in net-zero energy scenarios without battery storage is 67.57% based on baseline scenarios. It is slightly lower than that in net-zero energy scenarios with battery storage due to a higher grid import when the battery storage is absent from the community. The maximum carbon emission saving potential is achieved in the net-zero energy PolyU group without battery storage with a carbon emission decline of up to 91.36% for about 27562.53 tCO₂ compared with the baseline scenario. And the maximum carbon emission cost saving potential is obtained in the net-zero energy community with battery storage at about US\$ 1170.57k, compared with the baseline scenario relying on the utility grid and external hydrogen refill.

Table 7.6 Decarbonisation potential of net-zero energy buildings and the community

Carbon emission analysis	Carbon emissions tCO ₂	Equivalent carbon emission cost US\$ k
Baseline scenarios without renewable energy		
Community	68476.43	1643.43
PolyU	30167.55	724.02
ICC	22746.99	545.93
Resid	15561.90	373.49
Net-zero energy scenarios with battery storage		
Community	19702.87 (-71.23%)	472.87 (US\$ -1170.57k)
PolyU	2737.61 (-90.93%)	65.70 (US\$ -658.32k)
ICC	3183.72 (-86.00%)	76.41 (US\$ -469.52k)

Carbon emission analysis	Carbon emissions tCO ₂	Equivalent carbon emission cost US\$ k
Resid	3801.13 (-75.57%)	91.23 (US\$ -282.26k)
Net-zero energy scenarios without battery storage		
Community	22206.00 (-67.57%)	532.94 (US\$ -1110.49k)
PolyU	2605.02 (-91.36%)	65.52 (US\$ -661.50k)
ICC	2732.63 (-87.99%)	65.58 (US\$ -480.34k)
Resid	4341.61 (-72.10%)	104.20 (US\$ -269.29k)

7.6 Sensitivity analysis on time-of-use grid penalty cost model

The grid import estimation is defined as the ratio of the peak building electrical load, and the grid export estimation is defined as the ratio of the rated renewable energy capacity as explained in the time-of-use grid penalty cost model. A sensitivity analysis is conducted to investigate the impact of these two ratios on the grid penalty cost for the net-zero energy community with battery storage. It is indicated from Fig. 7.11(a) that the penalty cost of grid import power during off-peak time increases with the import estimation ratio, as a low import estimation is preferred by the utility grid to encourage more excess import in off-peak time. While the penalty cost of grid import power during on-peak time shows a negative correlation with the import estimation ratio, because a high import estimation is preferred by the utility grid to reduce unplanned grid import in on-peak time. The penalty cost of grid export is however not affected by the import estimation ratio. Fig. 7.11(b) shows that the penalty cost of grid export in off-peak time declines with the export estimation ratio while the grid export penalty cost in on-peak time shows an opposite correlation as excess grid export is discouraged during off-peak time but welcomed during on-peak time. The total time-of-use grid penalty cost is US\$ -178.56k under the assumed condition with an import estimation ratio of 50% and export estimation ratio of 20%. Large amounts of bonus are achieved for both grid

export in off-peak time ($PC_{export_offpeak}$) at US\$ -499.18k as per Fig. 7.11(a) and grid import in on-peak time (PC_{import_onpeak}) at US\$ -338.88k as per Fig. 7.11(b). While a fine is imposed for both grid export in on-peak time (PC_{export_onpeak}) at US\$ 430.96k and grid import in off-peak time ($PC_{import_offpeak}$) at about US\$ 228.54k. Appropriate grid import and export estimation ratios should be set in net-zero energy building applications based on the grid power availability considering the peak electrical load and rated renewable energy capacity.

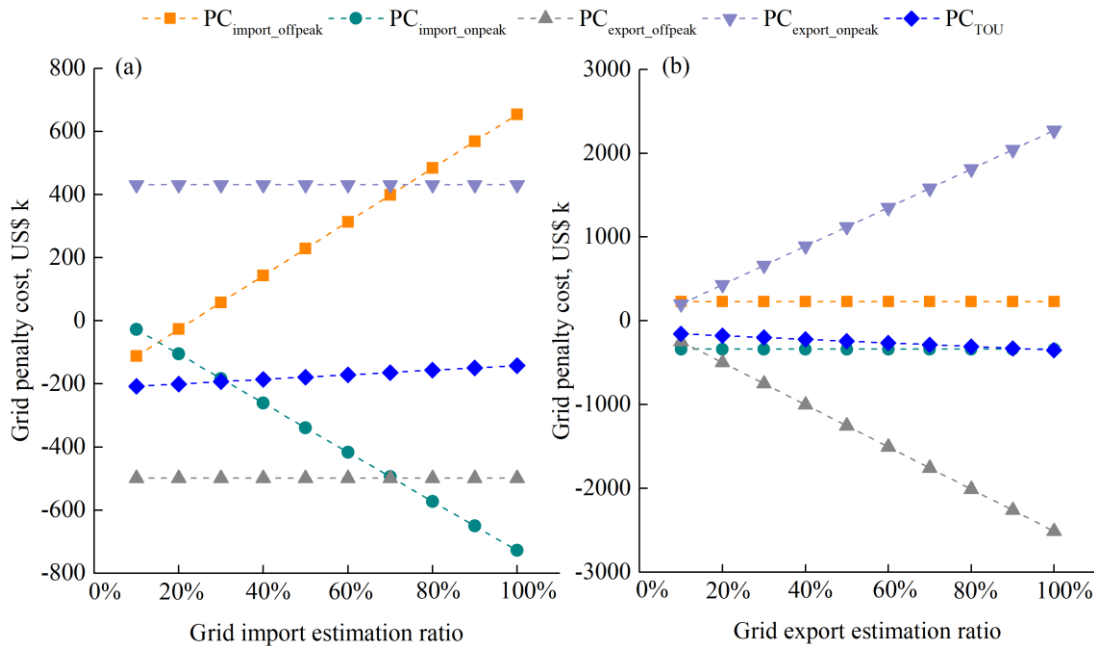


Fig. 7.11 Impact of grid import estimation ratio and grid export estimation ratio on grid penalty cost of the community with battery storage

The impact of the penalty factor ratio of the grid penalty cost model is illustrated in Fig. 7.12. It is indicated that absolute values of penalty cost of grid import and grid export in both off-peak and on-peak time increase with the penalty factor. The penalty cost of grid import during off-peak time and grid export during on-peak time is positive with a fine to the community microgrid to charge unreached grid import in off-peak time and unmet grid export in on-peak time. While the penalty cost of grid import in on-peak time and grid export in off-peak time is negative with a

bonus to the community microgrid to reward unused grid import in on-peak time and unfed grid export in off-peak time. The total time-of-use penalty cost with the penalty factor ratio of 10% is about US\$ -178.56k, which can compensate for about 1.01% of the annual electricity bill of the net-zero energy community. And the maximum time-of-use penalty cost with the penalty factor ratio of 100% is about US\$ -1785.60k accounting for about 10.08% of the annual electricity bill.

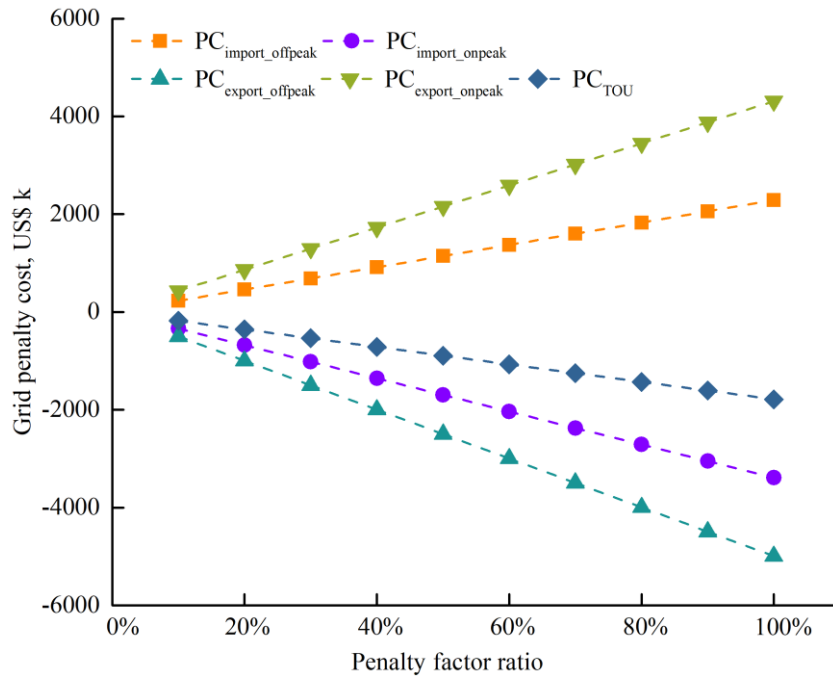


Fig. 7.12 Impact of penalty factor ratio on grid penalty cost of the community with battery

7.7 Summary of renewable energy systems with battery and hydrogen vehicle storage for the net-zero energy community

This chapter develops shared hybrid renewable energy and storage microgrid systems for a net-zero energy community consisting of campus, office and residential buildings, based on a combination of on-site collected and simulated building energy data. Three mobile hydrogen vehicle groups following different cruise schedules are integrated as transportation tools and

shared storage units together with stationary batteries. Multi-objective optimizations are conducted to size three net-zero energy buildings and the integrated net-zero energy community by coupling jEplus+EA with TRNSYS. Four net-zero energy scenarios without stationary battery storage and four baseline scenarios without renewable energy are also developed for the techno-economic-environmental performance comparison. Important findings are concluded as below:

(1) The net-zero energy residential building group achieves the maximum renewable energy self-consumption ratio, load cover ratio and hydrogen system efficiency of about 97.33%, 75.06% and 60.92% in four net-zero energy scenarios with battery storage. Battery storage improves the self-consumption ratio, load cover ratio and hydrogen system efficiency performance of the net-zero energy community, and enhances the load cover ratio of all four net-zero energy scenarios by up to 28.96% in the office building group.

(2) A time-of-use grid penalty cost model evaluating grid import and grid export during on-peak and off-peak periods is developed, to achieve the flexibility and economy between the renewable energy microgrid and utility grid. It is suggested that appropriate grid import and export estimation ratios should be set in net-zero energy building and community applications, based on the grid power availability considering the peak electrical load and rated renewable energy capacity.

(3) The net grid import energy is reduced by 71.23% - 90.93% in four net-zero energy scenarios with battery storage and by 72.10% - 91.36% in four net-zero energy scenarios without battery storage compared with baseline scenarios without renewable energy. The grid penalty cost reductions of 145.36% - 158.92% and 135.05% - 164.41% are achieved in net-zero energy scenarios with and without battery storage compared with baseline scenarios. The net-zero energy community has higher grid flexibility with lower grid penalty cost than three individual building

groups. Battery storage contributes to the grid relief of the net-zero energy community with a 29.40% penalty cost reduction.

(4) The lifetime net present value of four net-zero energy scenarios with battery storage is increased by 22.39% - 96.17% compared with baseline scenarios. The lifetime net present value of the community and office building group without battery storage is increased by 75.12% and 15.37% respectively on top of baseline scenarios. While the net present value is reduced by about 6.45% of US\$ 7.62M and 1.90% of US\$ 2.16M for the campus and residential building group without battery storage compared with baseline scenarios. Therefore, economic benefits can be obtained by applying hybrid renewable energy and hydrogen vehicle storage systems to the campus and residential building groups.

(5) Substantial environmental benefits can be achieved in all net-zero energy scenarios with significant reductions in carbon emissions and costs compared with baseline scenarios. The carbon emissions decline by 71.23% - 90.93% in four net-zero energy scenarios with battery storage achieving a carbon emission cost saving of US\$ 282.26k - 1170.57k. And about 67.57% - 91.36% of the carbon emission reduction for a cost of US\$ 269.29k - 1110.49k can be achieved in four net-zero energy scenarios without battery storage.

(6) The comprehensive feasibility study of net-zero energy buildings and their community is presented considering the system supply performance, lifetime cost and decarbonisation potential. The detailed comparison results based on net-zero energy scenarios without battery storage and baseline scenarios without renewable energy offer clear guidance to relative stakeholders for future large-scale renewable energy installations in urban areas. Moreover, the proposed time-of-use grid penalty cost model provides significant references to achieve the power grid resilience and economy for large-scale renewable energy system deployment in urban communities.

CHAPTER 8 PEER-TO-PEER ENERGY TRADING OPTIMIZATION OF A NET-ZERO ENERGY COMMUNITY WITH RENEWABLE ENERGY SYSTEMS INTEGRATING HYDROGEN VEHICLE AND BATTERY VEHICLE STORAGE

This chapter intends to develop the peer-to-peer energy trading management and optimization platform of a diversified net-zero energy community with hybrid renewable energy system integrated with hydrogen vehicle storage and battery vehicle storage. An individual peer trading price model is proposed for the diversified community, consisting of building groups with different energy distributions and grid pricing schemes. The time-of-use peer trading management strategies are developed for both uniform and individual trading price modes to improve the power flexibility and economy of the utility grid. Multi-objective peer-to-peer trading optimizations of the net-zero energy community integrated with both hydrogen vehicles and battery vehicles are conducted to find optimal configurations of vehicle numbers and time-of-use management operations. An improved peer-to-peer trading management strategy is further proposed considering the peer trading priority and complementary operations of hybrid vehicle storages, to enhance the grid integration, decarbonisation and economy.

8.1 Peer-to-peer energy trading of net-zero energy communities with renewable energy systems integrating hydrogen vehicle storage

8.1.1 Framework of peer energy trading of the net-zero energy community with renewable energy and hydrogen vehicle storage systems

This study develops a diversified net-zero energy community powered by hybrid renewable energy systems integrated with three groups of hydrogen vehicle (HV) storage to study the peer-to-peer (P2P) energy trading with the overall framework shown in Fig. 8.1. The net-zero energy community means the diversified community installed with renewable energy and storage systems, achieving a net-zero energy operation with annual balanced electrical demand and renewable energy generation. The utility grid is connected with the community allowing surplus renewable energy export and grid import for unmet electrical load, as there is time mismatch between the electrical demand and on-site renewable generation/storage supply. Fundamental units are integrated in the net-zero energy community including the university campus building group (the Hong Kong Polytechnic University - PolyU), commercial office building group (the International Commerce Center - ICC) and high-rise residential building group (public residences with standard layout - Resid). The load profiles of three building groups are obtained from actual annual energy consumption data and dynamic simulation data as per local surveys and codes. Hybrid renewable energy sources of solar PV and wind turbine systems with advantageous and complementary characteristics are developed for the net-zero energy community. 1000 HVs following different cruise schedules are allocated to three building groups serving as both the daily cruise and energy storage tools.

An individual peer energy trading price model is proposed for the diversified community to allocate an individual peer selling/buying price for each building group, according to their intrinsic energy surplus-demand features and grid import prices. The uniform peer trading price model, with a same peer trading price for all peers developed for household communities, is also adapted for the net-zero energy community for comparison analysis. And time-of-use P2P trading management strategies based on the time-of-use grid penalty cost model are further developed for

the two peer trading price modes to improve the power flexibility and economy of the utility grid in community applications.

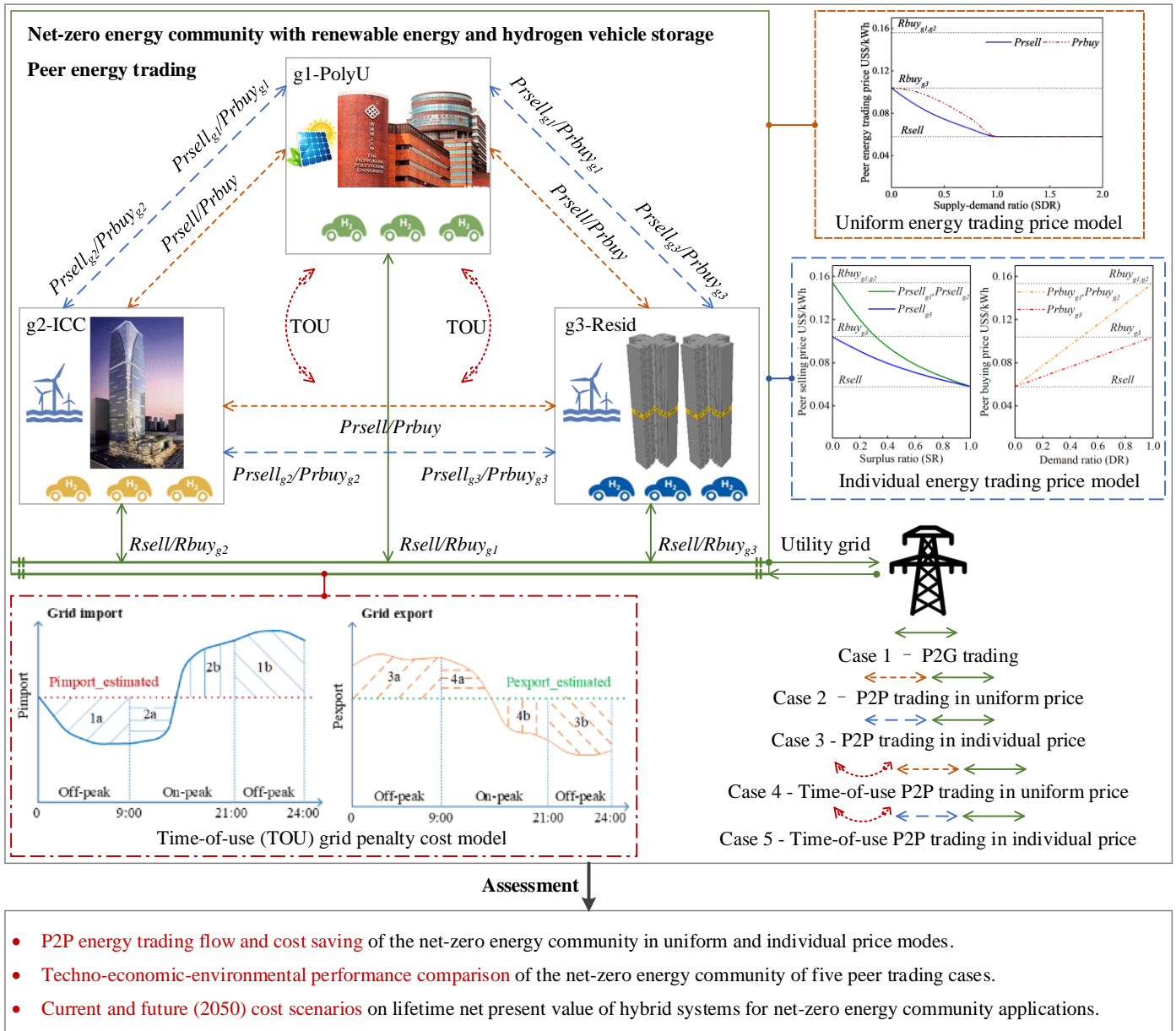


Fig. 8.1 Framework of peer energy trading of the net-zero energy community

Five peer trading cases with different energy trading management strategies are developed to study the peer-to-grid (P2G) and P2P energy trading behavior of three building groups in the net-zero energy community. Case 1 serves as the baseline case where the building groups only trade

energy with the utility grid rather than trade with their peers. Case 2 adopts P2P energy trading in the uniform price mode where the building groups trade surplus energy with their peers prior to the utility grid, and a uniform energy selling/buying price is utilized for P2P trading in the community depending on the dynamic total energy surplus and demand. Case 3 adopts P2P energy trading in the individual price mode where the building groups trade surplus energy with their peers prior to the utility grid, and an individual energy selling/buying price is set for each building group community depending on its intrinsic energy surplus and demand. Different P2P energy trading rules should be followed in the uniform and individual energy trading price models. Case 4 and Case 5 further consider time-of-use energy trading management on top of Case 2 and Case 3, based on the time-of-use grid penalty cost model to improve grid power flexibility and economy in large-scale net-zero energy community applications.

To assess the peer trading management in the net-zero energy community with hybrid renewable energy and HV storage systems, the energy sharing flow and energy trading cost saving of the net-zero energy community of typical P2P trading cases are analyzed. And the detailed techno-economic-environmental performances of the peer trading cases with different peer trading price modes and management strategies are compared, including renewable energy self-consumption and load coverage, annual energy trading flow, time-of-use grid penalty cost, annual electricity cost and equivalent carbon emissions. Furthermore, the lifetime NPV of hybrid renewable energy and HV storage systems under the current and future cost scenarios is evaluated to provide economic references to develop net-zero energy communities in the near future.

8.1.2 System modelling of peer energy trading of the net-zero energy community with renewable energy and hydrogen vehicle storage systems

Hybrid renewable energy and HV systems are developed for power supply to the typical community for a net-zero energy building operation with annual balanced electrical demand and renewable energy generation as shown in Fig. 8.2. The rooftop solar PV system of 41,200 kW is installed for electricity supply to the campus building group, with a tilted angle of 22° employing maximum power point tracking devices. The offshore wind turbine systems of 13,500 kW and 9200 kW are developed for electricity supply to the office and residential building groups.

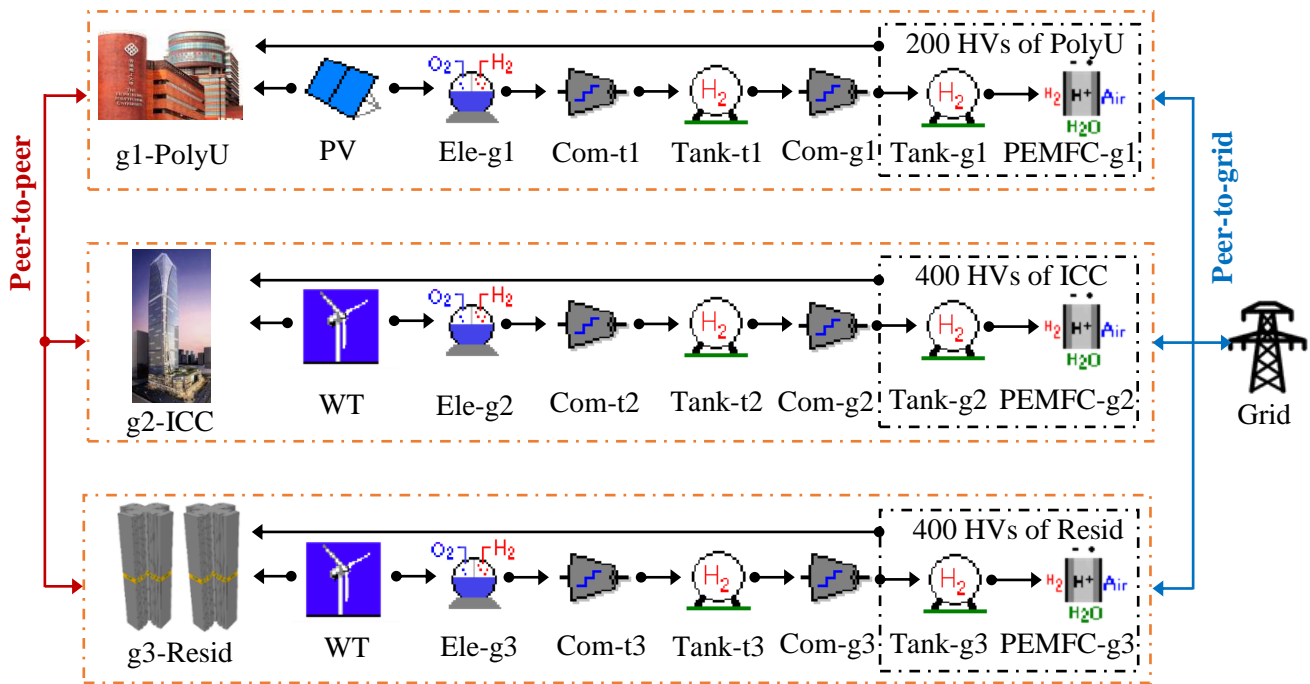


Fig. 8.2 Hybrid renewable energy and HV systems for the net-zero energy community

Three building groups with different operational functions and renewable energy configurations in the net-zero energy community can not only exchange power with the utility grid, but also make P2P energy trading among the community. Five cases with varied energy trading modes are developed as shown in Fig. 8.3.

(1) In Case 1 (baseline P2G case), three building groups make energy trading only with the utility grid and do not share energy with peers in the community as per Fig. 8.3(a).

(2) In Case 2 and Case 3, the P2P energy trading among the community is managed prior to the P2G energy trading as per Fig. 8.3(b). And a uniform price is adopted for the community P2P energy trading in Case 2, while an individual price is assigned to each building group in Case 3, according to the proposed individual peer trading price model.

(3) Case 4 and Case 5 are further developed considering grid time-of-use operation in the P2P energy trading management, to improve the power flexibility and economy of the utility grid as per Fig. 8.3(c). A uniform peer energy trading price mode is adopted in Case 4 and an individual peer energy trading price mode is adopted in Case 5.

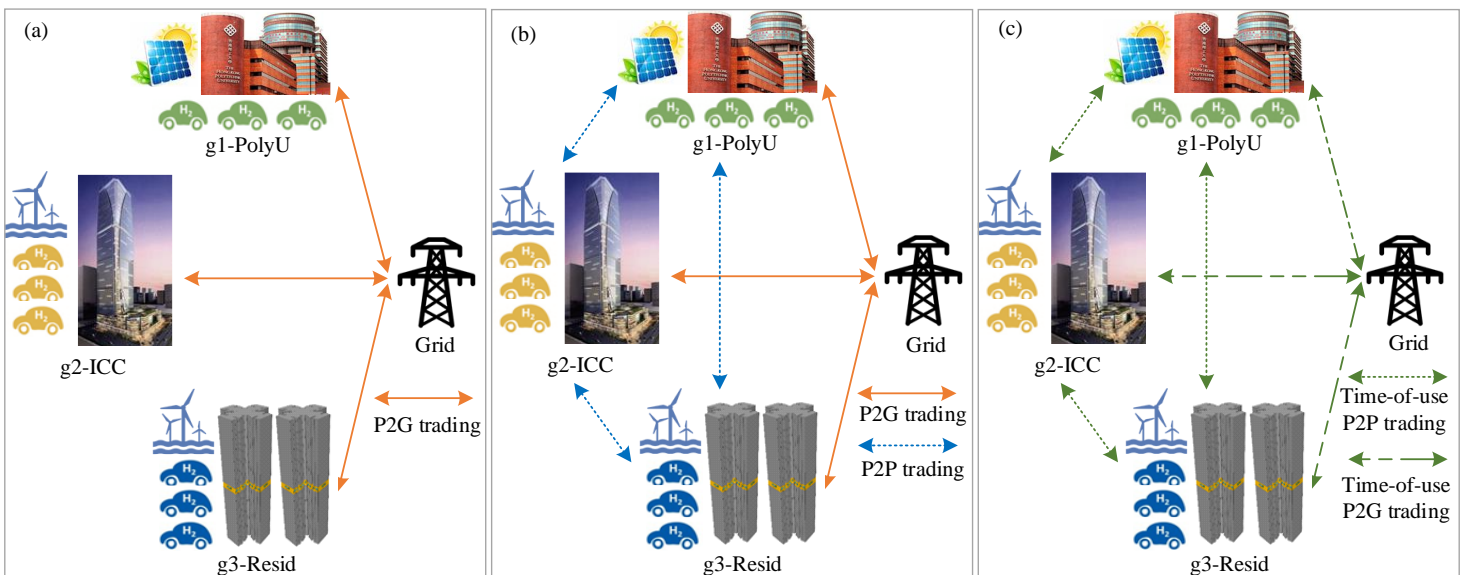


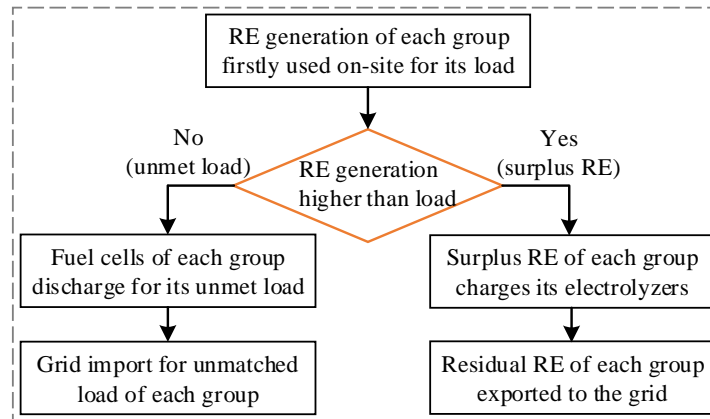
Fig. 8.3 Schematic of energy trading in the net-zero energy community of five cases

(Note: (a) only P2G trading - Case 1; (b) P2P trading in uniform price mode - Case 2 and in individual price mode - Case 3; (c) time-of-use P2P trading in uniform price mode - Case 4 and in individual price mode - Case 5.)

8.1.3 Energy management of five net-zero energy community cases with renewable energy and hydrogen vehicle storage systems

(1) Energy management strategy of baseline peer-to-grid case (Case 1)

The energy management strategy of the hybrid renewable energy and HV storage system in Case 1 is shown in Fig. 8.4, where the building groups in the net-zero energy community do not share energy with other peers but only trade with the utility grid. Specifically, the renewable energy generation of each building group is firstly used on-site to cover the building electrical load. Then surplus renewable energy is used to drive electrolyzers of the hydrogen storage system to generate and store hydrogen, when the FSOC of the stationary hydrogen storage tank is lower than its maximum level ($FSOC_{ti_max} < 0.95$). And the dynamic charging power is also limited by the electrical current density of electrolyzers (within 40 - 400 mA/cm² [102]). The residual renewable energy is lastly fed into the utility grid. For the unmet building load supplied by the on-site renewable energy, the parked HVs can be operated to supply power when the FSOC of the mobile hydrogen storage tank is higher than its minimum level ($FSOC_{gi_min} > 0.1005$), to support one-day cruise and keep above the atmosphere pressure. Finally, the utility grid supplies power for unmatched load.



(a)

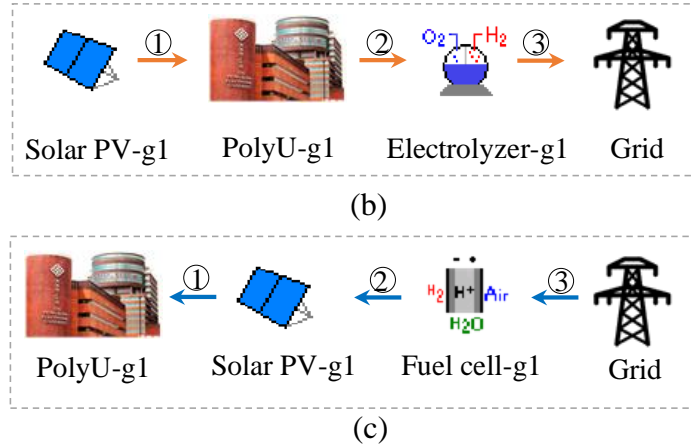


Fig. 8.4 Energy management strategy of Case 1 (a) simplified diagram (b) renewable generation flow priority of group 1 (c) load matching flow priority of group 1

The detailed energy management strategy of the hybrid renewable energy and HV storage system in Case 1 with only peer-to-grid trading is shown in Fig. 8.5.

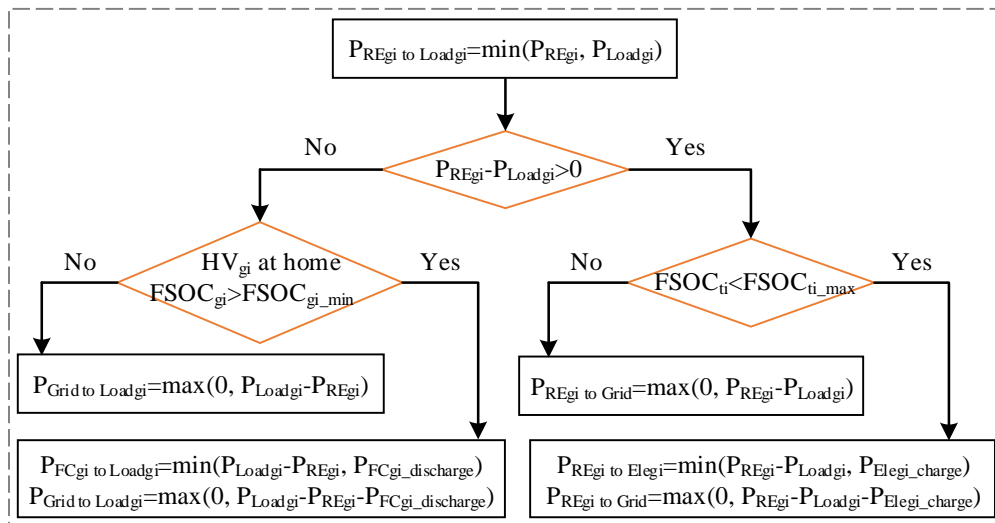
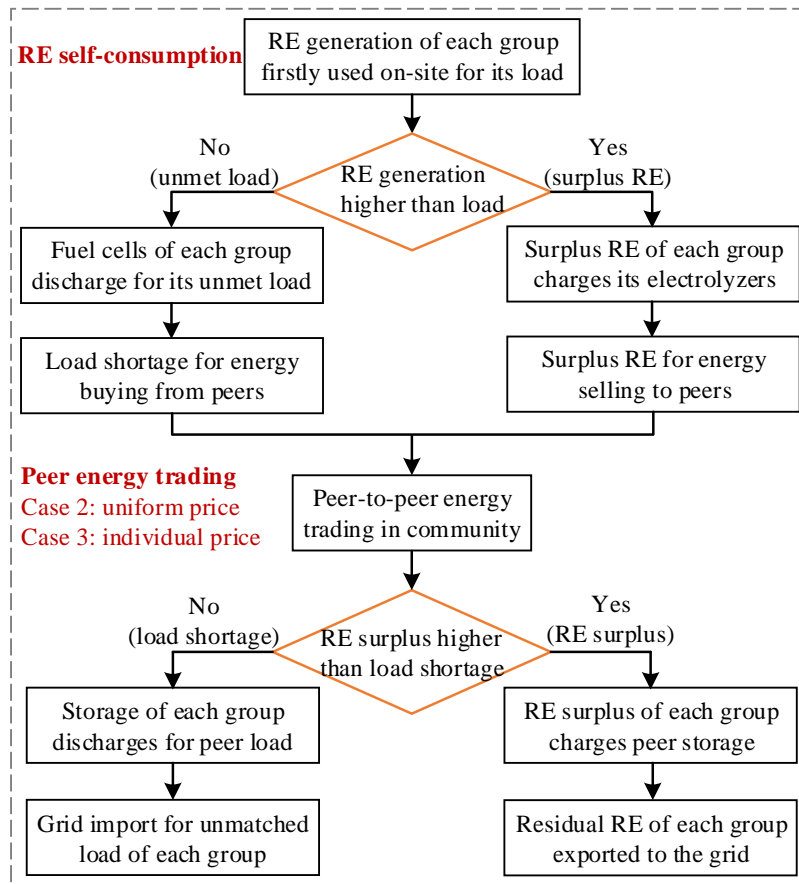


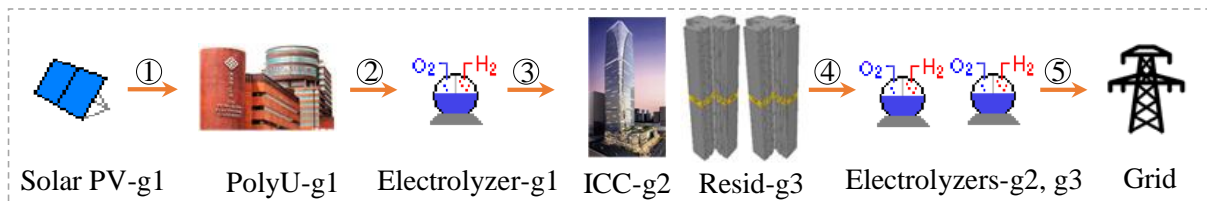
Fig. 8.5 Detailed energy management strategy of Case 1 (only P2G)

(2) Energy management strategy of peer-to-peer energy trading cases (Case 2 in uniform price mode and Case 3 in individual price mode)

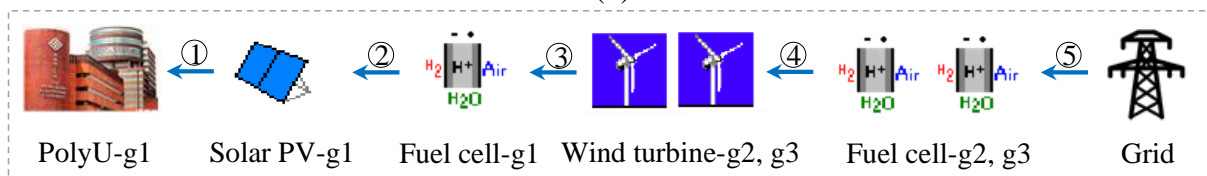
The energy management strategy of the P2P energy trading cases (Case 2 in uniform price and Case 3 in individual price) is presented in Fig. 8.6.



(a)



(b)



(c)

Fig. 8.6 Energy management strategy of Case 2 and Case 3 (a) simplified diagram (b) renewable generation flow priority of group 1 (c) load matching flow priority of group 1

Renewable energy generation of each building group is firstly utilized on site for the building itself including electrical load and electrolyzers. Then surplus renewable energy of each building

group after the self-consumption is shared to meet the unmet load of other community peers. Afterwards, the residual renewable energy of each building group is delivered to charge the hydrogen storage systems of other community peers before being exported to the grid. The building group with load shortage after buying peer renewable energy can also buy energy from hydrogen storage systems of its peers. The detailed energy flow priority of renewable energy generation and load matching in Case 2 and Case 3 is shown in Fig. 8.6 (b-c), taking group 1 as a detailed demonstration.

The detailed energy management strategy of the hybrid renewable energy and HV storage system in Case 2 with P2P energy trading in the uniform price mode is shown in Fig. 8.7. The basic trading rules should be followed in the P2P energy trading process in the uniform price mode:

- 1) Surplus energy from renewable sources (PV/wind) or storage sources (fuel cells) of one peer is shared to meet the unmatched load of other peers prior to electrolyzers of other peers.
- 2) When more than one peer with surplus renewable power or storage power are available for sharing to the third peer, the peer with higher surplus power has the peer trading priority considering the energy trading convenience.
- 3) When more than one peer with unmatched demand need to buy energy from the third peer, the peer with a higher grid electricity price has the peer trading priority, so as to reduce the overall electricity bills of the community.

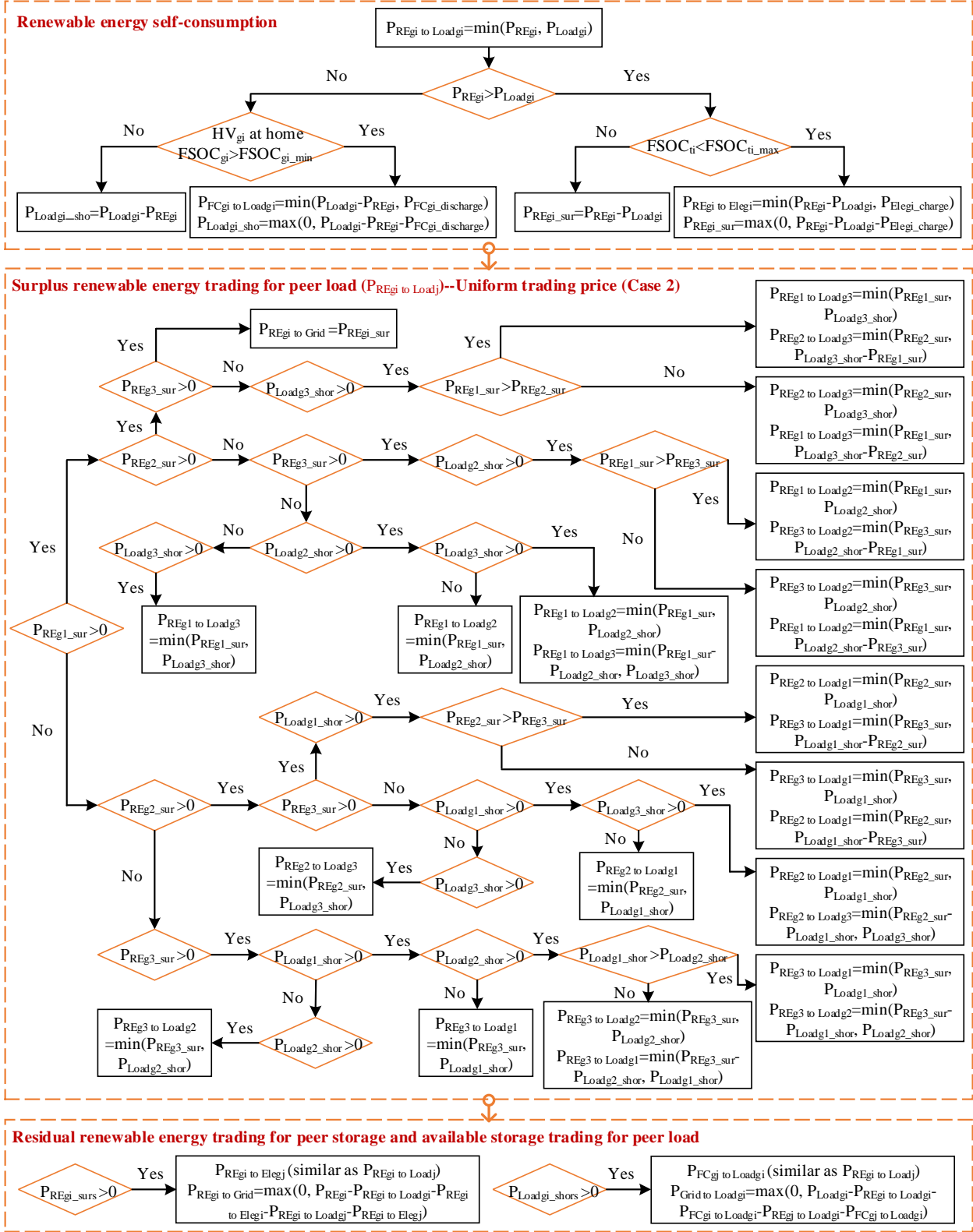


Fig. 8.7 Energy management strategy of Case 2 (P2P trading in uniform price mode)

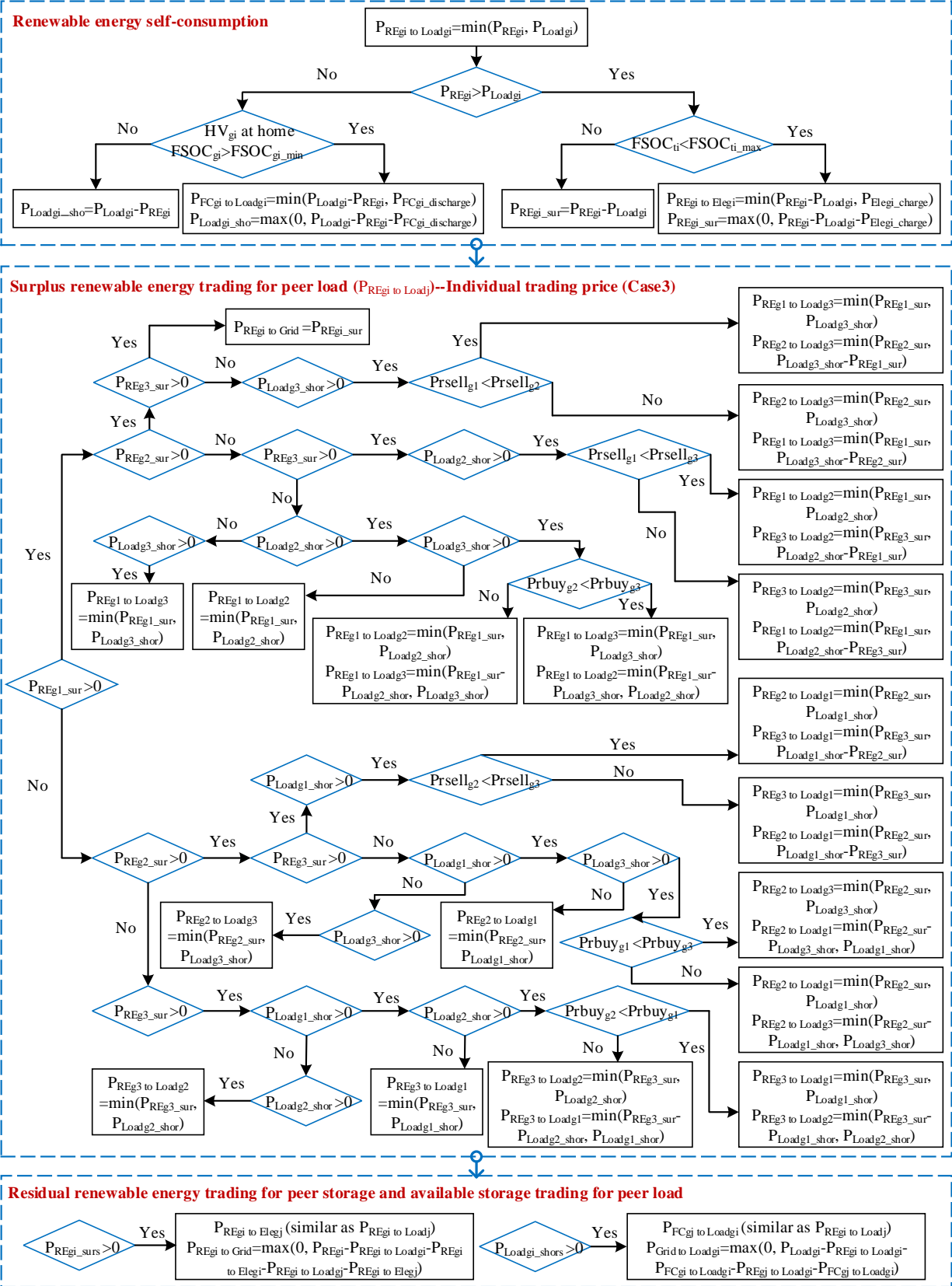


Fig. 8.8 Energy management strategy of Case 3 (P2P trading in individual price mode)

The detailed energy management strategy of the hybrid renewable energy and HV storage system in Case 3 with P2P energy trading in the individual price mode is shown in Fig. 8.8. As an individual trading price is allocated to each building group according to its own renewable energy surplus and load shortage, the P2P trading rules in Case 3 are different from Case 2 as below:

1) When more than one peer with surplus renewable power or storage power are available for sharing to the third peer with unmatched demand, the peer with a lower selling price has the energy trading priority.

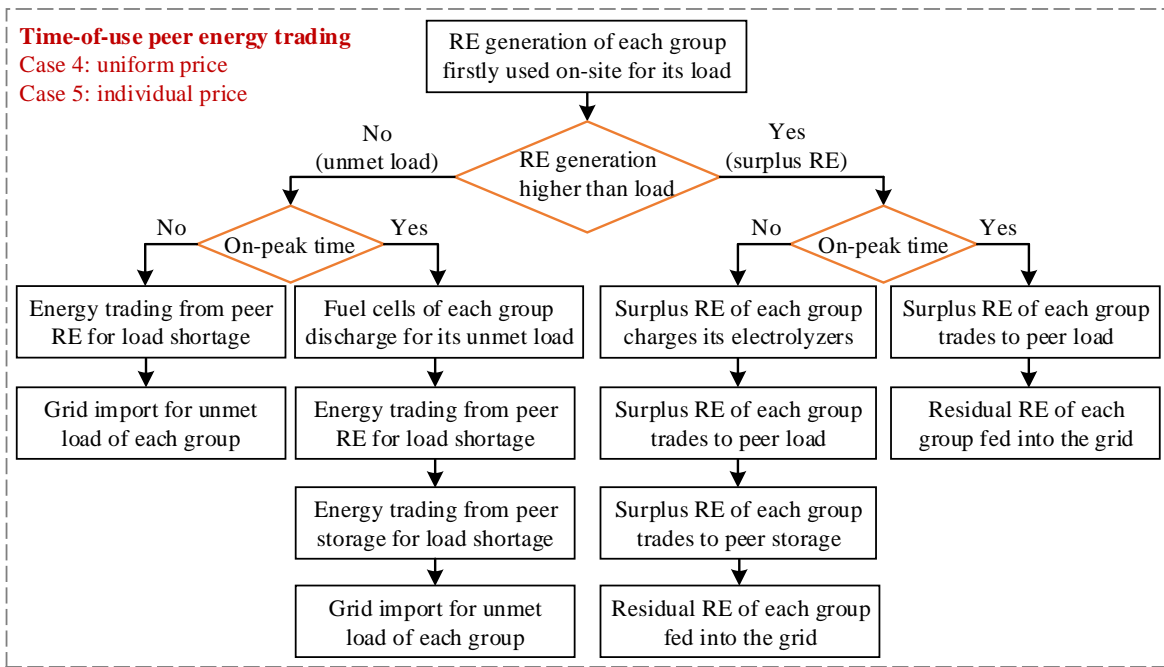
2) When more than one peer with unmatched demand need to buy energy from the third peer with surplus energy, the peer with a higher buying price has the peer trading priority.

3) The dynamic trading price is the minimum value of selling price of the seller and buying price of the buyer to encourage internal energy sharing in the net-zero energy community.

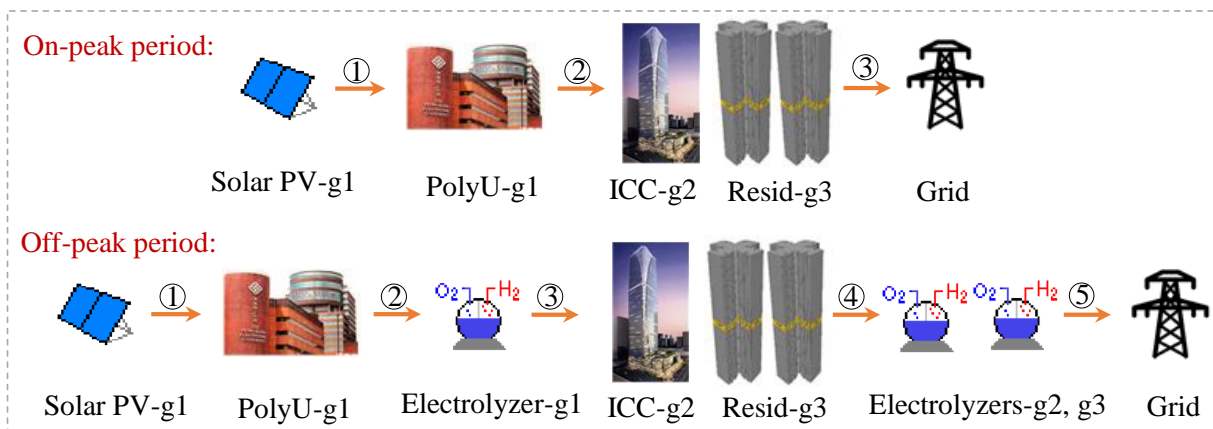
(3) Energy management strategy of time-of-use peer-to-peer energy trading cases (Case 4 in uniform price mode and Case 5 in individual price mode)

The time-of-use P2P energy trading is proposed to improve the power flexibility and economy between the net-zero energy community and utility grid, with the simplified diagram shown in Fig. 8.9 (a). The renewable energy generation is exported into the grid after supplying to electrical load of three building groups during on-peak time, while it is also available for hydrogen storage systems of three building groups during off-peak time. Because a higher energy export during on-peak time and a lower energy export during off-peak time are preferred by the utility grid. Both renewable energy and hydrogen storage are available for the electrical load of buildings during on-peak time, while only renewable energy is utilized for meeting building load during off-peak time. Since a lower energy import during on-peak time and a higher energy import during off-peak time

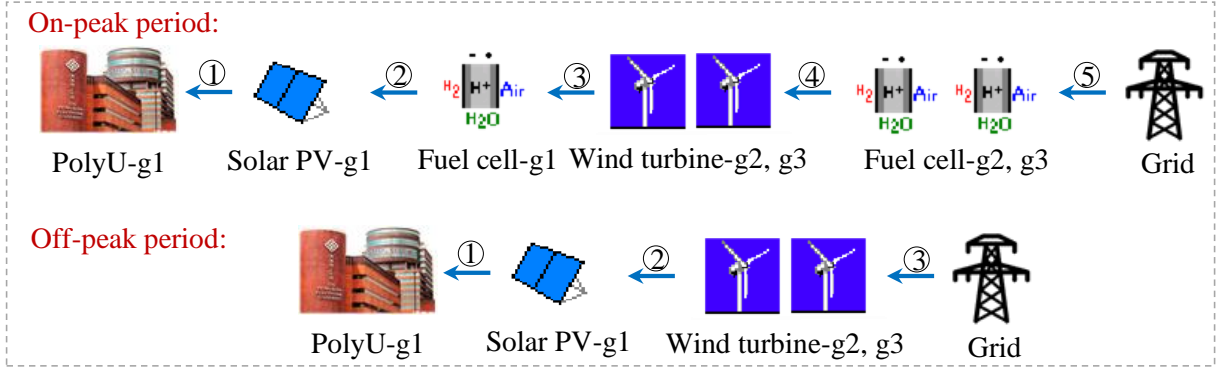
are encouraged by the utility grid, to address the power congestion and improve the economic performance through power shifting. The detailed energy flow priority of renewable energy generation and load matching in Case 4 and Case 5 is shown in Fig. 8.9(b-c), taking group 1 as a detailed demonstration.



(a)



(b)



(c)

Fig. 8.9 Energy management strategy of Case 4 and Case 5 (a) simplified diagram (b) renewable generation flow priority of group 1 (c) load matching flow priority of group 1

Therefore, the surplus renewable energy available for peer load sharing and the load shortage for peer energy trading in the time-of-use P2P trading process can be formulated as Eqs. (8.1-8.2).

$$P_{REgi_sur} = (P_{REgi} - P_{REgi\ to\ Loadgi}) \cdot T_{onpeak} + (P_{REgi} - P_{REgi\ to\ Loadgi} - P_{REgi\ to\ Elegi}) \cdot T_{offpeak} \quad (8.1)$$

$$P_{Loadgi_shor} = (P_{Loadgi} - P_{REgi\ to\ Loadgi} - P_{FCgi\ to\ Loadgi}) \cdot T_{onpeak} + (P_{Loadgi} - P_{REgi\ to\ Loadgi}) \cdot T_{offpeak} \quad (8.2)$$

where $P_{REgi\ to\ Loadgi}$ is the self-consumed renewable power of group i to meet its electrical load, kW. $P_{REgi\ to\ Elegi}$ is the self-consumed renewable power of group i to charge its electrolyzers, kW. T_{onpeak} is the on-peak time and $T_{offpeak}$ is the off-peak time. $P_{FCgi\ to\ Loadgi}$ is the energy from hydrogen storage of group i to meet its electrical load, kW. It is assumed that the on-peak period is the daily period between 9:00 and 21:00 and the off-peak period comprises all other hours according to the local power grid company [104].

The energy trading of renewable energy sharing for peer storage only operates in off-peak period to enhance the grid flexibility. The residual renewable energy after self-consumption and

supplying to peer load (P_{REgi_surs}) is available for trading to peer storage as per Eq. (8.3). The energy shortage of the hydrogen storage system after self-sufficiency (P_{Elegi_shor}) is formulated as Eq. (8.4).

$$P_{REgi_surs} = (P_{REgi} - P_{REgi\ to\ Loadgi} - P_{REgi\ to\ Elegi} - P_{REgi\ to\ Loadgj}) \cdot T_{offpeak} \quad (8.3)$$

$$P_{Elegi_shor} = (P_{Elegi} - P_{REgi\ to\ Elegi}) \cdot T_{offpeak} \quad (8.4)$$

where $P_{REgi\ to\ Loadgj}$ is the peer trading renewable power of group i to meet the electrical load of group j , kW.

The energy trading of hydrogen storage sharing for peer load only operates during on-peak period to relieve the power grid. The load shortage after self-sufficiency and peer renewable energy trading (P_{Loadgi_shors}) needing to be met by the peer storage is shown in Eq. (8.5). And the hydrogen storage after self-consumption (P_{FCgi_avai}) available for peer sharing is formulated as Eq. (8.6).

$$P_{Loadgi_shors} = (P_{Loadgi} - P_{REgi\ to\ Loadgi} - P_{FCgi\ to\ Loadgi} - P_{REgj\ to\ Loadgi}) \cdot T_{onpeak} \quad (8.5)$$

$$P_{FCgi_avai} = (P_{FCgi} - P_{FCgi\ to\ Loadgi}) \cdot T_{onpeak} \quad (8.6)$$

where $P_{REgj\ to\ Loadgi}$ is the peer trading renewable power of group j to meet the electrical load of group i , kW.

Finally, the energy trade between building group i with the utility grid is formulated as Eqs. (8.7-8.8).

$$P_{REgi\ to\ Grid} = (P_{REgi} - P_{REgi\ to\ Loadgi} - P_{REgi\ to\ Loadgj}) \cdot T_{onpeak} \\ + (P_{REgi} - P_{REgi\ to\ Loadgi} - P_{REgi\ to\ Elegi} - P_{REgi\ to\ Loadgj} - P_{REgi\ to\ Elegi}) \cdot T_{offpeak} \quad (8.7)$$

where $P_{REgi\ to\ Grid}$ is the energy from renewable sources of building group i to the grid, kW. $P_{REgi\ to\ Eelj}$ is the peer trading renewable power of group i to charge the electrolyzers of group j , kW.

$$P_{Grid\ to\ Loadgi} = (P_{Loadgi} - P_{REgi\ to\ Loadgi} - P_{FCgj\ to\ Loadgi} - P_{REgj\ to\ Loadgi} - P_{FCgj\ to\ Loadgi}) \cdot T_{onpeak} + (P_{Loadgi} - P_{REgi\ to\ Loadgi} - P_{REgj\ to\ Loadgi}) \cdot T_{offpeak} \quad (8.8)$$

where $P_{Grid\ to\ Loadgi}$ is the energy from the utility grid to meet the electrical load of building group i , kW. $P_{FCgj\ to\ Loadgi}$ is the peer trading energy from hydrogen storage of group j to meet the electrical demand of group i , kW.

8.1.4 Peer energy trading results of the net-zero energy community with renewable energy and hydrogen vehicle storage systems

This section firstly analyzes the energy sharing flow and trading cost saving of typical P2P trading cases in the net-zero energy community. Then detailed techno-economic-environmental performances of five cases are discussed, including the renewable energy self-consumption and load coverage, energy trading flow, time-of-use grid penalty cost, electricity cost and carbon emissions. Finally, the system lifetime NPV is evaluated under the current and future cost scenarios.

(1) Analysis on typical peer-to-peer energy trading cases of the net-zero energy community

The renewable energy generation and load matching flow of the net-zero energy community in Case 2 with P2P energy trading in the uniform price mode are discussed as per Fig. 8.10. It is indicated that about 26.93% of renewable energy generation (13488.01 MWh) in the campus building group is shared to peers, which otherwise needs to be fed into the utility grid if the P2P trading is not adopted.

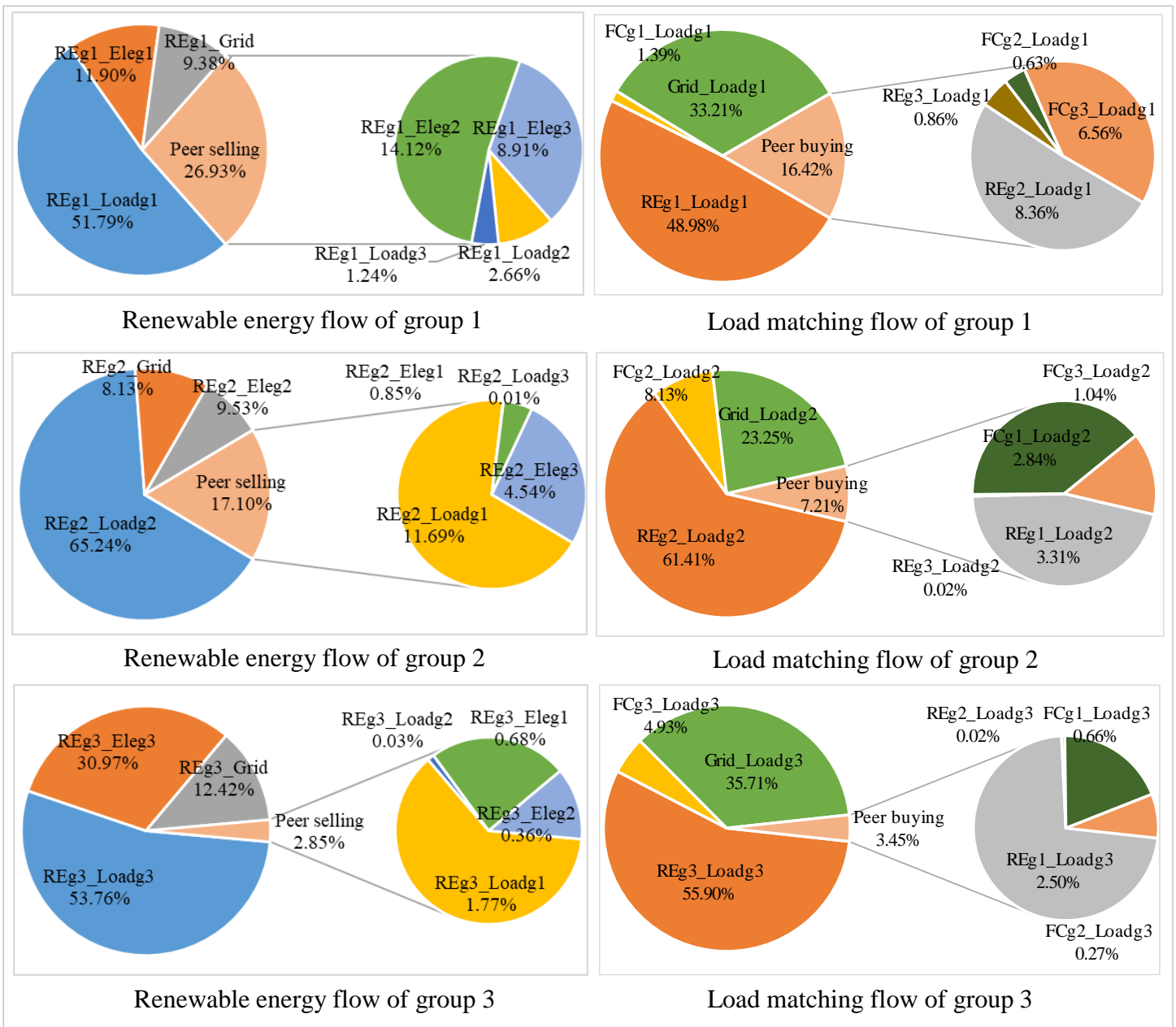
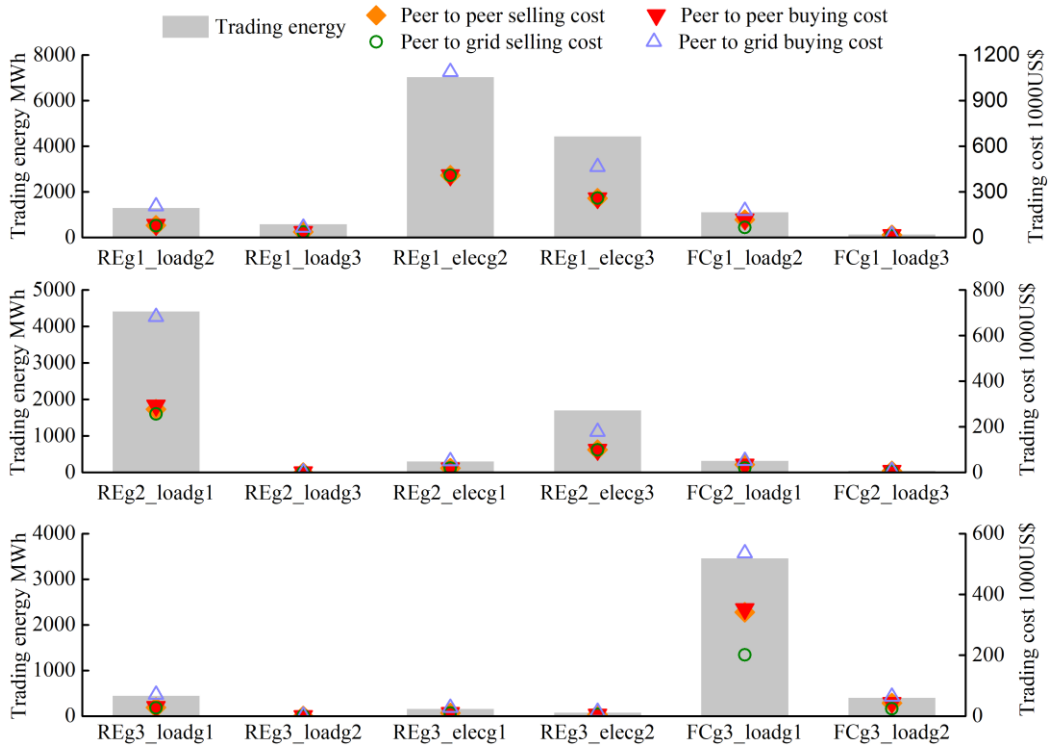


Fig. 8.10 Annual renewable energy flow and load matching in Case 2 (P2P in uniform price)

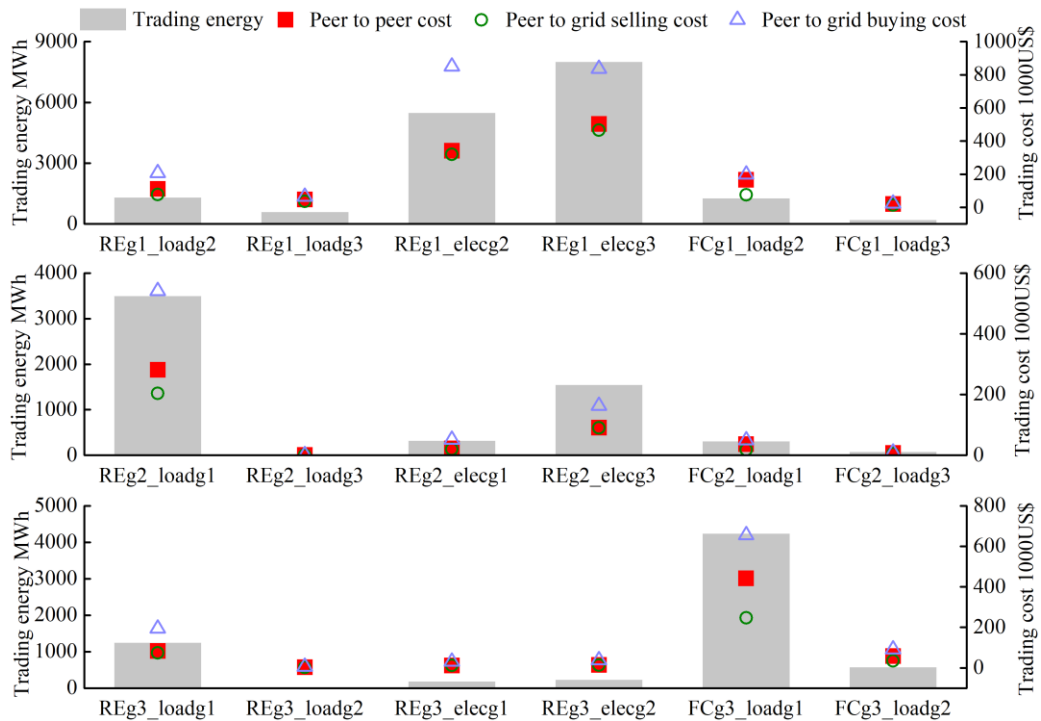
The peer selling energy in the office and residential building groups accounts for about 17.10% and 2.85% of its renewable energy generation respectively, lower than that in the campus building group with a good complementarity. Majority of peer selling energy is traded for storage charging in the campus building group while more peer selling energy is shared for peer load matching in the office and residential buildings. Because less peer load of the office and residential buildings

is in demand when surplus renewable energy generation of the campus buildings is available. The on-site self-consumption of the renewable supply is significantly improved with P2P sharing by 18.19% in the net-zero energy community. Building groups can also buy energy from peers with available renewable and storage power, where about 16.42% of electrical load (8696.27 MWh) of the campus buildings is supported by peers. The peer buying energy of office and residential buildings takes for 7.21% and 3.45% of the annual load respectively, which is lower than that of the campus building group with the maximum annual load. The annual average load coverage of the net-zero energy community is also enhanced with peer energy sharing by 10.55%.

The P2P trading energy and cost of three building groups in the net-zero energy community of Case 2 with the uniform price mode are shown in Fig. 8.11(a). The peer selling cost of the trading energy is not higher than the peer buying cost, as the P2P energy selling price is not greater than the P2P energy buying price as explained in the uniform price model. The P2P selling cost keeps above the P2G selling cost and the P2P buying cost keeps below the P2G buying cost to effectively encourage peer energy trading in the net-zero energy community. The P2P trading energy and cost of three building groups in the net-zero energy community of Case 3 with the individual price mode are shown in Fig. 8.11(b). There is little cost difference between the P2P selling cost and P2P buying cost as the dynamic trading price is the minimum value of selling price of the seller and buying price of the buyer as explained in trading rules of the individual price model. And it can be found that the P2P trading cost is not lower than the P2G selling cost but not higher than the P2G buying cost.



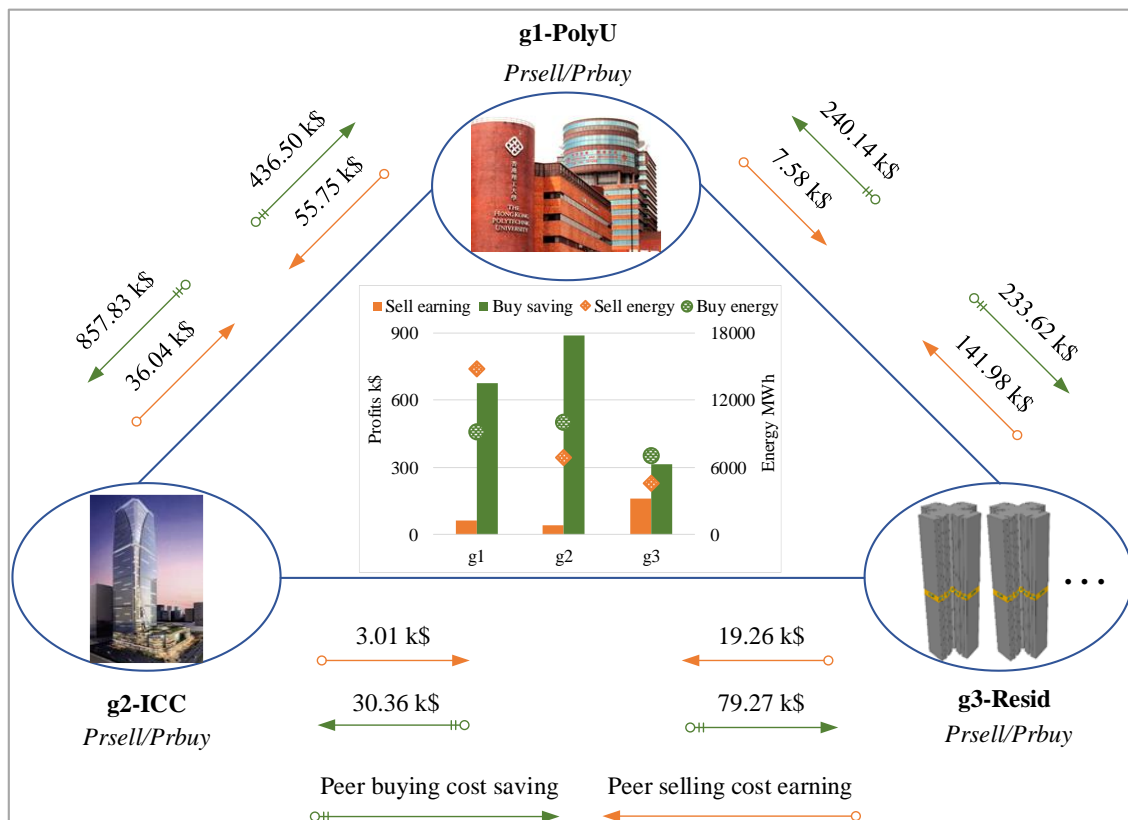
(a)



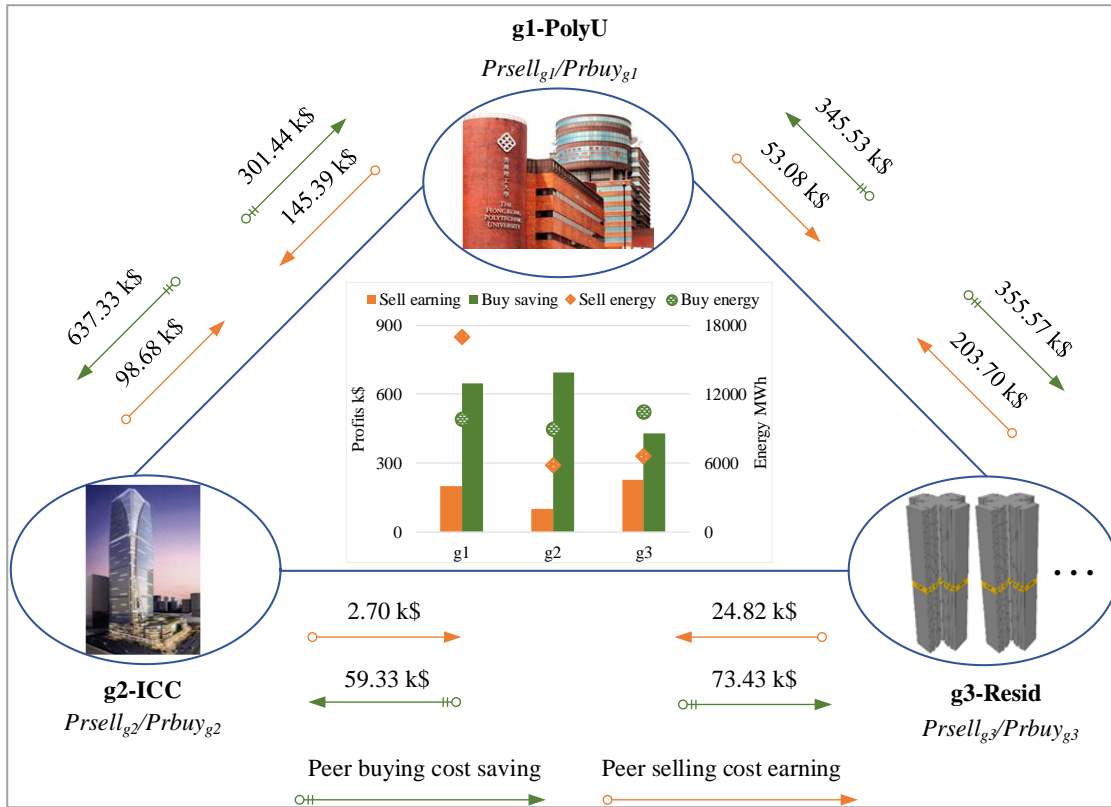
(b)

Fig. 8.11 P2P trading energy and cost in Case 2 (a, P2P trading in uniform price) and Case 3 (b, P2P trading in individual price)

Large amounts of economic profits can be achieved in the P2P energy trading management compared with the P2G energy trading management in Case 2 as per Fig. 8.12(a), where up to US\$ 888.18k of electricity bill can be saved in the office building group (g2) by the P2P buying. The total cost saving resulted from P2P energy trading (selling and buying) of the campus and office building groups is about US\$ 739.97k and US\$ 927.23k respectively, which is much higher than that of the residential building group at US\$ 474.14k. Because a smaller grid electricity rate ($R_{buy_{g3}} < R_{buy_{g1, g2}}$) is adopted for the uniform price model to ensure the peer energy selling price lower than the grid energy selling price. About US\$ 263.63k of peer selling earning and US\$ 1877.72k of peer buying saving can be obtained with the total trading profits of about US\$ 2141.34k in the net-zero energy community with the P2P trading management.



(a)



(b)

Fig. 8.12 P2P trading cost saving in Case 2 (a, P2P trading in uniform price) and Case 3 (b, P2P trading in individual price)

A relatively balanced energy trading profits among three building groups in the net-zero energy community is observed in Case 3 adopting the individual price mode as per Fig. 8.12(b). The peer energy buying saving of the campus and office building groups is higher than that of the residential building group, as the grid electricity buying price of non-residential buildings is higher than residential buildings in the community. And the P2P selling saving of the residential building group is the highest of about US\$ 228.53k, although the P2P selling energy of the campus building group is the highest of 17037.06 MWh. About US\$ 2301.01k of energy trading profits can be obtained in the net-zero energy community with US\$ 528.38k of peer selling earning and

US\$ 1772.63k of peer buying saving. The energy trading profits of Case 3 in the individual trading price mode are 7.46% higher than that in Case 2 in the uniform trading price mode.

(2) Comparison of five peer trading cases of the net-zero energy community

The self-consumption ratio (SCR) of renewable energy supplied to the community load and storage of five net-zero energy cases is compared as per Fig. 8.13, together with the load cover ratio (LCR) of the community met by on-site renewable energy and storage. It is indicated that Case 1 with only P2G trading has the minimum SCR and LCR of 73.64% and 59.54%, respectively. The SCR and LCR can be improved by 16.71% and 10.12% in Case 2 with P2P trading in the uniform price mode, as more renewable energy generation is utilized on site for peer sharing. And both SCR and LCR can be further enhanced in Case 3 with P2P trading in the individual price mode by 18.76% and 11.23% on top of the P2G trading (Case 1). The SCR and LCR are decreased when considering grid time-of-use management in the P2P trading (Case 4 and Case 5), since the energy trading is limited by the time-of-use management, but it is still higher than that of the baseline P2G case (Case 1).

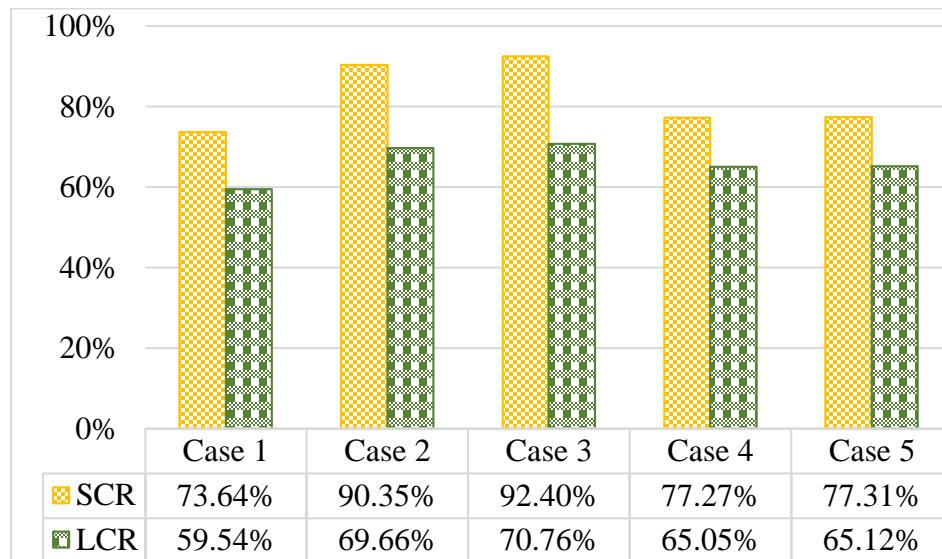


Fig. 8.13 Renewable energy self-consumption and load coverage of five cases

(Note: Case 1: P2G trading, Case 2: P2P trading in uniform price, Case 3: P2P trading in individual price, Case 4: TOU P2P trading in uniform price, Case 5: TOU P2P trading in individual price.)

The energy supply of each building group with the hybrid renewable energy and HV storage system can be used to meet its internal electrical load, trade with the community peers and the utility grid according to the management strategies as compared in Fig. 8.14. The internal consumption indicates the annual energy supply from the renewable energy generation and hydrogen storage of each building group to meet its internal electrical load. The peer trading energy means the annual energy exchange among peers in the net-zero energy community, and the grid trading energy indicates the net grid imported energy. It is found that the internal consumption of Case 1 with only P2G trading is higher than other cases with P2P trading, as the renewable sources and storage in Case 1 are not shared with others peers. Both peer trading energy and grid trading energy of cases considering time-of-use management (Case 4 and Case 5) are lower than cases without time-of-use management (Case 2 and Case 3) to maintain the grid power flexibility. Specifically, reductions of 52.40% on the peer trading energy and 32.06% on grid trading energy are observed in the uniform trading price case when considering time-of-use management (Case 4 compared with Case 2). And reductions of 56.66% and 34.24% on the peer trading energy and grid trading energy are achieved in the individual trading price case considering time-of-use management (Case 5 compared with Case 3). The grid trading energy in Case 4 and Case 5 considering time-of-use operation is also lower than Case 1 with only P2G trading by 8.78% and 8.93% respectively. Therefore, the time-of-use trading management cases achieve the best grid power flexibility.

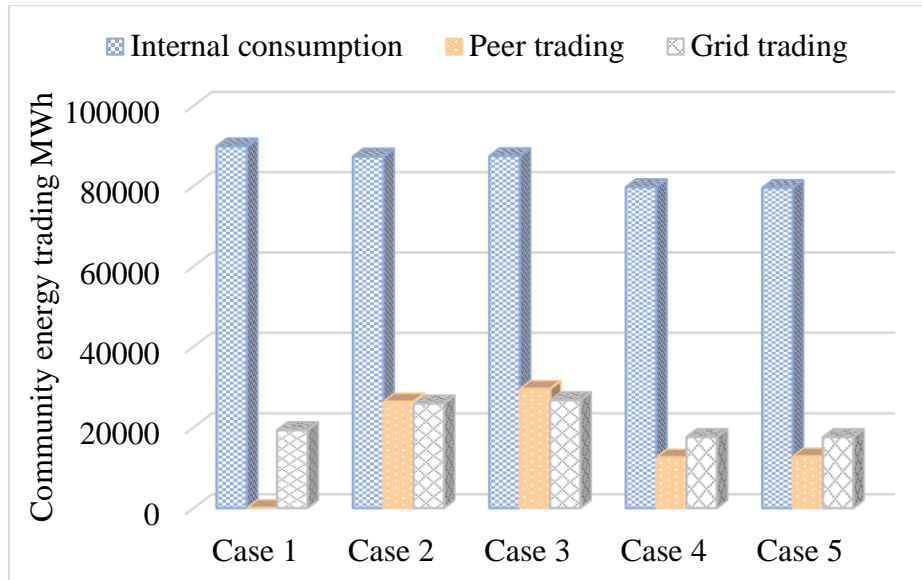


Fig. 8.14 Annual energy trading of five cases

(Note: Case 1: P2G trading, Case 2: P2P trading in uniform price, Case 3: P2P trading in individual price, Case 4: TOU P2P trading in uniform price, Case 5: TOU P2P trading in individual price.)

The time-of-use grid penalty cost covering the grid import and export during the on-peak and off-peak periods of five net-zero energy community cases is compared in Fig. 8.15. The penalty cost of grid import in off-peak time and grid export in on-peak time is positive with an economic fine, as the grid imported energy in off-peak time is less than the import estimation and the grid exported energy in on-peak time is also under the export estimation. While the penalty cost of grid import in on-peak time and grid export in off-peak time is negative with an economic bonus, as the grid imported energy in on-peak time and grid exported energy in off-peak time are below the import and export estimation. The total penalty cost in Case 1 with only P2G trading is about US\$ -168.99k, and the bonus is reduced to US\$ -40.96k in Case 2 and to US\$ -3.52k in Case 3 when considering P2P trading in the net-zero energy community with more power exchange with the utility grid. While the grid penalty cost in Case 4 and Case 5 considering time-of-use P2P trading management is the minimum at about US\$ -409.26k and US\$ -410.43k with the maximum bonus.

The grid penalty cost in Case 4 and Case 5 is reduced by 142.18% and 142.87% compared with the P2G case indicating the best grid economic flexibility.

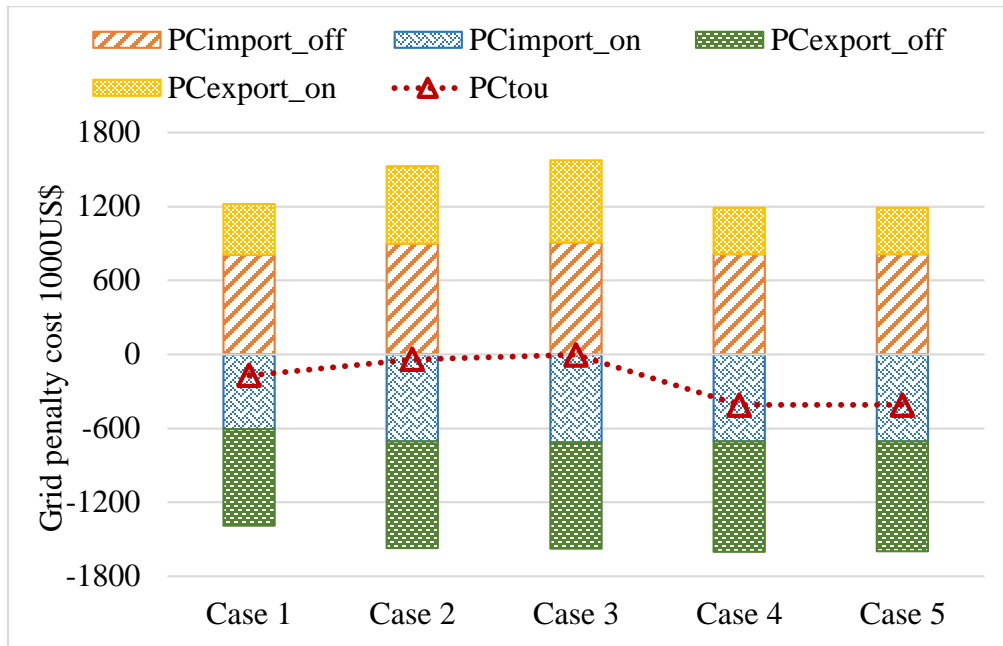


Fig. 8.15 Time-of-use grid penalty cost of five cases

(Note: Case 1: P2G trading, Case 2: P2P trading in uniform price, Case 3: P2P trading in individual price, Case 4: TOU P2P trading in uniform price, Case 5: TOU P2P trading in individual price.)

The annual electricity cost of five net-zero energy community cases indicating the net annual bill of energy selling and buying cost from both peers and utility grid is compared as per Fig. 8.16. The net annual bill of Case 1 in the P2G trading operation is the maximum of about US\$ 5370.04k, and it is reduced by 26.47% and 16.16% in Case 2 and Case 3 with P2P trading in the uniform and individual trading price modes. The annual electricity cost of Case 4 and Case 5 considering grid flexibility management is higher than that of Case 2 and Case 3, as the peer trading is limited by the grid time-of-use consideration. But the net annual cost in Case 4 and Case 5 is still less than that of Case 1 with only P2G trading by 13.75% and 14.54% for the uniform price mode and individual price mode, respectively.

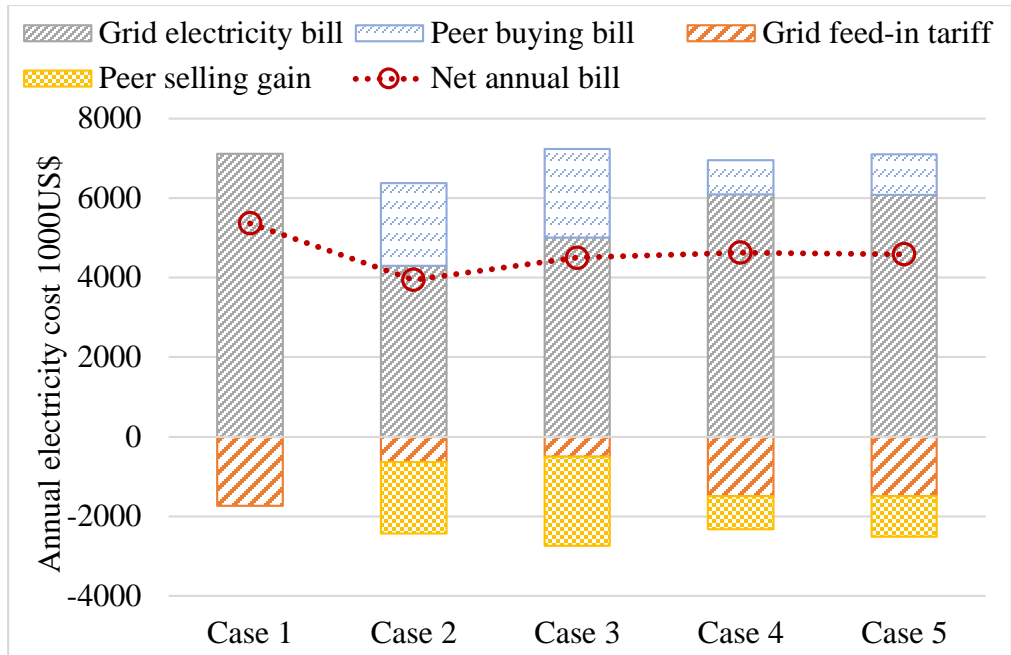


Fig. 8.16 Annual electricity cost of five cases

(Note: Case 1: P2G trading, Case 2: P2P trading in uniform price, Case 3: P2P trading in individual price, Case 4: TOU P2P trading in uniform price, Case 5: TOU P2P trading in individual price.)

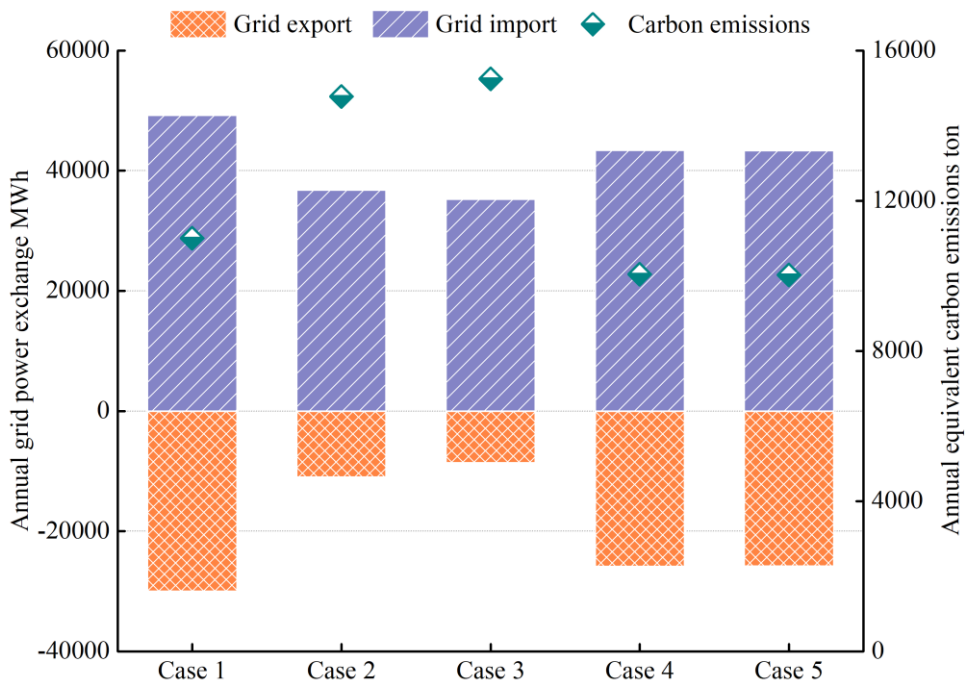


Fig. 8.17 Annual equivalent carbon emissions of five cases

(Note: Case 1: P2G trading, Case 2: P2P trading in uniform price, Case 3: P2P trading in individual price, Case 4: TOU P2P trading in uniform price, Case 5: TOU P2P trading in individual price.)

The annual equivalent carbon emissions calculated from the annual power exchange between the net-zero energy community and the utility grid of five cases are shown in Fig. 8.17. The annual equivalent carbon emissions of Case 1 with only P2G trading are about 11006.08 tons. It is increased by 34.26% and 38.50% in Case 2 and Case 3 with P2P trading in the uniform and individual price modes, although the grid import and export energy are reduced. Because the net grid imported energy of Case 2 and Case 3 is higher than that of Case 1. The carbon emissions in Case 4 and Case 5 considering the grid time-of-use P2P trading are the minimum of about 10039.35 tons and 10023.72 tons, lower by 8.78% and 8.93% than that in Case 1 with only P2G trading management. This is because that the grid import during on-peak time and grid export during off-peak time are limited by the time-of-use management.

(3) Lifetime net present value of renewable energy and hydrogen vehicle storage systems in current and future cost scenarios

The hybrid renewable energy and HV storage systems are projected for large penetrations for building power supply in urban areas with significant cost decline in the near future supported by advanced technology development and increased governmental subsidy. The lifetime NPV of the net-zero energy community powered by the hybrid renewable energy and HV storage systems in the current cost scenario and future cost scenario (2050) is compared as per Fig. 8.18. It is indicated that the system NPV in the current cost scenario of five net-zero energy community cases is about US\$ 670.53 - 689.02M, and it is reduced by 54.40% - 55.90% in the future cost scenario to US\$ 295.71 - 314.20M. Case 2 with the P2P energy trading in the uniform price mode shows the minimum lifetime NPV with the lowest grid trading cost with detailed items shown in Fig. 8.18(b).

The initial cost accounts for 71.62% of the lifetime NPV of the hybrid renewable energy and HV storage system for the community power supply in the current cost scenario, followed by the maintenance cost at 14.34% and trading bill at 12.37%, respectively. The system initial cost and maintenance cost can be reduced by 61.49% and 63.11% when considering the cost reduction in the future scenario in 2050, with a total cost reduction of 55.90% on the lifetime NPV in Case 2.

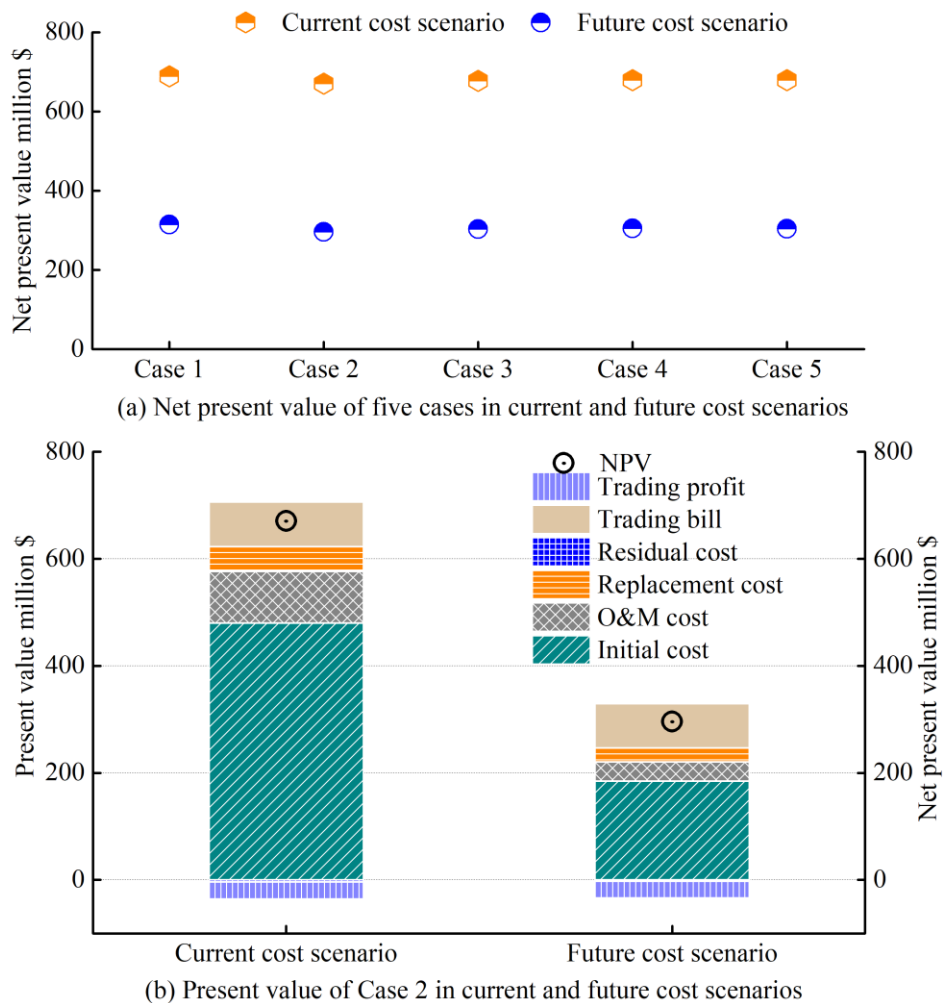


Fig. 8.18 Lifetime NPV of five cases in current and future cost scenarios

(Note: Case 1: P2G trading, Case 2: P2P trading in uniform price, Case 3: P2P trading in individual price, Case 4: TOU P2P trading in uniform price, Case 5: TOU P2P trading in individual price.)

8.1.5 Summary of peer-to-peer energy trading of the net-zero energy community with renewable energy systems integrating hydrogen vehicle storage

This study develops peer-to-peer energy trading management approaches for a net-zero energy community with fundamental units of university campus, commercial office and high-rise residential building groups based on actual energy consumption and simulation data. The hybrid solar photovoltaic and wind turbine systems are developed for power supply to the net-zero energy community integrated with three hydrogen vehicle groups for both daily commuting and energy storage based on the TRNSYS platform. Important findings of the present study are summarized as below:

(1) An individual peer-to-peer energy trading price model is proposed for peer energy sharing in diversified communities to allocate an individual peer selling/buying price to each building group according to its intrinsic energy surplus-demand characteristic and grid import electricity price. The superiority and economic benefits of the proposed individual peer energy trading price model for diversified building communities are demonstrated in comparison with that of the uniform peer trading price model generally for home building communities. The time-of-use peer energy trading management strategies in the uniform and individual peer trading price modes are further developed to improve the power flexibility and economy of the utility grid.

(2) The peer-to-peer energy trading improves the renewable energy self-consumption and on-site load coverage of the net-zero energy community compared with the baseline peer-to-grid energy trading, by 18.76% and 11.23% respectively for the individual peer trading price mode, as more renewable energy generation is utilized on site for peer sharing. The individual trading price mode can improve the peer-to-peer energy trading profits of the net-zero energy community by 7.46% with increased peer trading energy and increased peer selling earnings, compared with the

uniform trading price mode. The proposed time-of-use peer trading management strategies achieve significant improvements in both the grid power flexibility and grid economy on top of the peer-to-grid trading, with reductions of 8.93% in the net grid import energy and 142.87% in the annual grid penalty cost for the individual trading price mode, since the grid import during on-peak time and grid export during off-peak time are limited by the time-of-use management.

(3) The time-of-use peer-to-peer trading reduces the annual electricity cost of the net-zero energy community with less net grid import energy compared with the baseline peer-to-grid trading, by 14.54% for the individual trading price mode. Obvious environmental benefits are obtained in the time-of-use peer trading management with reduced net grid import energy, with about 8.93% (982.36 tCO₂) of carbon emission reductions for the individual price mode. The lifetime net present value of the hybrid renewable energy and hydrogen vehicle system applied in the net-zero energy community can be reduced by 54.40% - 55.90% in the future cost scenario compared with the current cost scenario, showing a promising application potential in the near future.

(4) The peer trading management in a net-zero energy community with hybrid renewable energy and hydrogen vehicle storage systems is presented. The detailed techno-economic-environmental performance comparison on the net-zero energy community in different peer trading price modes and management strategies provides clear guidance for renewable energy installation and management within high-density urban contexts. The proposed individual peer energy trading price model and time-of-use peer trading management strategies provide significant references for relative stakeholders for peer trading management in large-scale diversified urban communities.

8.2 Peer-to-peer trading optimizations on the net-zero energy community integrated with energy storage of hydrogen and battery vehicles

8.2.1 Framework of peer energy trading optimizations on the net-zero energy community integrated with energy storage of hydrogen and battery vehicles

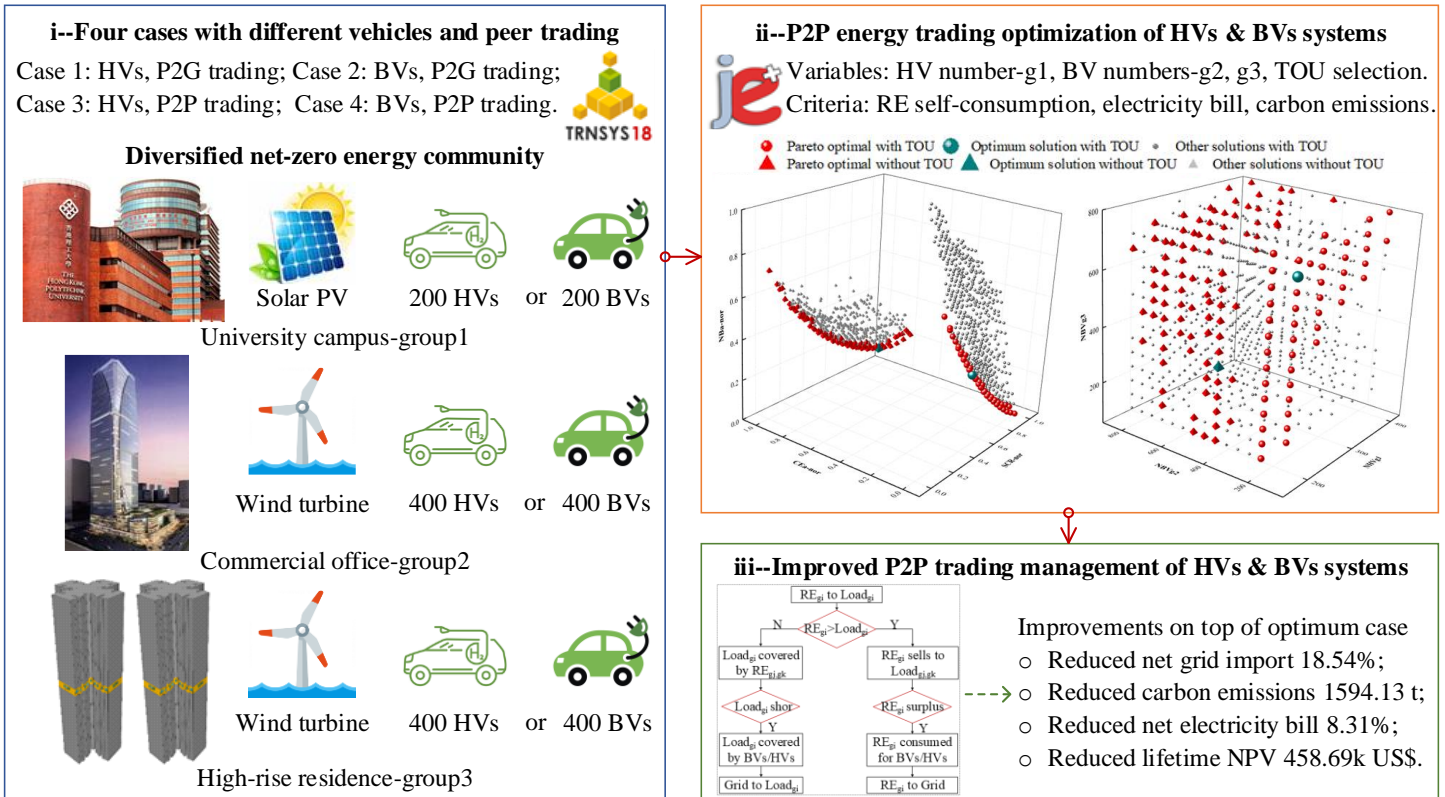


Fig. 8.19 Framework of peer trading optimizations on the net-zero energy community integrated with HVs and BVs

This study presents the P2P energy trading management and optimization approaches on a diversified net-zero energy community integrated with hydrogen vehicle (HV) and battery vehicle (BV) storage, with the overall framework as shown in Fig. 8.19. Hybrid solar PV and offshore wind turbine systems, with advantageous and complementary characteristics, are developed for power supply to the net-zero energy community, with annual balanced electrical loads and

renewable energy generations. The HV and BV groups with different cruise schedules are integrated with the hybrid renewable energy systems, serving as both energy storage units and cruise tools for the building occupants.

Firstly, four net-zero energy community cases are developed with different energy storage vehicles and peer trading management strategies, to compare the application feasibility of HV-integrated and BV-integrated renewable energy systems in either P2G or P2P trading operation. Specifically, Case 1 allocates three HV groups to the diversified net-zero energy community with only P2G trading management. Case 2 allocates three BV groups to the diversified net-zero energy community with only P2G trading management. Case 3 allocates three HV groups and introduces P2P energy trading in the diversified community. And Case 4 allocates three BV groups in the community with P2P energy trading management. Detailed techno-economic-environmental performances of these four cases are compared to explore the superiority of HV storage and BV storage systems in either P2G or P2P trading management strategy, in terms of the on-site renewable energy self-consumption, on-site load coverage, grid integration and carbon emissions, annual electricity bill and lifetime NPV.

Secondly, the P2P energy trading optimizations are conducted on the diversified net-zero energy community integrated with both HV and BV storage units, to investigate the interactive impact of vehicle numbers and time-of-use (TOU) management on the techno-economic-environmental performances of hybrid renewable energy systems. Four optimization variables are assigned including the number of integrated HVs in the university campus buildings, the number of integrated BVs in the commercial office buildings, the number of integrated BVs in the high-rise residential buildings, and the TOU management selection signal. And the technical, economic and environmental performance indicators of the renewable energy and hybrid vehicle storage

system are adopted as optimization criteria, including the on-site renewable energy self-consumption, annual net electricity bill, and annual equivalent carbon emissions. The application of the TOU management strategy on optimizing the techno-economic-environmental performances of hybrid renewable energy and vehicle storage systems is clearly presented, based on the distribution of the Pareto optimal set of optimization objectives. And the optimal interactive relationship of the TOU management strategy and equipped vehicle numbers in three diversified building groups for a comprehensive optimization is reported, based on the distribution of the Pareto optimal set of optimization variables. The multi-objective P2P energy trading optimization results can provide guidance for the application and management of hybrid renewable energy and green vehicle energy storage systems for achieving carbon neutrality in integrated building and transport sectors.

Based on the final optimum solution obtained from the decision-making strategy of the minimum distance to the utopia point method, an improved P2P energy trading management strategy is further proposed to enhance the dynamic peer energy trading of the hybrid renewable energy system with both HVs and BVs for the diversified net-zero energy community. The surplus renewable energy of each building group is shared and traded for the load shortage of other building peers prior to its vehicle storage, to increase the on-site load coverage and reduce grid power pressure. And the storage charging and discharging of BV systems are prior to HV systems to make complementary operations of hybrid storage units in the diversified community. The underlying mechanism for the complementary operations is that, BV systems have a higher utilization efficiency and a lower charging starting power but a smaller charging rate limit and lower charging availability, while HV systems have a larger charging rate and higher charging availability but a higher charging starting power and a lower efficiency. The techno-economic-

environmental superiority of the improved P2P trading management strategy is demonstrated, through the comparison with the optimum solution of the multi-objective optimization. And significant reductions can be achieved in the net grid import, annual equivalent carbon emissions, annual net electricity bill and lifetime NPV for the net-zero energy community.

8.2.2 System modelling of hybrid renewable energy systems for the net-zero energy community integrated with hydrogen vehicles or battery vehicles

This section develops HV-integrated renewable energy systems and BV-integrated renewable energy systems for power supply to the typical diversified net-zero energy community, given the promising development of HVs and BVs as the mostly widely used green vehicles. Multiple functions are served for the green vehicles when integrated with hybrid renewable energy systems, including storing surplus renewable energy as the energy storage unit, supplying power for load shortage as the energy supply unit, as well as serving as the daily cruise tools of occupants in the corresponding building group. The transient simulation model of the hybrid renewable energy system integrated with three HV storage groups is developed for the diversified net-zero energy community, considering the P2G trading (Case 1) and P2P trading (Case 3) managements as shown in Fig. 8.20.

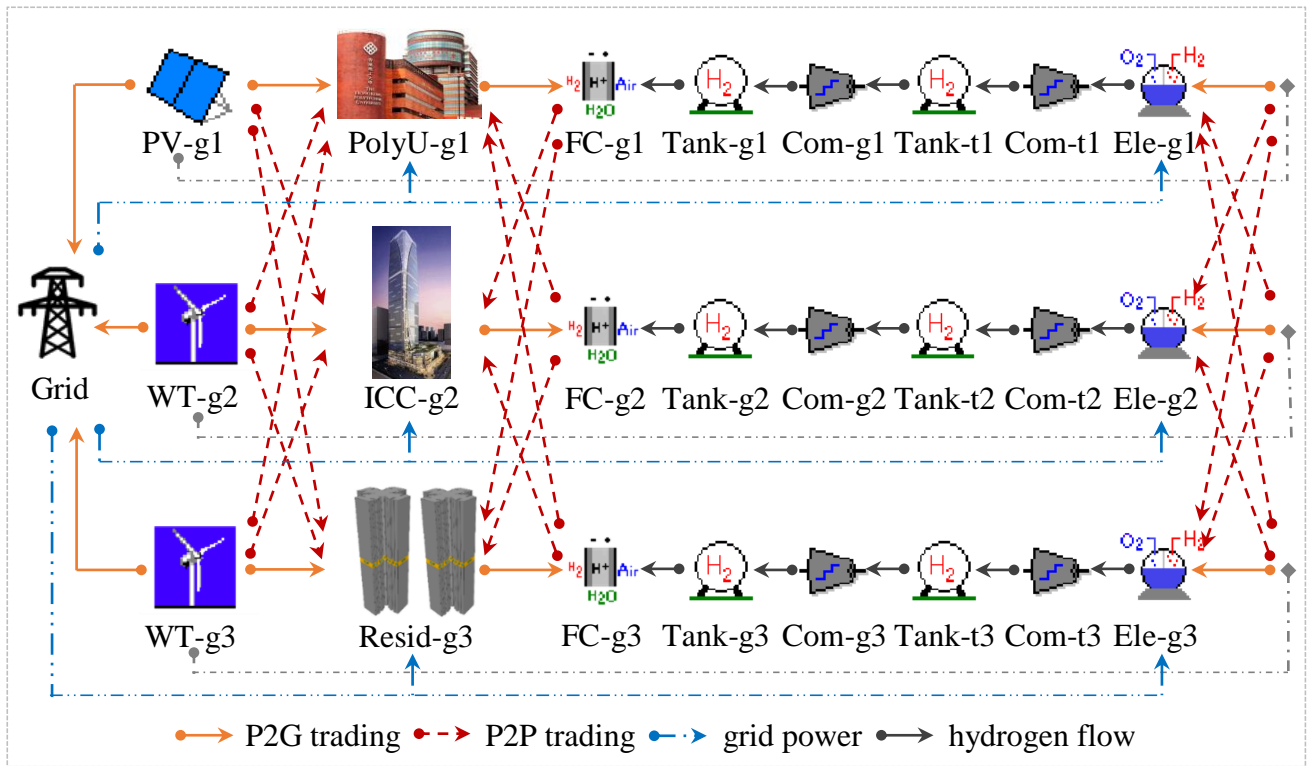


Fig. 8.20 Schematic of HV-integrated renewable energy systems with P2G (Case 1) and P2P trading (Case 3) of the diversified net-zero energy community

The transient simulation model of the hybrid renewable energy system integrated with three BV storage groups is also developed for the diversified net-zero energy community with P2G energy trading (Case 2) and P2P energy trading (Case 4) as shown in Fig. 8.21. The vehicle number and operation schedule in each group keep the same with that in the HV-integrated renewable energy systems. And the storage capacity of each BV is 75 kWh, as comparable to that of the HV. Type 47a is adopted to model the battery vehicle based on the energy balance mechanism, according to the commercial product of “Tesla Model S 75” [100]. A maximum electricity storage state of charge at 0.95 is set for the BV, and a minimum state of charge at 0.39 is set to cover one-day cruise and keep above the minimum vehicle storage level.

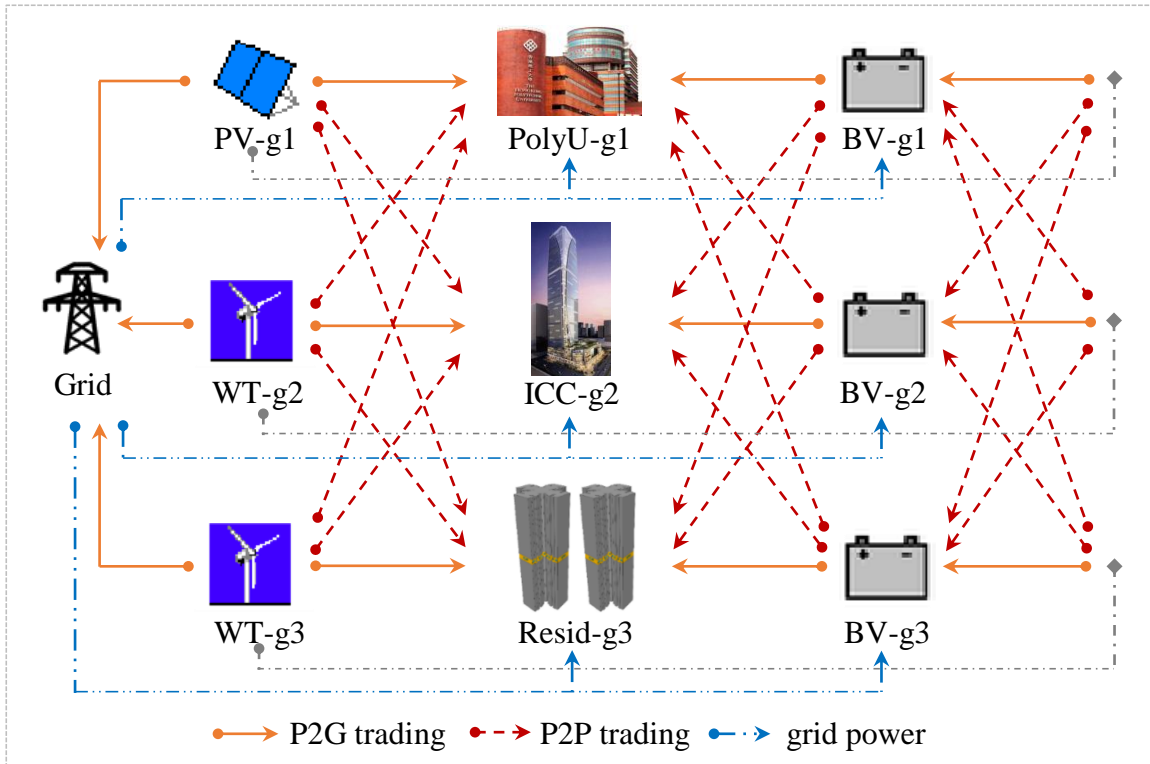


Fig. 8.21 Schematic of BV-integrated renewable energy systems with P2G (Case 2) and P2P trading (Case 4) of the diversified net-zero energy community

Obvious differences between the BV storage system and HV storage system are considered in the energy management of hybrid renewable energy systems applied in the diversified net-zero energy community. On the one hand, the HV system has superior performances than the BV system for the charging time availability and charging rate limit. Renewable energy can be stored in the HV system via driving stationary electrolyzers to generate hydrogen and store in the stationary storage tanks, so that the HV system can store renewable energy even though HVs are not parked in buildings. While, only parked BVs can be charged for the BV system. And the charging rate limit of the BV system (1C for the lithium-ion battery) is stricter than the HV system (current density of 400 mA/cm^2 for the advanced alkaline electrolyzer). On the other hand, the BV system has superior advantages than the HV system in terms of the initial charging power, energy

efficiency and investment cost. The electrolyzers can be only started when the input power is above its initial charging power (current density of 40 mA/cm² for the advanced alkaline electrolyzer), while BVs can be started without strict power limitations. Moreover, the utilization efficiency of the BV system is much higher than that of the HV system.

Table 8.1 Four community cases with different storage vehicles and energy trading strategies

Net-zero energy community cases	Case 1	Case 2	Case 3	Case 4
Three HV groups	√	--	√	--
Three BV groups	--	√	--	√
P2G trading only	√	√	--	--
P2P trading management	--	--	√	√

Four net-zero energy community cases are developed and compared with different storage vehicle and energy trading strategies as shown in Table 8.1. Namely, Case 1: HVs are installed in each building group with only P2G trading in the community; Case 2: BVs are installed in each building group with only P2G trading in the community; Case 3: HVs groups are installed in each building group with P2P trading in the community; Case 4: BVs groups are installed in each building group with P2P trading in the community. The vehicle number in each building group of these four cases keeps the same, with 200 vehicles in the university campus buildings (group 1), 400 vehicles in the commercial office buildings (group 2) and 400 vehicles in the high-rise residential buildings (group 3) according to the building functions and scales.

8.2.3 Peer-to-peer energy trading optimization and improved peer energy management of the net-zero energy community with both hydrogen vehicles and battery vehicles

(1) Peer-to-peer energy trading optimization

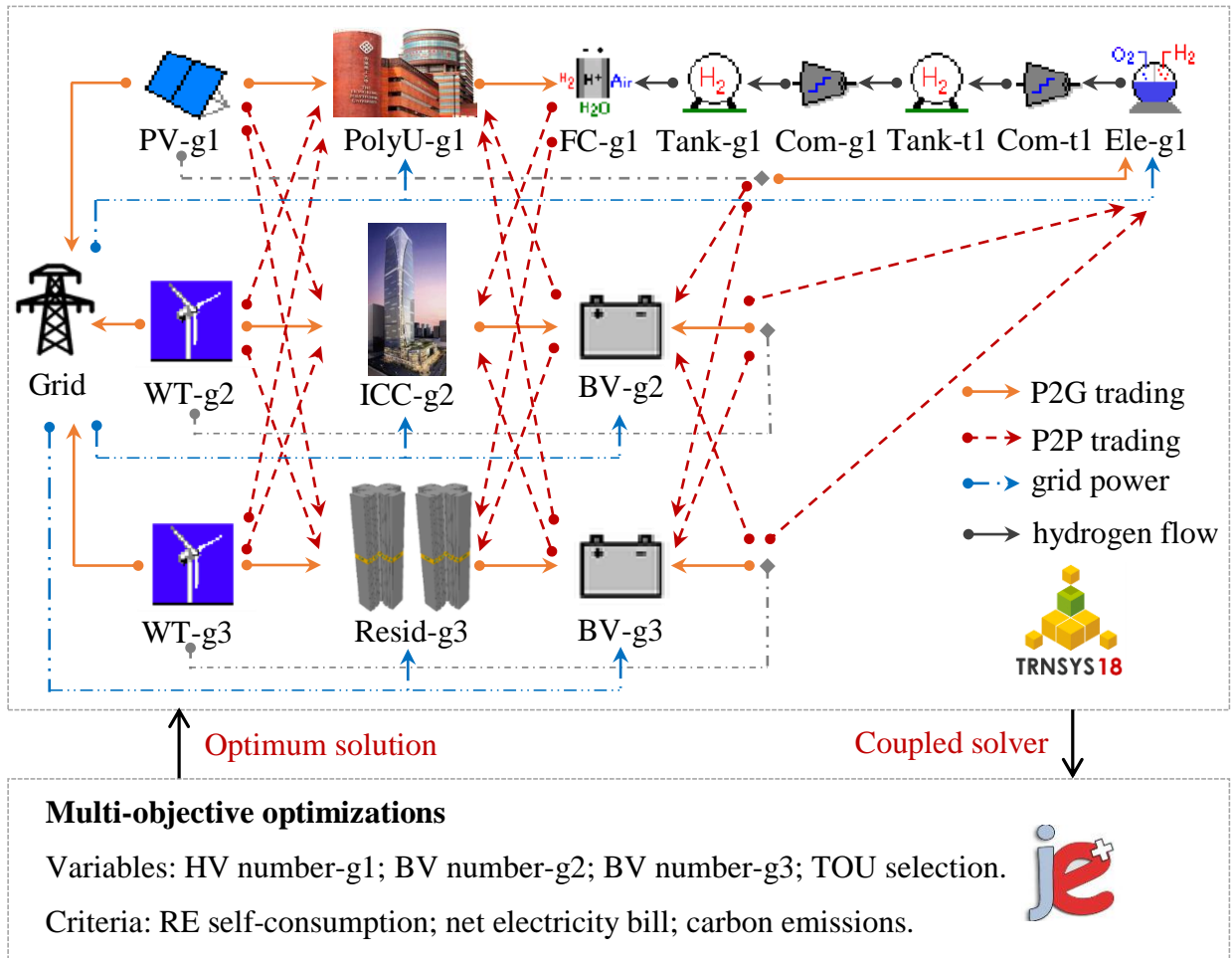


Fig. 8.22 Multi-objective optimization on renewable energy systems with both HVs and BVs

The P2P energy trading optimization of the diversified net-zero energy community with both HVs and BVs is further analyzed, to explore the interactive impact of vehicle numbers and TOU management on the techno-economic-environmental performances of hybrid renewable energy systems, with the schematic as shown in Fig. 8.22. The hybrid renewable energy system model integrated with HVs (group 1 campus buildings) and BVs (group 2 office buildings and group 3 residential buildings) is firstly established. The building groups in the diversified net-zero energy community trade energy with both building peers and the utility grid.

Then, multi-objective optimizations on the diversified net-zero energy community are conducted based on the coupled TRNSYS and jEplus+EA platform. The vehicle numbers integrated with three building groups and the TOU management selection signal are adopted as optimization variables. The HVs are integrated with the university campus buildings (group 1) searching within the range of 150 - 400 at an increment of 50. The BVs are integrated with the commercial office buildings (group 2) and high-rise buildings (group 3), both searching within the range of 150 - 800 at an increment of 50. And the TOU management selection signal is searched between the value 0 (with TOU management) and 1 (without TOU management).

The detailed energy management strategy with TOU management in the P2P energy trading of the diversified net-zero energy community is shown in Fig. 8.23. During on-peak periods, surplus renewable energy after meeting its electrical load is shared with other building peers with load shortage, where the building peer with a lower selling price and more surplus renewable energy enjoys the energy trading priority. And residual renewable energy after covering the load shortage of all buildings is exported into the utility grid for higher power flexibility and economy during on-peak time. While during off-peak periods with the grid preference of a low energy export, surplus renewable energy after meeting internal electrical demand is utilized to charge storage vehicles and shared with other building peers with load shortage and storage shortage. The residual renewable energy after covering all the load shortage and storage shortage of buildings in the community is finally fed into the grid. In terms of covering the load shortage of the building during on-peak time, after being met by the self-owned renewable energy sources, the vehicle storage of the building group is utilized. Afterwards, the load shortage can be covered via buying energy from other building peers with surplus renewable energy and surplus storage, following the rule that, the building peer with a higher buying price and higher load shortage catches the energy

trading priority. The remaining load shortage after being satisfied by all surplus renewable energy and surplus storage is finally supported by the utility grid. While during off-peak time with the grid preference of a high energy import, the building group with load shortage buys energy from other building peers with surplus renewable energy, and then imports energy from the utility grid.

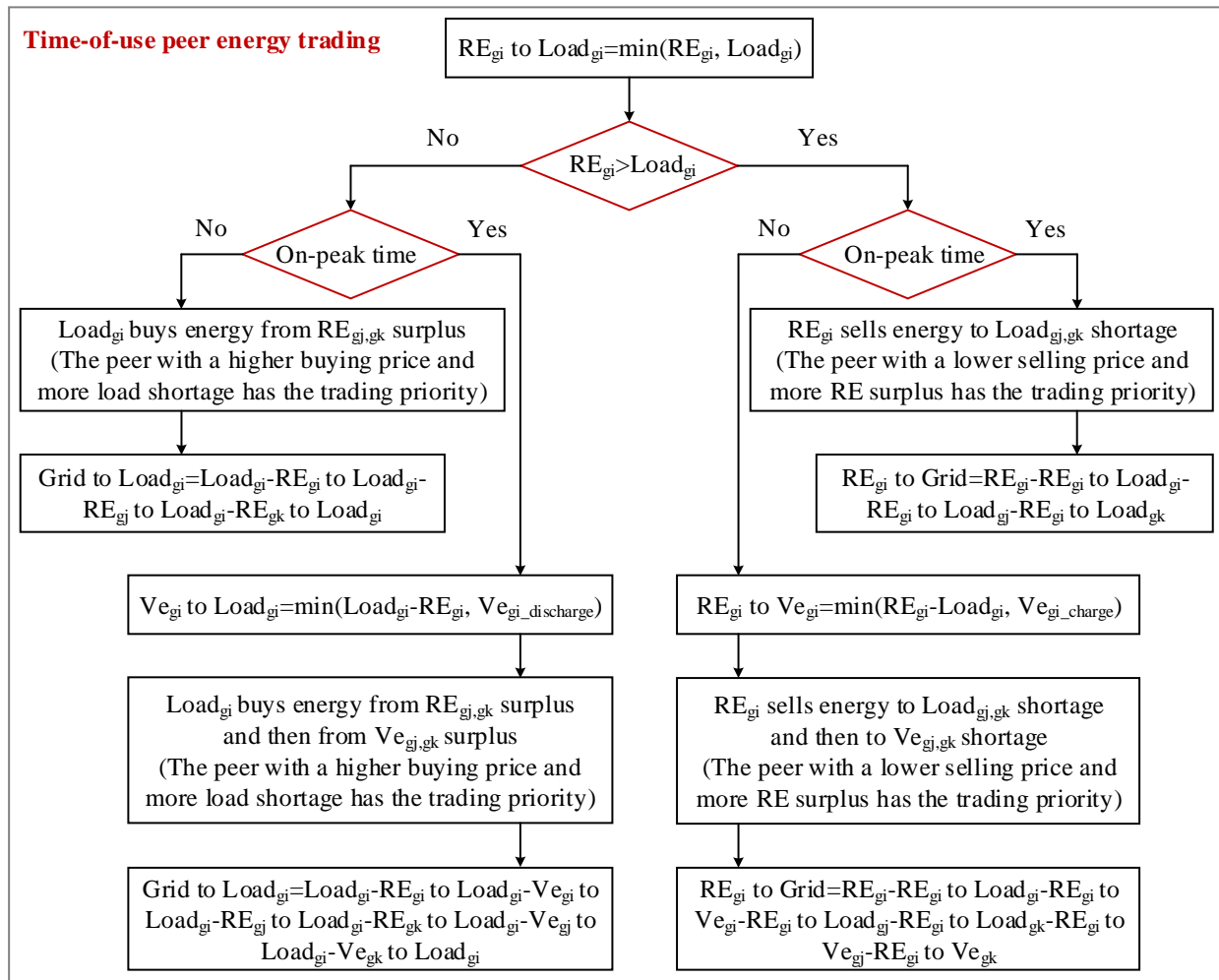


Fig. 8.23 Flowchart of renewable energy and vehicle systems with time-of-use P2P trading

The technical, economic and environmental performance indicators of renewable energy and hybrid vehicle storage systems are adopted as the optimization criteria, including the renewable energy on-site consumption, annual net electricity bill and annual equivalent carbon emissions.

(2) Improved peer-to-peer energy management

An improved P2P energy management strategy is proposed to further enhance the dynamic peer energy trading of the hybrid renewable energy system integrated with both HVs and BVs for power supply to the diversified net-zero energy community. Its superiority in the technical, economic and environmental performances is demonstrated in comparison with the final optimum solution obtained by the multi-objective optimizations. The main improvements of the improved P2P energy management on top of the optimization P2P management strategy of hybrid systems with both HVs and BVs lie in two aspects: (1) Surplus renewable energy of the building group is shared and traded for the load shortage of other building peers prior to its vehicle storage, to increase the on-site community load coverage and reduce grid power pressure. (2) The storage charging and discharging of the BV system are prior to the HV system to make complementary operations of the hybrid vehicle storages, as the BV system has a higher utilization efficiency and a lower charging starting power but a smaller charging rate limit and lower charging availability, while the HV system has a larger charging rate and higher charging availability but a higher charging starting power and a lower efficiency.

The detailed energy management strategy of the improved case is explained in Fig. 8.24. Surplus renewable energy generation of the building group after meeting its own electrical load is shared with other building peers with load shortage, where the building peer with a lower selling price and higher renewable energy surplus has the energy trading priority. And residual renewable energy after meeting all load demand of the community peers is then utilized to charge three groups of storage vehicles, where the BV charging is prior to the HV charging to make complementary operations of the hybrid vehicle storages. Finally, extra renewable energy is exported into the utility grid. As for the load shortage of the building group after being satisfied by its renewable energy sources, it is then covered by the shared energy from other building peers with surplus

renewable energy, where the building peer with a higher buying price and more load shortage enjoys the trading priority. The building group still with load shortage can then be met by the integrated three groups of storage vehicles, where the BV discharging is prior to the HV discharging. And the remaining load shortage is lastly covered by the utility grid.

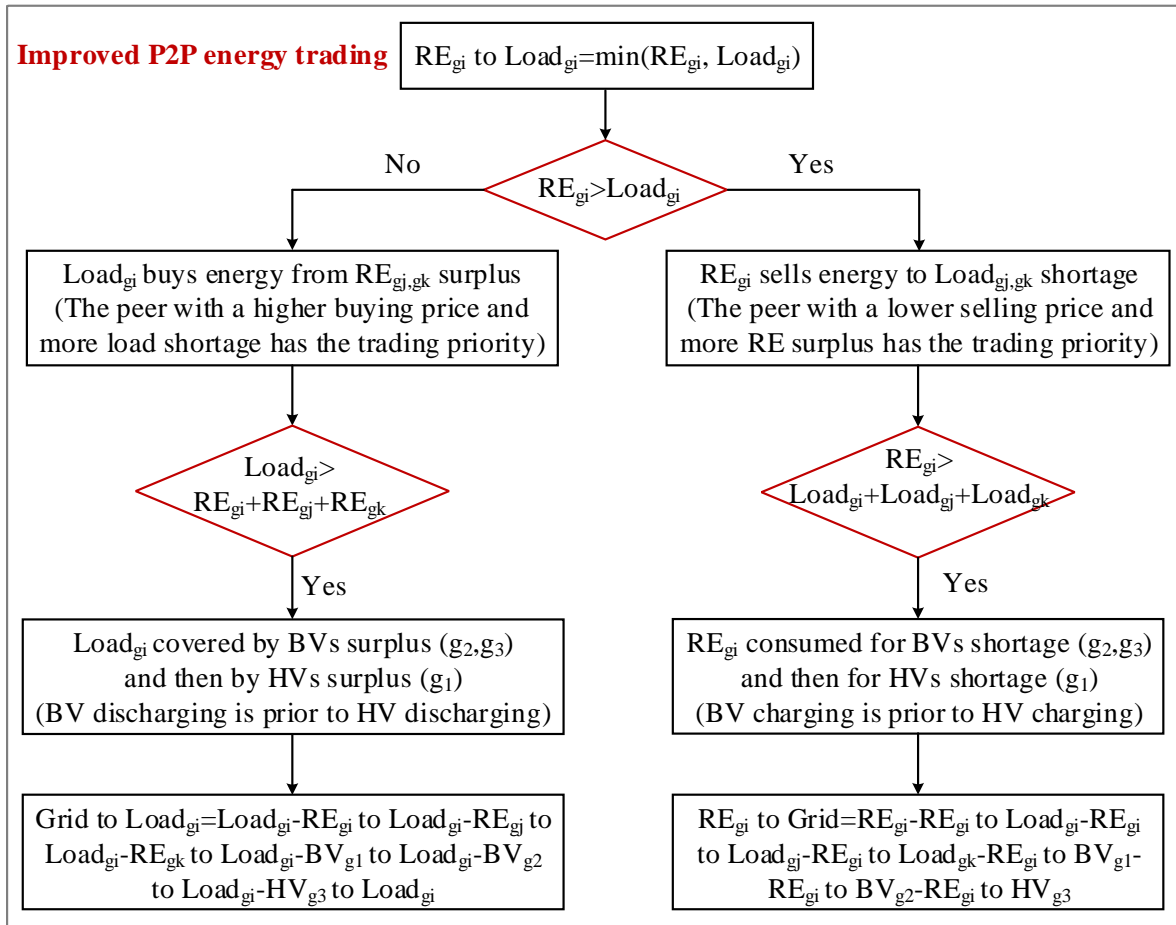


Fig. 8.24 Flowchart of improved P2P strategy of the community with both HVs and BVs

8.2.4 Comparison results of hydrogen vehicles-integrated and battery vehicles-integrated renewable energy systems for the net-zero energy community

The technical, economic and environmental performances of these four net-zero energy community cases with different vehicle types and peer energy trading managements are compared,

concerning the on-site renewable energy self-consumption, on-site load coverage, grid integration, carbon emissions, annual electricity bill and lifetime net present value.

(1) On-site renewable energy self-consumption of four net-zero energy community cases

The renewable energy supply from solar PV and wind sources for the net-zero energy community is firstly utilized to meet electrical load and charge vehicle storage in the building itself, then to be either exported into the grid in the P2G trading management (Case 1 and Case 2), or shared to peer load and vehicle storage before being exported into the grid in the P2P trading management (Case 3 and Case 4). So the renewable energy consumption for self-load in the four cases is almost the same, while consumption for other parts differs greatly as shown in Fig. 8.25. It is indicated that more renewable energy is utilized on site for the HV-integrated hybrid system for both P2G trading management (Case 1) and P2P trading management (Case 3) with a SCR increment of 13.09% and 16.82% respectively, compared with the BV-integrated cases (Case 2 and Case 4). The main reason is that the charging availability of HVs is higher than BVs which only can be charged when parking in buildings. So the utility grid needs to absorb much more renewable energy in the BV-integrated system, higher by 49.67% in the P2G trading and 171.30% in the P2P trading compared with the HV-integrated system. It is also found that the P2P energy trading improves the on-site renewable energy consumption for both the HV-integrated system (Case 3) and the BV-integrated system (Case 4), where the SCR is increased by 16.54% and 12.82% respectively on top of the P2G trading cases (Case 1 and Case 2), as more renewable energy can be shared for peer load and storage.

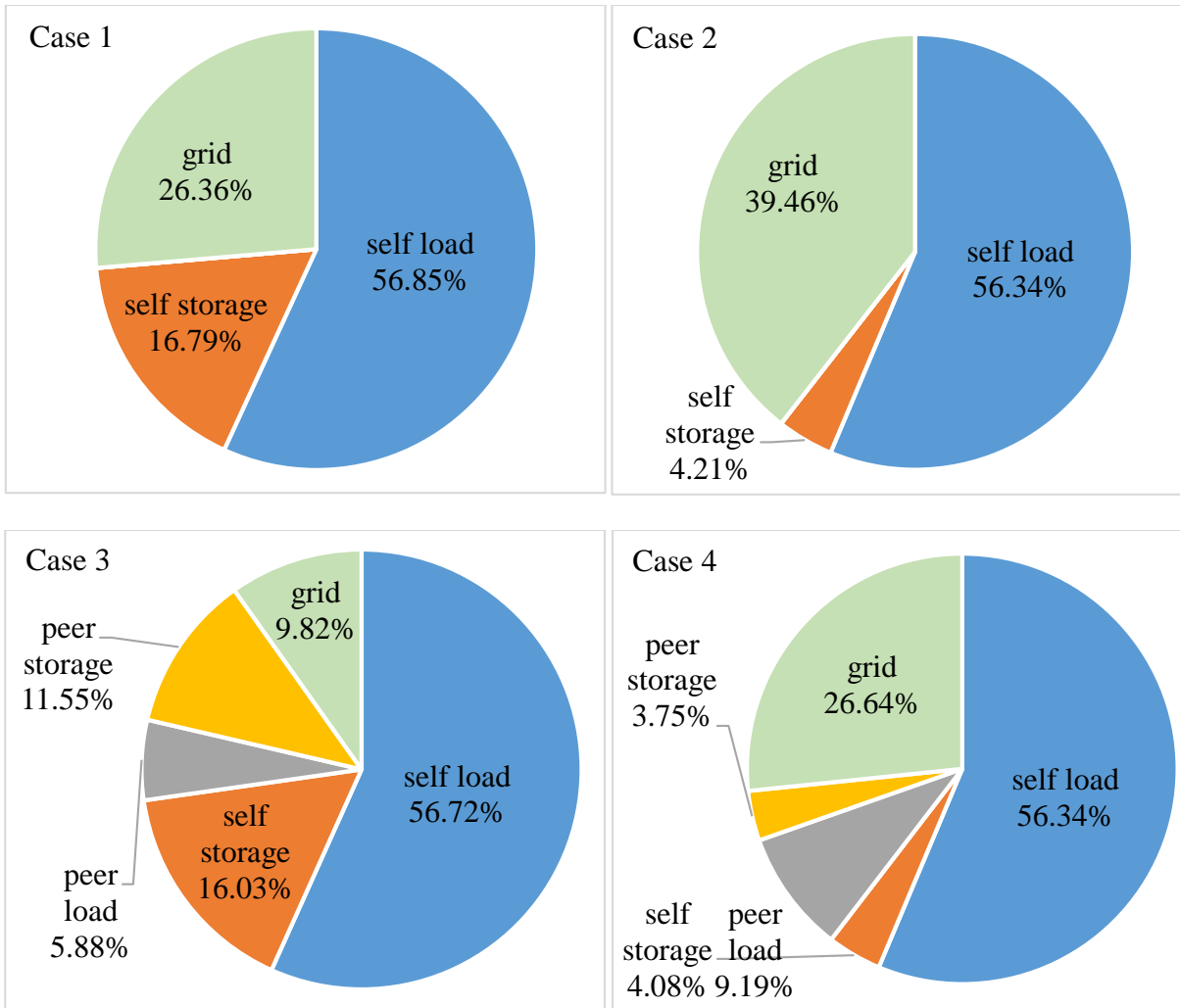


Fig. 8.25 Comparison of renewable energy self-consumption of four cases with HVs or BVs
 (Note: Case 1: HVs-based system in P2G trading; Case 2: BVs-based system in P2G trading; Case 3: HVs-based system in P2P trading; Case 4: BVs-based system in P2P trading.)

(2) On-site load coverage of four net-zero energy community cases

The renewable energy systems integrated with vehicle storage units are developed for meeting electrical demand of buildings in the net-zero energy community, with the on-site load coverage comparison as shown in Fig. 8.26. It is indicated that the on-site load coverage of the HV-integrated system is slightly higher than that of the BV-integrated system, by 3.45% for the

P2G trading (Case 1 vs. Case 2) and 1.64% for the P2P trading management (Case 3 vs. Case 4), as more renewable energy is absorbed by the HV storage. And an obvious enhancement on the LCR of the net-zero energy community is observed by introducing P2P trading compared with the P2G trading, higher by 10.10% for the HV-integrated system (Case 3 vs. Case 1) and 11.91% for the BV-integrated system (Case 4 vs. Case 2), since part of building load can be covered by surplus energy of peer renewable generation and storage for the P2P trading management. Therefore, the utility grid can be significantly relieved by adopting the P2P trading management, with less grid power import by 25.62% for the HV-integrated system (Case 3 vs. Case 1) and 27.13% for the BV-integrated system (Case 4 vs. Case 2).

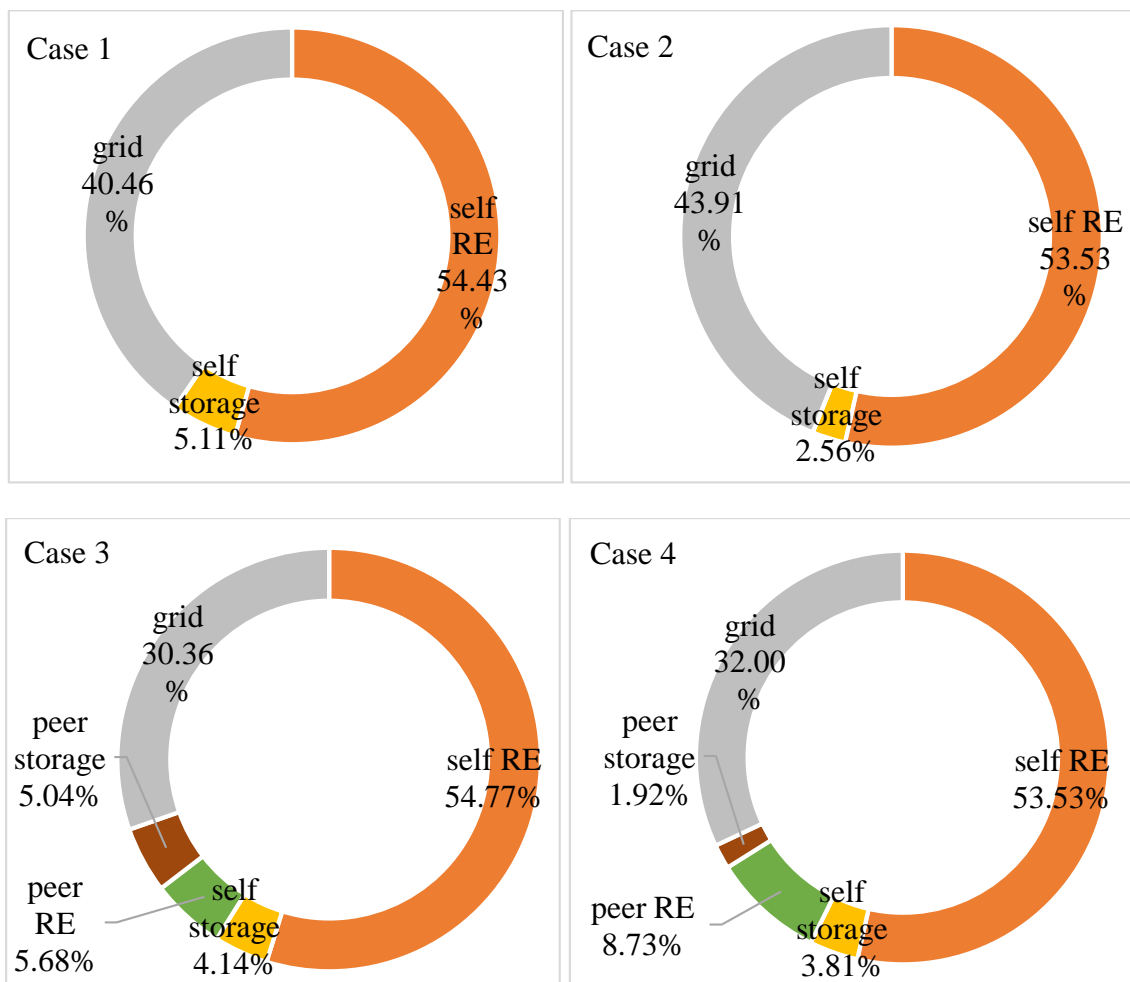


Fig. 8.26 Comparison of on-site load coverage of four cases with HVs or BVs

(Note: Case 1: HVs-based system in P2G trading; Case 2: BVs-based system in P2G trading; Case 3: HVs-based system in P2P trading; Case 4: BVs-based system in P2P trading.)

(3) Grid integration and carbon emissions of four net-zero energy community cases

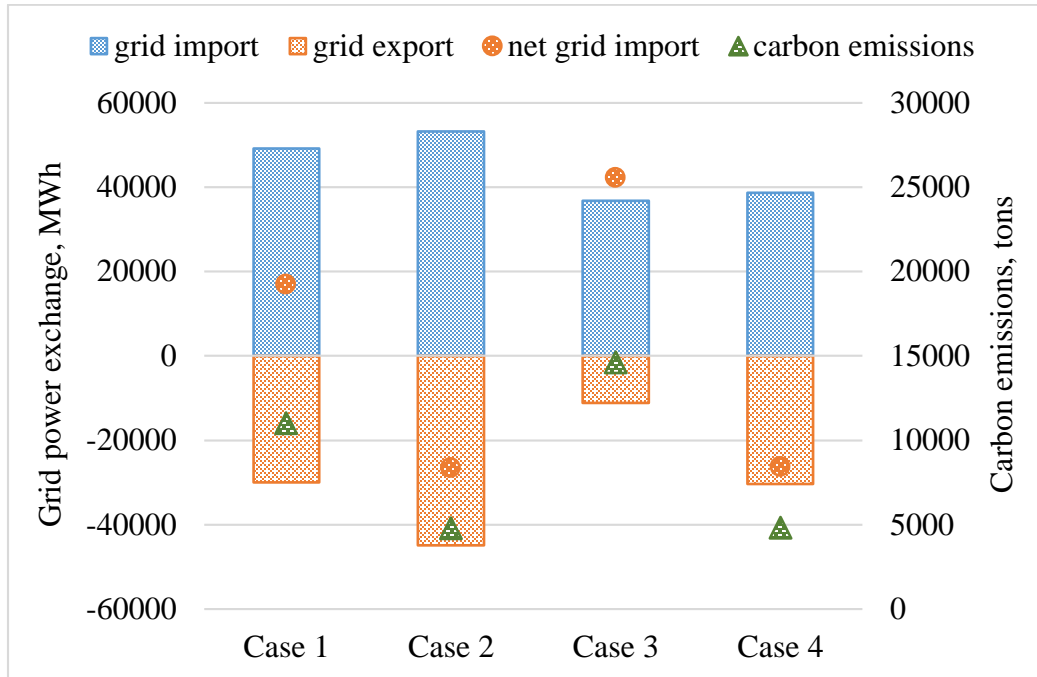


Fig. 8.27 Grid integration and carbon emissions of four cases with HVs or BVs

(Note: Case 1: HVs-based system in P2G trading; Case 2: BVs-based system in P2G trading; Case 3: HVs-based system in P2P trading; Case 4: BVs-based system in P2P trading.)

The power integration between the diversified net-zero energy community and the utility grid varies with the storage vehicle types and energy trading management modes as shown in Fig. 8.27. It is indicated that the BV-integrated hybrid system performs better in the grid integration, with much less net grid import than the HV-integrated system by 56.60% for the P2G trading (Case 2 vs. Case 1) and 67.05% for the P2P trading (Case 4 vs. Case 3). This is mainly because more renewable energy generation is exported into the utility grid in the BV-integrated system with less storage charging availability. And the utilization efficiency of the BV storage system (90.06% -

93.55%) is much higher than the HV storage system (40.81% - 42.42%), considering both energy storage and transportation functions. While, the P2P energy trading increases the net grid import for both HV and BV storage systems, with less grid export compared with P2G trading cases. Significant decarbonisation benefits are observed in the BV-integrated systems induced by lower net grid import compared with the HV-integrated systems, reduced by 6229.02 tons for the P2G trading (Case 2 vs. Case1) and 9803.21 tons for the P2P trading (Case 4 vs. Case 3). But the P2P energy trading increases carbon emissions of the diversified community compared with the P2G trading, especially for the HV storage system higher by 32.85% at 3615.37 tons (Case 3 vs. Case 1), as more renewable energy is used for peer load and storage rather than exported into the grid.

(4) Annual electricity bill of four net-zero energy community cases

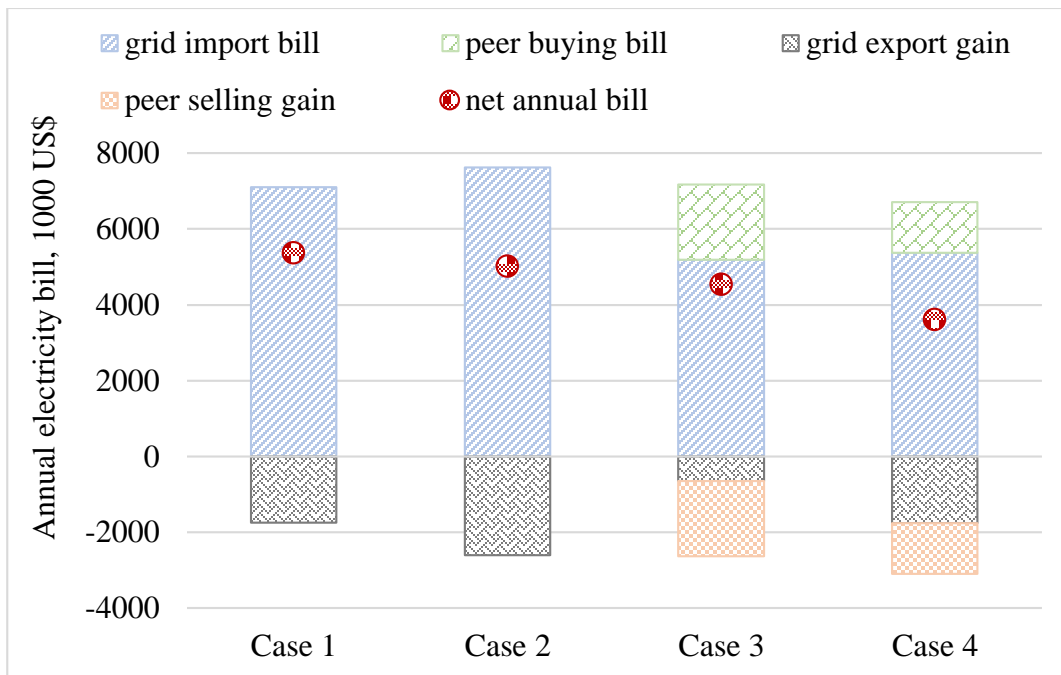


Fig. 8.28 Annual electricity bill of four cases with HVs or BVs

(Note: Case 1: HVs-based system in P2G trading; Case 2: BVs-based system in P2G trading; Case 3: HVs-based system in P2P trading; Case 4: BVs-based system in P2P trading.)

The building groups in the net-zero energy community pay electricity bills for both the utility grid imported power and peer bought power, and achieve electricity gains for the grid exported power and peer sold power as shown in Fig. 8.28. It is indicated that the BV-integrated systems enjoy lower net annual bill than the HV-integrated systems, reduced by 6.60% (US\$ 354.35k) for the P2G trading (Case 2 vs. Case 1) and 20.50% (US\$ 931.52k) for the P2P trading (Case 4 vs. Case 3), as more renewable energy is available for feeding into the grid with export gain in the BV-integrated systems. And the P2P trading reduces the annual electricity bill of the diversified community, lower by 15.37% (US\$ 825.34k) for the HV-integrated system (Case 3 vs. Case 1) and 27.96% (US\$ 1402.50k) for the BV-integrated system (Case 4 vs. Case 2). The main reason is that less power is needed from the utility grid with a higher cost than the peer trading energy.

(5) System lifetime net present value of four net-zero energy community cases

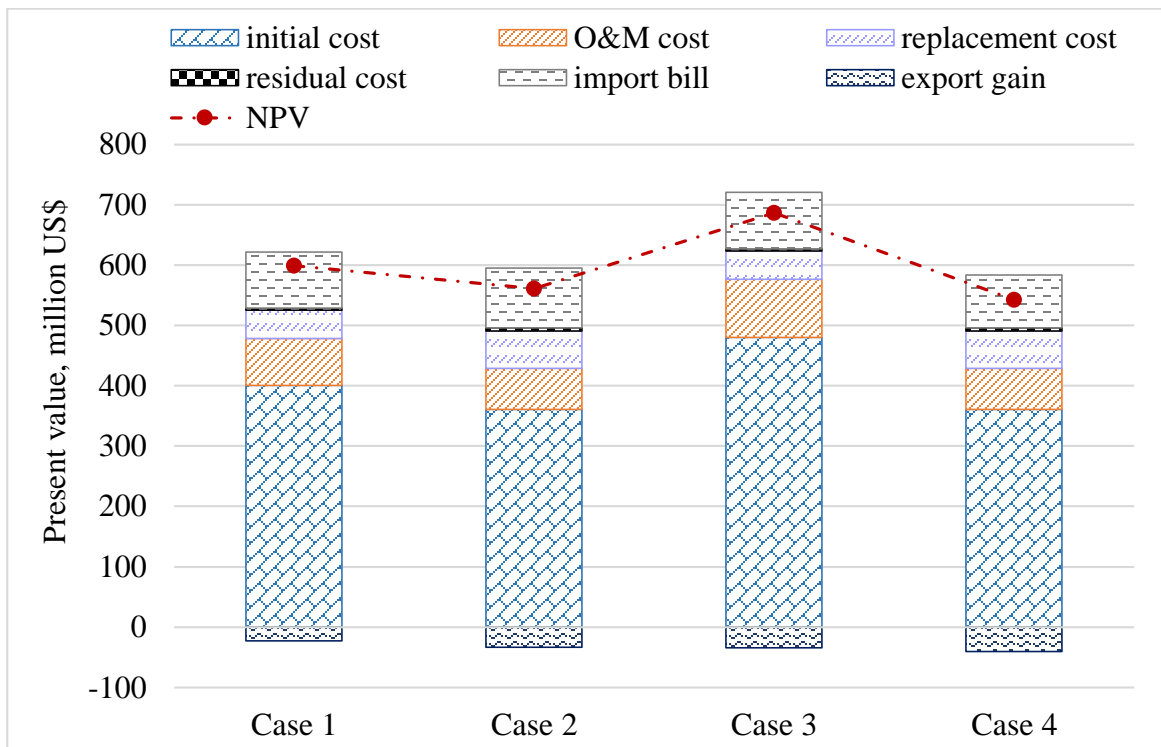


Fig. 8.29 System lifetime net present value of four cases with HVs or BVs

(Note: Case 1: HVs-based system in P2G trading; Case 2: BVs-based system in P2G trading; Case 3: HVs-based system in P2P trading; Case 4: BVs-based system in P2P trading.)

The system NPV of the hybrid renewable energy systems integrated with three groups of HVs or BVs during a service lifetime of 20 years is analysed, considering the initial cost, O&M cost, replacement cost, residual cost, electricity import bill and electricity export gain, as per Fig. 8.29. The comparison results show that the present value of initial cost of the HV-integrated system is higher than that of the BV-integrated system, as more components are installed in the HV storage system including electrolyzers, compressors, hydrogen storage tanks and hydrogen vehicles. And the present value of net electricity bill of HV-integrated systems is higher than that of BV-integrated systems with higher grid export gains. So the lifetime NPV of HV-integrated systems is higher than that of BV-integrated systems, by 6.74% (US\$ 37.81M) for the P2G trading (Case 1 vs. Case 2) and 26.38% (US\$ 143.22M) for the P2P trading (Case 3 vs. Case 4). The present value of initial cost and O&M cost of the HV-integrated system with P2P trading management (Case 3) is increased by 19.80% and 23.83% compared to that with only P2G trading (Case 1), since more electrolyzers need to be installed in the community with higher charging power. The present value of electricity export gain (including grid export gain and peer selling gain) with P2P trading management is higher by 51.42% than that without P2P trading. So the lifetime NPV of the HV-integrated system with P2P trading (Case 3) is higher than that with only P2G trading (Case 1) by 14.55% for US\$ 87.16M. In terms of the BV-integrated system, the present value of investment cost with P2P trading (Case 4) is the same with that with only P2G trading (Case 2). While, the present value of net electricity bill of the BV-integrated system with P2P trading is 27.96% lower than that with P2G trading. So the lifetime NPV of the BV-integrated system with P2P trading (Case 4) is lower than that with only P2G trading (Case 2) by 3.25% for US\$ 18.25M.

8.2.5 Multi-objective optimization results on the net-zero energy community integrated with both hydrogen vehicles and battery vehicles

- Pareto optimal with TOU ● Optimum solution with TOU ● Other solutions with TOU
- ▲ Pareto optimal without TOU ▲ Optimum solution without TOU ▲ Other solutions without TOU

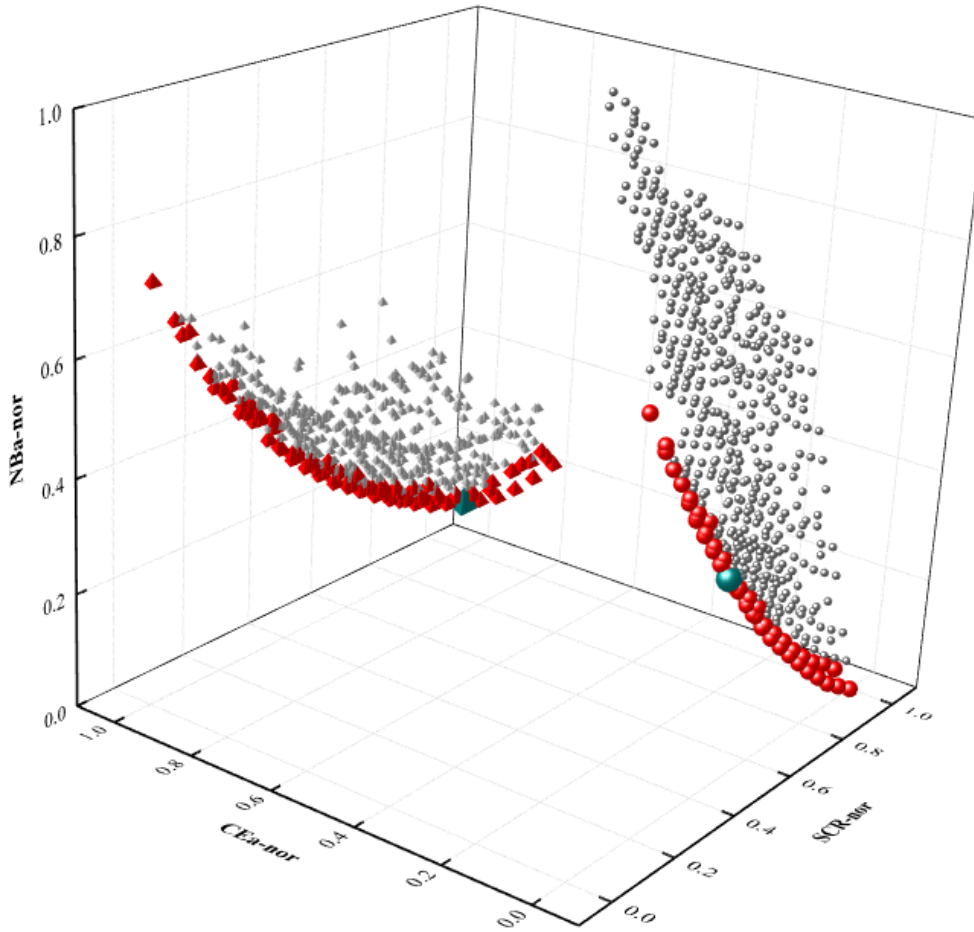


Fig. 8.30 Pareto optimal and final optimum results of hybrid PV-wind-HV-BV systems under TOU and non-TOU management strategies

The three-dimensional Pareto optimal and final optimum results of the multi-objective optimization on hybrid PV-wind-HV-BV systems are shown in Fig. 8.30, optimizing three groups of vehicle numbers and TOU management selection signals, considering the on-site renewable energy utilization, annual electricity bill and carbon emissions. Two obvious Pareto optimal surfaces are observed for TOU and non-TOU management approaches, with a clear trade-off

conflict among the focused technical, economic, and environmental criteria in normalized values. Namely, both TOU management and non-TOU management strategies can be selected in the hybrid renewable energy systems with different vehicle numbers for a comprehensive techno-economic-environmental optimization in the net-zero energy community. The final optimum solutions of TOU and non-TOU management approaches as highlighted in the cyan ball and tetrahedron are obtained using the decision-making strategy of the minimum distance to the utopia point method.

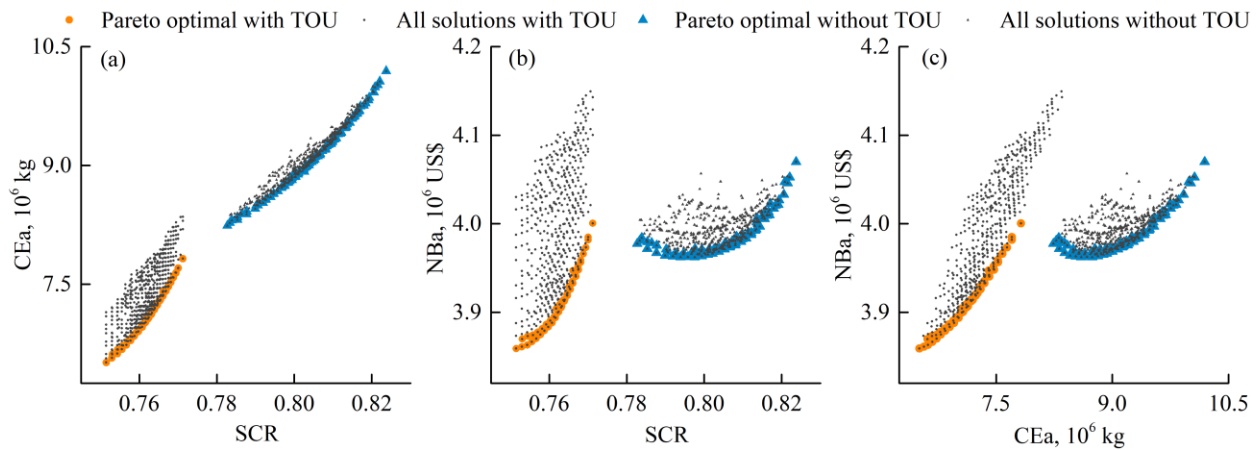


Fig. 8.31 Projection distribution of Pareto optimal and final optimum results

The two-dimensional projections of Pareto optimal solutions under TOU and non-TOU managements are shown in Fig. 8.31 for a clear demonstration. It is indicated that the Pareto optimal solutions with TOU management achieve lower SCR than that without TOU management, as per Fig. 8.31(a) and (b), since the utilization of on-site renewable energy is limited by the time-of-use power management to increase grid export and reduce grid import during on-peak periods, and to increase grid import and reduce grid export during off-peak periods. While most Pareto optimal solutions of TOU management obtain lower carbon emissions and lower annual electricity bill compared with that of non-TOU management as per Fig. 8.31(c), as the net grid imported

energy is reduced with TOU management. Therefore, TOU management should be adopted when solely focusing on the economic and environmental performances (*CEa-NBa*) of the hybrid PV-wind-HV-BV systems applied in the net-zero energy community. While, both TOU and non-TOU management approaches can achieve balanced results when considering the techno-economic (*SCR-CEa*) or techno-environmental (*SCR-NBa*) performances, with appropriate vehicle numbers in diversified building groups.

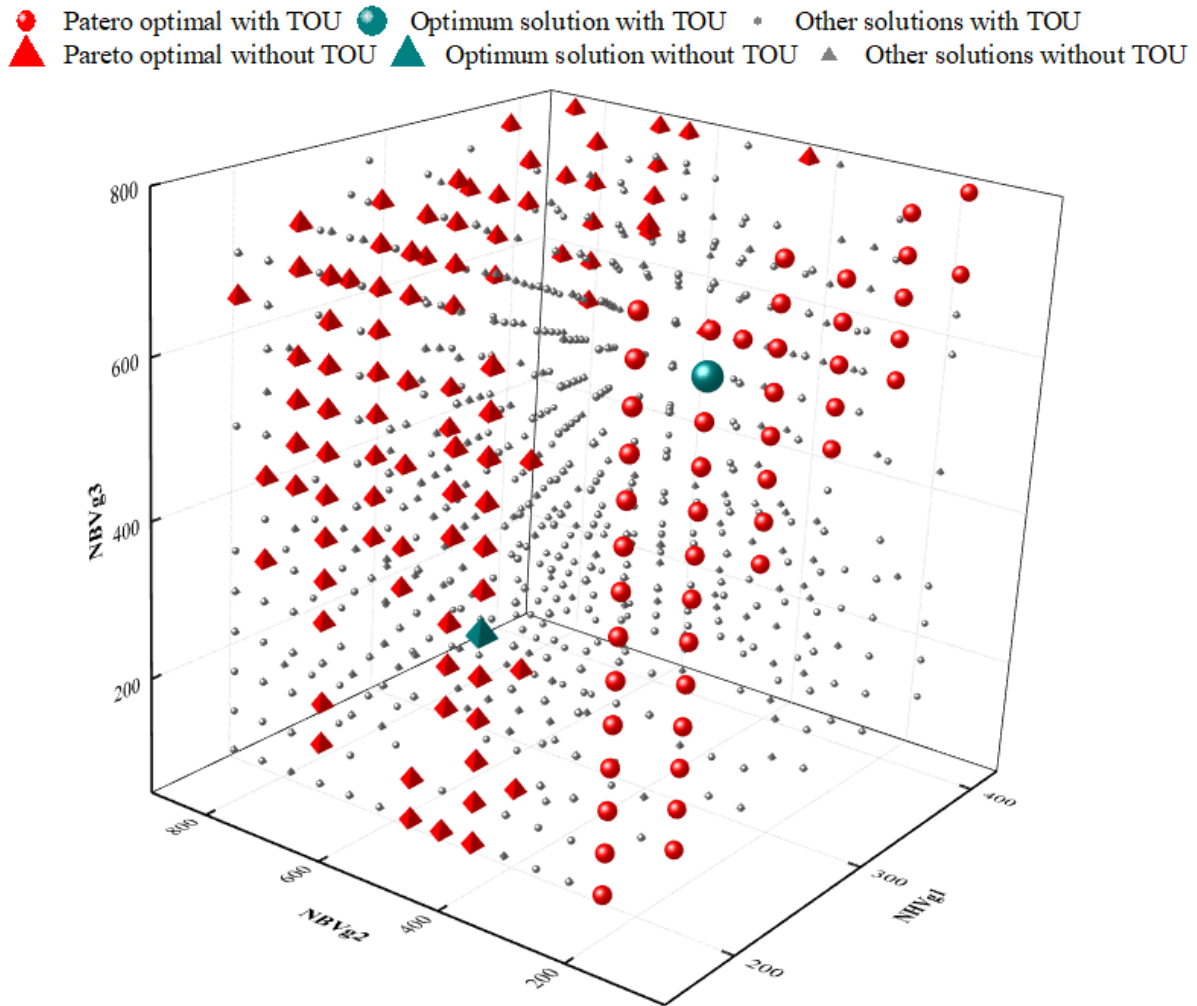


Fig. 8.32 Distribution of sizing vehicle numbers of Pareto optimal and final optimum solutions under TOU and non-TOU management strategies

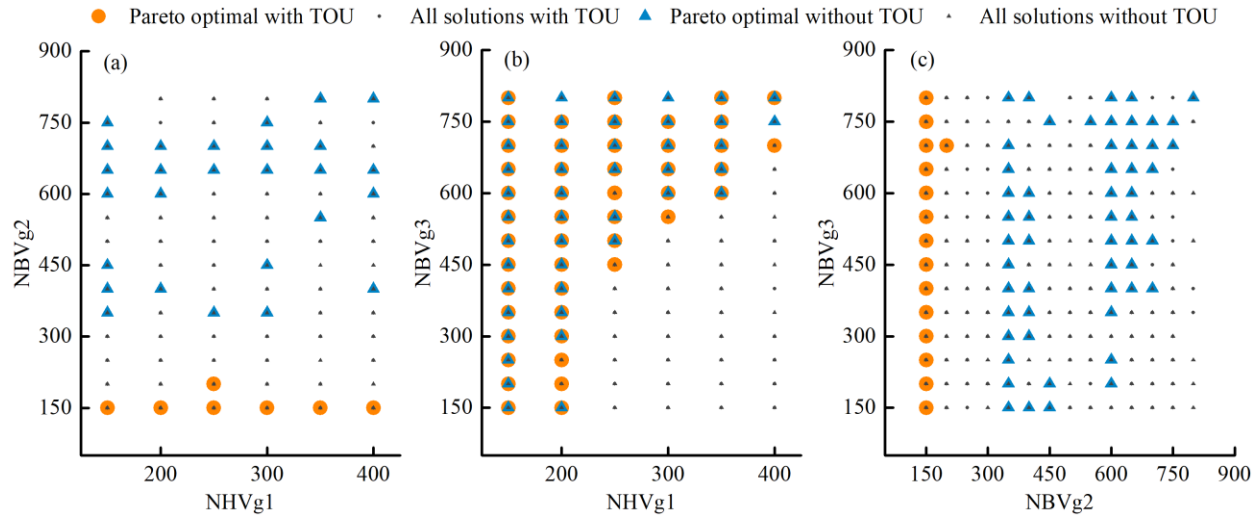


Fig. 8.33 Projection distribution of sizing vehicle numbers under TOU and non-TOU strategies

The distribution of sizing vehicle numbers of three building groups in the net-zero energy community of Pareto optimal and final optimum solutions under TOU and non-TOU managements is shown in Fig. 8.32, with the two-dimensional projections as shown in Fig. 8.33. The results indicate that the Pareto optimal solutions of TOU management are obtained with a relatively low BV number in group 2, as per Fig. 8.33(a) and (c), since BVs in group 2 (commercial office buildings) are assumed to be parked in buildings only during the on-peak periods, and only parked BVs have charging or discharging availability. And less vehicles in group 2 with lower charging availability has relatively lower impact on decreasing renewable energy *SCR* under TOU management, so a relatively superior performance can be achieved in decreasing *CEa* and *NBa*. It is also found that most of optimal solutions of non-TOU management are obtained with large vehicle numbers with higher charging availability for a higher *SCR*. The final optimum solution under TOU management obtained from the minimum distance to the utopia point method is achieved with the vehicle numbers of three groups for 200, 150, 700, respectively. And the final optimum solution under non-TOU management is achieved with 150 HVs in group 1, 350 BVs in group 2 and 400 BVs in group 3. It can be found that TOU management should be adopted when

the number of integrated BVs in group 2 is relatively small, for achieving a comprehensive optimal results in technical, economic and environmental performances (*SCR-CEa-NBa*). While TOU management should not be applied when the BV number in group 2 is relatively large.

8.2.6 Improved peer trading management results of the net-zero energy community integrated with both hydrogen vehicles and battery vehicles

In this section, an improved peer-to-peer energy trading management strategy is proposed, and the techno-economic-environmental superiority is demonstrated through the comparative analysis with the multi-objective optimum case.

(1) Power flow of optimum and improved cases

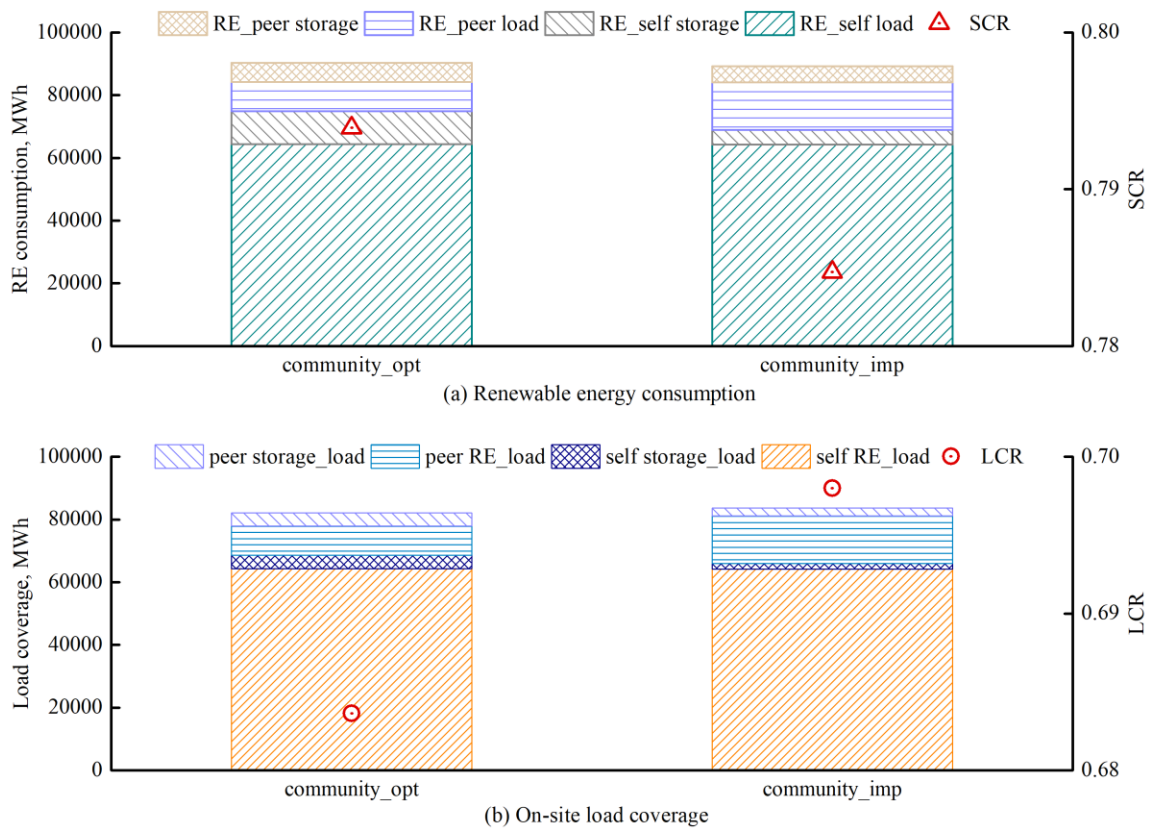


Fig. 8.34 Renewable energy consumption and load coverage of optimum and improved cases

(Note: the ‘opt’ and ‘imp’ are abbreviations of the optimum case and the improved case.)

The annual energy flow of the hybrid PV-wind-HV-BV system for power supply to the net-zero energy community for the optimum and improved cases is firstly analyzed to compare the on-site renewable energy consumption and load coverage. It is indicated that the more renewable energy is consumed for meeting the peer load in the net-zero energy community for the improved case, 61.43% higher than the optimum case as per Fig. 8.34(a). While less on-site renewable energy is available for the self-storage and peer storage, lower by 55.42% and 14.10% respectively. The main reason is that the on-site renewable energy is utilized for peer load prior to storage vehicles in the improved case, while a reversed priority is adopted in the optimum case. The SCR of renewable energy for the improved case is slightly lower than the optimum case by 0.92% in the net-zero energy community integrated with both BVs and HVs, changing from 79.39% to 78.47%. Regarding the on-site load coverage of the net-zero energy community integrated with both HVs and BVs, a 1.44% improvement in the LCR is observed for the improved case based on the optimum case as per Fig. 8.34(b). The peer trading energy is improved by 31.19% on top of the optimum case, and less demand is required from storage vehicles. Meanwhile, the utilization efficiency of the hybrid vehicle storages is reduced from 68.27% in the optimum case to 58.23% in the improved case with less charging availability.

(2) Improvement in grid integration and decarbonisation benefits

The grid integration and decarbonisation performances of the hybrid PV-wind-HV-BV system can be significantly improved by prioritizing energy trading to peer load before energy consumption to self-storage, compared with the optimum case with a reversed energy flow as shown in Fig. 8.35. The results show that the grid export of three building groups in the net-zero energy community all increases for the improved case with a rising range of 2.93% - 4.88%, compared with the optimum case. And an overall reduction in the community grid import of about

4.53% (1741.36 MWh) and an overall increment in the community grid export of about 4.46% (1045.58 MWh) are observed for the improved case. The net grid power import from the utility grid of the net-zero energy community is therefore markedly reduced in the improved case by around 18.54% of 2786.94 MWh. Meanwhile, obvious decarbonisation benefits are achieved by adopting the improved P2P energy trading management strategy in the net-zero energy community, with the annual equivalent carbon emissions reduced by 18.54% for 1594.13 tons.

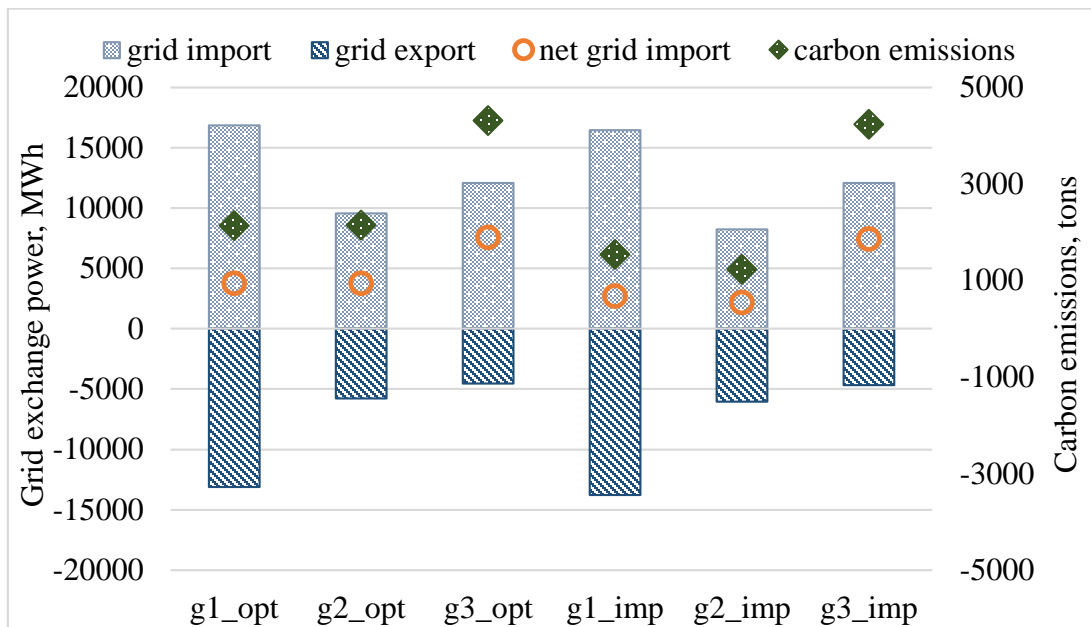


Fig. 8.35 Annual grid power exchange and carbon emissions of the optimum and improved cases
(Note: the ‘opt’ and ‘imp’ are abbreviations of the optimum case and the improved case.)

(3) Improvement in annual electricity bill and lifetime NPV

In addition to achieving improvements in technical and environmental aspects of the hybrid PV-wind-HV-BV system, the economic improvement is also observed in the proposed improved case on top of the optimum case as per Fig. 8.36. As shown in Fig. 8.36(a), it is indicated that the annual electricity bill of grid imported energy is reduced in the improved case by US\$ 268.45k, while the annual electricity bill of peer imported energy is increased by US\$ 217.08k. Because

less energy is imported from the utility grid and more energy is imported from the community peers, and the peer trading cost is more favorable than the grid trading cost in the individual peer trading price mode. And both the grid export gain and peer export gain are increased in the improved case by US\$ 60.64k and 217.08k, respectively. A total reduction in the net annual electricity bill of about US\$ 329.09k is achieved, lower by 8.31% compared with the optimum case. Moreover, the lifetime NPV of the hybrid PV-wind-HV-BV system with the improved P2P energy trading management strategy is also cut down as shown in Fig. 8.36(b). The system investment cost is slightly higher in the improved case by US\$ 3.82M as more electrolyzers are needed, while the system electricity bill is lower by US\$ 4.28M. So the system lifetime NPV of the improved case is lower than that of the optimum case by US\$ 458.69k, mainly contributed by the reduced electricity bills.

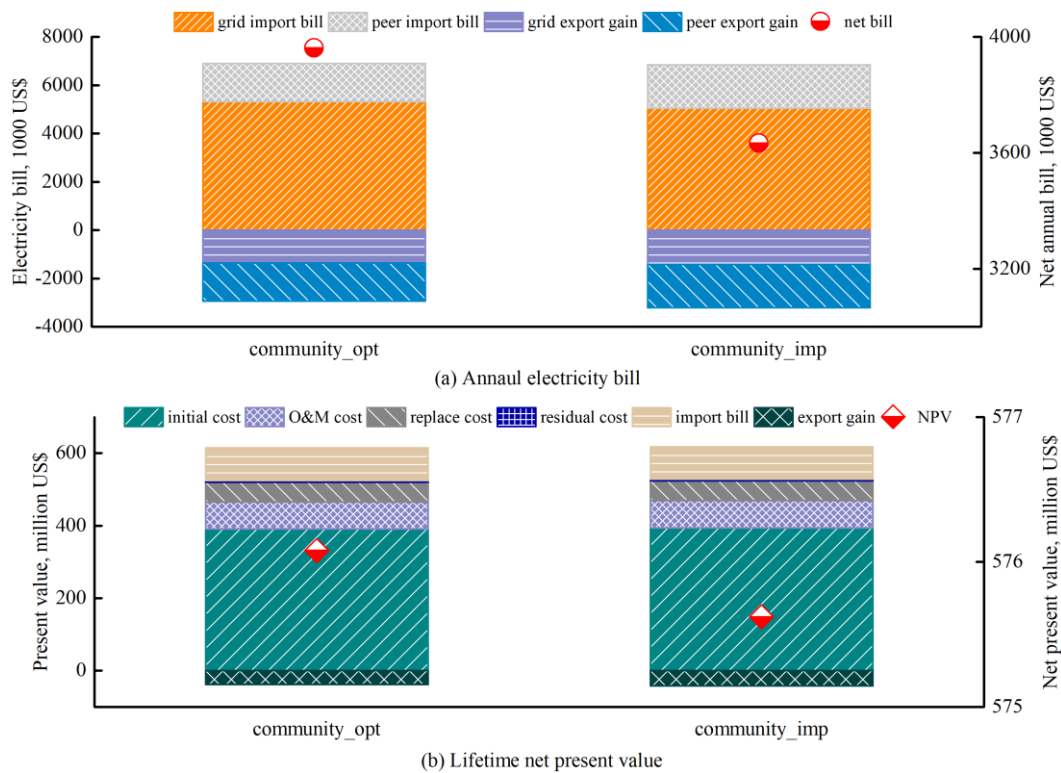


Fig. 8.36 Annual electricity bill and lifetime NPV of the optimum and improved cases

(Note: the ‘opt’ and ‘imp’ are abbreviations of the optimum case and the improved case.)

8.2.7 Summary of peer-to-peer trading optimizations on the net-zero energy community integrated with energy storage of hydrogen and battery vehicles

This study presents the newly developed peer-to-peer energy trading management and optimization approaches of hybrid renewable energy systems for power supply to a typical diversified net-zero energy community integrated with hydrogen vehicles and battery vehicles based on actual energy use data and simulations. Firstly, four net-zero energy community cases are developed and compared with different vehicle types and peer trading management approaches, to explore the techno-economic-environmental performance superiority of hydrogen vehicle-integrated and battery vehicle-integrated renewable energy systems under peer-to-grid trading and peer-to-peer trading managements. Secondly, the multi-objective peer-to-peer trading optimizations of renewable energy systems with hybrid energy storage of hydrogen vehicles and battery vehicles are developed, to find optimal configurations of vehicle numbers in diversified building groups and time-of-use management operations, for a comprehensive optimization considering the system supply, electricity cost and decarbonisation benefits. Furthermore, an improved peer-to-peer trading management strategy is proposed on top of the optimum solution obtained by the multi-objective optimizations, to further enhance the system grid integration, decarbonisation and economic cost performances, via improving the peer trading management and making complementary operations on the hybrid energy storage of hydrogen vehicles and battery vehicles. Important conclusions are drawn as follows:

(1) The hydrogen vehicle-integrated hybrid renewable energy systems achieve superior performances on the on-site renewable energy self-consumption (higher by 16.82%) and load coverage (higher by 1.64%), compared with the battery vehicle-integrated systems under the peer-to-peer trading management. While the battery vehicle-integrated systems perform better in terms

of the grid integration (67.05% less net grid import), decarbonisation benefits (9803.21 tons CO₂ reduced), net annual electricity bill (lower by 20.50%) and lifetime net present value (lower by 26.38%). And the utilization efficiency of the battery vehicle-integrated system (90.06% - 93.55%) is much higher than the hydrogen vehicle-integrated system (40.81% - 42.42%) considering both energy storage and transportation functions.

(2) The peer-to-peer energy trading management improves the technical performances and electricity bills of the diversified net-zero energy community in terms of the renewable energy self-consumption (higher by 16.54%), load coverage (higher by 10.10%) and annual electricity bill (lower by 15.37%) for the hydrogen vehicle-integrated systems compared with the peer-to-grid trading. But the carbon emissions of the net-zero energy community are increased by 32.85% (3615.37 tons), as more renewable energy is utilized for peer load and storage rather than being exported into the utility grid.

(3) The multi-objective peer trading optimizations indicate an optimal interactive relationship between the time-of-use management selection and equipped vehicle numbers for the diversified building groups in the net-zero energy community with hybrid renewable energy systems integrated with both hydrogen vehicles and battery vehicles. For the techno-economic-environmental optimization in the typical net-zero energy community, the time-of-use management strategy should be adopted when the number of integrated battery vehicles in commercial office buildings is relatively small, and the strategy without time-of-use management is preferred when the numbers of integrated green vehicles in diversified building groups are relatively high. And the time-of-use management strategy should be adopted when focusing on the system economic and environmental performances, while both management approaches can

achieve balanced results when considering the techno-economic or techno-environmental performances, with appropriate vehicle numbers in the diversified building groups.

(4) Obvious improvements can be achieved by the proposed improved peer-to-peer energy trading management strategy of renewable energy and hybrid vehicle storage systems applied in the diversified net-zero energy community, including the grid integration (18.54% less net grid import), decarbonisation benefits (1594.13 tons less carbon emissions), net electricity bill (lower by 8.31%) and lifetime net present value (reduced by US\$ 458.69k) on top of the optimum solution.

(5) The present study develops peer energy trading approaches for a diversified community, via comparing four typical net-zero energy cases with different storage vehicles and peer trading managements, developing multi-objective peer trading optimizations, and proposing an improved peer trading management strategy. The techno-economic-environmental superiority of hydrogen vehicle-integrated and battery vehicle-integrated renewable energy systems is distinguished, and the optimal interactive relationship between the vehicle numbers and system management strategy is demonstrated. The comprehensive results provide significant guidance for stakeholders to install and manage renewable energy and green vehicle systems for net-zero energy communities towards carbon neutrality in the integrated building and transport sectors in urban areas.

CHAPTER 9 CONCLUSIONS AND RECOMMENDATIONS

FOR FUTURE WORK

9.1 Summary of research findings and contributions

This thesis develops a comprehensive and systematic research framework on hybrid renewable energy and electrical energy storage systems for power supply to both a single building and building communities in urban regions, for achieving a carbon neutral energy framework in the near future. Three parts of work have been conducted including the system models and preliminary experiments, hybrid renewable energy and storage systems for one single building, and hybrid renewable energy and storage systems for the building community. This thesis studies the hybrid renewable energy and storage system applications by conducting practical experimental tests, proposing novel energy management strategies, formulating improved technical and economic assessment indicators, developing robust system planning and optimization approaches, establishing flexible grid integration models, and presenting systematic peer-to-peer energy trading management and optimization platforms. It makes significant contributions on helping researchers and policy makers to design and evaluate hybrid renewable energy and storage systems for both a single building and communities. And it also provides major stakeholders with clear guidance to develop renewable energy applications in the integrated building and transport sectors towards carbon neutrality. An integrated simulation and optimization platform of hybrid renewable energy and storage systems can be established with the developed models and codes for building and community applications. The input conditions include local conditions of a specific site including local renewable energy resources, energy storage applicability, electricity tariff schemes (grid tariff, feed-in tariff) and demand distributions. The output conditions include optimal system sizing

configurations, detailed techno-economic-environmental feasibility assessment indicators, optimal management strategies and settings. This integrated platform would provide significant guidance for the industry, such as consulting companies, to promote renewable energy and storage systems in integrated building and transport sectors for achieving carbon neutrality in urban areas. The main research findings and conclusions are summarized for each section as follows.

9.1.1 System modelling and preliminary experiments of hybrid renewable energy and storage systems

The detailed system modelling and evaluation methodology of hybrid renewable energy and storage systems are presented as per Chapter 3 for applications in the single building and communities within urban contexts. The dynamic simulation models on hybrid renewable energy and storage systems are specified involving the main components (i.e. energy demand, energy supply, energy storage, grid integration and energy management). And detailed design optimization methods are explained to optimize the system size configurations, grid operational limits and energy management strategies. Different decision-making strategies are explained to determine the final optimum solution, including the weighted sum method, minimum distance to the utopia point method, and analytical hierarchy process method. Meanwhile, key assessment indicators are formulated to evaluate the technical (supply performance, energy storage, grid integration), economic (lifetime net present value, improved levelized cost of energy) and environmental (annual equivalent carbon emissions and corresponding costs) aspects of the hybrid renewable energy and storage systems.

Experiments on an actual solar photovoltaic and battery storage system are conducted, under the maximizing self-consumption and time-of-use strategies, to investigate the system operational performance and validate the energy balance based battery model and energy management strategy

in TRNSYS modelling (as per Chapter 4). It is indicated that the root mean square deviations between the tested and simulated battery state of charge for the maximizing self-consumption and time-of-use strategies are 1.49% and 0.94%, respectively. And the maximum error deviations between the tested and simulated state of charge for these two strategies are 0.03 and 0.04, which validated the energy balance based battery model and energy management strategy in TRNSYS modelling.

9.1.2 Design optimization of photovoltaic and battery systems for a low-energy building

Following the system modelling and evaluation methodology in Chapter 3 and preliminary experiments in Chapter 4, the design application of an actual solar photovoltaic and battery system is studied for a low-energy office building (Chapter 5). A novel energy management strategy is proposed considering the battery cycling aging, grid relief and local time-of-use pricing. Both single-criterion and multi-criterion optimizations are conducted, by comprehensively considering technical, economic and environmental performances of the system, based on decision-making strategies including the weighted sum and minimum distance to the utopia point methods.

It is indicated that the single-criterion optimizations achieve superior performances in the energy supply, battery storage, utility grid and whole system aspect respectively over the existing scenario of the target building. The multi-criterion optimization considering all performance indicators shows that the solar photovoltaic self-consumption and utilization efficiency can be increased by 15.0% and 48.6%, while the standard deviation of net grid power, battery cycling aging and CO₂ emission can be reduced by 3.4%, 78.5% and 34.7% respectively. The significance and impact of design parameters are further quantified by both local and global sensitivity analyses. This study can provide references for the optimum energy management of solar photovoltaic and

battery storage systems in low-energy buildings, and guide the renewable energy and storage system design to achieve higher penetration of renewable applications into urban areas.

9.1.3 Energy planning of renewable energy and hybrid storage systems for a high-rise building

Succeeding to the study on solar photovoltaic and battery storage applications for a low-energy office building, the energy planning of hybrid renewable energy and storage systems for a typical high-rise residential building is presented. It includes battery storage based renewable energy systems, and hybrid battery and hydrogen vehicle storage based renewable energy systems (Chapter 6).

For the battery storage based renewable energy systems, three typical renewable application scenarios (solar photovoltaic, solar photovoltaic-wind, solar photovoltaic-wind-battery) are investigated. A comprehensive technical optimization criterion is developed integrating the energy supply, battery storage, building demand and grid relief indicators. And the improved levelized cost of energy considering detailed renewables benefits is formulated, including the feed-in tariff, transmission loss saving, network expansion saving and carbon reduction benefit. It is indicated that the solar photovoltaic system covers 16.02% of the annual load at a levelized cost of energy of 0.5252 US\$/kWh, and the solar photovoltaic-wind system covers 53.65% of the annual load at the lowest levelized cost of energy of 0.1251 US\$/kWh. The added battery storage improves the annual average load cover ratio and self-consumption ratio by 14.08% and 16.56% respectively, while the optimum solar photovoltaic-wind-battery system covers 81.29% of the annual load at an affordable levelized cost of energy of 0.2230 US\$/kWh.

While for the hybrid battery and hydrogen vehicle storage based renewable energy systems, two energy management strategies are developed with different operation priorities of the battery

and hydrogen storage technologies. Multi-objective optimizations are conducted to select the optimum management strategy and configuration of the hybrid solar photovoltaic-wind-battery-hydrogen system. Techno-economic indicators are developed for the multi-objective optimizations, and four decision-making strategies are further applied to search the final optimum solution for major stakeholders with different preferences. The research results indicate that the management strategy with hydrogen storage prior to battery storage has a wider applicability, and this strategy should be selected when focusing on the supply-grid integration or supply-economy performance. The annual average self-consumption ratio, load cover ratio and hydrogen system efficiency are about 84.79%, 76.11% and 77.06% respectively in the end-user priority case. The annual absolute net grid exchange is about 4.55 MWh in the transmission system operator priority case. The lifetime net present value of the investor priority case is about US\$ 3.64M, 29.88% less than the equivalent priority case. Final optimum solutions show positive environmental impacts with negative annual carbon emissions. Such a techno-economic-environmental feasibility analysis of the hybrid system provides major stakeholders with valuable energy planning references to promote renewable applications in urban areas for achieving carbon neutrality in the near future.

9.1.4 System optimization of renewable energy and storage systems for a diversified net-zero energy community

In addition to study the application of hybrid renewable energy and storage systems for one single building, its further system optimization in diversified building communities is also focused as per Chapter 7. The hybrid renewable energy systems integrated with stationary battery and mobile hydrogen vehicle storage are developed for a net-zero energy community consisting of campus, office and residential buildings. A time-of-use grid penalty cost model evaluating grid import and export during on-peak and off-peak periods is proposed, to achieve the power grid

flexibility and economy. Multi-objective optimizations are conducted to size net-zero energy buildings and the community considering the renewable energy self-consumption, on-site load coverage and grid penalty cost.

The study results indicate that battery storage improves the renewable energy self-consumption, load coverage, hydrogen system efficiency and grid integration of the net-zero energy community. Grid penalty cost reductions of 145.36% - 158.92% and 135.05% - 164.41% are achieved in net-zero energy scenarios with and without battery storage, compared with baseline scenarios without renewable energy. The lifetime net present value of four net-zero energy scenarios with battery storage is increased by 22.39% - 96.17% compared with baseline scenarios, while it is reduced by 6.45% of US\$ 7.62M and 1.90% of US\$ 2.16M in net-zero energy campus and residential buildings without battery storage. Substantial environmental benefits are also achieved in net-zero energy scenarios with and without battery storage, for reducing carbon emissions by 71.23% - 90.93% and 67.57% - 91.36%, respectively. This comprehensive techno-economic-environmental feasibility study can offer significant guidance for relative stakeholders to develop renewable energy applications for net-zero energy urban buildings and communities.

9.1.5 Peer-to-peer energy trading optimization of a net-zero energy community with renewable energy and storage systems

To further promote the penetration of hybrid renewable energy and storage systems in building communities, the dynamic peer-to-peer energy trading management and optimization platform of a diversified net-zero energy community is established integrating both hydrogen vehicles and battery vehicles (Chapter 8).

For the peer-to-peer energy trading of the net-zero energy community with renewable energy systems integrating hydrogen vehicle storage, hybrid solar photovoltaic and wind turbine systems

are developed for power supply to the diversified community integrated with three hydrogen vehicle storage groups. An individual peer energy trading price model is proposed for the diversified community to allocate an individual peer trading price to each building group, according to its intrinsic energy characteristic and grid import price. The time-of-use peer trading management strategies are further developed for both uniform and individual energy trading price modes to improve the grid flexibility and economy. The study results indicate that the peer energy trading management in the individual trading price mode improves the renewable energy self-consumption ratio by 18.76% and load cover ratio by 11.23% for the net-zero energy community compared with the peer-to-grid trading. The time-of-use trading management in the individual trading price mode can reduce the net grid import energy by 8.93%, grid penalty cost by 142.87%, annual electricity cost by 14.54%, and equivalent carbon emissions by 8.93% (982.36 tCO₂), respectively. This comprehensive feasibility study on the typical community with the proposed peer trading price model and management strategies provides significant guidance for renewable energy and hydrogen storage applications in large-scale communities within high-density urban contexts.

In terms of the peer-to-peer trading optimizations on the diversified net-zero energy community integrated with hydrogen and battery vehicles, typical net-zero energy community models are developed and compared with different energy storage vehicle types (hydrogen vehicle/battery vehicle) and energy trading modes (peer-to-grid/peer-to-peer). Multi-objective peer-to-peer trading optimizations of the net-zero energy community integrated with both hydrogen vehicles and battery vehicles are conducted to find optimal configurations of vehicle numbers and time-of-use management operations. An improved peer-to-peer trading management strategy is further proposed considering the peer trading priority and complementary operations of

hybrid vehicle storages, to enhance the grid integration, decarbonisation and economy. The study results indicate that the hydrogen vehicle-integrated system achieves superior system supply performances, while the battery vehicle-integrated system performs better on the grid integration, economic and environmental aspects. The time-of-use management strategy should be adopted when the number of integrated battery vehicles in commercial office buildings is relatively small, and the strategy without time-of-use management is preferred when the numbers of integrated vehicles in diversified building groups are relatively high for a comprehensive techno-economic-environmental optimization. Obvious improvements can be achieved by the improved peer trading management strategy, with reductions on the net grid import by 18.54%, carbon emissions by 1594.13 tons, net electricity bill by 8.31% and lifetime net present value by US\$ 458.69k. This comprehensive feasibility study on the diversified net-zero energy community provides significant references for stakeholders to install and manage renewable energy and green vehicle storage systems towards carbon neutrality in the integrated building and transport sectors in urban areas.

9.2 Recommendations for future research

This thesis presents a systematic study on hybrid renewable energy and storage systems for power supply to both a single building and communities in urban regions for achieving the carbon neutral development in the near future. The novel energy management strategies, improved technical and economic indicators, flexible grid integration models, robust system planning optimizations, and systematic peer-to-peer energy trading management and optimization approaches are developed. Typical electrical energy storage technologies are covered, including stationary battery storage, mobile battery vehicle storage, mobile hydrogen vehicle storage and their hybrids, by practical experiments, transient system simulations, coupled optimizations,

techno-economic-environmental assessments and sensitivity analyses. However, there are still aspects to be further investigated, due to the limited time and experimental unavailability.

Firstly, this thesis conducted preliminary experiments on the solar photovoltaic and battery storage system under two typical energy management strategies. Further experimental studies on hybrid renewable energy and storage systems need to be carried out, to promote the practical applications of renewable energy systems, such as hybrid solar photovoltaic-wind systems with battery vehicles or hydrogen vehicles. The flexible energy control algorithms of the hybrid systems should be developed and validated in the testing platforms installed with solar photovoltaic panels, wind turbines and hybrid storage technologies.

Secondly, this thesis considers the battery cycling aging only based on an empirical equation. While the dynamic battery degradation (both cycling and calendar aging) in the renewable energy operation and management needs to be further researched. And the lifetime degradation of hydrogen vehicle systems (i.e. fuel cell, electrolyzer) should also be studied for renewable energy system applications.

Thirdly, the application feasibility of hybrid renewable energy and storage systems in a large-scale city/region needs to be studied, considering the local power supply resources, renewable energy potential, energy storage availability and energy demand predictions. The system design optimizations and energy management controls for the city-scale applications will be explored in further research.

REFERENCES

- [1] International Energy Agency. Global energy and CO₂ status report: The latest trends in energy and emissions in 2018. 2019.
- [2] REN 21. Renewables 2020 global status report. 2020.
- [3] International Energy Agency. 2019 global status report for buildings and construction: towards a zero-emissions, efficient and resilient buildings and construction sector. 2019.
- [4] Environment Bureau. Hong Kong's Climate Action Plan 2030+. 2017.
- [5] International Energy Agency. GlobalABC roadmap for buildings and construction 2020-2050: towards a zero-emission, efficient, and resilient buildings and construction sector. 2020.
- [6] International Renewable Energy Agency. Global renewables outlook: Energy transformation 2050. 2020.
- [7] Tomas Kåberger RZ. 2019 global power sector developments: RE finally dominated growth. 2019.
- [8] Yan J, Yang Y, Campana PE, He J. City-level analysis of subsidy-free solar photovoltaic electricity price, profits and grid parity in China. *Nature Energy*. 2019;4:709-17.
- [9] International Renewable Energy Agency. Future of solar photovoltaic: Deployment, investment, technology, grid integration and socio-economic aspects. 2019.
- [10] International Renewable Energy Agency. Power to change - Solar and wind cost reduction potential to 2030 in the G20 countries. 2019.
- [11] International Renewable Energy Agency. Future of wind: Deployment, investment, technology, grid integration and socio-economic aspects. 2019.
- [12] REN 21. Renewables in cities: 2019 global status report. 2019.

- [13] International Institute for Sustainable Development SDG Knowledge Hub. 77 countries, 100+ cities commit to net zero carbon emissions by 2050 at Climate Summit. 2019.
- [14] International Institute for Sustainable Development SDG Knowledge Hub. European Commission launches green deal to reset economic growth for carbon neutrality. 2019.
- [15] World Resources Institute. Zero carbon buildings for all initiative launched at UN Climate Action Summit. 2019.
- [16] Xinhua News. Xi Focus: Xi announces China aims to achieve carbon neutrality before 2060. 2020.
- [17] The World Bank. 2019. Year in review: 2019 in 14 charts.
- [18] Liu J, Chen X, Cao S, Yang H. Overview on hybrid solar photovoltaic-electrical energy storage technologies for power supply to buildings. *Energy Conversion and Management*. 2019;187:103-21.
- [19] International Renewable Energy Agency. Renewable energy statistics 2019. 2019.
- [20] Kousksou T, Bruel P, Jamil A, El Rhafiki T, Zeraouli Y. Energy storage: Applications and challenges. *Solar Energy Materials and Solar Cells*. 2014;120:59-80.
- [21] Chatzivasileiadi A, Ampatzi E, Knight I. Characteristics of electrical energy storage technologies and their applications in buildings. *Renewable and Sustainable Energy Reviews*. 2013;25:814-30.
- [22] Kim J, Suharto Y, Daim TU. Evaluation of Electrical Energy Storage (EES) technologies for renewable energy: A case from the US Pacific Northwest. *Journal of Energy Storage*. 2017;11:25-54.

- [23] Beaudin M, Zareipour H, Schellenberglabe A, Rosehart W. Energy storage for mitigating the variability of renewable electricity sources: An updated review. *Energy for Sustainable Development*. 2010;14:302-14.
- [24] Amirante R, Cassone E, Distaso E, Tamburrano P. Overview on recent developments in energy storage: Mechanical, electrochemical and hydrogen technologies. *Energy Conversion and Management*. 2017;132:372-87.
- [25] Chen H, Cong TN, Yang W, Tan C, Li Y, Ding Y. Progress in electrical energy storage system: A critical review. *Progress in Natural Science*. 2009;19:291-312.
- [26] Hadjipaschalis I, Poullikkas A, Efthimiou V. Overview of current and future energy storage technologies for electric power applications. *Renewable and Sustainable Energy Reviews*. 2009;13:1513-22.
- [27] Queensland Government. Types of battery energy storage. 2018.
- [28] Clean Energy Council. Guide to installing a household battery storage system. 2018.
- [29] Argyrou MC, Christodoulides P, Kalogirou SA. Energy storage for electricity generation and related processes: Technologies appraisal and grid scale applications. *Renewable and Sustainable Energy Reviews*. 2018;94:804-21.
- [30] Akbari H, Browne MC, Ortega A, Huang MJ, Hewitt NJ, Norton B, et al. Efficient energy storage technologies for photovoltaic systems. *Solar Energy*. 2018.
- [31] REN 21. Renewables 2019 global status report-renewable electricity generation costs. 2019.
- [32] Wood Mackenzie. U.S. energy storage monitor: 2019 year in review executive summary. 2020.
- [33] European Association for the Storage of Energy and Delta Energy & Environment. European Market Monitor on Energy Storage – Latest Status and Trends in Europe Edition 4.0. 2020.

- [34] G. Hering. At ‘tipping point’, battery-backed solar homes gain foothold on New England grid. 2019.
- [35] S. Vorrath. Australia’s big battery market set to add ‘at least’ 500MWh in 2020. 2020.
- [36] R. McCarthy. What technology is winning the energy storage race? 2019.
- [37] BloombergNEF. Scale-up of solar and wind puts existing coal, gas at risk. 2020.
- [38] IHS Markit. IHS Markit’s 10 Cleantech Trends in 2020. 2020.
- [39] Power Engineering. Lithium-ion startups attract lion’s share of energy storage venture capital in 2019. 2020.
- [40] International Energy Agency. Global EV Outlook 2020: Entering the decade of electric drive? 2020.
- [41] International Energy Agency. The future of hydrogen: Seizing today’s opportunities. 2019.
- [42] Buttler A, Spliethoff H. Current status of water electrolysis for energy storage, grid balancing and sector coupling via power-to-gas and power-to-liquids: A review. *Renewable and Sustainable Energy Reviews*. 2018;82:2440-54.
- [43] Bruce S, Temminghoff M, Hayward J, Schmidt E, Munnings C, Palfreyman D, et al. National Hydrogen Roadmap. Pathways to an economically sustainable hydrogen industry in Australia. 2018.
- [44] Advanced Fuel Cells Technology Collaboration Programme. AFC TCP Survey on the number of fuel cell electric vehicles, hydrogen refuelling stations and targets. 2019.
- [45] International Energy Agency. Global EV outlook 2019: overcoming the challenges of transport electrification. 2019.
- [46] FuelCells Works. Korean government announces roadmap to become the world leader in the hydrogen economy. 2019.

- [47] Strategy Advisory Committee of the Technology Roadmap for Energy Saving and New Energy Vehicles and Society of Automotive Engineers of China. Hydrogen Fuel Cell Vehicle Technology Roadmap. 2016.
- [48] California Fuel Cell Partnership. The California fuel cell revolution a vision for advancing economic, social, and environmental priorities. 2018.
- [49] Ministry of Economy Trade and Industry Japan. Compilation of the revised version of the strategic roadmap for hydrogen and fuel cells. 2016.
- [50] Hydrogen Council. Hydrogen scaling up. A sustainable pathway for the global energy transition. 2017.
- [51] Fathabadi H. Novel stand-alone, completely autonomous and renewable energy based charging station for charging plug-in hybrid electric vehicles (PHEVs). *Applied Energy*. 2020;260:114194.
- [52] Robledo CB, Oldenbroek V, Abbruzzese F, van Wijk AJM. Integrating a hydrogen fuel cell electric vehicle with vehicle-to-grid technology, photovoltaic power and a residential building. *Applied Energy*. 2018;215:615-29.
- [53] Cao S, Alanne K. The techno-economic analysis of a hybrid zero-emission building system integrated with a commercial-scale zero-emission hydrogen vehicle. *Applied Energy*. 2018;211:639-61.
- [54] Farahani SS, Bleeker C, van Wijk A, Lukszo Z. Hydrogen-based integrated energy and mobility system for a real-life office environment. *Applied Energy*. 2020;264:114695.
- [55] Cao S. The impact of electric vehicles and mobile boundary expansions on the realization of zero-emission office buildings. *Applied Energy*. 2019;251:113347.

- [56] Silverman RE, Flores RJ, Brouwer J. Energy and economic assessment of distributed renewable gas and electricity generation in a small disadvantaged urban community. *Applied Energy*. 2020;280:115974.
- [57] Bartolini A, Carducci F, Muñoz CB, Comodi G. Energy storage and multi energy systems in local energy communities with high renewable energy penetration. *Renewable Energy*. 2020;159:595-609.
- [58] Avilés A C, Oliva H S, Watts D. Single-dwelling and community renewable microgrids: Optimal sizing and energy management for new business models. *Applied Energy*. 2019;254:113665.
- [59] You C, Kim J. Optimal design and global sensitivity analysis of a 100% renewable energy sources based smart energy network for electrified and hydrogen cities. *Energy Conversion and Management*. 2020;223:113252.
- [60] Yan B, Di Somma M, Graditi G, Luh PB. Markovian-based stochastic operation optimization of multiple distributed energy systems with renewables in a local energy community. *Electric Power Systems Research*. 2020;186:106364.
- [61] Clairand J-M, Arriaga M, Cañizares CA, Álvarez-Bel CJIToSE. Power generation planning of Galapagos' microgrid considering electric vehicles and induction stoves. 2018;10:1916-26.
- [62] Mazzeo D, Oliveti G, Baglivo C, Congedo PM. Energy reliability-constrained method for the multi-objective optimization of a photovoltaic-wind hybrid system with battery storage. *Energy*. 2018;156:688-708.
- [63] Bingham RD, Agelin-Chaab M, Rosen MA. Whole building optimization of a residential home with PV and battery storage in The Bahamas. *Renewable Energy*. 2019;132:1088-103.

- [64] Salata F, Ciancio V, Dell'Olmo J, Golasi I, Palusci O, Coppi M. Effects of local conditions on the multi-variable and multi-objective energy optimization of residential buildings using genetic algorithms. *Applied Energy*. 2020;260:114289.
- [65] Ferrara M, Rolfo A, Prunotto F, Fabrizio E. EDeSSOpt – Energy Demand and Supply Simultaneous Optimization for cost-optimized design: Application to a multi-family building. *Applied Energy*. 2019;236:1231-48.
- [66] Waibel C, Evins R, Carmeliet J. Co-simulation and optimization of building geometry and multi-energy systems: Interdependencies in energy supply, energy demand and solar potentials. *Applied Energy*. 2019;242:1661-82.
- [67] González-Mahecha RE, Lucena AFP, Szklo A, Ferreira P, Vaz AIF. Optimization model for evaluating on-site renewable technologies with storage in zero/nearly zero energy buildings. *Energy and Buildings*. 2018;172:505-16.
- [68] Elkadeem MR, Wang S, Azmy AM, Atiya EG, Ullah Z, Sharshir SW. A systematic decision-making approach for planning and assessment of hybrid renewable energy-based microgrid with techno-economic optimization: A case study on an urban community in Egypt. *Sustainable Cities and Society*. 2020;54:102013.
- [69] Ghorbani N, Kasaeian A, Toopshekan A, Bahrami L, Maghami A. Optimizing a hybrid wind-PV-battery system using GA-PSO and MOPSO for reducing cost and increasing reliability. *Energy*. 2018;154:581-91.
- [70] Ghaffari A, Askarzadeh A. Design optimization of a hybrid system subject to reliability level and renewable energy penetration. *Energy*. 2020;193:116754.

- [71] Ma T, Javed MS. Integrated sizing of hybrid PV-wind-battery system for remote island considering the saturation of each renewable energy resource. *Energy Conversion and Management*. 2019;182:178-90.
- [72] Huang Z, Xie Z, Zhang C, Chan SH, Milewski J, Xie Y, et al. Modeling and multi-objective optimization of a stand-alone PV-hydrogen-retired EV battery hybrid energy system. *Energy Conversion and Management*. 2019;181:80-92.
- [73] Neves D, Scott I, Silva CA. Peer-to-peer energy trading potential: An assessment for the residential sector under different technology and tariff availabilities. *Energy*. 2020;205:118023.
- [74] Nguyen S, Peng W, Sokolowski P, Alahakoon D, Yu X. Optimizing rooftop photovoltaic distributed generation with battery storage for peer-to-peer energy trading. *Applied Energy*. 2018;228:2567-80.
- [75] Alam MR, St-Hilaire M, Kunz T. Peer-to-peer energy trading among smart homes. *Applied Energy*. 2019;238:1434-43.
- [76] Long C, Wu J, Zhou Y, Jenkins N. Peer-to-peer energy sharing through a two-stage aggregated battery control in a community Microgrid. *Applied Energy*. 2018;226:261-76.
- [77] Fernandez E, Hossain MJ, Mahmud K, Nizami MSH, Kashif M. A Bi-level optimization-based community energy management system for optimal energy sharing and trading among peers. *Journal of Cleaner Production*. 2021;279:123254.
- [78] Hahnel UJJ, Herberz M, Pena-Bello A, Parra D, Brosch T. Becoming prosumer: Revealing trading preferences and decision-making strategies in peer-to-peer energy communities. *Energy Policy*. 2020;137:111098.
- [79] Hackbarth A, Löbbeck S. Attitudes, preferences, and intentions of German households concerning participation in peer-to-peer electricity trading. *Energy Policy*. 2020;138:111238.

- [80] Zhou Y, Wu J, Song G, Long C. Framework design and optimal bidding strategy for ancillary service provision from a peer-to-peer energy trading community. *Applied Energy*. 2020;278:115671.
- [81] Li Z, Ma T. Peer-to-peer electricity trading in grid-connected residential communities with household distributed photovoltaic. *Applied Energy*. 2020;278:115670.
- [82] Tushar W, Saha TK, Yuen C, Morstyn T, McCulloch MD, Poor HV, et al. A motivational game-theoretic approach for peer-to-peer energy trading in the smart grid. *Applied Energy*. 2019;243:10-20.
- [83] Esmat A, de Vos M, Ghiassi-Farrokhfal Y, Palensky P, Epema D. A novel decentralized platform for peer-to-peer energy trading market with blockchain technology. *Applied Energy*. 2021;282:116123.
- [84] Wang Z, Yu X, Mu Y, Jia H. A distributed Peer-to-Peer energy transaction method for diversified prosumers in Urban Community Microgrid System. *Applied Energy*. 2020;260:114327.
- [85] Peng J, Lu L. Investigation on the development potential of rooftop PV system in Hong Kong and its environmental benefits. *Renewable and Sustainable Energy Reviews*. 2013;27:149-62.
- [86] De Soto W, Klein SA, Beckman WA. Improvement and validation of a model for photovoltaic array performance. 2006;80:78-88.
- [87] Duffie JA, Beckman WA. *Solar engineering of thermal processes*: John Wiley & Sons; 2013.
- [88] Chen X, Yang H, Peng J. Energy optimization of high-rise commercial buildings integrated with photovoltaic facades in urban context. *Energy*. 2019;172:1-17.
- [89] Liu J, Cao S, Chen X, Yang H, Peng J. Energy planning of renewable applications in high-rise residential buildings integrating battery and hydrogen vehicle storage. *Applied Energy*. 2021;281:116038.

- [90] Wind turbine models. Hummer H21.0-100kW. 2017.
- [91] International Energy Agency Statistics. Electric power transmission and distribution losses (% of output) Hong Kong SAR, China. 2018.
- [92] Paul Ayeng'o S, Axelsen H, Haberschusz D, Sauer DU. A model for direct-coupled PV systems with batteries depending on solar radiation, temperature and number of serial connected PV cells. *Solar Energy*. 2019;183:120-31.
- [93] Jiang Y, Kang L, Liu Y. A unified model to optimize configuration of battery energy storage systems with multiple types of batteries. *Energy*. 2019;176:552-60.
- [94] Hesse H, Martins R, Musilek P, Naumann M, Truong C, Jossen AJE. Economic optimization of component sizing for residential battery storage systems. 2017;10:835.
- [95] Pena-Bello A, Barbour E, Gonzalez MC, Patel MK, Parra D. Optimized PV-coupled battery systems for combining applications: Impact of battery technology and geography. *Renewable and Sustainable Energy Reviews*. 2019;112:978-90.
- [96] Cai J, Zhang H, Jin X. Aging-aware predictive control of PV-battery assets in buildings. *Applied Energy*. 2019;236:478-88.
- [97] Liu J, Wang M, Peng J, Chen X, Cao S, Yang H. Techno-economic design optimization of hybrid renewable energy applications for high-rise residential buildings. *Energy Conversion and Management*. 2020;213:112868.
- [98] Liu J, Chen X, Yang H, Li Y. Energy storage and management system design optimization for a photovoltaic integrated low-energy building. *Energy*. 2020;190:116424.
- [99] Chen B, Jiang H, Sun H, Yu M, Yang J, Li H, et al. A new gas–liquid dynamics model towards robust state of charge estimation of lithium-ion batteries. *Journal of Energy Storage*. 2020;29:101343.

- [100] Toyota USA NEWSROOM. Toyota Mirai product information. 2019.
- [101] Solar Energy Laboratory Univ. of Wisconsin-Madison. TRNSYS 18 a transient system simulation program, Volume 4 mathematical reference. 2017.
- [102] Cao S, Alanne K. Technical feasibility of a hybrid on-site H₂ and renewable energy system for a zero-energy building with a H₂ vehicle. *Applied Energy*. 2015;158:568-83.
- [103] Voss K, Sartori I, Napolitano A, Geier S, Gonçalves H, Hall M, et al. Load matching and grid interaction of net zero energy buildings. *EUROSUN 2010 International Conference on Solar Heating, Cooling and Buildings*2010.
- [104] China Light and Power Hong Kong Limited. *Tariff and charges*. 2020.
- [105] Liu N, Yu X, Wang C, Li C, Ma L, Lei J. Energy-sharing model with price-based demand response for microgrids of peer-to-peer prosumers. *IEEE Transactions on Power Systems*. 2017;32:3569-83.
- [106] Hongkong Electric Company. *Billing, payment and electricity tariffs*. 2020.
- [107] Zhang Y, Jankovic L. *An Interactive Optimisation Engine for Building Energy Performance Simulation*. 2017.
- [108] Magnier L, Haghghat F. Multiobjective optimization of building design using TRNSYS simulations, genetic algorithm, and Artificial Neural Network. *Building and Environment*. 2010;45:739-46.
- [109] Lee U, Park S, Lee I. Robust design optimization (RDO) of thermoelectric generator system using non-dominated sorting genetic algorithm II (NSGA-II). *Energy*. 2020;196:117090.
- [110] Chen X, Yang H, Zhang W. Simulation-based approach to optimize passively designed buildings: A case study on a typical architectural form in hot and humid climates. *Renewable and Sustainable Energy Reviews*. 2018;82:1712-25.

- [111] Saaty RW. The analytic hierarchy process—what it is and how it is used. *Mathematical modelling*. 1987;9:161-76.
- [112] Das R, Wang Y, Putrus G, Kotter R, Marzband M, Herteleer B, et al. Multi-objective techno-economic-environmental optimisation of electric vehicle for energy services. *Applied Energy*. 2020;257:113965.
- [113] International Renewable Energy Agency. Renewable power generation costs in 2017. 2018.
- [114] Electrical and Mechanical Services Department. Introduction to feed-in tariff of renewable energy in Hong Kong. 2018.
- [115] China Light and Power Hong Kong Limited. Electricity price adjustment. 2018.
- [116] China Light and Power Hong Kong Limited. Large power tariff. 2020.
- [117] Ricke K, Drouet L, Caldeira K, Tavoni M. Country-level social cost of carbon. *Nature Climate Change*. 2018;8:895-900.
- [118] Ministry of Housing and Urban-Rural Construction of the People's Republic of China. Design standard for energy efficiency of public buildings. 2015.
- [119] University of Wisconsin. TRNSYS 18. 2017.
- [120] National Renewable Energy Laboratory. Weather Data Sources.
- [121] National Development and Reform Commission. Notice of the national development and reform commission on improving the feed-in tariff mechanism for photovoltaic power generation. 2019.
- [122] Magnor D, Sauer DUJEP. Optimization of PV battery systems using genetic algorithms. 2016;99:332-40.
- [123] China Southern Power Grid. Industrial and commercial electricity price in Shen Zhen. 2019.

- [124] Delgarm N, Sajadi B, Delgarm S, Kowsary F. A novel approach for the simulation-based optimization of the buildings energy consumption using NSGA-II: Case study in Iran. *Energy and Buildings*. 2016;127:552-60.
- [125] Chen X, Yang H, Sun K. A holistic passive design approach to optimize indoor environmental quality of a typical residential building in Hong Kong. *Energy*. 2016;113:267-81.
- [126] Chaianong A, Bangviwat A, Menke C, Breitschopf B, Eichhammer W. Customer economics of residential PV–battery systems in Thailand. *Renewable Energy*. 2020;146:297-308.
- [127] Hong Kong Housing Authority. Standard block typical floor plans. 2016.
- [128] Chen H, Lee WL, Yik FWH. Applying water cooled air conditioners in residential buildings in Hong Kong. *Energy Conversion and Management*. 2008;49:1416-23.
- [129] Hong Kong Building Environmental Assessment Method Society. An environmental assessment for new buildings Version 4/04. 2004.
- [130] Hong Kong Electrical and Mechanical Services Department. Guidelines on Performance-based Building Energy Code. 2007.
- [131] Wan KSY, Yik FWH. Building design and energy end-use characteristics of high-rise residential buildings in Hong Kong. *Applied Energy*. 2004;78:19-36.
- [132] Jung W, Jeong J, Kim J, Chang D. Optimization of hybrid off-grid system consisting of renewables and Li-ion batteries. *Journal of Power Sources*. 2020;451:227754.
- [133] Campbell M AP, Blunden J, Smeloff E, Wright S. The Drivers of the Levelized Cost of Electricity for Utility-Scale Photovoltaics. SunPower Corp. 2008.
- [134] Li J, Zhang X, Zhou X, Lu L. Reliability assessment of wind turbine bearing based on the degradation-Hidden-Markov model. *Renewable Energy*. 2019;132:1076-87.
- [135] Global petrol prices. Hong Kong electricity prices. 2019.

- [136] China Light and Power Hong Kong Limited. 2018 Annual report. 2018.
- [137] Gao X, Yang H, Lu L. Investigation into the optimal wind turbine layout patterns for a Hong Kong offshore wind farm. *Energy*. 2014;73:430-42.
- [138] Cao S, Sirén K. Impact of simulation time-resolution on the matching of PV production and household electric demand. *Applied Energy*. 2014;128:192-208.
- [139] The University of Wisconsin Madison. TRNSYS 18. 2017.
- [140] Zhou Y, Cao S. Coordinated multi-criteria framework for cycling aging-based battery storage management strategies for positive building–vehicle system with renewable depreciation: Life-cycle based techno-economic feasibility study. *Energy Conversion and Management*. 2020;226:113473.
- [141] Ma T, Yang H, Lu L, Peng J. Optimal design of an autonomous solar–wind-pumped storage power supply system. *Applied Energy*. 2015;160:728-36.
- [142] Wang D, Cao X. Impacts of the built environment on activity-travel behavior: Are there differences between public and private housing residents in Hong Kong? *Transportation Research Part A: Policy and Practice*. 2017;103:25-35.
- [143] Ramadhani F, Hussain MA, Mokhlis H, Fazly M, Ali JM. Evaluation of solid oxide fuel cell based polygeneration system in residential areas integrating with electric charging and hydrogen fueling stations for vehicles. *Applied Energy*. 2019;238:1373-88.
- [144] Gökçek M, Kale C. Techno-economical evaluation of a hydrogen refuelling station powered by Wind-PV hybrid power system: A case study for İzmir-Çeşme. *International Journal of Hydrogen Energy*. 2018;43:10615-25.

- [145] Assaf J, Shabani B. Transient simulation modelling and energy performance of a standalone solar-hydrogen combined heat and power system integrated with solar-thermal collectors. *Applied Energy*. 2016;178:66-77.
- [146] Toyota Motor Sales. 2019 Mirai fuel cell electric vehicle. 2020.
- [147] Killer M, Farrokhseresht M, Paterakis NG. Implementation of large-scale Li-ion battery energy storage systems within the EMEA region. *Applied Energy*. 2020;260:114166.
- [148] GlobalData. Further falling inverter prices – market value declining. 2018.
- [149] Baldwin D. Development of high pressure hydrogen storage tank for storage and gaseous truck delivery. Hexagon Lincoln LLC, Lincoln, NE (United States); 2017.
- [150] Kim I, Kim J, Lee J. Dynamic analysis of well-to-wheel electric and hydrogen vehicles greenhouse gas emissions: Focusing on consumer preferences and power mix changes in South Korea. *Applied Energy*. 2020;260:114281.
- [151] Freitas Gomes IS, Perez Y, Suomalainen E. Coupling small batteries and PV generation: A review. *Renewable and Sustainable Energy Reviews*. 2020;126:109835.
- [152] International Energy Agency. *The Future of Hydrogen. Seizing today's opportunities*. 2019.
- [153] Transport Department. *The annual traffic census*. 2018.
- [154] California fuel cell partnership. *Cost to refill*. 2019.